EFFICIENCY OF SOIL AQUIFER TREATMENT IN THE REMOVAL OF WASTEWATER CONTAMINANTS AND ENDOCRINE DISRUPTORS

A study on the removal of triclocarban and estrogens and the effect of chemical oxygen demand and hydraulic loading rates on the reduction of organics and nutrients in the unsaturated and saturated zones of the aquifer

By

Helen Michelle Korkor ESSANDOH

A thesis submitted for the degree of

Doctor of Philosophy

at the

School of Engineering, Design and Technology

University of Bradford

2011

ABSTRACT

EFFICIENCY OF SOIL AQUIFER TREATMENT IN THE REMOVAL OF WASTEWATER CONTAMINANTS AND ENDOCRINE DISRUPTORS

Keywords: *artificial wastewater, chemical oxygen demand, endocrine disrupting compounds, estrogens, hydraulic loading rate, removal efficiency, saturated zone, soil aquifer treatment, triclocarban, unsaturated zone*

This study was carried out to evaluate the performance of Soil Aquifer Treatment (SAT) under different loading regimes, using wastewater of much higher strength than usually encountered in SAT systems, and also to investigate the removal of the endocrine disruptors triclocarban (TCC), estrone (E1), 17β-estradiol (E2) and 17α-ethinylestradiol (EE2). SAT was simulated in the laboratory using a series of soil columns under saturated and unsaturated conditions.

Investigation of the removal of Chemical Oxygen Demand (COD), Biochemical Oxygen Demand (BOD), Dissolved Organic Carbon (DOC), nitrogen and phosphate in a 2 meter long saturated soil column under a combination of constant hydraulic loading rates (HLRs) and variable COD concentrations as well as variable HLR under constant COD showed that at fixed HLR, a decrease in the influent concentrations of DOC, BOD, total nitrogen and phosphate improved their removal efficiencies. It was found that COD mass loading applied as low COD wastewater infiltrated over short residence times would provide better effluent quality than the same mass applied as a COD with higher concentration at long residence times. On the other hand relatively high concentrations coupled with long residence time gave better removal efficiency for organic nitrogen. Phosphate removal though poor under all experimental conditions, was better at low HLRs.

In 1 meter saturated and unsaturated soil columns, E2 was the most easily removed estrogen, while EE2 was the least removed. Reducing the thickness of the unsaturated zone had a negative impact on removal efficiencies of the estrogens whereas increased DOC improved the removal in the saturated columns. Better removal efficiencies were also obtained at lower HLRs and in the presence of silt and clay.

Sorption and biodegradation were found to be responsible for TCC removal in a 300 mm long saturated soil column, the latter mechanism however being unsustainable. TCC removal efficiency was dependent on the applied concentration and decreased over time and increased with column depth. Within the duration of the experimental run, TCC negatively impacted on treatment performance, possibly due to its antibacterial property, as evidenced by a reduction in COD removals in the column.

COD in the 2 meter column under saturated conditions was modelled successfully with the advection dispersion equation with coupled Monod kinetics. Empirical models were also developed for the removal of TCC and EE2 under saturated and unsaturated conditions respectively. The empirical models predicted the TCC and EE2 removal profiles well. There is however the need for validation of the models developed.

TABLE OF CONTENTS

ABSTRACT i

TABLE OF FIGURES x

TABLE OF TABLES xv

ACKNOWLEDGEMENTS xvii

PUBLICATIONS AND CONFERENCE PROCEEDINGS xix

NOMENCLATURE xxi

1 INTRODUCTION 1

1.1 Background 1

1.2 Research Objectives 5

1.3 Justification for Study 6

1.4 Scope of Research 8

1.5 Organization of Thesis 9

2 LITERATURE REVIEW 11

2.1 Introduction 11

2.2 Contaminants of Concern in Wastewater Treatment 11

2.3 Soil Aquifer Treatment 12

2.3.1 Pre-treatment of Wastewater for SAT Systems 16

2.3.1.1 Characteristics of Applied Wastewater 17

2.3.1.2 Soil and Aquifer Properties 17

2.3.1.3 Uses of Recovered Groundwater 19

2.4 Mass Transport and Transformation Processes 21

2.4.1 Advective Transport 22

2.4.2 Diffusive Transport 23

2.4.3 Mechanical Dispersion and Hydrodynamic Dispersion 25

2.4.4 The Sorption Process 27

2.4.5 The Biodegradation Process 29

2.4.5.1 Aerobic Oxidation 32

2.4.5.2 Denitrification 34

2.4.5.3 Sulphate Reduction 35

2.4.6 Advection–Dispersion Transport 36

2.4.6.1 Initial and Boundary Conditions 37

2.4.6.2 Advection-Dispersion Transport with Sorption and Reaction 38

2.4.6.3 Kinetics of Biodegradation 40

2.5 Fate of Contaminants in Effluents Undergoing SAT 42

2.5.1 Removal Mechanisms in SAT 43

2.5.2 Fate of Particulates 45

2.5.3 Fate of Dissolved Organic and Inorganic Contaminants 46

2.5.4 Fate of Pathogens 49

2.6 Performance of SAT Systems 51

2.6.1 Level of Effluent Pre-treatment 53

2.6.2 Site Characteristics 54

2.6.3 Operating Conditions 55

2.7 Reduction in Soil Hydraulic Conductivity during SAT 56

2.7.1 Bacterial Biomass and Community Structure in Soils 59

2.8 Endocrine Disrupting Compounds 63

2.8.1 Introduction 63

2.8.2 Mechanisms of Action of Endocrine Disrupting Compounds 64

2.8.3 Estrogens 65

2.8.3.1 Structure and Properties of E1, E2 and EE2 66

2.8.3.2 Sources of Environmental Estrogens 68
2.8.3.3 Effects of Exposure to Estrogens 73
2.8.3.4 Transformation Processes and Mechanisms for Removal of Estrogens 74
2.8.3.5 Redox Conditions and Estrogen Transformation 76
2.8.4 3, 4, 4´-trichlorocarbanilide (Triclocarban) 78
2.8.4.1 Sources of Triclocarban in the Environment 79
2.8.4.2 Effects of TCC Exposure on Living Organisms 80
2.8.4.3 Removal of Triclocarban during Wastewater Treatment and Mechanisms for Removal 82
3 MATERIALS AND METHODS 86
3.1 Introduction 86
3.2 Studies on Wastewater Hydraulic Loading Rates and COD Effects on Removal Efficiency of Wastewater Parameters during SAT 89
3.2.1 Soil Column Description and Setup 89
3.2.2 Column Startup and General Operation 92
3.2.3 Residence Time Distribution Studies 95
3.2.4 SAT Simulations 97
3.2.5 Soil Column Soil Biomass Measurements 100
3.2.6 Abiotic Soil Column Experiments 102
3.3 Studies on the Removal of Estrogens under Saturated and Unsaturated Soil Conditions 102
3.3.1 Soil Column Description and Setup 103
3.3.1.1 Description and Calibration of SWT5 Tensiometers 106
3.3.1.2 Description and Calibration of Soil Moisture Sensors 111

3.3.2 Soil Characterisation 116
3.3.2.1 Grain Size Distribution 116
3.3.2.2 Atterberg Limits 117
3.3.2.3 Hydraulic Conductivity 119
3.3.3 Soil Column Experiments 123
3.3.3.1 Experimental Conditions and Wastewater Sampling 125
3.3.3.2 Soil Sampling 128
3.4 Studies on Triclocarban (TCC) Removal 128
3.4.1 Description of Setup 128
3.4.2 Soil Column Start-Up and Operation 130
3.5 Instruments and Analytical Methods for Wastewater Characterisation 131
3.5.1 Dissolved Oxygen and pH Measurement 131
3.5.2 Dissolved Organic Carbon (DOC) Analysis 132
3.5.2.1 Principle of Operation of TOC Analyser 132
3.5.2.2 Calibration of TOC Analyser 133
3.5.2.3 Sample Analysis 134
3.5.3 Chemical Oxygen Demand Analysis 135
3.5.4 Biochemical Oxygen Demand Analysis 135
3.5.5 Total Kjeldahl Nitrogen and Ammonia Nitrogen Analysis 137
3.5.6 Anions Analysis 138
3.5.6.1 Principle of Operation 139
3.5.6.2 Instrument Calibration 140
3.5.6.3 Sample Analysis 142
3.5.7 Analysis of Estrogens and Triclocarban 142
3.5.7.1 Principle of Operation of LCMS 143

3.5.7.2 Optimisation and Calibration of LCMS 144

3.5.7.3 Wastewater Sample Preparation and Estrogen Analysis..... 146

3.5.7.4 Sample Preparation and TCC Analysis 148

3.5.8 Phospholipid Fatty Acid Analysis of Soil Column Packing Material 149

3.5.8.1 Principle of Operation of GCMS..... 149

3.5.8.2 Calibration of GCMS 150

3.5.8.3 Sample Preparation..... 154

3.5.8.4 GCMS Analysis..... 156

3.6 Summary of Experiments..... 156

4 RESULTS AND DISCUSSIONS 161

4.1 Introduction 161

4.2 Removal of Synthetic Wastewater Parameters under Varying Hydraulic Loading Rates and Chemical Oxygen Demand..... 161

4.2.1 2-meter Soil Column Hydraulic Properties 162

4.2.2 Soil Column Experiments 167

4.2.2.1 Mass Loading Rates on the Soil Column 167

4.2.2.2 Redox Conditions in the Soil Column..... 171

4.2.2.3 Dissolved Organic Carbon, Biochemical and Chemical Oxygen Demand Removal under Constant Chemical Oxygen Demand and Variable Hydraulic Loading Rates 180

4.2.2.4 Dissolved Organic Carbon, Biochemical and Chemical Oxygen Demand Removal under Variable Chemical Oxygen Demand and Constant Hydraulic Loading Rate 184

4.2.2.5 Organic Matter Removal by Adsorption in the Soil Column.... 189

4.2.2.6 Nitrogen Removal under Constant Chemical Oxygen Demand and Variable Hydraulic Loading Rates 190
4.2.2.7 Nitrogen Removal under Variable Chemical Oxygen Demand and Constant Hydraulic Loading Rate 194
4.2.2.8 Phosphate Removal 196
4.2.3 Chemical Oxygen Demand Balance in the Soil Column 199
4.2.4 Correlations between Electron Donor and Electron Acceptors 202
4.2.5 Microbial Concentration Profile in the Soil Column 204
4.2.6 Soil Column Reaction Kinetics 206
4.2.7 Comparison of Removal Efficiencies under Varying Chemical Oxygen Demand and Hydraulic Loading Rates 209
4.2.8 Conclusions 211
4.3 Removal of Estrone, 17β-Estradiol and 17α-Ethinylestradiol under Saturated and Unsaturated Soil Conditions 213
4.3.1 Soil and Hydraulic Characteristics of 1-meter Soil Columns 213
4.3.1.1 Hydraulic Residence Time 214
4.3.1.2 Unsaturated Hydraulic Conductivity 216
4.3.1.3 Soil Matric Potential and Water Content 217
4.3.2 Soil Column Dissolved Organic Carbon Removal and Nitrogen Transformation Processes 219
4.3.2.1 Saturated Soil Columns 220
4.3.2.2 Phospholipid Fatty Acid Analysis of Soil Samples 222
4.3.2.3 Wastewater Treatment under Unsaturated Conditions 229
4.3.3 Investigation of Estrogens Removal 238
4.3.3.1 Estrogen Removal under Unsaturated Conditions 239

4.3.3.2 Estrogen Removal in Saturated Silica Sand under Variable Hydraulic Loading Rates and Dissolved Organic Carbon Concentration 243

4.3.3.3 Estrogen Removal in Saturated Sand-Silt-Clay Mix under Variable Hydraulic Loading Rates and Dissolved Organic Carbon Concentration 248

4.3.4 Conclusions 251

4.4 Removal of Triclocarban during Soil Aquifer Treatment and its Effects on Chemical Oxygen Demand Removal 253

4.4.1 TCC Solid Phase Extraction Recovery Tests 254

4.4.2 Soil Column Experiments 255

4.4.2.1 Influent Triclocarban Loading Rates 255

4.4.2.2 Triclocarban Reduction in the Soil Column 255

4.4.2.3 Evaluation of Triclocarban Removal Mechanisms in the Soil Column 258

4.4.3 Conclusions 265

5 MODEL DEVELOPMENT 267

5.1 Introduction 267

5.2 Model for Chemical Oxygen Demand Removal 267

5.2.1 Development of Fate Controlling Equations 268

5.2.1.1 Mass Balance in the Liquid Phase 269

5.2.1.2 Mass Balance in the Solid Phase 274

5.2.2 Boundary Conditions 274

5.2.3 Estimation of COD Transport Parameters and Degradation Rate Constants 276

5.2.3.1 Hydraulic and Hydrodynamic Parameters 276
5.2.3.2 Rate Constants 276
5.2.3.3 Ratio of Oxygen to Organic Material Consumed 277
5.2.4 Modelling Results 279
5.3 Model for Triclocarban Removal 281
5.4 Model for 17α-Ethinylestradiol (EE2) Removal under Unsaturated Conditions 287
5.5 Conclusions 290
6 CONCLUSIONS AND RECOMMENDATIONS 292
6.1 Conclusions 292
6.1.1 Removal of Chemical Oxygen Demand, Biochemical Oxygen Demand, Dissolved Organic Carbon, Nitrogen and Phosphate 292
6.1.2 Removal of Estrogens 294
6.1.3 Removal of Triclocarban 296
6.1.4 Modelling 297
6.2 Recommendations 297
REFERENCES 300
APPENDIX A 336
APPENDIX B 342
APPENDIX C 352
APPENDIX D 363

TABLE OF FIGURES

Figure 1.1 Schematic diagram of soil aquifer treatment 2

Figure 2.1 Schematic diagrams of soil aquifer treatment systems with recovery of renovated water 20

Figure 2.2 Processes affecting the movement and fate of contaminants in the subsurface environment 22

Figure 2.3 Schematic representation of factors causing pore-scale longitudinal dispersion 26

Figure 2.4 Schematic representation of sorption processes 28

Figure 2.5 Electron tower showing positions of sulphate, nitrate and oxygen 31

Figure 2.6 Removal mechanisms in the vadose zone during SAT 44

Figure 2.7 Nitrogen inputs and transformation in a SAT system 48

Figure 2.8 Cyclopentanophenathrene ring of estrogens 65

Figure 2.9 Structure of conjugated estrogen, Premarin 66

Figure 2.10 Structure of estrone 67

Figure 2.11 Structure of 17β-estradiol 67

Figure 2.12 Structure of 17α-ethinylestradiol 67

Figure 2.13 Common conjugated forms of estrone and 17β-estradiol 69

Figure 2.14 Metabolism and excretion of 17α-ethinylestradiol after ingestion 70

Figure 2.15 Structure of Triclocarban 79

Figure 2.16 Proposed biodegradation pathway of triclocarban 84

Figure 3.1 2-meter soil column setup 90

Figure 3.2 Fluorescein calibration curve 96

Figure 3.3 Phosphate calibration curve 102

Figure 3.4 1-meter soil column setup 104

Figure 3.5 SWT5 Tensiometer 107

Figure 3.6 Calibration setup for tensiometers 109

Figure 3.7 Calibration curves for SWT5 tensiometers 111

Figure 3.8 ThetaProbe soil moisture sensor 112

Figure 3.9 Calibration curves for soil moisture sensors 115

Figure 3.10 Silica sand grading curve 117

Figure 3.11 Experimental setup for the development of soil moisture retention curve 121

Figure 3.12 Silica sand moisture retention curve 122

Figure 3.13 Experimental stages for estrogen studies 125

Figure 3.14 Schematic diagram of 300 mm soil column setup 129

Figure 3.15 Dissolved organic carbon calibration curve 134

Figure 3.16 Anion calibration curves 141

Figure 3.17 Estrogen calibration curves 145

Figure 3.18 Triclocarban calibration curve 146

Figure 3.19 Calibration curves of bacterial acids methyl esters 154

Figure 4.1 Concentration versus time tracer response at varying hydraulic loading rates using 50 mg pulse input of fluorescein tracer 164

Figure 4.2 Mass loadings of wastewater parameters to the soil column 170

Figure 4.3 Dissolved oxygen mass removal rate against soil column depth 172

Figure 4.4 Nitrate mass removal rate against soil column depth at 20 °C 175

Figure 4.5 Sulphate mass removal rate against soil column depth at 20 °C 178

Figure 4.6 Mass removal rate of DOC, BOD and COD with soil column depth at 135 mg L^{-1} COD and variable HLRs of 44 cm d^{-1}, 88 cm d^{-1} and 169 cm d^{-1} 182

Figure 4.7 Mass removal rate of DOC, BOD and COD with soil column depth at HLR of 169 cm d^{-1} and variable COD of 135 mg L^{-1}, 81 mg L^{-1} and 42 mg L^{-1} 185

Figure 4.8 Nitrogen mass removal rate against column depth at constant COD of 135 mg L^{-1} and variable HLR of 44 cm d^{-1}, 88 cm d^{-1} and 169 cm d^{-1} 191

Figure 4.9 pH profile in soil column under experimental conditions HC-5, HC-10, HC-20, MC-20 and LC-20 at 20 °C..... 192

Figure 4.10 Influence of pH with oxidation states of ammonia-nitrogen 192

Figure 4.11 Nitrogen mass removal rate against column depth at constant HLR of 169 cm d^{-1} and variable COD of 135 mg L^{-1}, 81 mg L^{-1} and 42 mg L^{-1} 195

Figure 4.12 Phosphate removal rate against column height..... 196

Figure 4.13 Correlations between wastewater parameters at constant COD of 135 mg L^{-1} COD and varying HLR at 20 °C 203

Figure 4.14 Soil column microbial profile 204

Figure 4.15 Test for mixed-order reaction rate for dissolved oxygen, nitrate and sulphate 208

Figure 4.16 Test for mixed-order reaction rate for chemical oxygen demand, dissolved organic carbon and biochemical oxygen demand..... 209

Figure 4.17 Comparison of mass removal under investigated experimental conditions..... 210

Figure 4.18 Hydraulic residence time distribution curves in 1 m soil columns..... 215

Figure 4.19 Moisture retention curve and unsaturated hydraulic conductivity of silica sand..... 217

Figure 4.20 Dissolved organic carbon, oxygen, sulphate and nitrate removal efficiencies at 20°C in saturated soil columns, SC2 and SC3, at HLR of 81.5 cm d^{-1} 221

Figure 4.21 Peak areas against column height for depths for the various fatty acids identified in SC2 and SC3 227

Figure 4.22 Volumetric water content profiles and DOC and sulphate removal efficiencies at differing water table levels in unsaturated silica sand column (SC1).....230

Figure 4.23 Schematic diagram of nitrogen transformation processes within the soil column 234

Figure 4.24 Nitrogen removal at differing water table levels in SC1 235

Figure 4.25 Water content and estrogen removal efficiency in unsaturated silica sand column (SC1).....240

Figure 4.26 Estrogen removal efficiency in saturated silica sand column (SC2) ..244

Figure 4.27 Estrogen removal efficiency in silica sand/silt/clay mix column (SC3)... 249

Figure 4.28 TCC solid phase extraction recovery tests.....254

Figure 4.29 TCC concentration against time at different depths of the soil column ... .256

Figure 4.30 Percentage removal of TCC in the soil column.....257

Figure 4.31 Effect of TCC addition on COD concentration in the soil column 261

Figure 4.32 TCC mass balance in the soil column.....263

Figure 5.1 Schematic diagram of COD transport in the soil column controlled by advection, dispersion and reaction.....268

Figure 5.2 Schematic diagram of mass flow at entrance of soil column 274

Figure 5.3 Modelled COD removal for an initial concentration of 136 mg L^{-1} applied at a HLR of 169 cm d^{-1}.....279

Figure 5.4 Modelled COD removal for an initial concentration of 136 mg L^{-1} applied at a HLR of 88 cm d^{-1}.....280

Figure 5.5 Modelled COD removal for an initial concentration of 136 mg L^{-1} applied at a HLR of 44 cm d^{-1}.....280

Figure 5.6 Fraction of TCC remaining against mass applied at various soil column depths.....282

Figure 5.7 Fraction of TCC remaining per mass applied against soil column depth. 283

Figure 5.8 Comparison of model predicted TCC concentrations to measured concentrations at various depths.....285

Figure 5.9 EE2 removal against soil column height in the unsaturated soil column at various water table heights.....288

Figure 5.10 Modelled and experimental data for EE2 removal against soil column depth at various water table heights.....289

TABLE OF TABLES

Table 2.1 Characteristics of SAT systems 14

Table 2.2 Typical performance data for SAT systems 52

Table 2.3 Expected effluent quality from SAT systems 53

Table 2.4 Suggested loading cycles for SAT systems 55

Table 2.5 PLFA often used as biomarkers for specific groups of microorganisms 61

Table 2.6 Physical and chemical properties of E1, E2 and EE2 67

Table 2.7 Amount of E1, E2 and EE2 excreted daily by humans 70

Table 2.8 Concentrations of estrogens in wastewater treatment plant effluents in different countries 72

Table 2.9 Physical and chemical properties of TCC 79

Table 2.10 TCC concentrations measured in wastewater effluents 80

Table 3.1 Summary of equipment and instruments used 88

Table 3.2 Composition of synthetic wastewater 93

Table 3.3 Influent characteristics 98

Table 3.4 Experimental conditions 98

Table 3.5 Properties of silica sand, silt and clay used in 1 meter soil columns 119

Table 3.6 Influent characteristics to 1 meter soil column 124

Table 3.7 SC1 sampling locations 126

Table 3.8 SC2 and SC3 experimental conditions 127

Table 3.9 Masses of compounds in 1 L of 1000 mg L^{-1} anion standards 141

Table 3.10 Composition of BAME mix 151

Table 3.11 Summary of experiments and operating conditions for 2 meter soil column 157

Table 3.12 Summary of experiments and operating conditions for unsaturated soil column 158

Table 3.13 Summary of experiments and operating conditions for 1 meter silica sand and silica sand/silt/clay columns 159

Table 3.14 Summary of experiments and operating conditions for 300 mm soil column 160

Table 4.1 Summary of soil column hydraulic characteristics.....165

Table 4.2 Influent characteristics.....168

Table 4.3 Experimental conditions 168

Table 4.4 Comparison of predicted and actual COD removal in 2000 mm of the soil column.....201

Table 4.5 1 meter soil column hydraulic properties 216

Table 4.6 Pressure and water content in 1 m unsaturated soil column.....218

Table 4.7 Wastewater influent characteristics for SC1, SC2 and SC3 220

Table 4.8 Fatty acids identified in soil column samples by GCMS analysis.....224

Table 4.9 TCC concentration in soil column sand.....259

Table 5.1 COD kinetic parameters estimated from soil column concentration profile.....277

Table 5.2 Percentage errors between predicted and measured TCC concentrations 286

Table 5.3 Percentage errors between predicted and measured EE2 concentrations. 290

ACKNOWLEDGEMENTS

I wish to acknowledge the immense contribution of my supervisors Dr Chedly Tizaoui and Dr Mostafa Mohamed to this research. Their dedication and support have brought about the successful completion of this research. The input of Professor Gary Amy of King Abdullah University/ UNESCO-IHE, Professor Damir Brdjanovic of UNESCO-IHE and Dr Bukari Ali of Kwame Nkrumah University of Science and Technology (KNUST) towards this research is also acknowledged.

I am very grateful to Mr John Purvis and Glen Burton of the School of Engineering, Design and Technology (SoEDT) for being so accommodating and facilitating the smooth running of my research program, and also Mr Andy Birch and Mr Mick Cribb for their immense contribution. I also wish to thank Dr Fatima Mahieddine, Dr Anna Snelling and Dr Ben Stern for their help in specific aspects of my research. The invaluable contribution from technical staff of the SoEDT Workshop especially Mr Ian Mackay, Mr Mick Jagger, Phil Clegg, Mr Tony Dalton, Mr Dhiru Chavda, Owen Baines, Ms Joana Wood, and Mr C. Mistry towards the fabrication and successful running of the experimental setup is deeply appreciated. I am also really grateful for the input of Mr Arthur Kershaw towards the experimental setup. Many thanks also go to Mr Andrew Healey and Mr Dennis Farwell of the Institute of Pharmaceutical Innovation (IPI) and also to the technical staff of Archaeological, Geographical and Environmental Sciences (AGES) especially Mrs Usha Gohil and Mrs Belinda Hill for their help during the analytical stages of the research.

A big thank you also goes to my parents, siblings and parents in-laws for their prayers, support and encouragement. Finally, to my husband Ernest and children,

Mildred and Cyril, thank you for being so supportive and understanding when I had to be away at school so often.

Above all, my deep gratitude goes to God Almighty without whose intervention, this research would not have materialised.

This research was funded by the Netherlands Organisation for International Cooperation in Higher Education (Nuffic).

PUBLICATIONS AND CONFERENCE PROCEEDINGS

Three journal publications and one conference presentation have been derived from this research. These are outlined below:

1. ESSANDOH, H. M. K., TIZAOUI, C., MOHAMED, M. H. A., AMY, G. & BRDJANOVIC, D. (2010) Fate of triclocarban during soil aquifer treatment: soil column studies. *Water Science and Technology,* 61 (7)**,** 1779-1785.

2. ESSANDOH, H. M. K., TIZAOUI, C., MOHAMED, M. H. A., AMY, G. & BRDJANOVIC, D. (2011) Soil aquifer treatment of artificial wastewater under saturated conditions. *Water Research,* 45 (14)**,** 4211-4226.

3. ESSANDOH, H. M. K., TIZAOUI, C. & MOHAMED, M. H. A. (2012) Removal of estrone (E1), 17β-estradiol (E2) and 17α-ethinylestradiol (EE2) during soil aquifer treatment of a model wastewater. *Separation Science and Technology,* 47 (6), 777-787.

4. ESSANDOH, H. M. K., TIZAOUI, C., MOHAMED, M. H. A., AMY, G. & BRDJANOVIC, D. Fate of triclocarban during soil aquifer treatment (PC 252). Advanced Oxidation Processes 5 (AOP5). 5th IWA Specialist Conference/ 10th IOA-EA3G Berlin Conference on Oxidation Technologies for Water and Wastewater Treatment, 30th March – 2nd April 2009, Berlin. CUTEC Serial Publication No. 72, 90. CUTEC-Institut GmbH, PAPIERFLIEGER VERLAG, Clausthal-Zellerfeld.

This thesis is dedicated to my children Mildred and Cyril

NOMENCLATURE

Notation	Description and dimensions	Units
A	Cross-sectional area (L^2)	cm^2
b	Microbial decay rate (T^{-1})	
B_1	Dissolved oxygen of seed control before incubation (ML^{-3})	$mg\ L^{-1}$
B_2	Dissolved oxygen of seed control after incubation (ML^{-3})	$mg\ L^{-1}$
b_c	Active biomass concentration (ML^{-3})	
b_d	Microbial decay rate (T^{-1})	
C	Solute concentration (ML^{-3})	
C_c	Coefficient of curvature	
C_o	Initial solute concentration (ML^{-3})	
C_{oc}	Natural organic carbon concentration (ML^{-3})	
C_t	Solute concentration at time t (ML^{-3})	
C_u	Coefficient of uniformity	
d	Dispersion number	
D	Soil column coefficient of axial dispersion (L^2T^{-1})	cm^2min^{-1}
D^*	Effective diffusion coefficient (L^2T^{-1})	
D_1	Dissolved oxygen of diluted sample immediately after preparation (ML^{-3})	$mg\ L^{-1}$
D_2	Dissolved oxygen of diluted sample after 5-day incubation at 20 ºC (ML^{-3})	$mg\ L^{-1}$
d_{10}	Effective diameter (L)	mm
d_{30}	Grain diameter at 30 % passing (L)	mm
d_{50}	Average diameter (L)	mm
d_{60}	Grain diameter at 60 % passing (L)	mm

dC/dt	Change in concentration with time ($ML^{-3}T^{-1}$)	
dC/dx	Concentration gradient ($ML^{-3}L^{-1}$)	
dh/dl	Hydraulic gradient (LL^{-1})	
D_d	Diffusion coefficient (L^2T^{-1})	
D_m	Coefficient of longitudinal mechanical dispersion (L^2T^{-1})	
D_L	Hydrodynamic dispersion coefficient in principal direction of flow (L^2T^{-1})	
f	Fraction of seeded dilution water volume in sample to volume of seeded dilution water in seed control	
F	Ratio of oxygen to organic material (COD) consumed	
F_d	Mass flux of solute per unit area per unit time ($MT^{-1}L^{-2}$)	
F_x	One-dimensional advective mass flux ($MT^{-1}L^{-2}$)	
G	Ratio of oxygen to hydrocarbon consumed	
H	Concentration of hydrocarbon in pore fluid (ML^{-3})	
h	Thickness of unsaturated zone (L)	*mm*
h_b	Bubbling pressure (L)	*cm*
h_u	Maximum rate of hydrocarbon utilization per unit mass of aerobic microorganisms (T^{-1})	
k	Maximum specific substrate utilization rate/ reaction rate coefficient (T^{-1})	min^{-1}
k'	Soil column effective overall rate constant (T^{-1})	min^{-1}
$K(\theta)$	Unsaturated hydraulic conductivity at water content θ (LT^{-1})	$cm\ s^{-1}$
k_c	First order decay rate of natural organic carbon (T^{-1})	
K	Saturation constant of substrate/ constituent saturation constant (ML^{-3})	$mg\ L^{-1}$

K_c	Saturation constant of organic material/ COD (ML^{-3})	*mg L^{-1}*
K_d	Distribution coefficient (L^3M^{-1})	
K_h	Half-saturation constant of hydrocarbon (ML^{-3})	
K_o	Half-saturation constant of oxygen (ML^{-3})	
K_s	Saturated hydraulic conductivity (LT^{-1})	*cm s^{-1}*
l	Length of sample or distance along soil column (L)	
L	Soil column length (L)	
m	van Genuchten soil parameter	
m_T	Total cumulative mass of TCC (M)	*ng*
m_d	Mass of dry soil pat (M)	*g*
m_g	Mass of wax-coated sample in water (M)	*g*
M_t	Concentration of aerobic microorganisms (ML^{-3})	
m_w	Mass of wax-coated sample in air (M)	*g*
n	Porosity	
N	Axial dispersion of mass across soil column boundary ($MT^{-1}L^{-2}$)	
n_e	Effective porosity	
N_r	Number of complete-mix reactors in series	
O	Concentration of oxygen in pore fluid (ML^{-3})	
P	Fraction of wastewater sample volume to total combined volume	
Pe	Peclet number of longitudinal dispersion	
Q	Flow rate (L^3T^{-1})	*cm^{3}min^{-1}*
q	Hydraulic loading rate (LT^{-1})	*cm d^{-1}*
R	Retardation factor	

r	Rate of COD disappearance by reaction (T^{-1})	
r_c	Constituent reaction rate ($ML^{-3}T^{-1}$)	
R_{max}	Maximum reaction rate (T^{-1})	
r_s	Rate of COD mass sorption per unit mass of sand (T^{-1})	
s	Slope	
S	Mass of solute sorbed per unit mass of solid ($M\ M^{-1}$)	
S_e	Effective saturation	
S_p	Dimensionless slope	
t	Time (T)	
τ	Mean residence time (T)	*min*
τ_t	Theoretical residence time (T)	*min*
u	Average linear velocity of wastewater flow in soil column (LT^{-1})	*cm min*$^{-1}$
V	Volume (L^3)	
V_1	Volume of wet soil pat (L^3)	*cm*^{3}
VA_b	Volume of acid used for blank titration (L^3)	*mL*
VA_s	Volume of acid used for sample titration (L^3)	*mL*
V_B	Volume of BOD bottle (L^3)	*mL*
V_d	Volume of dry soil pat (L^3)	*cm*^{3}
v_i	Average linear velocity in the *i* direction (LT^{-1})	
V_l	Volume of liquid phase (L^3)	
V_{SP}	Volume of sample (L^3)	*mL*
V_s	Volume of solid phase (L^3)	
v_x	Average linear groundwater velocity (LT^{-1})	
w_1	Moisture content of soil	*%*

x	Relative concentration	
Y	Microbial yield coefficient (MM^{-1})	
z	Dimensionless length	
α_i	Dynamic dispersivity in the *i* direction (L)	
α_L	Longitudinal dynamic dispersivity (L)	
Δh	Head difference (L)	
Δl	Elemental length of soil column (L)	
Δt	Elemental time (T)	
θ	Volumetric water content (L^3L^{-3})	$cm^3\ cm^{-3}$
θ_r	Irreducible minimum water content (L^3L^{-3})	$cm^3\ cm^{-3}$
θ_s	Volumetric water content at saturation (L^3L^{-3})	$cm^3\ cm^{-3}$
ρ_b	Bulk density of aquifer (ML^{-3})	
ρ_p	Density of paraffin wax (ML^{-3})	$g\ cm^3$
ρ_s	Density of sand particles (ML^{-3})	
σ^2	Variance (T^2)	min^2
τ	Soil column residence time, (T)	*min*
τ_t	Theoretical residence time (T)	*min*
ω	Coefficient	

CHAPTER 1

1 INTRODUCTION

The importance of adequate sanitation and the availability of enough quantities of water for human consumption, industrial and agricultural use cannot be over emphasised as they play a vital role in maintaining a healthy livelihood and in the development of nations. Most human activities, involving water use, generate wastewater which must be treated to prescribed or acceptable standards before reuse or discharge into the environment to avoid pollution of the receiving water bodies.

As populations continue to increase with its associated problems of waste generation and contamination of surface water and groundwater, pressure on available water resources is increasing. This coupled with uneven distribution of water resources and periodic droughts around the world has brought about the need for innovative sources of water supply and local conservation. Highly treated wastewater effluents from municipal wastewater treatment plants are therefore now increasingly being considered as a reliable source of water supply (Tchobanoglous et al., 2003).

1.1 Background

Soil aquifer treatment (SAT) is a sustainable natural wastewater treatment technology, with the ability to generate high quality effluent from secondary treated wastewater for potable and non-potable uses. During SAT, well treated wastewater is ponded in infiltration basins and allowed to infiltrate through the unsaturated and saturated zones of the soil.

Treatment of the wastewater during infiltration involves physico-chemical and biological processes for the removal of contaminants in the effluent, and it has been reported that the technology is capable of removing almost all biochemical oxygen demand (BOD) and chemical oxygen demand (COD) (Bouwer et al., 1980; Idelovitch and Michail, 1984; Pescod, 1992), 99 - 100 % total suspended solids (TSS) and greater than 99 % viruses (Crites et al., 2000). High nitrogen removal (92.5 %) and 99.9 % phosphorus removal have also been reported (Crites et al., 2000).

Besides treatment, SAT offers the opportunity of aquifer recharge which is especially beneficial in arid areas. A schematic diagram of a SAT system is shown in Figure 1.1 (Fox et al., 2006).

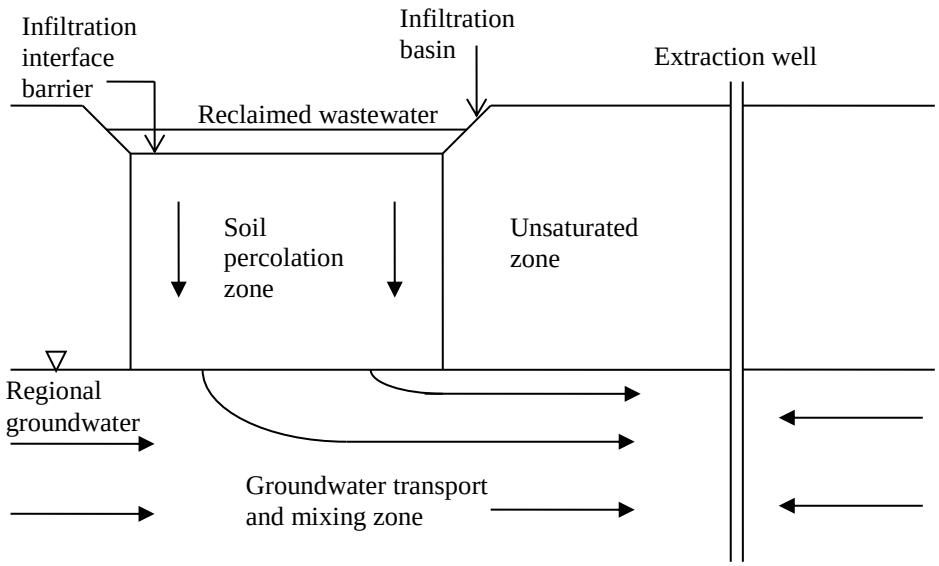

Figure 1.1 Schematic diagram of soil aquifer treatment

[Reproduced from Fox et al, 2006]

Concerns however exist over environmental and human health risks posed by the presence of persistent chemicals in wastewater effluents undergoing SAT. Some of these trace compounds are able to cause endocrine disruption in mammals in contact with it, and in recent years emerging contaminants such as Pharmaceuticals and Personal Care Products (PPCPs) (Coogan et al., 2007) as well as estrogens have become an issue of major concern. One such PPCP is 3, 4, 4´-trichlorocarbanilide, more commonly known as triclocarban (TCC). TCC (CAS registry number: 101-20-2) is a high production volume antimicrobial agent widely used in the formulation of personal care products especially antimicrobial soaps since the mid-20th century (TCC-Consortium, 2002; Heidler et al., 2006; Coogan et al., 2007; Cha and Cupples, 2009; Chalew and Halden, 2009). It is added for its germicidal properties and typical concentration in antimicrobial soaps is 2 % by weight (Chalew and Halden, 2009). As soaps and other personal care products are used atopically, TCC easily finds its way into the wastewater treatment system and associated aquatic environments (Miller et al., 2010). TCC is incompletely removed during conventional wastewater treatment and is disposed of with the wastewater effluent (Heidler et al., 2006). As such, TCC has now developed into one of the most persistent and commonly detected PPCPs in aquatic systems (Heidler and Halden, 2009).

Estrogens are also encountered in wastewater treatment and include the natural estrogens, estrone (E1), 17β-estradiol (E2), estriol (E3), and 17α-estradiol (17α) (Mansell and Drewes, 2004) and the synthetic estrogen 17α-ethinylestradiol (EE2). The natural estrogens are synthesised from cholesterol in the human body (Yen et al., 1999) and are responsible for the development of the female reproductive system (Mansell and Drewes, 2004) whilst EE2 is industrially synthesised from E2 and is

the active ingredient in oral contraceptive pills (Khanal et al., 2006; Combalbert and Hernandez-Raquet, 2010). These estrogens find their way into the wastewater treatment system via their excretion with urine and faeces. Trace amounts of estrogens, especially EE2, (even in the ng L^{-1} range of concentrations) are able to cause endocrine disruption in aquatic species in contact with them (Purdom et al., 1994).

Due to the endocrine disrupting nature of these estrogens as well as triclocarban, and since they are not parameters routinely tested for in wastewater treatment plant effluents, their behaviour during SAT needs to be well investigated in order to curtail groundwater pollution. Hitherto, the removal of triclocarban during soil aquifer treatment has not been studied and it is currently not known what effects this antimicrobial agent has on SAT.

Although quite a number of SAT systems exist, most of them employ well treated secondary effluents from conventional wastewater treatment or tertiary effluents. Therefore little work has been done to demonstrate the applicability of SAT in treating poorly treated effluents, effluent from waste stabilization ponds or even primary effluents. In addition, SAT has always involved wastewater infiltrating through an unsaturated soil zone before reaching the groundwater, and a minimum depth of 3 m to groundwater is usually recommended (Tchobanoglous et al., 1999) to safeguard the quality of the underlying aquifer. The unsaturated zone promotes biological activity for the removal of wastewater contaminants such as organic matter and also promotes nitrification due to its conduciveness for re-aeration mechanisms to occur, which ensure the continuous availability of dissolved oxygen

in this zone. The use of SAT in very shallow aquifers has therefore not been well explored. This research therefore focuses on the use of wastewater of much higher organic matter concentration (representing poorly treated effluents) than usually infiltrated in SAT systems and the removal of wastewater contaminants in a saturated system simulating a SAT system by-passing the unsaturated zone in view of the capability of infiltrating water during SAT to flow through preferential flow paths thereby avoiding effective contact with the unsaturated soil matrix (Tchobanoglous et al., 2003).

1.2 Research Objectives

The main aims of this study are therefore:

1. To evaluate the performance of SAT under unsaturated and/or saturated soil conditions for the treatment of wastewater of much higher concentrations than that which is normally encountered in SAT systems, simulating poorly treated secondary effluents, and
2. To investigate its potential for the removal of the endocrine disrupting compounds triclocarban and estrogens.

Specifically the objectives of this research are:

i. To study the removal of Chemical Oxygen Demand (COD), Biochemical Oxygen Demand (BOD), Dissolved Organic Carbon (DOC), nitrogen and phosphate during simulated SAT under different loading regimes (hydraulic and organic) using laboratory soil columns and synthetic wastewater under saturated conditions;

ii. To assess the removal of the estrogens E1, E2 and EE2 during SAT and the influence of wastewater hydraulic loading rates, organic carbon and soil properties on their removal efficiency under saturated conditions;

iii. To determine the impact of the height of groundwater table on the removal of E1, E2 and EE2. This would be investigated under unsaturated soil conditions;

iv. To study the removal of triclocarban in the saturated zone during SAT and the effects of TCC, which is an antimicrobial agent, on the performance of the SAT system;

v. To develop models for TCC and estrogen removal in the soil columns and also to model chemical oxygen demand removal based on the advection-dispersion equation.

1.3 Justification for Study

Although 75% of the world's land surface is covered with water, drinking water sources are not unlimited. Only about 0.62 % of the total volume of water is found in fresh water lakes, rivers and streams, and groundwater supplies, and is available for general livelihood and agricultural activities (Peavy et al., 1985). A greater proportion of the water consumed ultimately becomes wastewater and in the United States for example, it is estimated that about 60 % to 90 % of water demand is returned as wastewater (Tchobanoglous et al., 2003). To maintain a healthy environment and prevent outbreaks of disease, wastewater that is generated needs to be collected and appropriately treated to prescribed effluent standards before discharge into the environment. As the ultimate discharge point is a receiving water body, the wastewater needs to be treated to such a degree as to avoid pollution of the

receiving water body. These water bodies usually serve as a source of drinking water for people downstream and also a habitat for aquatic organisms. It is desirable that a high degree of treatment is attainable at the lowest possible cost, and this goal should be pursued. With fresh water sources very vulnerable to pollution, the limited surface water resources may dwindle in quality and quantity leading in the long term to fresh water shortages and the need for new water supply sources. Treated wastewater could be reclaimed and stored underground for future potable and non-potable uses. This makes studies into the use of SAT systems very important. Some of the immediate reasons include the following:

i. As there are high evaporation losses from surface storage reservoirs due to high ambient temperatures, the added benefit of aquifer recharge from SAT systems would store water underground, protected from evaporation losses and recontamination. This is important in view of expected population increases and resulting pressure on water resources for human consumption and industrial and agricultural use.
ii. SAT opens up the possibility of indirect potable water reuse.
iii. Increased base flow to rivers and streams from recharged aquifers would improve stream flow.
iv. Wastewater effluents have become the main source of estrogens in the environment due to their incomplete removal during conventional wastewater treatment (Allinson et al., 2010).
v. Although TCC has been in use for a long time it has been overlooked as a toxic environmental contaminant (Halden and Paull, 2005) and not much work has been done on its fate in the environment (Sapkota et al., 2007) and in indirect water reuse facilities (Ternes et al., 2007) nor on techniques such

as SAT for its removal from wastewater. Some studies have been carried out in the area of assessing the contamination posed by land application of TCC containing wastewater sludge to groundwater, by studying at its fate in soil. However the disposal of the accompanying liquid fraction via land disposal methods such as wastewater effluent irrigation practices or soil infiltration have not been studied much and in fact no studies have been carried out on the fate of TCC during soil aquifer treatment.

Studies under saturated soil conditions are necessary because as opposed to the unsaturated zone, groundwater environments are inclined to being devoid of dissolved oxygen due to non-replenishment of consumed oxygen during hydro chemical and biochemical reactions, as a result of no contact existing between the circulating groundwater and the atmosphere (Freeze and Cherry, 1979). Due to low oxygen water solubility, which ranges from 9 mg L^{-1} at 25 °C to 11 mg L^{-1} at 5 °C, even low concentrations of organic matter in groundwater can cause depletion of all the dissolved oxygen (Freeze and Cherry, 1979), which could impact negatively on the treatment process.

1.4 Scope of Research

Soil aquifer treatment would be simulated in the laboratory under unsaturated and saturated conditions in soil columns to simulate infiltration through the unsaturated (vadose) zone and the saturated zone (aquifer), respectively. The study will highlight further treatment of poor quality wastewater effluents using synthetic wastewater. Synthetic wastewater to be used would therefore be prepared to have much higher COD than effluents normally infiltrated in SAT systems.

Since the focus is on high COD effluents and high groundwater tables, COD modelling would entail the fitting of laboratory data obtained by infiltrating high COD wastewater through a saturated soil column, to the advection dispersion equation to obtain kinetic constants. Triclocarban and estrogen modelling would involve the development of empirical equations to suitably describe the removal process in the soil column. The purpose of the model development is to mathematically describe the treatment processes in the soil columns and to provide insight into the parameters and conditions influencing treatment for predictions to be made about removal efficiencies of the wastewater contaminants studied. Field testing of the models would however not be carried out and therefore the models would not be developed to the extent suitable for direct application under field conditions.

1.5 Organization of Thesis

This thesis is organized as follows:

A general introduction and brief description of soil aquifer treatment, as well as the research objectives and justification for the study undertaken are given in Chapter 1. Chapter 2 reviews existing literature on soil aquifer treatment, the estrogens E1, E2 and EE2 and triclocarban, and Chapter 3 presents the materials and laboratory methods employed to meet the set objectives. These include soil column setups, experimental protocols, instrumentation and analytical methods employed. The results on the removal of the aforementioned wastewater parameters and endocrine disruptors are presented and discussed in Chapter 4, followed by models developed for their removal in Chapter 5. Chapter 6 gives the derived conclusions from the

study as well as recommendations for further research. These are followed by the references used and appendices.

CHAPTER 2

2 LITERATURE REVIEW

2.1 Introduction

Water management practices are increasingly becoming an issue of major concern as fresh water resources are dwindling. To reduce the effects of pollution on our water bodies, the wastewater generated needs to be treated and the effluents properly disposed of. Effluents from treatment plants are usually disposed of into surface water bodies but they could also be used to recharge groundwater resources if properly handled. In cases where there are negative public perceptions about direct-treated wastewater reuse for potable or non-potable uses, aquifer recharge with treated wastewater would generally be more acceptable (Bouwer, 2002) because the water would be more associated with a natural source rather than with wastewater (Fox et al., 2006).

2.2 Contaminants of Concern in Wastewater Treatment

Wastewater contains a wide variety of contaminants that have the potential to pollute environmental resources especially water bodies. The composition and concentration varies according to the characteristics of the community generating the wastewater. Suspended solids are of concern as they tend to form sludge deposits and anaerobic conditions when they are discharged into water bodies. Biodegradable organics deplete dissolved oxygen during stabilisation of the organic matter by microorganisms. Septic conditions arise when all the oxygen has been consumed. The presence of the nutrients – nitrogen and phosphorus in discharged wastewater

can lead to eutrophication in surface water bodies and groundwater pollution. Priority pollutants such as arsenic, lead, mercury, benzene may have toxic, carcinogenic, mutagenic, and teratogenic effects. Heavy metals from commerce and industry and dissolved inorganics such as calcium, sodium and sulphate imparted from domestic water use have to be removed before wastewater can be reused. Refractory organics tend to persist even after conventional treatment and thus are of major concern. Besides, pathogens present in wastewater are responsible for the transmission of communicable diseases to those who come into contact with the water (Tchobanoglous et al., 2003).

2.3 Soil Aquifer Treatment

Soil Aquifer Treatment (SAT) is an inexpensive, low-technology (Bouwer, 2000) wastewater treatment and reclamation option, able to generate high quality effluent from secondary treated wastewater for potable and non-potable uses (Cha et al., 2006; Fox et al., 2006). SAT is usually applied for final polishing of secondary treated effluents with the intention of replenishing groundwater reserves (Droste, 1997). During SAT, the saturated and unsaturated zones of the soil act as the medium in which physicochemical and biological reactions occur (Cha et al., 2006), substantially reducing effluent parameters such as biochemical oxygen demand (BOD), total suspended solids (TSS) and pathogens to levels that even allow the use of the water for unrestricted irrigation (Bdour et al., 2009). SAT is also effective at removing nutrients (nitrogen and phosphorus) and trace metals (Kopchynski et al., 1996). Mixing of the infiltrated wastewater with the groundwater and the slow movement through the aquifer increases the contact time with the aquifer material leading to further purification of the water (Asano and Cotruvo, 2004; Dillon et al.,

2006). Thus under favourable soil and groundwater conditions for artificial groundwater recharge, partially treated wastewater can be highly upgraded by intermittently spreading the water in infiltration basins to allow its percolation through the soil and to the groundwater (Pescod, 1992; Tchobanoglous et al., 2003; Asano and Cotruvo, 2004).

While SAT has many positive attributes, there however still exists a potential for undesirable contamination of aquifers by pathogens, pharmaceuticals and other organic wastewater contaminants during SAT and this could be a great source of concern especially in arid and semi-arid areas where ground water is the only available source of drinking water (Cordy et al., 2004). In recent years, evidence has emerged on the limitations of SAT in the removal of polar and persistent emerging pollutants (Yu et al., 2009). Ethylenediaminetetraacetic acid (EDTA), x-ray contrast residuals (organic iodine) the antiepileptics primidone (Fox et al., 2006) and carbamazepine (Fox et al., 2006; Arye et al., 2011) are examples of compounds found to persist in SAT product waters. Artificial sweeteners have also been shown to persist during SAT (Scheurer et al., 2009). Besides these, SAT poses the risk of contamination of underlying aquifers with nitrates, which could cause methemoglobinemia in infants when ingested (Fryar et al., 2000). Nitrates are formed mainly in the unsaturated zone, by the nitrification process for oxidation of adsorbed wastewater ammonium ions in soil. Table 2.1 gives the characteristics of SAT systems.

Table 2.1 Characteristics of SAT systems

Characteristic	**Value**
Hydraulic application rate, m yr^{-1}	6 – 125
Soil permeability, cm h^{-1}	> 1
Soil type	Sand, sandy loam, loamy sand, gravels
Minimum pre-treatment	Primary
BOD_5 loading, kg ha^{-1} yr^{-1}	8,000 – 46,000
Depth to groundwater	3m; lesser depth acceptable where under drainage is provided
Application method	Surface
Land slope suitability	
0 – 12 %	High
12 – 20 %	Low
> 20 %	Do not use
Land use suitability	
Open or cropland	High
Partially forested	Moderate
Heavily forested	Low
Developed (residential, commercial or industrial)	Very low

(USEPA, 1981; Reed et al., 1988; Tchobanoglous et al., 1999)

Besides treatment, SAT offers the opportunity of aquifer recharge, thus operating as a system for seasonal and longer-term storage of water (Fox et al., 2006). The advantages offered by SAT over the use of surface water as discharge points and reservoirs include:

i. The low cost of storing water by artificial recharge compared to that of equivalent surface reservoirs;
ii. The existence of the aquifer's natural underground distribution system, which means surface pipelines or canals may not be needed for water transport;
iii. No constraints by site availability on water storage. In urban areas for example, the construction of surface reservoirs may be restricted because suitable sites may be unavailable or environmentally unacceptable (Tchobanoglous et al., 2003; Dillon et al., 2006);
iv. Natural protection of underground reservoirs from evaporation. Storage of water for seasonal or longer-term use can be accomplished without evaporation losses and associated salinity increases in the reservoir (Dillon et al., 2006; Fox et al., 2006);
v. Protection of groundwater from pollution and recontamination with coliforms and parasites by birds, mammals and humans (Fox et al., 2006);
vi. Exclusion of sunlight from the water which prevents the growth of algae and so eliminates the formation of water quality problems such as algae-derived taste and odour and the formation of disinfection by-products (Fox et al., 2006). Problems resulting from the growth of toxic cyanobacteria are also eliminated as the bacteria cannot grow in underground reservoirs.

Besides the above-mentioned advantages, aquifer recharge with wastewater before reuse also offers additional water quality benefits due to the additional treatment that occurs in the soil and aquifer. The recovered water from the wells is clear and free from odour (Fox et al., 2001). Public confidence in water recycling projects also increases when the reclaimed water is put back into natural systems such as streams and aquifers before recovery (Rowe, 1995; Dillon et al., 2006). The recycled water is

perceived as groundwater which is aesthetically superior and more acceptable to the public as a source of water (Fox et al., 2006).

Even though water generated from SAT is of much higher quality than the influent wastewater, it is of inferior quality to the native groundwater. It is therefore prudent that the SAT system is designed and managed such that mixing with the native groundwater is restricted and only a portion of the aquifer is used (Asano and Cotruvo, 2004; Dillon et al., 2006).

2.3.1 Pre-treatment of Wastewater for SAT Systems

Before application of wastewater to a SAT system, some form of pre-treatment is required. The type of pre-treatment needed for effluents to be applied in SAT systems depends on the characteristics of wastewater to be applied, the properties of the soil and aquifer, the final endpoint of the groundwater and the use to which the recovered groundwater would be put (NRC, 1994). Pre-application treatment for municipal sewage may be primary treatment, dissolved air flotation or treatment in waste stabilization ponds. Little work has however been done to demonstrate their applicability (Tchobanoglous et al., 2003; Asano and Cotruvo, 2004). Pre-treatment processes that generate effluents with high algal content are not very suitable for SAT systems because the algal cells could lead to severe clogging of infiltration basins (Asano and Cotruvo, 2004). The level of pre-treatment however does not have a major impact on the efficiency of aerobic biological reactions (Kopchynski et al., 1996).

2.3.1.1 Characteristics of Applied Wastewater

The most important effluent quality parameter is suspended solids as these tend to settle out of the effluent in the infiltration basins or are filtered out and accumulated at a short distance below the soil water interface, thereby reducing the permeability of the soil and retarding water movement into the subsurface. Other quality parameters of concern are total dissolved solids, the concentration of nutrients that stimulate biological growth and the concentration of calcium, magnesium and sodium which dictate the sodium absorption ratio of the soil. If the recharge water has a higher sodium absorption ratio than the native water, swelling and deflocculation of clay minerals contained in the aquifer can occur leading to lowered infiltration rates. Carbonates, phosphates and iron oxides in the recharge water can react with the native groundwater to form precipitates which can clog the pores in the soil. SAT systems can be effectively operated over a wide range of water quality. Higher quality effluents however allow higher infiltration rates to occur (NRC, 1994). Incompatible wastewaters such as industrial effluents from chemical industries, and containing heavy metals should be excluded from SAT systems (Tchobanoglous et al., 2003).

2.3.1.2 Soil and Aquifer Properties

The soil properties of importance in a SAT system are the soil's texture, permeability and the presence of organic matter, clay, iron or hardpan in the soil. The depth and compaction characteristics of the soil profile are also important considerations (NRC, 1994). The ideal soil for a SAT system is one that delivers high infiltration rates, which can be obtained from soils of coarse texture, while achieving efficient contaminant adsorption and removal, which on the other hand can be obtained more

from soils of fine texture (NRC, 1994). Due to the large pores in coarse textured soils they are inefficient in filtering out contaminants. The solid surfaces adjacent to the main flow paths are also relatively non-reactive thereby allowing high passage of contaminants. Soils which are structured with cracks or channels have large flow paths that allow the easy movement of material along these lines thereby bypassing a great proportion of the soil matrix. Fine textured soils though highly efficient in contaminant removal offer the disadvantage of low permeability and easy clogging of the pores. Fine sand, loamy sand or sandy loam with little structure is therefore a suitable soil option for SAT (Bouwer, 1985; Pescod, 1992).

Several studies have investigated the fate of organic and inorganic compounds during SAT. However only a few studies have focused on the characteristics of soil, which might influence the water quality of SAT treated effluents (Cha et al., 2006). Kopchynski et al., (1996) studied the effects of soil type and effluent pre-treatment on SAT. Quanrud et al., (1996a) also studied the effect of soil type on water quality improvement during soil aquifer treatment. Kopchinsky et al., (1996) found out that high infiltration rates can be maintained through porous sands, with high conversion efficiencies of substrates that can be aerobically biodegraded. The latter study revealed that during SAT great differences do not exist in the removal efficiency of organics between soils of different characteristics.

2.3.1.3 Uses of Recovered Groundwater

SAT systems may be designed for any of the following purposes:

i. Treatment followed by groundwater recharge to supplement water supplies or for the prevention of intrusion of salt-water particularly in coastal areas;
ii. Treatment followed by recovery of the water using under-drains or pumped withdrawal (wells), for irrigation or some other use;
iii. Treatment followed by groundwater flow and subsequent discharge into surface waters (Tchobanoglous et al., 2003).

Where the objective of the SAT system is for augmentation of existing water supply, wastewater would have to be treated to a very high quality before application to the system. A conservative approach follows the assumption that the soil and aquifer provide no treatment during passage of the effluent to the withdrawal point and thus the pre-treatment stage should bring the water to the level of quality acceptable for use. Adopting this approach is very expensive and opportunity should therefore be taken of the treatment offered by SAT (NRC, 1994). Typical methods for the recovery of the renovated water (Bouwer, 1991) are shown in Figure 2.1.

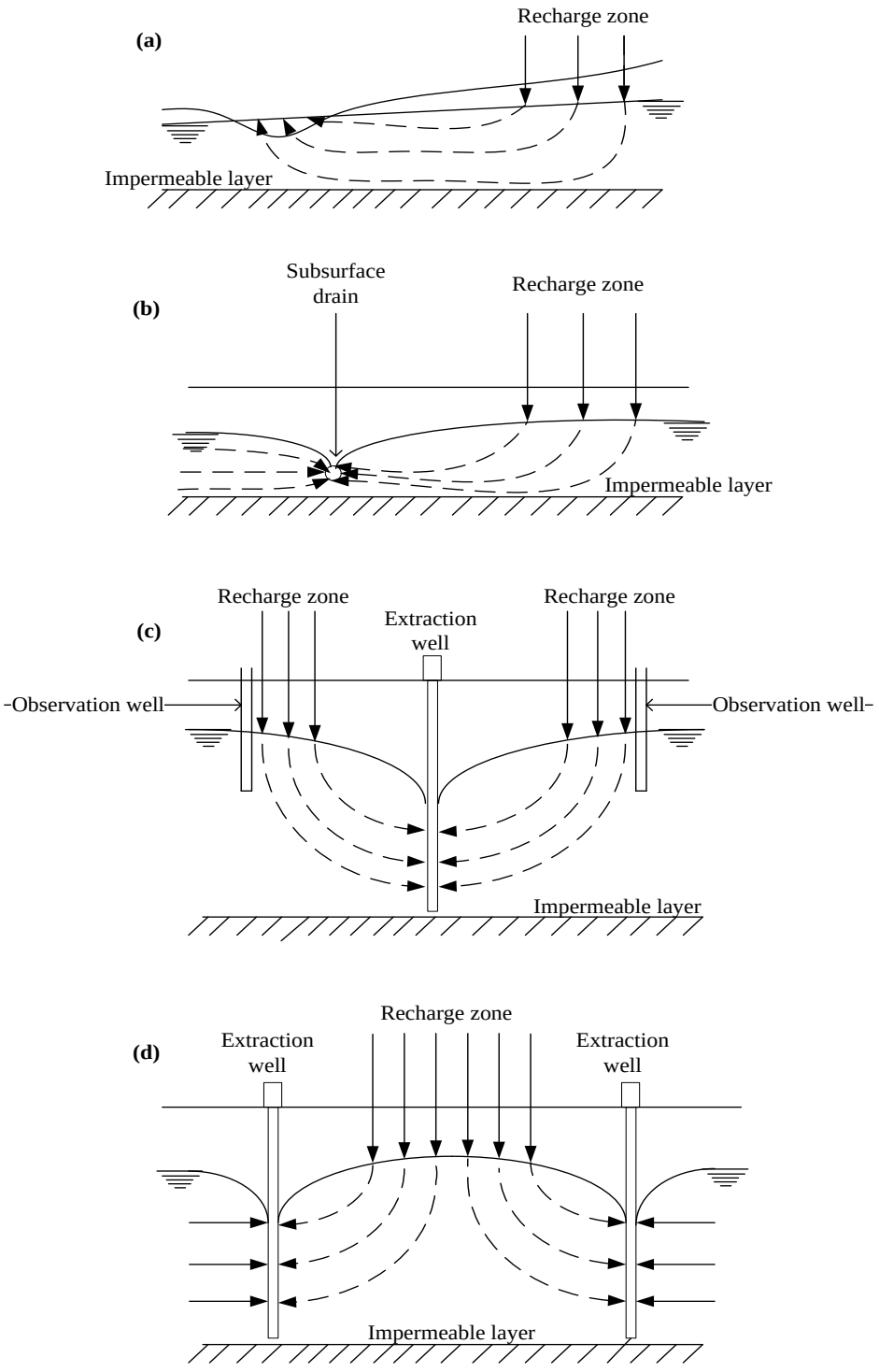

Figure 2.1 Schematic diagrams of soil aquifer treatment systems with recovery of renovated water

Discharge into: (a) a surface water body, (b) subsurface drains, (c) wells surrounding the basins, and (d) wells midway between parallel strips of basins.

[Reproduced from Bouwer, 1991]

2.4 Mass Transport and Transformation Processes

Pollutants are transported in the subsurface environment by three basic physical mechanisms. These are advection, diffusion and mechanical dispersion (Charbeneau, 2000). The concentration of the pollutants at any point and time *C(x, t)* is also influenced by adsorption and reaction (Charbeneau, 2000; Fetter, 2001). The basic equation governing the transport of pollutants is the conservation of mass equation (Bear, 1972; Freeze and Cherry, 1979; Domenico and Schwartz, 1998; Charbeneau, 2000) which states that, *"the rate of increase within the region is equal to the net mass flux into the region plus the increase in mass within the region due to biotic and abiotic processes"* (Charbeneau, 2000).

The important fate and transport processes that occur in the vadose zone can be summarised as:

i. Processes that cause losses: these are biological, chemical and photochemical degradation and volatilization;
ii. Processes that cause retardation: immobilization, sorption, ion exchange;
iii. Processes that affect mass transport: advection, diffusion and dispersion, residual saturation, preferential flow.

These processes determine the time and distance of travel and reduction in the levels of contaminants that occur as the effluent percolates the soil and moves down to the groundwater (Charbeneau, 2000). Figure 2.2 depicts the processes occurring in SAT (Charbeneau, 2000).

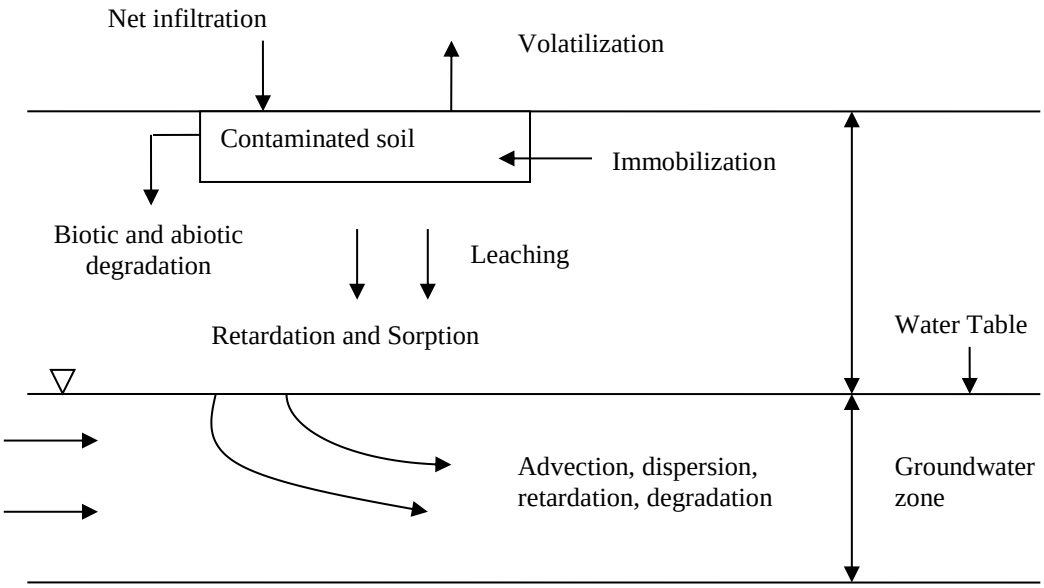

Figure 2.2 Processes affecting the movement and fate of contaminants in the subsurface environment

[Reproduced from Charbeneau, 2000]

The availability of adequate quantities of biodegradable organic carbon is necessary for the maintenance of biological and geochemical processes in the subsurface (Grischek et al., 1998; Aiken, 2002; Amiri et al., 2005). As bioavailable organic carbon in effluents limits soil biomass growth, the microorganisms in the soil are able to maintain a certain steady-state amount of viable soil biomass (Shackle et al., 2000).

2.4.1 Advective Transport

Advective transport or convection is the movement of a mass as it is carried along with the movement of the bulk fluid (Fetter, 1999; Charbeneau, 2000). Advection occurs as a result of head differences in the soil profile (Yong et al., 1992). Different species in the water are transported along with the flow of the water in the form of a

solute or suspension. Advection has the greatest influence in the mass transport process (Charbeneau, 2000). The bulk transport of the mass is proportional to the soil's hydraulic conductivity, the energy gradient and the local concentration. For a chemical present in an aqueous solution the one-dimensional advective mass flux, F_x ($MT^{-1}L^{-2}$), is given by:

$$F_x = v_x n_e C \quad \text{.....[2.1]}$$

where n_e is the effective porosity and C is the concentration of the solute (ML^{-3}). v_x is the average linear velocity (LT^{-1}), which is the rate at which the flux of water across the unit cross-sectional area of pore space occurs and is defined by:

$$v_x = \frac{K_s}{n_e}\frac{dh}{dl} \quad \text{.....[2.2]}$$

where K_s is the hydraulic conductivity (LT^{-1}) and $\frac{dh}{dl}$ is the hydraulic gradient (LL^{-1}) (Fetter, 1999).

2.4.2 Diffusive Transport

Diffusion is a mass transport process in which there are random molecular motions in a field where a concentration gradient is present (Charbeneau, 2000). There is therefore a net movement of the species under consideration from a region of higher concentration to one of lower concentration (Fetter, 1999; Charbeneau, 2000). Provided a concentration gradient exists diffusion will continue to take place even if the fluid is stationary (Fetter, 1999). In relation to advection, molecular diffusion occurs slowly (Logan, 1999) and causes mass transport over small distances especially in liquids. It is an important process during transport through soils of low permeability and volatilization of chemicals through soil and air. It also plays a role in the fate of non-aqueous phase liquids trapped in fractures and serves as a rate

limiting step in sorption of chemicals (Charbeneau, 2000). According to Fick's first law of diffusion, the diffusion mass flux is proportional to the concentration gradient and is given by:

$$F_d = - D_d \frac{dC}{dx} \quad \text{.....[2.3]}$$

where:

F_d = mass flux of solute per unit area per unit time ($ML^{-2}T^{-1}$)

D_d = diffusion coefficient (L^2T^{-1})

C = solute concentration (ML^{-3})

$\frac{dC}{dx}$ = concentration gradient ($ML^{-3}L^{-1}$)

Fick's second law gives the equation for diffusion in porous media where the concentration changes with time as:

$$\frac{\partial C}{\partial t} = D_d \frac{\partial^2 C}{\partial x^2} \quad \text{.....[2.4]}$$

where $\frac{\partial C}{\partial t}$ is the change in concentration with time ($ML^{-3}T^{-1}$).

As a result of the longer flow paths that have to be followed by the compounds in a solution flowing through a porous medium, diffusion is much slower and so is accounted for by applying another coefficient, ω, which is related to the tortuosity, to the diffusion coefficient. This gives rise to an effective diffusion coefficient, D^* (L^2T^{-1}) defined as:

$$D^* = \omega D_d \quad \text{.....[2.5]}$$

which replaces the diffusion coefficient D_d in Equation 2.4. The value of ω can be determined experimentally by conducting diffusion experiments where a solute is allowed to diffuse across a porous medium (Fetter, 1999).

2.4.3 Mechanical Dispersion and Hydrodynamic Dispersion

Mechanical dispersion is the transport of a solute relative to the bulk water movement that occurs when a concentration gradient exists and fluid particles that were once together move apart. The separation occurs because:

i. The fluid particles close to the walls of the pore channels tend to move more slowly than those nearer the centre;

ii. The differences in the dimensions of pores along the pore axes cause particle movement at different relative speeds;

iii. Adjacent particles moving in one channel can follow different streamlines thus crossing over into another channel and therefore travelling along longer paths (Fetter, 1999; Charbeneau, 2000);

iv. Variations in hydraulic conductivity of the medium cause solute molecules to move at different speeds even when uniform hydraulic gradient exists (Charbeneau, 2000).

The first three effects occur on a pore scale and are represented schematically in Figure 2.3 (Fetter, 2001).

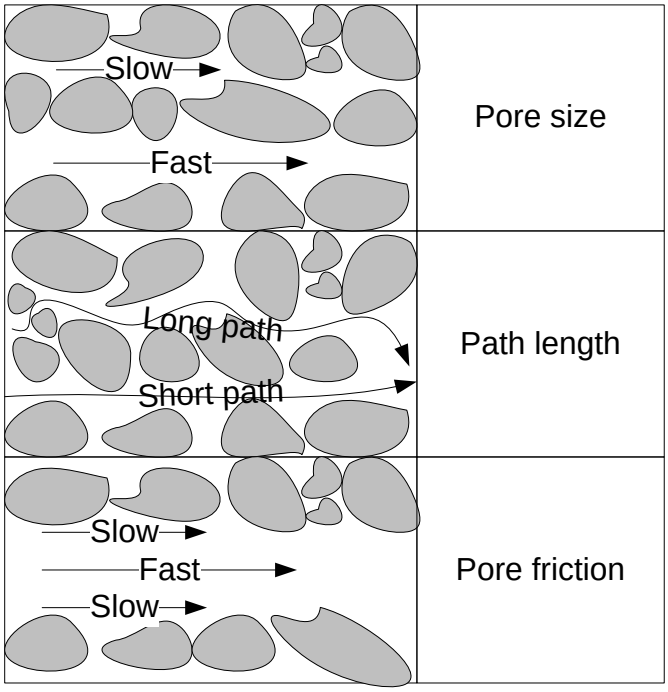

Figure 2.3 Schematic representation of factors causing pore-scale longitudinal dispersion

[Reproduced from Fetter, 2001]

Mixing of the solute with the ground water occurs along the direction of flow (longitudinal dispersion) and normal to the direction of flow (transverse dispersion) as the separation occurs. Describing mechanical dispersion in the principal direction of flow (longitudinal direction) by Fick's law and the amount of mechanical dispersion as a function of the average linear velocity, the coefficient of longitudinal mechanical dispersion, D_m (L^2T^{-1}) would be given by:

$$D_m = \alpha_i \, v_i \text{ …….. [2.6]}$$

where:

v_i = average linear velocity in the *i* direction (LT^{-1})

α_i = dynamic dispersivity in the *i* direction (L)

In ground water flow molecular diffusion and mechanical dispersion cannot be separated and are combined to obtain the hydrodynamic dispersion coefficient, D_L. Hence

$$D_L = \alpha_L v_i + D^* \quad \text{.....[2.7]}$$

where:

D_L = hydrodynamic dispersion coefficient parallel to the principal direction of flow i.e. longitudinal (L^2T^{-1})

α_L = longitudinal dynamic dispersivity (L) (Fetter, 1999)

2.4.4 The Sorption Process

Many chemical constituents tend to attach or sorb to the soil matrix (Charbeneau, 2000). Sorption is a collective term for the processes of adsorption, absorption, chemisorption and ion exchange (Fetter, 1999). In adsorption, the solute attaches to the surface of the solid particles whilst in absorption the solute particles diffuse into the soil particles due to their high porosity and are sorbed inside the particles. When a chemical reaction causes incorporation of the solute on the surface of a sediment, soil or rock by a chemical reaction, chemisorption is said to occur. Ion exchange occurs when cations in the solution are attracted to and held by electrostatic forces to the region close to a negatively charged clay mineral surface or anions are attracted to positively charged sites on broken edges of clay minerals or iron and aluminium oxides (Fetter, 1999). One chemical is then replaced with another on the surface of the soil (Appelo and Postma, 1994). These sorption processes are depicted in Figure 2.4 (Appelo and Postma, 1994).

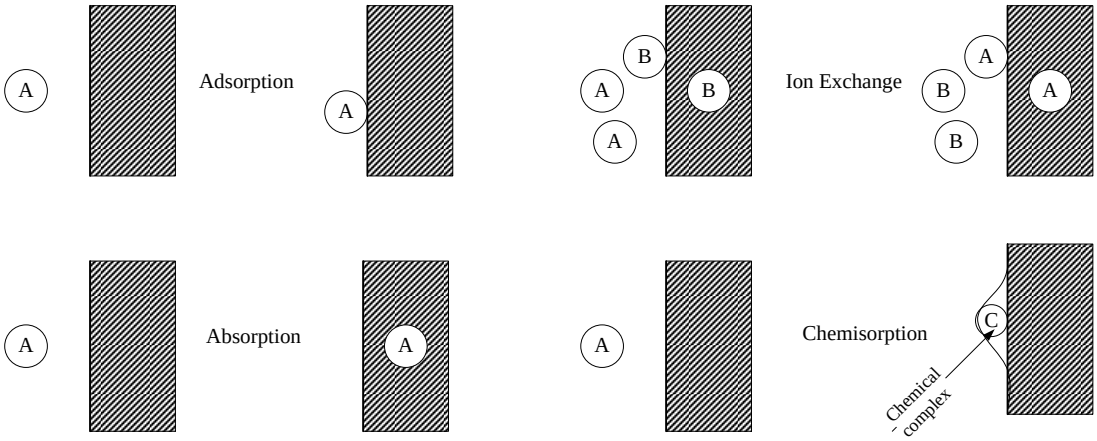

Figure 2.4 Schematic representation of sorption processes

[Reproduced from Appelo and Postma, 1994]

The concentration of the constituent in the liquid and solid phase (sorbed concentration) at equilibrium depends on its adsorption isotherm (Tchobanoglous et al., 2003). Adsorption isotherms describe the relationship between the sorbed mass and that remaining in the liquid phase. The most common adsorption isotherms are the Freundlich and the Langmuir isotherms (Domenico and Schwartz, 1998). Environmental concentrations are usually small enough to allow the use of a linear isotherm (Tchobanoglous et al., 1999), the simplest and most useful of which is the linear Freundlich isotherm (Domenico and Schwartz, 1998). This is given by:

$$S = K_d\, C \quad \text{.....[2.8]}$$

where:

S = mass of constituent sorbed per unit mass of solid (MM^{-1})

C = concentration of constituent in liquid (ML^{-3})

K_d = distribution coefficient (L^3M^{-1})

The rate of the sorption reactions at equilibrium may be expressed as:

$$r = \frac{\partial S}{\partial t} = K_d \frac{\partial C}{\partial t} \quad \text{.....[2.9]}$$

where *S* is the solid phase concentration of the sorbed mass (Tchobanoglous et al., 2003).

2.4.5 The Biodegradation Process

Biodegradation is an important process in SAT which brings about the breakdown of organic chemicals in soils by the action of microorganisms naturally present in the soil or introduced through engineered systems (Charbeneau, 2000). The microorganisms found in biological wastewater treatment systems include bacteria, algae, protozoa, viruses and fungi (Tchobanoglous et al., 2003), bacteria being the most predominant microbial species involved in the stabilisation of organic matter (Gray, 2004) and also the most important microorganisms in the groundwater environment for the catalysis of oxidation reduction processes (Freeze and Cherry, 1979). Some of the factors controlling the rate of biodegradation are:

i. The number and type of microorganisms present;
ii. The water solubility and toxicity of the organic chemical or its products to the microorganisms;
iii. The water content, pH and temperature of the soil;
iv. The presence of other nutrients necessary for microbial metabolism (Charbeneau, 2000);
v. The presence of electron acceptors such as oxygen (O_2), nitrate (NO_3), sulphate (SO_4) (Bitton, 1999), iron (III) hydroxide ($Fe(OH)_3$), manganese dioxide (MnO_2) and other oxidised organic compounds (Freeze and Cherry, 1979), and the oxidation-reduction potential (Charbeneau, 2000).

Microbial metabolism mechanisms that occur during stabilisation of the wastewater involve catabolic reactions which are exergonic and therefore release energy as well as anabolic reactions, which on the other hand are endergonic and use up the energy and chemical intermediates generated by catabolic reactions (Bitton, 1999). Bacteria possess an electron transport system (ETS) located within their cytoplasmic membrane, through which electrons are transported from an electron donor such as organic and inorganic compounds carried through a series of complex biochemical pathways to the final or terminal electron acceptor (TEA) (Bitton, 1999). During biological oxidation, energy stored in organic matter is released by dehydrogenation of the substrate (Gray, 2004). The energy produced in this catabolic reaction is transferred to compounds like adenosine triphosphate (ATP) which is a high energy phosphorylated compound. ATP consists of adenine, ribose which is a sugar composed of five carbons, three phosphates and two bonds which are high in energy. These high-energy bonds are able to release 7 500 calories of chemical energy upon hydrolysis of each ATP molecule to adenosine diphosphate (ADP). Some of this energy is used in anabolic reactions for the biosynthesis of new microbial cells and their growth and also for the maintenance of cells. Some of it is also used for movement, active transport or dissipated as heat (Bitton, 1999).

The order of preference of use of TEA is based on the highest free energy released per mole of substrate by the electron acceptor during microbial respiration (Bitton, 1999; Gray, 2004). The amount of adenosine triphosphate (ATP) formed during aerobic oxidative phosphorylation depends on the difference between the electron donor and electron acceptor redox potentials ($\Delta E_0'$) (Gray, 2004). Oxidation reduction reactions could be represented as occurring in an electron tower

comprising a range of reduction potentials for redox couples normally involved in biological reactions. Redox couples with more electronegative reduction potentials (E_0') are located at the top of the tower, whilst those with the highest positive reduction potentials are situated at the bottom. Electrons are donated from the top of the tower and accepted at various lower levels in the tower (Madigan and Martinko, 2006). Figure 2.5 shows the positions of sulphate, nitrate and oxygen redox couples in the electron tower, as well as the electrons accepted. As oxygen is situated at the lowest position in the electron tower it has the most positive reduction potential meaning the greatest tendency for accepting electrons than the other electron acceptors (Madigan and Martinko, 2006), and thus more ATP is released (Bitton, 1999).

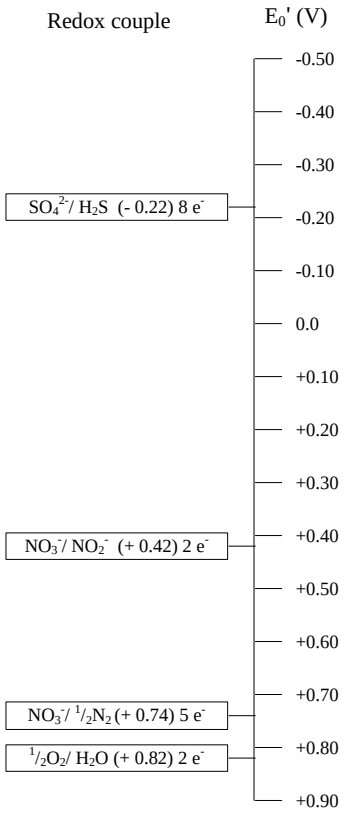

Figure 2.5 Electron tower showing positions of sulphate, nitrate and oxygen [Reproduced from Madigan and Martinko, 2006]

Free energy released (ΔG°) per electron equivalent are -78.14, -71.67 and 21.27 kJ for oxygen, nitrate and sulphate respectively (Tchobanoglous et al., 2003). Greater microbial assimilation of organic carbon as cell material thus results from the greater energy utilisation. In mixed microbial cultures, the microorganisms pursue the route with the highest energy yield so as to attain maximum cell synthesis. Aerobic and facultative bacteria first oxidise organics in the wastewater, depleting the dissolved oxygen. After the oxygen is used up, facultative and anaerobic bacteria utilize oxygen bound in nitrates and sulphates for the breakdown of any remaining organic matter (Gray, 2004). The biodegradation processes involving the use of oxygen, nitrate and sulphate are respectively known as aerobic oxidation, dissimilatory nitrate reduction (denitrification) and dissimilatory sulphate reduction (Bitton, 1999).

During biodegradation, oxygen competes with nitrate and sulphate as the final electron acceptor. This however does not preclude the occurrence of denitrification and sulphate reduction in cases where there are relatively high oxygen concentrations existing in the bulk wastewater. Denitrification processes and sulphate reduction have also been observed to occur in aerobic wastewater treatment processes such as in the biofilms of trickling filters (Bitton, 1999).

2.4.5.1 Aerobic Oxidation

Aerobic biodegradation of organic matter is fast, more complete and yields stable end products (Pescod, 1992) and is therefore the preferred route for biodegradation in many cases.

The biodegradation of wastewater represented by glucose proceeds according to the stoichiometric reaction of Equation 2.10 (Tchobanoglous et al., 2003):

$$C_6H_{12}O_6 + 6O_2 \rightarrow 6CO_2 + 6H_2O \quad \text{[2.10]}$$

From Equation 2.10, 6 moles of oxygen (molar mass of 32 g) is required to oxidise one mole of glucose (molar mass of 180 g).

$$COD_{glucose} = \frac{(Number\ of\ moles \times Molar\ mass\ of)O_2}{(Number\ of\ moles \times Molar\ mass\ of)\ C_6H_{12}O_6} \quad \text{[2.11]}$$

$$= \frac{6 \times 32}{1 \times 180} = 1.07\ g\ O_2/\ g\ glucose$$

Thus the chemical oxygen demand (COD) of glucose from Equation 2.11 is 1.07 g O_2/ g glucose.

The total COD consumed by aerobic heterotrophic bacteria during wastewater degradation is made up of the oxidized portion which supplies energy and that which is conserved in the biomass for cell synthesis. The stoichiometry relating the amount of oxygen consumed and the degradation of glucose is:

$$3C_6H_{12}O_6 + 8O_2 + 2NH_3 \rightarrow 2C_5H_7NO_2 + 8CO_2 + 14H_2O \quad \text{[2.12]}$$

$C_5H_7NO_2$ represents the bacterial cells and NH_3 growth nutrients.

From the stoichiometry of Equation 2.12, 8 moles of oxygen is required to oxidize 3 moles of glucose (having COD of 1.07 g O_2/ g glucose) to CO_2 and 2 moles of bacterial cells (molar mass of 113 g).

O_2 *requirement for COD removal*

$$= \frac{(Number\ of\ moles \times Molar\ mass\ of)\ O_2}{COD_{glucose} \times (Number\ of\ moles \times Molar\ mass\ of)\ C_6H_{12}O_6} \quad \text{[2.13]}$$

$$= \frac{8 \times 32}{1.07 \times 3 \times 180} = 0.44\ g\ O_2/\ g\ COD$$

Thus the oxygen requirement for COD removal from Equation 2.13 is 0.44 g O_2/ g COD used. The theoretical yield of bacterial cells, *Y*, obtained from Equation 2.14 is 0.39 g cells/ g COD used.

$$Y = \frac{\Delta(C_5H_7NO_2)}{\Delta(C_6H_{12}O_6 \text{ as } COD)} \quad \text{.....[2.14]}$$

$$= \frac{2 \times 113}{1.07 \times 3 \times 180} = 0.39 \text{ g cells/ g COD}$$

The COD of bacterial cells is also obtained from Equations 2.15 and 2.16 as 1.42 g O_2 /g cells.

$$C_5H_7NO_2 + 5O_2 \rightarrow 5CO_2 + NH_3 + 2H_2O \quad \text{.....[2.15]}$$

$$COD_{bacterial\ cells} = \frac{(Number\ of\ moles \times Molar\ mass\ of)O_2}{(Number\ of\ moles \times Molar\ mass\ of)\ C_5H_7NO_2} \quad \text{..... [2.16]}$$

$$= \frac{5 \times 32}{1 \times 113} = 1.42\ g\ O_2 / g\ cells$$

Thus the oxygen requirement for the bacterial cells is (0.39 x 1.42) g O_2/ g COD and the total amount of oxygen consumed per gram of COD removed, which is the sum of the oxygen used for oxidation of glucose (0.44 g) and that consumed during bacterial synthesis (0.55 g), is therefore 1 g (Tchobanoglous et al., 2003).

2.4.5.2 Denitrification

In wastewater, removal of nitrate could occur by assimilating or dissimilating means. During assimilating nitrate reduction, nitrate is reduced to ammonia which is used during cell synthesis (Bitton, 1999). This form of nitrate reduction occurs when ammonia is unavailable in the wastewater (Bitton, 1999; Tchobanoglous et al., 2003). Dissimilating nitrate reduction, also known as biological denitrification, involves the use of nitrate as an electron acceptor leading to its reduction

(Tchobanoglous et al., 2003). It proceeds by the reduction of nitrate to nitrogen gas through nitrite, nitric and nitrous oxide intermediaries as shown below (Bitton, 1999).

$$NO_3 \xrightarrow{\text{Nitrate reductase}} NO_2 \xrightarrow{\text{Nitrite reductase}} NO \xrightarrow{\text{Nitric oxide reductase}} N_2O \xrightarrow{\text{Nitrous oxide reductase}} N_2 \quad \text{.....[2.17]}$$

Denitrification is carried out in wastewater by facultative microorganisms belonging to the *Pseudomonas, Bacillus, Spirillum, Hyphomicrobium, Agrobacterium, Acinetobacter, Propionobacterium, Rhizobium, Corynebacterium, Cytophaga, Thiobacillus* and *Alcaligenes* genera, with the latter often found in soils (Bitton, 1999). Denitrification is commonly known to be inhibited by dissolved oxygen and therefore occurs only at very low dissolved oxygen concentration. It could however occur in anaerobic microsites present in an aerobic environment (Tchobanoglous et al., 1999). At very low nitrate-N concentrations (0.1 mg L^{-1}), the kinetics of utilization of substrate is influenced by the nitrate concentration (Tchobanoglous et al., 2003). In groundwater, the rate of denitrification is influenced by the residence time (Gu et al., 2007).

2.4.5.3 Sulphate Reduction

Sulphate reducing bacteria, which utilize sulphate in wastewater as the terminal electron acceptor when oxygen and nitrate are not present, are responsible for sulphate reduction. Sulphate reducers belong to bacteria genera such as *Desulfovibrio, Desulfotomaculum, Desulfobulbus, Desulfomonas, Desulfobacter, Desulfococcus, Desulfonema, Desulfosarcina, Desulfobacterium* and *Thermodesulfobacterium*. Carbon sources of low molecular weight such as

fermentation products of carbohydrates and proteins are used as electron donors (Bitton, 1999). Sulphate reduction proceeds according to the following equations (Bitton, 1999):

$$SO_4^{2-} + organic\ compounds \rightarrow S^{2-} + H_2O + CO_2 \text{ ……..……} [2.18]$$

$$S^{2-} + 2H^+ \rightarrow H_2S \text{ ……} [2.19]$$

Sulphate reducing bacteria are thought to be strict anaerobes. They are however able to tolerate oxygen in their environment and have been found to exist in activated sludge flocs (Lens et al., 1995). Their presence in this aerobic environment as well as in biofilms of rotating biological contactors and trickling filters has been attributed to the development of anoxic microsites in their environment and physiological adaptability of the anaerobic microorganisms (Lens et al., 1995). Oxygen concentration gradients across the thickness of biofilms contribute to the formation of anoxic and anaerobic zones in the deeper layers of the biofilm. Sulphate reduction has also been observed to occur consistently in well-oxygenated biomats (Canfield and Des Marais, 1991).

2.4.6 Advection–Dispersion Transport

The advection dispersion equation is the basic relationship that describes mass transport through porous media (Domenico and Schwartz, 1998; Charbeneau, 2000). The equation incorporates advection, mechanical dispersion and diffusion, and for one-dimensional flow in homogenous and isotropic saturated media, where flow is uniform and under steady state conditions, is given by (Freeze and Cherry, 1979):

$$\frac{\partial C}{\partial t} = D_L \frac{\partial^2 C}{\partial x^2} - v_x \frac{\partial C}{\partial x} \text{ ……} [2.20]$$

Soil column experiments can be used as a means of determining the hydrodynamic dispersion in porous media. To determine D_L, a conservative tracer (e.g., chloride) is fed into and moves upwards through the column. The concentration of the tracer at the effluent end is measured as a function of time and the breakthrough curve (BTC) developed. The problem is mathematically modelled and the experimental data fitted against the mathematical solution to the problem to determine the parameter values that best fit the theory and observed data. There are well established techniques for modelling advection-dispersion transport (Yong et al., 1992) and software packages such as CXTFIT, MODFLOW and BIOPLUME exist, which simplify the modelling process.

2.4.6.1 Initial and Boundary Conditions

In order to solve the partial differential equations of mass transport for a unique solution, supplementary equations that best fit the initial and boundary conditions of the system under consideration have to be imposed on the transport equation (Bear, 1972; Parker and Van Genuchten, 1984; Lee, 1999). In soil column experiments, the identification of the appropriate boundary conditions is crucial in order to interpret the laboratory data obtained and also to extrapolate the results to field conditions (Van Genuchten and Parker, 1984).

The initial condition is specified at time zero for all points along the soil column. The boundary conditions are usually specified at the entrance and exit of the soil column. They depend on the entry and exit conditions (Van Genuchten and Parker, 1984; Fetter, 1999) and account for the effects of the external environment on the system under consideration (Domenico and Schwartz, 1998). Principles of mass

conservation are used to formulate these boundary conditions (Fogler, 1992). Three types of boundary conditions exist (Fetter, 1999). The first-type also known as Dirichlet or concentration-type boundary condition is specified as a constant inlet concentration. The second-type or Neumann condition (Lee, 1999) is for a fixed gradient (Fetter, 1999) and the third-type, also called Cauchy or flux-type boundary condition, is specified for a constant inlet flux. Boundary conditions of the first and third type are often used for semi-finite (i.e. $0 \leq x \leq \infty$) and finite systems ($x = L$) (Van Genuchten and Parker, 1984; Charbeneau, 2000). Boundary conditions of the third-type are applicable to systems where the column does not have any physical connection with the entrance or exit reservoir and also for systems where even though there is a direct connection between the column and reservoir, the section before the entrance or after the exit can be considered as completely mixed and therefore dispersion and molecular diffusion can be neglected. This assumption implies that an infinitesimally thick boundary layer develops at the boundary between the assumed perfectly mixed condition at $x < 0$ and the soil in the column, $x > 0$, within which there occurs a discontinuous change in the parameters of the system from the conditions at $x < 0$ to $x > 0$ (Parker and Van Genuchten, 1984). At the exit of a finite system, an additional assumption made is that the solute concentration is continuous across the boundary (Van Genuchten and Parker, 1984).

2.4.6.2 Advection-Dispersion Transport with Sorption and Reaction

The effects of sorption and decay can also be included in the advection dispersion equation as shown in Equation 2.21 (Miller and Weber, 1984).

$$\frac{\partial C}{\partial t} = \underset{\text{(dispersion)}}{D_L \frac{\partial^2 C}{\partial x^2}} - \underset{\text{(advection)}}{v_x \frac{\partial C}{\partial x}} - \underset{\text{(sorption)}}{\frac{\rho_b}{\theta} \frac{\partial S}{\partial t}} + \underset{\text{(reaction)}}{\left(\frac{\partial C}{\partial t}\right)_{rxn}} \quad \text{.....[2.21]}$$

where:

C = concentration of solute in liquid phase (ML^{-3})

t = time (T)

D_L = longitudinal dispersion coefficient (L^2T^{-1})

v_x = average linear groundwater velocity (LT^{-1})

ρ_b = $\rho_s(1-\theta)$ is the bulk density of aquifer (ML^{-3})

ρ_s = density of the sand particles (ML^{-3})

θ = volumetric moisture content (L^3L^{-3}) or porosity for saturated media

S = amount of solute sorbed per unit weight of solid (MM^{-1})

rxn indicates a biological or chemical reaction of the solute other than sorption.

Substituting Equation 2.9 (i.e $\frac{\partial S}{\partial t} = K_d \frac{\partial C}{\partial t}$) into Equation 2.21 yields Equation 2.22.

$$\frac{\partial C}{\partial t} = D_L \frac{\partial^2 C}{\partial x^2} - v_x \frac{\partial C}{\partial x} - \frac{\rho_b}{\theta} \frac{\partial (K_d C)}{\partial t} + \left(\frac{\partial C}{\partial t}\right)_{rxn} \quad \text{.....[2.22]}$$

Rearranging

$$\frac{\partial C}{\partial t}\left(1 + \frac{\rho_b}{\theta} K_d\right) = D_L \frac{\partial^2 C}{\partial x^2} - v_x \frac{\partial C}{\partial x} + \left(\frac{\partial C}{\partial t}\right)_{rxn} \quad \text{.....[2.23]}$$

$R = \left(1 + \frac{\rho_b}{\theta} K_d\right)$ is the retardation factor and measures by how much the movement of the solute is slowed down compared to water by adsorption or reaction or both.

2.4.6.3 Kinetics of Biodegradation

Enzymatic activity occurring in bacteria is responsible for their capability to catalyse redox reactions involved in biodegradation processes in groundwater. The action of enzymes is through the reduction of reaction activation energies thereby increasing the redox rate (Lawrence and McCarty, 1970). For a single reaction in which a single substrate is reacting, the kinetics of the enzyme catalysed reaction was originally defined by Michaelis and Menten (1913). The Michaelis – Menten (M-M) equation representing enzyme kinetics can be written as (Benefield and Randall, 1980):

$$r = \frac{R_{max}\ [C]}{K + [C]} \quad \text{.....[2.24]}$$

where:

R_{max} = maximum reaction rate (T^{-1})

K = saturation constant given by the concentration of the substrate at half the reaction rate of R_{max} (ML^{-3})

C = concentration of substrate (ML^{-3})

Michaelis – Menten kinetics can be used in constant biomass systems in which the bio reactions are not limited by other compounds (Gong et al., 2011). Equations in the form of the M-M function can also be used to represent kinetic reactions in wastewater treatment involving multi-substrates as well as mixed cultures (Benefield and Randall, 1980) and is often applied in modelling contaminant transport in the subsurface (Holzbecher, 2007). Zero and first order reaction kinetics are also used (Schafer and Therrien, 1995). For a zero order reaction, the rate of the reaction is independent of the substrate concentration whilst for first and higher order kinetics, the reaction rate is a function of the concentration (Gray, 2004). The M-M kinetics approximates a zero order reaction when the saturation constant is much less than the

substrate concentration and first order when it far exceeds the substrate concentration (Gong et al., 2011).

The Monod function (Monod, 1949), which is similar to the M-M function, and its variants (Borden and Bedient, 1986; Widdowson et al., 1988; Baveye and Valocchi, 1989; Essaid et al., 1995) is also used often to model biodegradation of contaminants in the subsurface and under laboratory conditions (Rifai et al., 1989; Hunter et al., 1998; MacQuarrie and Sudicky, 2001; MacQuarrie et al., 2001; Kim et al., 2004; Lee et al., 2006; Bunsri et al., 2008). The Monod function, which gives the rate of growth of microorganisms in a biological system as a function of the substrate concentration has been rewritten in terms of rate of substrate utilisation as (Lawrence and McCarty, 1970):

$$\frac{dC}{dt} = \frac{k\, b_c\, C}{K + C} \quad \text{.....[2.25]}$$

where $\frac{dC}{dt}$ is the overall substrate utilisation rate, k is the maximum specific substrate utilization rate (T^{-1}), b_c is the active biomass concentration (ML^{-3}), C is the concentration of the substrate surrounding the biomass (ML^{-3}) and K is the saturation constant (ML^{-3}).

Borden and Bedient (1986) derived equations involving Monod kinetics, where the transport of hydrocarbons is coupled to the transport of dissolved oxygen, serving as an electron acceptor, and also to microbial dynamics. These equations are:

$$\frac{dH}{dt} = - M_t h_u \left(\frac{H}{K_h + H}\right)\left(\frac{O}{K_o + O}\right) \text{.....} \quad [2.26\ a]$$

$$\frac{dO}{dt} = - M_t h_u G \left(\frac{H}{K_h + H}\right)\left(\frac{O}{K_o + O}\right) \text{.....} \quad [2.26\ b]$$

$$\frac{dM_t}{dt} = M_t h_u Y\left(\frac{H}{K_h+H}\right)\left(\frac{O}{K_o+O}\right) + k_c Y C_{oc} - b_d M_t \quad \text{.....[2.26 c]}$$

where:

H = concentration of hydrocarbon in pore fluid (ML^{-3})

O = concentration of oxygen in pore fluid (ML^{-3})

M_t = concentration of aerobic microorganisms (ML^{-3})

h_u = maximum rate of hydrocarbon utilisation per unit mass of aerobic microorganisms (T^{-1})

K_h = half-saturation constant of hydrocarbon (ML^{-3})

K_o = half-saturation constant of oxygen (ML^{-3})

G = ratio of oxygen to hydrocarbon consumed

Y = microbial yield coefficient ie. mass of cells/ mass of hydrocarbon (MM^{-1})

k_c = first order decay rate of natural organic carbon (T^{-1})

C_{oc} = natural organic carbon concentration (ML^{-3})

b_d = microbial decay rate (T^{-1})

In cases where the microbial growth kinetics is limited by some secondary species, an inhibition factor is included in the kinetic expression.

2.5 Fate of Contaminants in Effluents Undergoing SAT

The water quality parameters of primary concern in SAT reuse schemes include organic compounds, nitrogen species, phosphorus, suspended solids and pathogenic organisms (NRC, 1994; Gungor and Unlu, 2005). There is also a concern over the presence of trace amounts of toxic substances remaining in wastewater even after the

most advanced treatment due to the potential short term or long term health effects posed (Tchobanoglous et al., 2003). Putting reclaimed water into the natural environment offers the opportunity for recycling and therefore the biodegradation of slowly degradable contaminants (Dillon et al., 2006).

2.5.1 Removal Mechanisms in SAT

Most SAT processes occur in the upper part of the vadose zone of the soil where the soil is of finer texture than the aquifer, organic content is higher, unsaturated flow occurs and oxygen content is variable ranging from aerobic to anaerobic (NRC, 1994). This is therefore the most active treatment zone (Crites et al., 2000) with the biomat (*schmutzdecke*) that develops at the infiltration surface accounting for a significant portion of the removal that occurs (Tchobanoglous et al., 2003). The complex physico-chemical and biological processes that occur in the vadose zone and in the aquifer to achieve treatment of the wastewater include filtration, chemical precipitation, adsorption, cation exchange, biodegradation of organics, nitrification, denitrification, biological recarbonation, bacterial die-off, and virus inactivation (Idelovitch and Michail, 1984; Asano, 1985; Kopchynski et al., 1996) complexation and chelation (Ward et al., 1985). These removal mechanisms are shown in Figure 2.6.

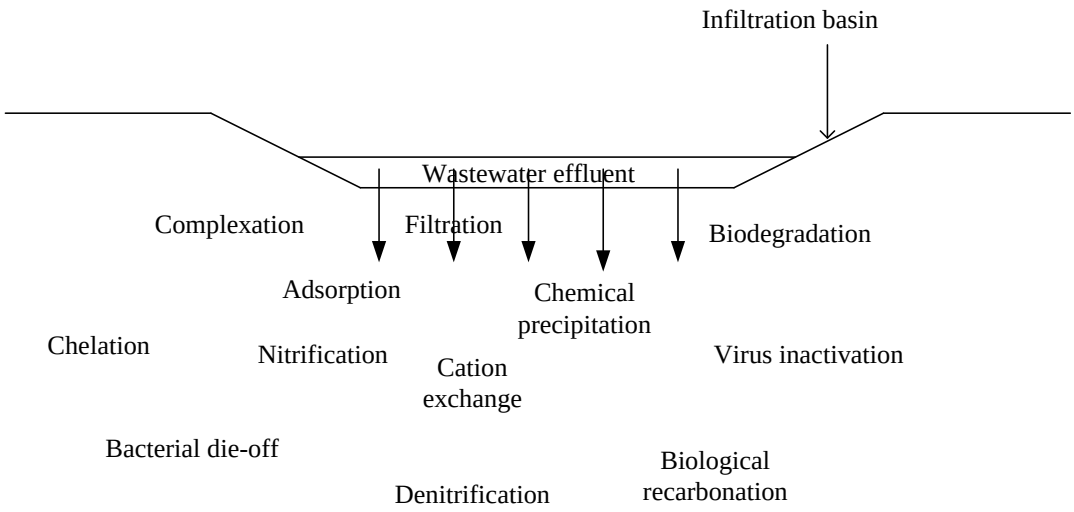

Figure 2.6 Removal mechanisms in the vadose zone during SAT

Nitrification is a two stage process facilitated by different species of chemo-autotrophic nitrifying bacteria. Nitrosification, which involves the oxidation of ammonium ions to nitrite is the first stage of nitrification and is often catalysed by bacteria belonging to the genus *Nitrosomonas* (Gray, 2004). Although other autotrophic bacteria genera such as *Nitrosococcus, Nitrosospira, Nitrosolobus* and *Nitrosovibrio* have also been identified (Belser, 1979) as capable of oxidizing ammonium to nitrite, *Nitrosomonas europa, Nitrosomonas oligocarbogenes* and *Nitrosomonas monocella* are three species often found during nitrosification (Gray, 2004). The oxidation process is as shown:

$$NH_4^+ + 1.5\,O_2 \rightarrow NO_2 + 2H^+ + H_2O \quad \text{.....[2.27]}$$

The second stage of nitrification is the oxidation of nitrite to nitrate. The bacteria genus *Nitrobacter* carry out this second stage, with *Nitrobacter winogradskyi* and *Nitrobacter agilis* being the species often isolated (Gray, 2004). Again other bacteria genera have also been found capable to converting nitrite to nitrate. These include

Nitrococcus, *Nitrospira*, *Nitrospina* and *Nitroeystis* (Tchobanoglous et al., 2003). The reaction for the conversion is as given by Gray (2004):

$$NO_2 + 0.5\,O_2 \rightarrow NO_3^- \quad \text{.....[2.28]}$$

The stoichiometry of nitrification requires that for complete nitrification to occur, 4.57 mg of oxygen should be available per 1 mg of ammonia-N present (Tchobanoglous et al., 2003).

Other processes that take place in the subsurface environment are chemical oxidation and reduction, dilution, volatilization and photochemical reactions (Tchobanoglous et al., 2003). The lifetime of the physico-chemical processes varies from short, for example the removal of sodium and boron, to very long as occurs for removal of trace elements. With careful operation and management of the SAT system, filtration by the upper soil layer and biological processes occurring can be effective indefinitely (Idelovitch and Michail, 1984). Since biological processes (biodegradation) dominate, SAT becomes a sustainable technology (Crites et al., 2000).

2.5.2 Fate of Particulates

SAT is a very efficient process for the removal of suspended solids (Crites et al., 2000). Suspended solids are removed by filtration as the water flows through the soil, with the soil matrix effectively retaining these filtered particles (Tchobanoglous et al., 2003). Complete removal of suspended solids could occur within 1 m of wastewater travel through the unsaturated zone (Pescod, 1992).

2.5.3 Fate of Dissolved Organic and Inorganic Contaminants

Inorganic contaminants are removed by processes including cation exchange, precipitation, surface adsorption and chelation and complexation (Ward et al., 1985). Phosphorus is partially removed mainly by adsorption and chemical precipitation (Asano, 1985; NRC, 1994). Although physical and chemical removal mechanisms, which are responsible for the removal of phosphorus, trace metals and non-biodegradable organics have limited capacity (Kopchynski et al., 1996), and the capacity of the soil in attenuating inorganic contaminants is not infinite, experimental studies have shown that large quantities of trace metal elements can be retained and a site used for groundwater recharge may thus be effective in retaining trace metals for a long time (Asano, 1985). With the exception of boron, strong attenuation being adsorption, ion exchange and complexation and precipitation of trace metals occurs within the soil especially under aerobic and alkaline conditions (NRC, 1994). The surfaces of clay minerals, soil organic matter and metal oxides serve as adsorption sites for the metals (Crites et al., 2000). Even though boron is not as easily removed as other metals, it can be adsorbed on clay (Pescod, 1992). Denitrification, which takes place when anaerobic conditions prevail, is the main nitrogen removal mechanism in SAT. Ammonia nitrogen is adsorbed from the infiltrating wastewater in the unsaturated zone where it is converted to nitrate by nitrification. During the wetting cycle, the nitrate is remobilised and transported to the saturated zone where it is denitrified.

Dissolved organic contaminants are removed by biodegradation and adsorption, the removal of the easily biodegradable fractions occurring within the first 60 cm or 1 m of travel through the soil (Crites et al., 2000; Tchobanoglous et al., 2003). Organic

nitrogen is hydrolysed to ammonium (ammonification) through the action of microorganisms (Gray, 2004). Mineralization of proteins into ammonium (NH_4^+) occurs by their conversion into peptides and amino acids by extracellular proteolytic enzymes, which are then transformed through oxidative or reductive deamination to ammonium (Bitton, 1999). The reactions are shown in Equations 2.29 and 2.30 (Bitton, 1999).

Oxidative deamination

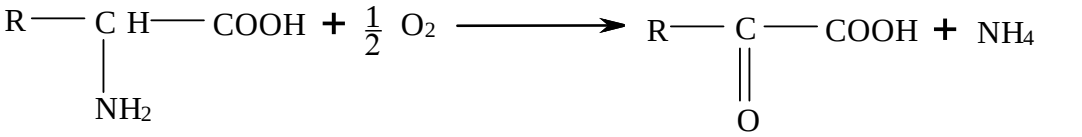

Amino acid Keto acid ……. [2.29]

Reductive deamination

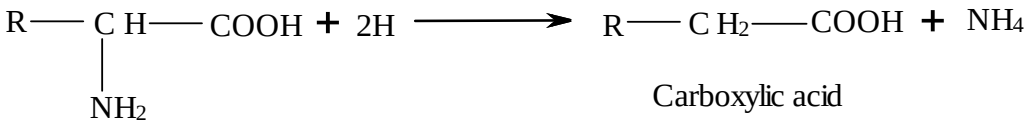

Amino acid Carboxylic acid …….. [2.30]

The dynamics involving the removal of nitrogen during SAT is quite complex due to its several oxidation states which are organic nitrogen, nitrogen gas (N_2), ammonia (NH_3), ammonium (NH_4^+), nitrite (NO_2) and nitrate (NO_3) (Crites et al., 2000). The input of nitrogen to a SAT system and its transformation is represented schematically in Figure 2.7 (Freeze and Cherry, 1979).

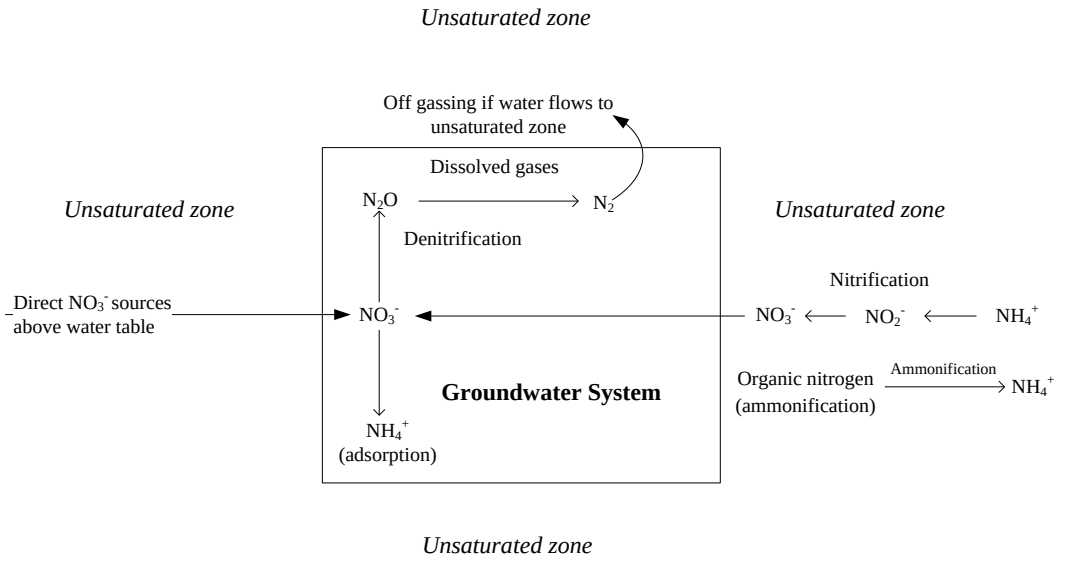

Figure 2.7 Nitrogen inputs and transformation in a SAT system

[Reproduced from Freeze and Cherry, 1979]

BOD is removed mainly by aerobic microorganisms in the soil. Removal of biodegradable organic carbon occurs within 30 cm of the soil depth (Rauch-Williams and Drewes, 2006). BOD and nitrogen removal are sustainable because they are achieved through biodegradation (Kopchynski et al., 1996). Although sorption and biodegradation are the main removal processes for effluent organic matter in SAT systems, only a few studies have been conducted to determine the relative contribution of each process to the overall removal (Quanrud et al., 1996b; Drewes and Fox, 1999; Fox et al., 2005).

Soil contaminants are also removed through volatilization, which is the mass transfer of chemical substances from the soil to the atmosphere. Contaminants vaporise into air pockets in the soil and are subsequently removed by diffusion to the ground surface or by vacuum extraction in wells. Factors influencing the rate of

volatilization of contaminants from the soil include the properties of the soil and contaminant and environmental conditions (Charbeneau, 2000).

2.5.4 Fate of Pathogens

Natural systems are generally robust in the removal of human pathogens (Dillon et al., 2006) in that they can still maintain a consistent level of efficiency under variations in environmental and operational conditions such as influent wastewater concentration and loading rates. There is however a risk of groundwater getting contaminated by bacteria during SAT under high hydraulic loading rates and in soils of coarse texture and high permeability (Crites et al., 2000). Removal mechanisms include adsorption, desiccation, radiation, filtration and predation (Crites et al., 2000).

Bacteria are removed mainly by filtration and viruses by adsorption (Asano, 1985; Pescod, 1992), a greater proportion of the removal attainable within 1 m of travel (Crites et al., 2000). Immobilised pathogens in the soil cease to reproduce and eventually die off (Pescod, 1992). The fate of pathogens in the subsurface environment is therefore dependent on their survival characteristics and retention in the soil matrix. These are controlled by the physical and chemical properties of the soil such as moisture holding capacity, pH, organic matter content, the nature of the microorganisms and climatic conditions such as rainfall and temperature (Bitton and Gerba, 1984; Tchobanoglous et al., 2003). Viruses are transported more easily through soil than bacteria. Their transport can however be retarded by the presence of small quantities of organic matter in the soil (Logan, 1999) and they are better retained in fine grained sandy loam than in sand (Quanrud et al., 2003a). Inactivation

and natural die-off rates of viruses and bacteria increase with increases in temperature. Over a temperature range of 5 ºC to 30 ºC die-off rates approximately double with every 10 ºC rise. The low pH of rainwater can cause desorption of viruses from the soil grains thus allowing movement of these pathogens with the infiltrating rainwater (Quanrud et al., 2003a; Tchobanoglous et al., 2003).

The fate of various wastewater contaminants such as organic matter (Quanrud et al., 1996b; Amy and Drewes, 2007; Zhao et al., 2007), trace organics (Amy and Drewes, 2007; Rauch-Williams et al., 2010), chlorination-by products (Amy et al., 1993; Quanrud et al., 1996b) nitrogen (Kopchynski et al., 1996; Bali et al., 2010) and pathogens (Quanrud et al., 2003a; Bali et al., 2010) has been studied in SAT systems (Fox et al., 2001). Most field studies carried out have involved deep unsaturated zones and secondary or tertiary effluents and several of the soil column studies have also been carried out with wastewater containing low concentrations of organic carbon. So far, limited work has been done to demonstrate the applicability and practicality of using SAT in treating poorly treated effluents or even primary effluents. In addition, complete reliance on the saturated zone without utilisation of the vadose zone in the treatment has never been explored. There is therefore the need for investigations on the efficiency of SAT under high organic loading rates and under saturated soil conditions especially in light of evidence that during infiltration, wastewater has the tendency to follow preferential flow paths and therefore able to bypass a greater proportion of the unsaturated soil matrix (Tchobanoglous et al., 2003). This is especially important in areas where the water table is high. Such a system would also have to be investigated with respect to operational parameters such as hydraulic loading rates to assess its performance efficiency. Although

dissolved organic carbon removal through a shallow vadose zone and under saturated soil conditions has been previously investigated (Chua et al., 2009), the wastewaters infiltrated were secondary and tertiary effluents and therefore had low DOC concentrations. Objective 1 of this research, which involves the infiltration of wastewater with much higher COD and DOC concentrations through the saturated soil, would therefore address this need.

Earlier studies carried out by Nema et al., (2001) found a correlation between the organic and hydraulic loading rates and effluent quality. It was observed that effluent biochemical oxygen demand (BOD), chemical oxygen demand (COD), suspended solids (SS), total kjeldahl nitrogen (TKN), ammonia nitrogen (NH_3) and phosphorus concentrations increased linearly with an increase in cumulative mass loading. Effluent quality with respect to these parameters was also found to deteriorate linearly with increase in cumulative hydraulic loading (Nema et al., 2001). These results were however found not to support previous studies carried out by Carlson et al., (1982) indicating that the hydraulic loading was a more important operating parameter than the organic loading in determining the effluent quality. Besides, these studies involved an unsaturated zone for the treatment and in recent years no further studies have been carried out.

2.6 Performance of SAT Systems

The performance of SAT systems is mainly dependent on three engineering factors. These are the characteristics of the infiltration site such as the type of soil overlying the aquifer, pre-treatment given to the wastewater, which determines the applied wastewater characteristics and the operating conditions such as the duration of the

wetting and drying cycles applied (Quanrud et al., 1996a; AWWA, 1998; Houston et al., 1999; Fox et al., 2006). Redox conditions and residence time can have a significant influence on the kinetics of dissolved organic carbon (DOC) degradation (Grünheid et al., 2005) and may affect the removal efficiency. Studies on a number of SAT sites have shown that 95 % to 99 % of total suspended solids removal is attainable (Crites et al., 2000). Typical performance data for BOD, nitrogen, phosphorus and faecal coliforms in SAT systems are summarized in Table 2.2. Expected effluent quality of treated water from SAT systems based on percolation of primary or secondary effluent through 4.5 m of soil is also given in Table 2.3.

Table 2.2 Typical performance data for SAT systems

Parameter	**Average loading rate (kg/ha.d)**	**Average removals (%)**	**Comments**
BOD	44.8 – 179.2	86 – 98	Higher values are associated with well- designed systems.
Nitrogen	3.36 – 41.4	10 – 93	Very dependent on pre-application treatment, BOD/N ratio, wet/dry cycle, hydraulic loading rate.
Phosphorus	1.12 – 13.4	29 – 99	Removals correlate closely with travel distance through soil.
Faecal coliforms	-	2 – 6 logs	Removals correlate with soil texture, travel distance through soil, and resting time.

Source: (WPCF, 1990)

Table 2.3 Expected effluent quality from SAT systems

Constituent	**Value (mg L^{-1})**	
	Average	**Maximum**
BOD	2	< 5
Suspended solids	2	< 5
Ammonia nitrogen as N	0.5	< 2
Total nitrogen as N	10	< 20
Total phosphorus as P	1	< 5

Source: (Tchobanoglous et al., 1999)

2.6.1 Level of Effluent Pre-treatment

The level of pre-treatment given to the wastewater determines the concentration of organic carbon applied to the SAT system and thus the redox condition under which degradation of target wastewater constituents would occur. Near the soil/water interface, biological activity is high, because this is where growth substrates and dissolved oxygen are at their highest concentrations. If organic carbon concentrations are high in the applied wastewater, most if not all of the dissolved oxygen would be utilised in this zone for the degradation of organic carbon and aerobic conditions would not pertain in the soil (Fox et al., 2006).

A substantial amount of nitrification and simultaneous denitrification can occur in SAT systems, thereby achieving nitrogen removal (Kanarek et al., 1993). Under predominantly aerobic conditions, nitrification occurs and a large fraction of the influent nitrogen is transformed to nitrate. High carbon content of the influent coupled with sufficient BOD levels would generate anoxic conditions to promote

denitrification of the nitrate-nitrogen. Long wet and dry cycles also enhance the denitrification process. Long wet cycles allow anoxic conditions needed for denitrification to develop and be maintained, whilst long drying times allow aerobic conditions needed for nitrification to be re-established (Gungor and Unlu, 2005).

2.6.2 Site Characteristics

SAT infiltration rates, sorption processes and biofilm formation on the soil are affected by soil properties. For the development of biofilms in the soil, adequate surface area is required for bacterial attachment. High infiltration rates at the beginning of SAT wet cycles would also occur in soils possessing high hydraulic conductivity (Fox et al., 2006) such as coarse textured soils. On the other hand, more efficient contaminant adsorption and removal can be obtained from soils of fine texture (NRC, 1994). Loamy sand receiving secondary effluent from conventional biological treatment is able to remove 95 % nitrogen when the operated on a 7 days wetting and 7 days drying cycle. Sandy clay loam and sandy loam can also be operated under both 7 days wetting and 7 days drying and 3 days wetting and 4 days drying cycles to meet the nitrification and denitrification requirements of SAT (Gungor and Unlu, 2005). Under continuous recharge conditions however, ammonia breakthrough can occur (Bouwer et al., 1980; Idelovitch and Michail, 1984; Amy et al., 1993; AWWA, 1998). Ammonia adsorption is a function of the cation exchange capacity of the soil (Fox et al., 2006), thus soils with high cation exchange capacity are required to adsorb ammonia in the infiltrating water (AWWA, 1998). Inorganic phosphorus is usually strongly sorbed in soils and sediments. Experiments carried out to measure phosphorus breakthrough times during SAT at the Shafdan Wastewater Treatment Plant for example showed that phosphorus contamination of

deep aquifers by the reclaimed effluents would not be a problem in the near future (Lin and Banin, 2006). The presence of a vadose zone is a requirement in SAT in order to promote the nitrification process for the transformation of nitrogen in the wastewater (Fox et al., 2006). Its depth could have an impact on the hydraulic function and the treatment efficiency by affecting the aeration and water content of the soil, the surface area of unsaturated soil available and the hydraulic retention time (Van Cuyk et al., 2001).

2.6.3 Operating Conditions

Wet and dry cycles have a key influence on nitrogen transformation processes in the soil. During the drying cycle, reaeration of the soil, which is essential for nitrification occurs (Fox et al., 2006). This transforms ammonia in the infiltrating water into nitrate. During ponding, dissolved oxygen becomes limited and anoxic conditions develop. This allows denitrification processes to occur, transforming nitrate into nitrogen gas. Loading cycles to maximize specific treatment objectives are given in Table 2.4.

Table 2.4 Suggested loading cycles for SAT systems

Treatment Objective	**Pre-treatment**	**Application Period, days**	**Drying period, days**
Maximize infiltration rates	Primary Secondary	1 – 2 1 – 3	5 – 7 4 – 5
Maximize nitrogen removal	Primary Secondary	1 – 2 7 – 9	10 – 14 10 – 15
Maximize nitrification	Primary Secondary	1 – 2 1 – 3	5 – 7 4 – 5

(USEPA, 1981)

2.7 Reduction in Soil Hydraulic Conductivity during SAT

The hydraulic conductivity of a soil describes how easily water can move through the pores of the soil and is an important property in determining the risk of pollution of groundwater by a contaminant plume. When a soil is inundated over a prolonged period, the hydraulic conductivity changes over time (Miyazaki and Seki, 2006).

Clogging layers develop in SAT infiltration basins during operation. They are undesirable as they are much less permeable than the natural soil leading to reductions in infiltration rates (Bouwer, 2002). Besides lowered hydraulic performance, excessive clogging could lead to anaerobic conditions developing in the soil and reduced treatment efficiency. On the other hand the development of the clogging layer to a balanced extent such that it does not become too restrictive on hydraulic conductivity is desirable as it could promote sorption, biotransformation and pathogen inactivation and elimination (Van Cuyk et al., 2001).

Microorganisms present in the soil may directly or indirectly cause a decrease in the hydraulic conductivity of the soil (Miyazaki and Seki, 2006). A diverse population of microorganisms exist in soils, the most predominant being bacteria, fungi and actinomycetes. There are about 10^7 to 10^8 bacteria in every 1 g of soil with the largest numbers being found in the surface layer. Bacterial numbers decrease exponentially with depth of soil (Ishizawa and Toyoda, 1964) reducing to about one tenth of the number at the surface at a depth of 50 cm and to less than one thousandth at a soil depth of 100 cm. Previous studies carried out at SAT sites have found the concentration of total viable soil biomass in the infiltration zone of SAT infiltration basins to be positively correlated with the concentration of biodegradable organics in the applied effluent (Rauch-Williams and Drewes, 2006).

The clogging of the infiltration surface and soil, and subsequent reduction in hydraulic conductivity is caused by physical, chemical and biological processes (Bouwer, 2002; Miyazaki and Seki, 2006). Physical processes in SAT infiltration basins leading to clogging of the infiltration surface include suspended solids deposition and accumulation in the basin. Suspended solids may be organic or inorganic and includes silt and clay particles, sludge, algae and other microorganisms. The downward movement of fine soil particles and accumulation of these in denser or finer areas in the soil also form a thin subsurface clogging layer (Bouwer, 2002). Microorganisms also destroy the structure of the soil by attacking organic materials in the soil. This causes the soil particles to disperse leading to a reduction in hydraulic conductivity (Martin, 1945).

Chemical processes contributing to clogging include anaerobic inorganic precipitation that occurs in the soil pores (Kamon et al., 2002). Chemicals such as calcium carbonate, phosphate and gypsum could precipitate in and on the soil (Bouwer, 2002). Microbial gas production also greatly contributes to a reduction in the hydraulic conductivity (Poulovassilis, 1972). Soils submerged continuously tend to create an environment that supports anaerobic microbial activity, especially when an ample source of carbon is available. Anaerobic breakdown of the carbon leads to the production of methane gas, a portion of which is stored as gas bubbles in the soil (Bouwer, 2002; Miyazaki and Seki, 2006). Nitrogen gas may also be trapped in soil pores (Bouwer, 2002). The gas is produced by nitrification/denitrification processes occurring in the soil for the removal of nitrogen from the infiltrating wastewater. Dissolved air in the infiltrating wastewater could also lead to reductions in infiltration rates. In cases where the soil or aquifer is warmer than the recharge

water, the water warms up and inherent air is displaced from the water and becomes trapped in the soil pores (Bouwer, 2002).

Biological processes leading to clogging include the build-up of algae and bacterial flocs on the bottom of infiltration basins (Bouwer, 2002). As the bacterial population in the soil increases, products of microbial metabolism accumulate in soil pores (Frankenberger et al., 1979). Biomass and biofilms also develop in and on the surfaces of the soil particles. These are able to cause a reduction in the size of soil pores or even block them completely (Bouwer, 2002; Kamon et al., 2002), thereby reducing the available pore space for water flow leading to a reduction in hydraulic conductivity. In soil columns the greatest reduction in hydraulic conductivity occurs at the inlet end to the column where a bacterial mat forms (Miyazaki and Seki, 2006).

Two hypotheses describe the clogging in soils due to the activity of bacteria. They are the biofilm model and the microcolony model. In the biofilm model, a film of bacteria covers the walls of the pores in the soil. The bacterial cells in the film are intimately associated with a meshwork of exopolymers or glycocalyx. In the microcolony model, the bacteria consume substrates and electron acceptors in the soil water and grow in microcolonies that are dispersed on the surface of the soil particles. The mechanisms of clogging due to microrganisms are still being investigated. Out of the studies that have already been carried out a greater number support the microcolony concept (Miyazaki and Seki, 2006).

The importance of applying wastewater intermittently in the SAT system i.e. a cyclic operation consisting of a period of application followed by a drying period is to improve the treatment performance and help maintain infiltration rates over a long period (Droste, 1997). The drying periods employed allow the clogging layer to dry, shrink, decay and break up thus restoring infiltration rates. Periodically, the dry clogging layer is removed mechanically and the soil bottom of the basins scarified to further improve infiltration (Bouwer, 2002). When using secondary effluents, implementing an operation regime of 1 to 3 days wastewater application period followed by a 4 to 5 day drying period would maximize infiltration rates (USEPA, 1981). With proper management a SAT system operated with periodic drying to reduce clogging should be sustainable indefinitely (NRC, 1994).

2.7.1 Bacterial Biomass and Community Structure in Soils

A number of methods have been developed to determine the microbial community structure and biomass in soils. Deoxyribonucleic acid (DNA) based fingerprint methods have been developed and are commonly used for describing the community structure. These methods are based on variations in ribosomal ribonucleic acid (rRNA) of microbial communities (Leckie, 2005). Microscopy can also be used for the enumeration of microorganisms in soils. It is however not suitable for use on coarse sands. Phospholipids fatty acid (PLFA) analysis is another widely used method for characterising microbial communities in soil and offers the advantage of deriving information on both community structure and total microbial biomass from the same sample (Findlay and Dobbs, 1993). It is based on the differences in the fatty acids contained in the cell membranes of diverse organisms (Leckie, 2005) and

as no culturing of samples is required, the method is not selective but covers the entire range of the microbial community (Findlay and Dobbs, 1993).

The cell membranes of viable organisms contain fatty acids as a component of its phospholipids, which are essential components of its cells. Fatty acids may be straight chained, branched or cyclic and could also be saturated or unsaturated (O'Leary, 1962). Unique to bacteria are the cyclopropane, β-OH and branched chain fatty acids (Lechevalier, 1989). Specific types of fatty acids are usually predominant in a given group of organisms and are used as biomarkers for that group of microorganisms (Zelles, 1999; Leckie, 2005). The phospholipids fatty acids often used as biomarkers are shown in Table 2.5.

Fatty acids are named according to the total number of carbon atoms it contains, followed by the degree of unsaturation or the number of double bonds, and the position of the double bond from the aliphatic end, ω, of the molecule. *cis* or *trans* double bonds are denoted by the suffix *c* or *t* respectively and indicate the position of the adjacent hydrogen atoms to the double bond (Findlay and Dobbs, 1993; Zelles, 1999). In *cis* isomers, the two adjacent hydrogen atoms are bound on the same side of the double bond in the carbon chain whilst in *trans* isomers, they are bound on opposite sides of the double bond (Valenzuela and Morgado, 1999). For example the PLFA 16:1ω5c means that the fatty acid has 16 carbon atoms and possesses one double bond situated at the 5^{th} carbon counting from the aliphatic end of the molecule with the two adjacent hydrogen atoms bound on the same side of the double bond. Prefixes *a*, *i*, *cy*, *br* and *d* are used to signify *anteiso*, *iso* and *cyclopropyl* branched, *branching* type unknown and *dicarboxylic* acids respectively

(Findlay and Dobbs, 1993; Zelles, 1999). The position of the methyl group in the molecule is indicated by a number followed by ME. In an OH fatty acid, the prefixes α and β denote that OH groups of the molecule are located at positions 2 and 3 respectively (Zelles, 1999).

Table 2.5 PLFA often used as biomarkers for specific groups of microorganisms

Type of PLFA	**Indicator for**	**PLFA used as biomarker**	**Comments**
Monoenoic unsaturated and cyclopropane unsaturated	Gram-negative bacteria	16:1ω5c, 16:1ω7c, 16:1ω7t, 16:1ω9c, a16:0, cy17:0, 18:1ω5c, 18:1ω7c, 18:1ωtc, 18:1ω9c, cy19:0a	Occur in lesser amounts in Gram-positive bacteria and eukaryotes
Terminally branched and 10Me branched saturated	Gram-positive bacteria	i14:0, i15:0, a15:0, i16:0, a17:0, i18:0, 10Me16:0	Occur in some Gram-negative bacteria (sulphate-reducers)
Saturated straight chain (< 20 Carbon atoms) Methyl branch on 10th carbon Polyenoic unsaturated	Bacteria (non-specific) Actinomycetes Fungi	14:0, 16:0, 18:0 10Me16:0, 10Me17:0, 10Me18:0 18:2ω6 (18:1ω9c, 18:3ω3)	 Occur in other eukaryotes and bacteria
Saturated straight chain (> 20 Carbon atoms)	Microeukaryotes, higher plants, mosses	20:0, 21:0, 22:0, 23:0, 24:0, 25:0, 26:0	
Polyunsaturates	Microeukaryotes	20:3ω6, 20:4ω6	Rare in bacteria
Ratio of monoenoic precursors to cyclopropane PLFA	Stress indicator	16:1ω7c/cy17:0, 16:1ω8c/cy19:0	Ratio < 0.5 occurs in healthy non-stressed populations
Trans/cis ratio of monoenoic PLFA	Stress indicator	16:1ω7t/16:1ω7c, 16:1ω8t/16:1ω8c	Ratio < 0.5 occurs in healthy non-stressed populations

(Leckie, 2005)

Following the description of the soil aquifer treatment system and a review of its performance with respect to characteristic wastewater parameters and mechanisms for their removal, literature on the properties of endocrine disrupting compounds, specifically triclocarban and the estrogens estrone (E1), 17β-estradiol (E2) 17α-ethinylestradiol (EE2) and their removal from wastewater are now reviewed and presented in the next section.

2.8 Endocrine Disrupting Compounds

2.8.1 Introduction

The problem of endocrine disruption from environmental pollution has in recent years developed into a major human health and environmental issue. Many man-made chemicals released into the environment have suspected endocrine disrupting capabilities (Birkett, 2003a). An endocrine disrupter may be defined as *"An exogenous agent that interferes with the synthesis, secretion, transport, binding, action, or elimination of natural hormones in the body that are responsible for the maintenance of homeostasis, reproduction, development, and/or behaviour"* (USEPA, 1997). Compounds that cause endocrine disruption include:

i. Steroid hormones such as estrogens;

ii. Pesticides, herbicides and fungicides;

iii. Surfactants such as nonylphenol and its ethoxylates;

iv. Polyaromatic compounds such as polyaromatic hydrocarbons;

v. Polychlorinated biphenyls and polybrominated flame retardants;

vi. Organic oxygen compounds such as phthalates, dioxins and bisphenol A (Birkett, 2003b);

vii. Antimicrobials such as triclocarban which has recently been shown to possess endocrine disrupting properties (Chen et al., 2008).

2.8.2 Mechanisms of Action of Endocrine Disrupting Compounds

Endocrine disruption occurs when there is an interaction of endocrine disruptors with hormone receptors causing a change in the natural patterns of response of the endocrine system. Endocrine disrupting compounds (EDCs) could act as mimics, blockers, stimulators, endocrine flushers, enzyme flushers or destructors (Birkett, 2003a). Most endocrine disrupting compounds cause reproduction interferences (Wuttke et al., 2010).

The mechanisms of action of EDCs are by:

i. Binding to the hormone receptor and activating a response (agonistic effect), thus mimicking a natural hormone and having adverse effects on biological functions;
ii. Binding to and occupying hormone receptor sites in cells, but generating no response (antagonistic effect) thus blocking the natural hormone from carrying out its normal interacting functions;
iii. Stimulating the formation of more hormone receptors, thus amplifying the effects of both natural and foreign hormones;
iv. Accelerating the breakdown of hormones and their elimination from the body, leading to hormone depletion;
v. Deactivating enzymes responsible for the breakdown of hormones in the body, leading to excess hormones in the system and problems with signalling;
vi. Altering the structure of natural hormones or pattern of hormone synthesis thus destroying the ability of the hormone to carry out its function (Birkett, 2003a).

2.8.3 Estrogens

Estrogens may be defined as *"any of a family of steroid hormones that regulate and sustain female sexual development and reproductive function"* (Birkett, 2003a). They are biologically active compounds synthesized from cholesterol (Ying et al., 2002) and have a tetracyclic molecular framework comprising a phenol ring (A), two cyclohexane rings (B, C) and a cyclopentane ring (D) (Khanal et al., 2006). Figure 2.8 shows the general structure of estrogens. Estrogens are also known as C18 steroids due to the 18 carbon atoms they possess in their structure.

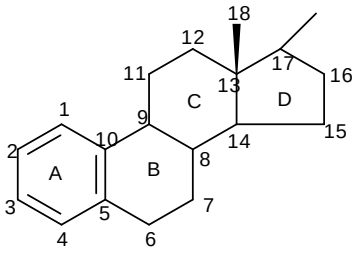

Figure 2.8 Cyclopentanophenathrene ring of estrogens

Estrogens may be natural or synthetic. Natural steroidal estrogens include estrone (E1), 17β-estradiol (E2), estriol (E3), and 17α-estradiol (17α) (Mansell and Drewes, 2004). These estrogens are primarily synthesized in the ovaries of humans and animals but could also be produced in the brain, hypothalamus, adipose tissue, testis and placenta (Combalbert and Hernandez-Raquet, 2010). Estrogens are responsible for the development of the female reproductive system (Mansell and Drewes, 2004) and also important in maintaining healthy breasts, skin and brain (Ying et al., 2002). The synthetic estrogen 17α-ethinylestradiol (EE2) is industrially synthesised from E2 by the addition of an ethinyl group and is the active ingredient in oral contraceptive pills (Khanal et al., 2006; Combalbert and Hernandez-Raquet, 2010). Conjugated

forms of E1 are also used as active ingredients in drugs used for hormone replacement therapy (Arcand-Hoy et al., 1998). These conjugated estrogens are blends of salts of estrogen sulphate esters. An example is the drug Premarin, $C_{18}H_{21}NaO_5S$, (Figure 2.9) with main components sodium estrone sulphate and sodium equilin sulphate, used to treat the symptoms of menopause (DRUGBANK, 2011).

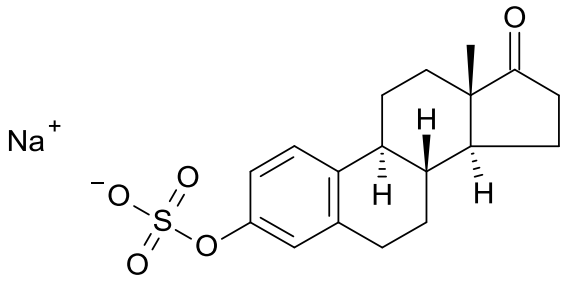

Figure 2.9 Structure of conjugated estrogen, Premarin

2.8.3.1 Structure and Properties of E1, E2 and EE2

Figures 2.10 – 2.12 show the structures of estrone (E1), 17β-estradiol (E2) and 17α-ethinylestradiol (EE2). Differences in the compounds arise from the configuration of the D-ring at the C16 and C17 positions of the structure, with estrone possessing a carbonyl group on C17 and 17β-estradiol having a hydroxyl group on C17 pointing upward of the molecular plane (Carlos, 1998; Khanal et al., 2006). 17α-ethinylestradiol possesses an ethinyl group on the D-ring (Birkett, 2003a). The physical and chemical properties (water solubility, octanol-water partition coefficients (K_{ow}), and the Henry's Law constant (H_c)) of the estrogens are given in Table 2.6.

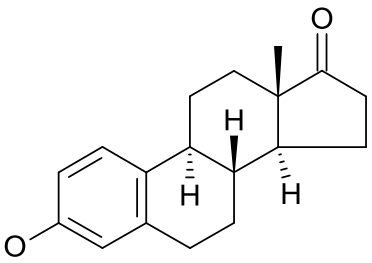

Figure 2.10 Structure of estrone

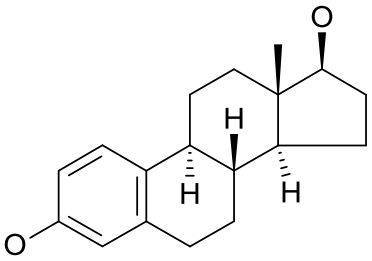

Figure 2.11 Structure of 17β-estradiol

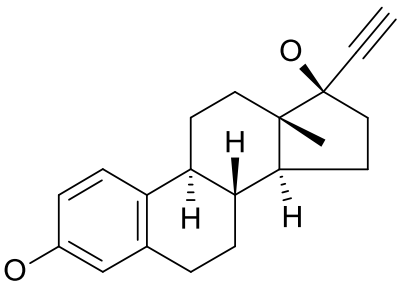

Figure 2.12 Structure of 17α-ethinylestradiol

Table 2.6 Physical and chemical properties of E1, E2 and EE2

Compound	**Molecular formula**	**Molecular mass (g/mol)** [a]	**Aqueous solubility (mgL^{-1})** [b]	**Log K_{ow}** [b]	**H_c ($atm\ m^3\ mol^{-1}$)** [b]
Estrone	$C_{18}H_{22}O_2$	270.37	12.42	3.43	6.2×10^{-7}
17β-estradiol	$C_{18}H_{24}O_2$	272.39	12.96	3.94	6.3×10^{-7}
17α-ethinylestradiol	$C_{20}H_{24}O_2$	296.40	4.83	4.15	3.8×10^{-7}

[a](Conroy et al., 2007), [b](Langford and Lester, 2003)

2.8.3.2 Sources of Environmental Estrogens

Humans and livestock are the main source of estrogens with large amounts being excreted in urine and smaller amounts in faeces (Khanal et al., 2006; Combalbert and Hernandez-Raquet, 2010). In the liver, estrogens are converted into biologically inactive conjugated forms of sulphate, glucuronide or sulphoglucuronide by substitution of their hydroxyl groups in positions C3 or C17 or both (Birkett, 2003b; Khanal et al., 2006; Combalbert and Hernandez-Raquet, 2010). Commonly reported conjugated forms of E1 and E2 (Johnson and Williams, 2004; Racz and Goel, 2010) are shown in Figure 2.13. Figure 2.14 also shows the metabolism of EE2 after ingestion and its excretion from the body (Johnson and Williams, 2004).

Conjugated forms of estrogens have little biological activity and are more soluble than the unconjugated or free forms of the estrogens. They are thus easily excreted from the body through urine (Combalbert and Hernandez-Raquet, 2010) and are therefore the main form in which estrogens are excreted (D'Ascenzo et al., 2003). Estrogens excreted with faeces on the other hand are mainly in the free form, having been deconjugated by intestinal flora in the gut (Adlercreutz and Järvenpää, 1982). Outside the body or during wastewater treatment the conjugated estrogens, especially the glucuronides (D'Ascenzo et al., 2003), are broken down by faecal bacteria into their free forms, which present much greater estrogenic activity (Desbrow et al., 1998). A summary of the amounts of E1, E2 and EE2 excreted daily by humans is given in Table 2.7.

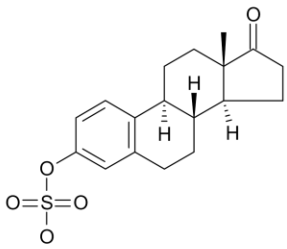

Estrone-3-sulphate

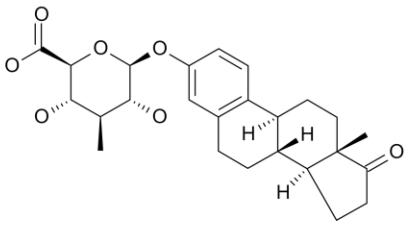

Estrone-3-glucuronide

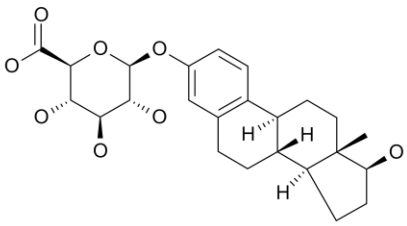

17β-estradiol-3-glucuronide

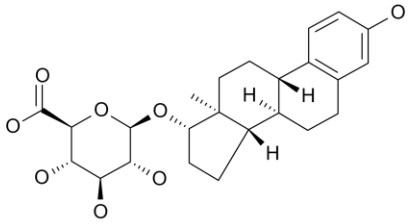

17β-estradiol-17-glucuronide

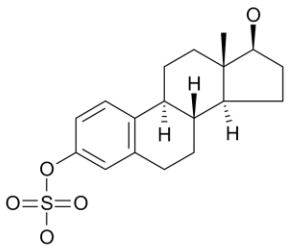

17β-estradiol-3-sulphate

Figure 2.13 Common conjugated forms of estrone and 17β-estradiol

[Reproduced from Johnson and Williams, 2004; Racz and Goel, 2010]

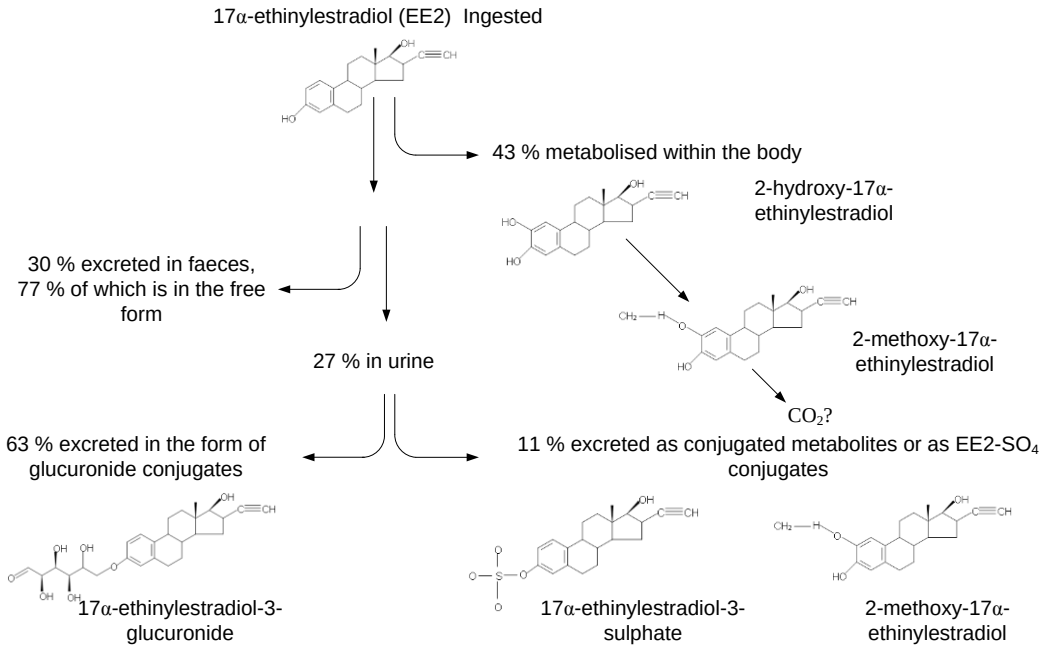

Figure 2.14 Metabolism and excretion of 17α-ethinylestradiol after ingestion [Reproduced from Johnson and Williams, 2004]

Table 2.7 Amount of E1, E2 and EE2 excreted daily by humans

Category	**Amount excreted (µg d^{-1})**		
	E1	**E2**	**EE2**
Women			
of reproductive age (15 – 59)[a]	5 – 31	3 – 19	-
pregnant[a]	600 – 940	170 – 330	-
using oral contraceptives[b]			35
Men[b]	3.9	1.6	-

[a](Combalbert and Hernandez-Raquet, 2010); [b](Johnson et al., 2000)

As the conventional wastewater treatment process is not specifically designed with EDCs as target contaminants for removal (Drewes et al., 2005), estrogens are incompletely removed during treatment and it is not surprising that wastewater treatment plant effluents have become the main source of estrogens in the

environment (Allinson et al., 2010). Natural and synthetic estrogens present the greatest endocrine disrupting activity in domestic wastewater effluents (Desbrow et al., 1998; Snyder et al., 2001). E1, E2 and EE2 are the most active EDCs (Desbrow et al., 1998), as they are able to exert their physiological effects at much lower concentrations than the other estrogens (Arnon et al., 2008). EE2 has the highest estrogenic activity followed by E2, and although E1 only has half the potency of E2, in wastewater effluents it is often found at more than double the concentration of E2 (Johnson and Sumpter, 2001) due to its slower rate of degradation (Rodgers-Gray et al., 2000). Due to the much higher concentrations of E1 in the aquatic environment, it is potentially the most important endocrine disruptor among all the estrogens (D'Ascenzo et al., 2003). It has been established for surface waters a total "potential no effect concentration" (PNEC) of 1.0 ng L^{-1} as a weighted sum of estrone (E1), 17β-estradiol (E2), and 17α-ethinylestradiol (EE2) (PNEC = 10EE2 + E2 + E1/3). The individual PNEC values for each of these EDCs are 3.0, 1.0, and 0.1 ng L^{-1} for E1, E2 and EE2 respectively (Young et al., 2004). A few examples of a range of estrogen concentrations observed in sewage treatment plant effluents in some countries are given in Table 2.8. Other sources of estrogens in water bodies include run off from farmlands used for rearing livestock (Matthiessen et al., 2006). Low concentrations of estrogens have been detected in aquifers recharged with wastewater effluents or in areas where animal manure or wastewater treatment plant sludge is applied on the overlying agricultural land in the catchment area. They have also been detected in spring water from some aquifers indirectly recharged with wastewater through irrigation practices (Gibson et al., 2007) or animal husbandry (Peterson et al., 2000). Hohenblum et al (2004) also attributed presence of estrogens in groundwater to agricultural practices and contamination from domestic sewage.

Septic tank systems have also been identified as a contributor to estrogens found in groundwater (Swartz et al., 2006).

Table 2.8 Concentrations of estrogens in wastewater treatment plant effluents in different countries

Wastewater Treatment Process	**Country**	**Concentration in effluent (ng L^{-1})**			**Reference**
		E1	**E2**	**EE2**	
Activated sludge	Italy	5 – 30	3 – 8	ND	(Laganà et al., 2004)
Activated sludge	Italy	17 ± 7	1.6 ± 1.9	NM	(D'Ascenzo et al., 2003)
Activated sludge	Italy	2.5 – 82.1	0.44 – 3.5	0.3 – 1.7	(Baronti et al., 2000)
Activated sludge	Italy	< 0.5 – 54	< 0.5 – 7	< 0.5 – 2.2	(Johnson et al., 2000)
Activated sludge	Portugal	<LOD – 85	< LOD – 2.3	< LOD	(Sousa et al., 2010)
Summarised from a variety of treatment processes	UK	1 – 80	0.1 - 90	< 0.1 – 4.3	(Fenlon et al., 2010)
Activated sludge, Biological percolating filter + sand filter	UK	< 0.4 – 12.2	< 0.4 – 4.3	< 0.4 – 3.4	(Williams et al., 2003)
Activated sludge	UK	6.68 ± 4.15	0.65 ± 0.35	0.78 ± 0.09	(Filby et al., 2010)
Activated sludge	The Netherlands	< 0.4 – 47	< 0.4 – 12	< 1.8	(Johnson et al., 2000)
Activated sludge	China	8.3 – 14.0	8.7 – 32.4	ND	(Zhang et al., 2011)
Activated sludge	France	6.2 ± 0.8 – 7.2 ± 0.8	4.5 ± 1.0 – 8.6 ± 0.9	3.1 ± 0.6 – 4.5 ± 0.8	(Cargouët et al., 2004)
Bio-filter	France	4.3 ± 0.6	6.6 ± 1.4	2.7±0.8	(Cargouët et al., 2004)
Activated sludge	Germany	9 (mean) 70 (max)	<1 (mean) 3 (max)	1 (mean) 15 (max)	(Ternes et al., 1999)
Activated sludge	Canada	3 (mean) 48 (max)	6 (mean) 64 (max)	9 (mean) 42 (max)	(Ternes et al., 1999)
Activated sludge	Canada	8.7 – 75	<1 – 7.4	<1	(Lee et al., 2004)

LOD – Limit of Detection; ND – Not Detected; NM – Not Measured

2.8.3.3 Effects of Exposure to Estrogens

Estrogens have been detected in effluent receiving water bodies (Ternes et al., 1999; Hashimoto et al., 2007; Miya et al., 2007; Pauwels et al., 2008; Gabet-Giraud et al., 2010) at concentrations high enough to cause endocrine disruption of some aquatic species (Khanal et al., 2006).

Natural estrogens are biologically active in the blood of several mammals at concentrations as low as 2 to 3 pg mL^{-1} (Tyler et al., 1998). Due to the high affinity of hormone receptor sites for hormones, very low concentrations of hormones are sufficient to generate responses (Birkett, 2003a). The feminization of male fish in waters polluted by wastewater effluents has been attributed to the presence estrogens in the effluent (Purdom et al., 1994; Jobling et al., 1998). Exposure to EE2, even in concentrations as low as 1 to 10 ng L^{-1}, could significantly increase the amount of the blood protein vitellogenin in the plasma of fish (Purdom et al., 1994). Vitellogen is an egg yolk protein precursor which is estrogen-dependent and specific to female fish (Jobling and Tyler, 2003).

The presence of EDCs in treated wastewater used for drinking water augmentation is of great concern due to their potential harmful effects on human health (Mansell and Drewes, 2004). Decrease in the quality and quantity of human sperm over the years is thought to have been caused by exposure to them (Birkett, 2003a). Other health issues believed to be brought about by EDCs such as increased incidence of testicular and prostate cancer, undescended testes (cryptorchidism), malformation of the penis (hypospadias) and breast cancer in women have not been well substantiated (Birkett, 2003a).

The interference of EDCs with reproduction as agonists or antagonists of the steroidal sex hormones (estrogens and androgens) could have serious consequences for sexual differentiation of animals, and is also a source of major concern (Wuttke et al., 2010).

2.8.3.4 Transformation Processes and Mechanisms for Removal of Estrogens

The physicochemical properties of estrogens and site-specific environmental conditions control their distribution and partitioning in the environment (Ying et al., 2002). Environmental conditions include pH, temperature, the presence of suitable microorganisms to carry out the degradation process and the presence of other organics which may either enhance or limit biodegradation of the estrogens (Lim et al., 2007). Physical and chemical properties governing the mechanisms for their removal and biotransformation pathways during treatment are water solubility, octanol-water partition coefficients (K_{ow}) and Henry's Law constant (H_c). The octanol-water partition coefficients influence the partitioning and sorption of the estrogen and the Henry's Law constant determines the potential for evaporation or volatilization. Log K_{ow} of less than 2.5 indicates low sorption potential whilst a value above 4 demonstrates a high potential for sorption (Langford and Lester, 2003). Due to the strong hydrophobic properties of estrogens, sorption is an important mechanism for their removal from wastewater. The H_cs of the estrogens however are much less than 10^{-3} mol^{-1} m^{-3} and thus the likelihood of their volatilisation is very low (Langford and Lester, 2003).

SAT has great potential for the removal of E1 and E2 due to their good rates of degradation under aerobic and anoxic conditions (Ke et al., 2007; Suarez et al., 2010). Secondary wastewater effluent samples collected from SAT infiltration ponds show a marked reduction of estrogenic activity over 24 hours (Conroy et al., 2007). EE2 is however more persistent in anoxic environments such as may pertain in aquifers that are artificially recharged by SAT or direct injection (Ke et al., 2007). Several studies have been carried out on the removal of estrogens in activated sludge treatment plants (Khanal et al., 2006; Racz and Goel, 2010) and their behaviour in soils under laboratory conditions. Not as much attention has been focussed on their removal during SAT.

Estrogens have been found to be removed mainly by sorption and aerobic biodegradation during percolation through the subsurface soil (Fox et al., 2006). In Fox et al's (2006) unsaturated soil column studies simulating SAT, adsorption was found to be the primary removal mechanism. About 79 % of E2 was removed by adsorption after 5.2 to 7.4 hours effective contact time with silica sand. In batch studies with different soil types, removal efficiencies were found to be higher in soils with higher organic, silt and clay contents. About 99 % removal of E2 was attainable in aerobic biologically active saturated and unsaturated columns packed with silica sand. The removal was found to be independent of total biomass activity (Fox et al., 2006). Sorption alone is not a sustainable contaminant removal process in the soil as substances removed by adsorption have the potential to remobilise (Mansell et al., 2004).

Cordy et al (2004) carried out a proof-of-concept experiment to verify if pathogens and pharmaceutical and organic compounds in wastewater including E1, E2 and EE2 would contaminate ground water during SAT. 2.4 m long unsaturated soil columns were used for this purpose. The concentrations of the estrogens in the wastewater effluent infiltrated however were already below the detection limit of 5 ng L^{-1} and as such were not detected in the column effluent. Cordy et al (2004) however concluded that there is the potential for contamination of ground water by pathogens, pharmaceuticals and other organic wastewater contaminants during SAT. Studies of two SAT sites, which had been in operation for more than thirteen years, found the presence of E2, though in low concentrations, after 1.5 m of wastewater infiltration at one site and after 5 m at the other. No breakthrough of hormones into the underlying groundwater however occurred (Fox et al., 2006).

2.8.3.5 Redox Conditions and Estrogen Transformation

In soil column studies, aerobic and anoxic conditions were not found to be of importance in the removal of E2 (Mansell and Drewes, 2004). E1 and E2 are readily biodegradable under a range of temperature and moisture conditions in agricultural soils. EE2 on the other hand has been found to be more resistant to biodegradation or mineralisation than E1 and E2 (Colucci et al., 2001; Jürgens et al., 2002; Stumpe and Marschner, 2009).

E2 was found to degrade slowly in sediments under strict batch anaerobic conditions, the rate and extent of degradation being dependent on the electron acceptor (iron, sulphate, carbon dioxide or nitrate). EE2 however remained resistant to biodegradation, even after several months (Czajka and Londry, 2006). The resistance

of EE2 to degradation partly stems from the presence of the ethinyl group in position 17α, which shields the compound from oxidation to E1 (Gomes and Lester, 2003). In nitrifying environments of activated sludge EE2 has been found to biodegrade quite well (Vader et al., 2000; Shi et al., 2004; Dytczak et al., 2008) and the removal has been attributed to cometabolic transformation mediated by ammonium oxidizing bacteria (Vader et al., 2000; Yi and Harper, 2007). Nitrification in the unsaturated zone followed by denitrification in the saturated zone during SAT is a crucial process for nitrogen removal. It is advantageous that the cometabolic process can proceed without prior adaptation of nitrifying bacteria (Vader et al., 2000) thus providing a barrier against groundwater contamination. Other studies however conclude that at environmentally relevant estrogen and ammonia concentrations, degradation of EE2 is rather mediated by heterotrophic bacteria (Gaulke et al., 2008).

In quite a number of studies, E2 has been observed to transform to its metabolite E1 (Colucci et al., 2001; Jürgens et al., 2002; Czajka and Londry, 2006; Stumpe and Marschner, 2009). Researchers carrying out laboratory microcosm incubation experiments have attributed the transformation to abiotic oxidation processes (Colucci et al., 2001) as well as to microbial oxidation (Czajka and Londry, 2006; Stumpe and Marschner, 2009). Removal of E1 was however found to be only biologically mediated (Colucci et al., 2001). Partial conversion of E1 to E2 under methanogenic conditions has also been observed by some authors, the conversion thought to have occurred as a result of the reduction of the ketone of E1 to the alcohol form of E2 (Czajka and Londry, 2006). The overall biodegradation process for the removal of estrogens from soils infiltrated with wastewater is a complex

process which is dependent on the presence of a stable microbial community in the soil system, substrate concentrations and the availability of nutrients for microbial sustenance (Das et al., 2004).

While the removal of estrogens in during conventional wastewater treatment such as activated sludge and has been well studied, their removal during SAT has not been fully explored. During SAT wastewater infiltrates through layers of saturated and unsaturated subsurface soils and the level of groundwater is expected to fluctuate. Studies undertaken at infiltration sites and in soil columns to assess the removal of wastewater estrogens have so far not addressed this situation. Also, due to the biotransformation of E1, E2 and EE2 from one form to the other, their behaviour as a mixture in the infiltrating wastewater needs to be investigated at short intervals within the soil profile. Information available in this respect is scarce. Objectives 2 and 3 of this study are therefore designed to help bridge these gaps in knowledge.

2.8.4 3, 4, 4´-trichlorocarbanilide (Triclocarban)

3, 4, 4´-trichlorocarbanilide or triclocarban (TCC) is a polychlorinated binuclear aromatic urea pesticide having 36.7 % chlorine content by weight (Halden and Paull, 2005). TCC is hydrophobic and non-volatile in nature with low solubility, high octanol-water partition coefficient (K_{ow}) and high soil adsorption coefficient (K_{oc}). It thus tends to sorb onto soil and sediment (Heidler et al., 2006; Sapkota et al., 2007; Ying et al., 2007). The NH group (Ying et al., 2007), high chlorine content and presence of aromatic rings imparts biodegradation resistance to the compound and the possibility of it persisting in the environment for a long period of time (Halden

and Paull, 2005; Ying et al., 2007). The structure of TCC is shown in Figure 2.15 and its physical and chemical properties are summarised in Table 2.9.

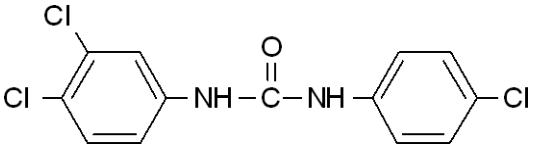

Figure 2.15 Structure of Triclocarban

Table 2.9 Physical and chemical properties of TCC

Property	**Value**
Formula	$C_{13}H_9Cl_3N_2O$
Molecular weight (g mol^{-1})	315.59
Chorine content (wt %)	36.7
Water solubility (mg L^{-1} at 25 °C)	0.65 – 1.55
$Log_{10}K_{ow}$ (at pH 7 and 25 °C)	4.9
Melting point (°C)	140

(Halden and Paull, 2005)

2.8.4.1 Sources of Triclocarban in the Environment

TCC is washed down the drain through household activities and enters water resources through the discharge of wastewater effluents (Heidler et al., 2006; Coogan et al., 2007; Sapkota et al., 2007), leaking sewer pipes and combined sewer overflows (Halden and Paull, 2005). Other potential sources are runoff from land that has been either amended with sludge from wastewater treatment for agricultural purposes or served as a disposal site (Heidler et al., 2006; Ying et al., 2007; Topp et al., 2008) or irrigated with wastewater effluents (Ternes et al., 2007). Wastewater

TCC concentrations in some treatment plants in the UK and US range from 0.4 µg L^{-1} to as high as 200 µg L^{-1}. Concentrations up to 6 µg L^{-1} have been measured in effluents from some wastewater treatment plants in New Jersey (Halden and Paull, 2005). Table 2.10 summarises concentrations measured in some wastewater effluents.

Table 2.10 TCC concentrations measured in wastewater effluents

Country	**TCC concentration (ng L^{-1})**	**Reference**
U.S.	110 ± 10	(Halden and Paull, 2005)
	100 – 6000	(Chalew and Halden, 2009)
	80 – 12 000	(TCC-Consortium, 2002)
	170 ± 30	(Heidler et al., 2006)
	50 – 330	(Klein et al., 2010)
	18 - 130	(Trenholm et al., 2008)
China	23.9 – 342	(Zhao et al., 2010)

2.8.4.2 Effects of TCC Exposure on Living Organisms

TCC imposes toxic influences on a quantity of living organisms (Chalew and Halden, 2009). Manufacturers have labelled TCC with the risk phrase R45 and R46, which indicates the chemical has the potential to act as a carcinogen and also cause heritable disease (Halden and Paull, 2005). Studies have found TCC to have a negative impact on reproduction of rats and the survival and body weight of their offspring. In rabbits, it also caused dose-related maternal toxicity, abortions, weight loss and even death (Nolen and Dierckman, 1979). TCC may adversely affect aquatic organisms such as fish and crustacea (Ying et al., 2007; Chalew and Halden,

2009) and also has the potential to bioaccumulate in algal species and snails (Coogan et al., 2007; Coogan and La Point, 2008). The minimum algistatic concentration toxic to algae is 6 µg L^{-1}, and concentrations above 1.46 µg L^{-1} and 5 µg L^{-1} cause chronic toxicity to aquatic invertebrates and fish respectively (TCC-Consortium, 2002). TCC has also been found to accumulate in the root tissues and translocate into the beans of the soybean plant upon exposure of the crop to biosolids containing TCC and irrigation with contaminated wastewater (Wu et al., 2010).

Mono and di-chlorinated anilines which are TCC breakdown products exhibit ecotoxic, genotoxic and hematotoxic characteristics (Gledhill, 1975). TCC exposure has been linked to methemoglobinemia in humans (Johnson et al., 1963) and can also cause endocrine disruption due to its potential to act as a sex steroid amplifier. In male rats, a diet containing TCC in combination with administered testosterone significantly increased the size of all sex accessory organs. TCC exposure could also cause developmental defects such as cryptorchidism and hypospadias and diminished reproductive function in adults such as a decrease in sperm quality. In females, the amplification of androgens as a result of exposure to TCC could result in disturbance in ovulation and upset the functioning mechanisms of the ovaries. Neurogenesis could also be compromised as a result of TCC exposure in the uterus (Chen et al., 2008).

The composition of biofilm communities and their architecture are very sensitive to environmental stress. Alterations could occur in the thickness of the biofilms, in the distribution of the microbial cells or in the community structure. At a concentration of 10 µg L^{-1}, significant changes were found to occur in river biofilm community

composition. There was a shift from a community composed mainly of autotrophs to one dominated by heterotrophs. Suppression of the utilization of carbon, carboxylic acids and amino acids by microorganisms was also evident (Lawrence et al., 2009).

2.8.4.3 Removal of Triclocarban during Wastewater Treatment and Mechanisms for Removal

Physical, chemical and biological processes are responsible for attenuation of TCC in the environment. Limited information is available on the transformation and mineralization of TCC by bacteria growth (Miller et al., 2010). It has been found to be removed to some extent by biodegradation (Gledhill, 1975) and sorption to sludge, inorganic particles and microbes (TCC-Consortium, 2002). Its biodegradation, though slow, is favoured in aerobic environments. Under anaerobic conditions, TCC has been found to be resistant to biodegradation (Heidler et al., 2006; Ying et al., 2007). In a study on activated sludge treatment about 21 % of TCC was observed to have been biotransformed, lost or could not be accounted for, 76 % partitioned into the sludge where no significant transformation occurred, and the remaining 3 % passed through the plant with the effluent (Heidler et al., 2006). TCC has been detected in effluents at concentrations ranging from 76 ng L^{-1} to 12 000 ng L^{-1} (TCC-Consortium, 2002) and in surface waters at less than 30 ng L^{-1} to 6750 ng L^{-1} (Halden and Paull, 2005).

Different TCC half-lives ranging from 80 days to 231 days have been reported to occur in aerobic soil (Ying et al., 2007; Wu et al., 2009; Cha and Cupples, 2010). 34 % to 53 % TCC removal was attained after 100 days in a range of soils using laboratory microcosms (Cha and Cupples, 2010). Under anaerobic conditions

however minimal biodegradation of TCC occurred over a period of 70 days (Ying et al., 2007). Access to compounds by soil microorganisms is limited when they are sorbed and therefore bioavailability limitations impact negatively on biodegradation rates in soils (Cha and Cupples, 2010). The kinetics and degree to which TCC would sorb or desorb in a natural system is influenced by the kind of organic carbon available and the attainment of equilibrium conditions. The presence of high organic matter would lead to greater sorption and reduced bioavailability (Chalew and Halden, 2009). Leaching models suggest that there is low likelihood for groundwater contamination by TCC due to its very low leaching potential (Cha and Cupples, 2010). Recently, bacteria belonging to the *Alcaligenaceae* family have been identified as capable of utilising TCC and non-chlorinated carbanilide (NCC) as sole carbon sources for growth. The metabolic capability of these bacteria suggests they could be used as an avenue for remediation of TCC polluted environments. TCC concentrations must however be high enough, such as pertains in digested sludge, to sustain their growth (Miller et al., 2010). A TCC biodegradation pathway based on a number of studies has been proposed by Miller et al (2010) and is shown in Figure 2.16. It was proposed that the first step of the degradation pathway is by hydrolysis of the urea bridge of the compound, giving rise to 4-chloroaniline and 3,4-dichloroaniline. Next, deamination of 4-chloroaniline occurs in bacteria and also hydroxylation by an aniline dioxygenase. This results in the production of 4-chlorocatechol. 3,4-dichloroaniline is also degraded into monochloroaniline, probably via dehalogenation, which may in turn undergo deamination and hydroxylation by a dioxygenase enzyme into 4-chlorocatechol. The degradation of 4-chlorocatechol then occurs in *meta*-cleavage and *ortho*-cleavage pathways via 2,3-catechol or 1,2-catechol dioxygenase enzymes, resulting in the production of 5-

chloro-2-hydroxymuconic acid semialdehyde and 3-chloro-*cis,cis*-muconate respectively. 5-chloro-2-hydroxymuconic acid semialdehyde and 3-chloro-*cis,cis*-muconate are lastly degraded by intermediate metabolic pathways and the subsequent bacterial assimilation of carbon and nitrogen occurs (Miller et al., 2010).

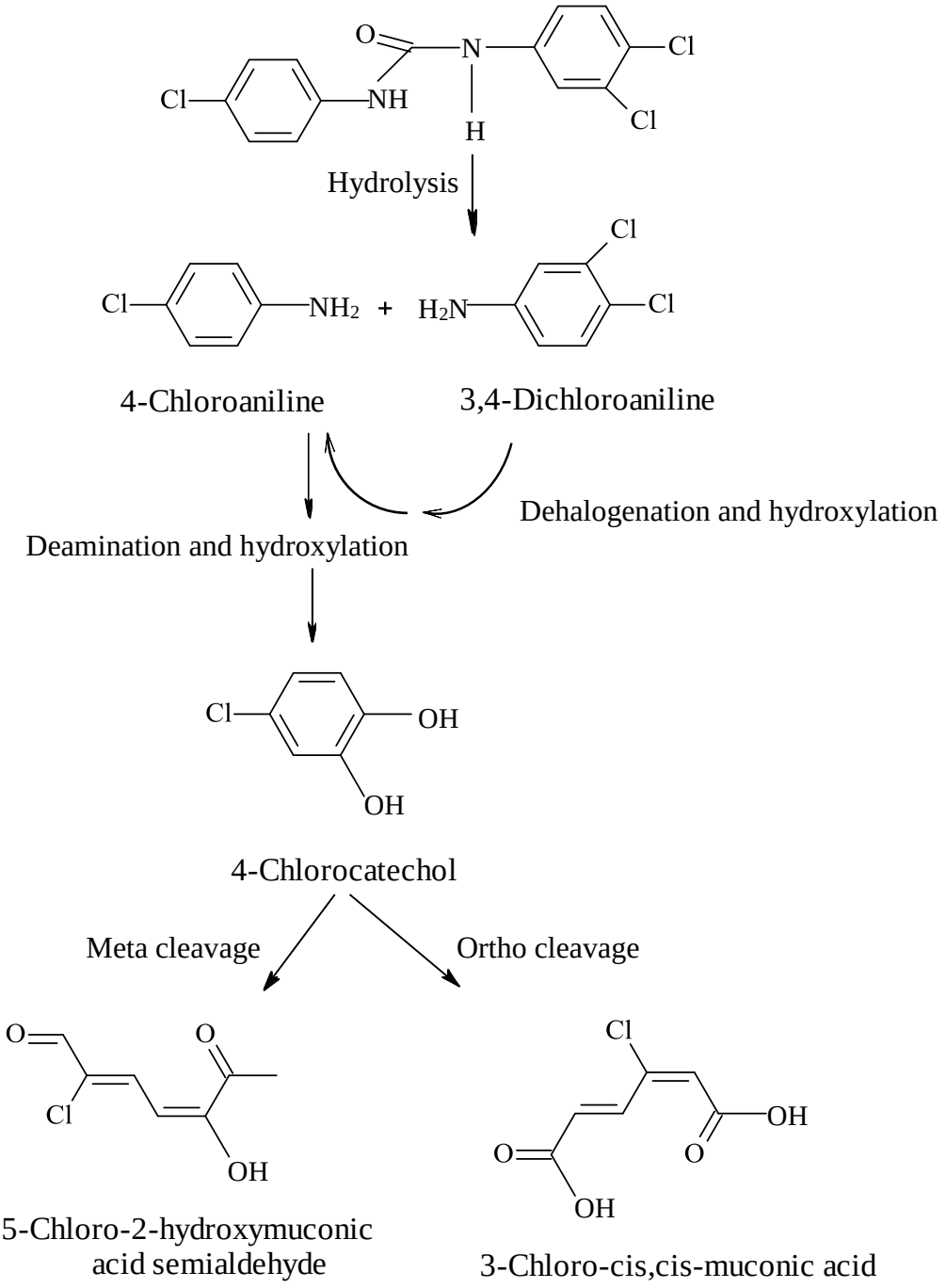

Figure 2.16 Proposed biodegradation pathway of triclocarban

[Reproduced from Miller et al, 2010]

While the removal of TCC from wastewater has been studied in the activated sludge process and also its behaviour in soil under aerobic and anaerobic conditions has been investigated, its removal during passage through the soil in a soil aquifer treatment system has not been assessed and currently there is no information on the efficiency of SAT for the removal of TCC as well as the effects of TCC, if any, on the performance of the SAT system. The purpose of Objective 4 of this study is therefore for the elucidation of this area of research.

CHAPTER 3

3 MATERIALS AND METHODS

3.1 Introduction

This chapter details the procedures followed to achieve the set objectives of this research. Soil aquifer treatment (SAT) was simulated in the laboratory under saturated and unsaturated conditions using long and short soil columns. These are a 2 metre long column, a set of three 1 metre long columns and a short column of length 300 mm. The 2 metre soil column was filled with silica sand and used to investigate the performance of SAT under different hydraulic and organic loading rates. Wastewater parameters measured during the experiments were chemical oxygen demand, biochemical oxygen demand, dissolved organic carbon, nitrogen (nitrate, ammonia nitrogen, organic nitrogen and total nitrogen), phosphate, pH, temperature and dissolved oxygen. Estrogen removal under saturated and unsaturated conditions was studied in 1 metre long soil columns filled with silica sand and also with a mixture of silica sand, silt and clay, whilst triclocarban (TCC) removal was explored using the 300 mm long column containing silica sand as packing material.

1 m soil columns were used to study estrogen removal because results from the 2 m column revealed that a greater part of the removal of wastewater parameters that was realised for the whole 2 m length of the soil column occurred within the first few centimetres. Since the fate of TCC during SAT has never been studied, it was also thought prudent to carry out the studies on a small scale, hence the use of a short column for TCC studies. Required residence times in the soil column can be obtained by selecting the appropriate hydraulic loading rate.

A description of the setups used for the experiments, instruments employed, experimental and calibration protocols and analytical procedures used to measure the concentrations of the parameters of interest are presented. Table 3.1 gives a summary of the main equipment/instruments used in the soil column setups and for the analyses carried out.

Calibration of some of the instruments used was needed in order to be able to convert readings from them into meaningful information in the data format required. The instruments calibrated were:

i. SWT5 Tensiometers
ii. ThetaProbe soil moisture sensors
iii. Ion chromatograph
iv. UV/Vis Spectrophotometer
v. TOC analyser
vi. LCMS
vii. GCMS

The setup and procedures adopted for the calibration of these instruments are detailed in later sections.

Table 3.1 Summary of equipment and instruments used

		Instruments/ Equipment
Setup	Soil column setup	Peristaltic pump Flow meter Water bath Refrigerator
	Instruments	SWT5 tensiometers ThetaProbe soil moisture sensors - type ML2x CONMARK 314 stainless steel digital pocket thermometers UV-Vis spectrophotometer
	Data collection	Data logger Computer Voltage stabilizer
Analysis	Chemical Oxygen Demand (COD)	Hach COD reactor Hach DR/2400 spectrophotometer
	Biochemical Oxygen Demand (BOD)	Hach Sension 6 dissolved oxygen meter
	Dissolved Organic Carbon (DOC)	ISCO Total organic carbon (TOC) analyser with low temperature oxidation
	Total Kjeldahl Nitrogen (TKN)	Tecator 2006 digestor Tecator Kjeltec System 1002 distilling unit
	Ammonia-Nitrogen (NH_3-N)	Tecator Kjeltec System 1002 distilling unit
	Nitrate-Nitrogen (NO_3-N)	Dionex series 4000i Ion chromatograph
	Nitrite-Nitrogen (NO_2-N)	Dionex series 4000i Ion chromatograph
	Phosphate (PO_4)	Dionex series 4000i Ion chromatograph
	Sulphate (SO_4)	Dionex series 4000i Ion chromatograph
	Dissolved Oxygen (DO)	Hach SenseIon 6 Dissolved oxygen meter
	pH	Oakton pH/mV/°C pH 11 series meter
	Triclocarban (TCC)	Liquid chromatograph-mass spectrometer (LCMS)
	Estrogens- liquid samples	LCMS 12-port disposable liner SUPELCO Visiprep™ SPE vacuum manifold and Visidry™ drying attachment
	Estrogens-soil samples	Sonicator LCMS
	Phospholipid Fatty Acid Analysis (PLFA)	Flask shaker Centrifuge Ultraviolet-Visible (UV-Vis) spectrophotometer Gas chromatograph-mass spectrometer (GCMS)

3.2 Studies on Wastewater Hydraulic Loading Rates and COD Effects on Removal Efficiency of Wastewater Parameters during SAT

A 2 m soil column was used to study the effect of wastewater COD and hydraulic loading rates on the removal of DOC, COD, BOD, nitrogen and phosphate.

3.2.1 Soil Column Description and Setup

Figure 3.1 shows a schematic drawing of the soil column setup. A photo gallery of the setup can be found in Appendix A. The column used for this study was made of acrylic tube with an inner diameter 140 mm and length 2000 mm. 10 mm thick flanges were fabricated and attached to the top and bottom of the column. Eight holes were drilled at equal intervals around the circumference of the top and bottom flanges of the column into which helicoil inserts were screwed. These inserts facilitated the tight closure of the tube with top and bottom caps without sustaining any cracks in the tube flanges. The top and bottom caps were fabricated from solid perspex and PVC blocks respectively. The inner part of the top cap was machined to a 15 ° ridge and the apex fitted with a radiator valve for bleeding air out of the column. A threaded hole was also provided slightly offset from the centre of the cap and fitted with a hose adapter. This served as the exit from the column. A 10 mm thick PVC distributor cut out in the form of a labyrinth was mounted on the inner surface of the bottom cap to facilitate even distribution of water over the entire cross section of the column. A 6 mm diameter hole was drilled midway through the thickness of the bottom cap along its cross section. One end of the hole was to serve as an entry port to the column, and the other end was used as a drain.

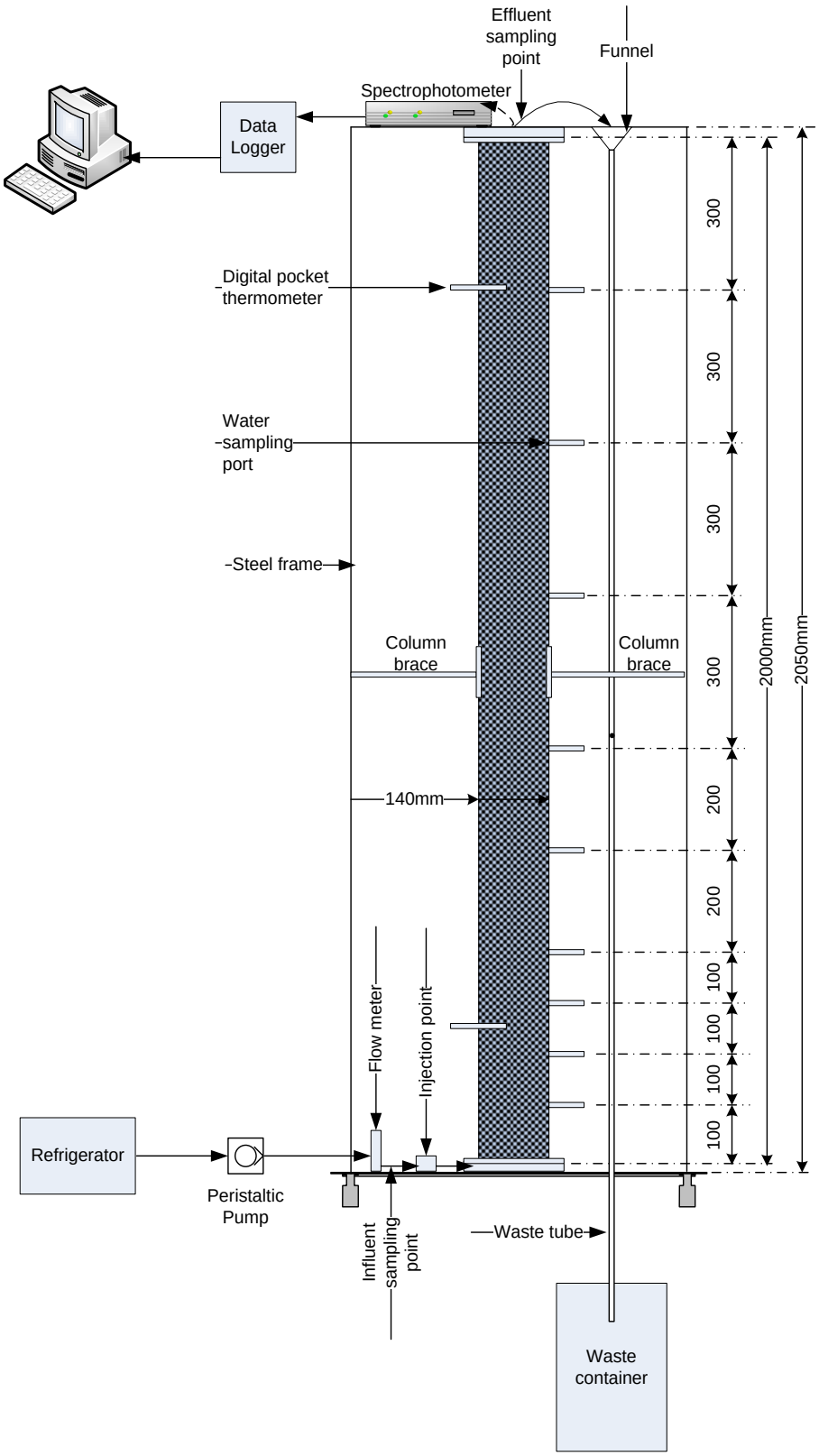

Figure 3.1 2-meter soil column setup

Another 6 mm diameter hole was drilled at right angles in the centre of the cap to serve as an access hole for wastewater into or out of the column. The drain hole was fitted with a 12 mm plastic ball valve and the entry hole with a quickfit/ quick disconnect coupling fitted to a 6 mm inner diameter stainless steel tube. To maintain a water tight seal, a gasket was placed between the tube and the end caps before securing them together with threaded screws complete with washers.

Water sampling points consisting of 3.2 mm inner diameter stainless steel tubes were provided at ten points (100 mm, 200 mm, 300 mm, 400 mm, 500 mm, 600 mm, 800 mm, 1100 mm, 1400 mm and 1700 mm) from the bottom of the column. These sampling tubes extended to the centre of the column's cross section. The sampling ports were closed by means of flexible tubing and a clip. 12 mm plastic ball valves were also provided at 100 mm, 300 mm, 600 mm, 1050 mm, 1400 mm and 1700 mm for soil sampling. Eight valves were equally spaced around the circumference of the column at each level. CONMARK 314 stainless steel digital pocket thermometers were inserted at 170 mm from the bottom and 170 mm from the top of the column to monitor the column temperature. An injection port consisting of a down-turned T-shaped glass tube with access via a screw cap with a septum stopper at the bottom of the 'T' was provided in the influent line at the column entry for injection of a tracer during residence time studies. The column was mounted in a steel frame with a wooden bottom support. A funnel and tubing arrangement was provided on the frame at the same height as the top of the column for discharge of the effluent from the column.

The column was packed to a density of 1.55 g cm^{-3} under saturated conditions with uniform silica sand of effective diameter of 0.51 mm and average diameter of 0.75 mm, obtained from WBB Minerals. Sieve analysis was performed to obtain the grading curve for the sand. The uniformity coefficient of the sand and porosity of the packing were found to be 1.6 and 0.41 respectively. Water saturated conditions in the column was achieved by ensuring that the water level in the column was always above the surface of the sand during packing. Sand was poured into the column using a funnel and large diameter tube arrangement. To ensure uniform packing, the water level in the column was maintained at 50 mm above the surface of the sand and the exit of the tube always kept at an equal height above the water surface so that the sand particles dropped from the same height. During filling, the tube was gently moved over the entire cross section of the column to uniformly distribute the sand. The tubing was shortened as the column filled up. After filling, the column was wrapped with aluminium foil to shut out light and discourage the growth of algae during operation. A Watson-Marlow 505S peristaltic pump with variable speed was used to deliver wastewater to the column through soft tygon tubing and a flow meter, which was fully opened and used for monitoring of flow to the column.

3.2.2 Column Startup and General Operation

The sand column was set up in a controlled temperature room set at 20 °C ± 0.5 °C. Synthetic wastewater was prepared by dilution in tap water of a stock solution containing chemicals in concentrations as shown in Table 3.2. All chemicals used were of analytical grade and were obtained from VWR International. The stock solution was prepared in deionised water and is based on the OECD standard sewage (OECD, 1996) and modified by Prochaska and others (Prochaska et al., 2007). The

substitution of NH_4Cl for urea in the original OECD recipe by Prochaska *et al* (2007) was preferred, as urea is usually not found in effluents due to its fast rate of decomposition (Tchobanoglous et al., 2003). Also the addition of glucose in the preparation as a carbon source provides an avenue for easy manipulation of the COD of the influent without changing the concentrations of the other chemicals in the preparation. The prepared stock solution was kept in the fridge at 4 °C and dilutions prepared daily and aerated continuously with laboratory air for application to the column. Aeration was required to keep the influent wastewater aerobic. After three to four days the solution was discarded and a fresh one was prepared.

Table 3.2 Composition of synthetic wastewater

Chemical	**Concentration ($g\ L^{-1}$)**
Peptone	9.60
Meat extract	6.60
Glucose	12.00
Sodium chloride (NaCl)	0.42
Ammonium chloride (NH_4Cl)	3.42
Calcium chloride dihydrate ($CaCl_2.2H_2O$)	0.24
Magnesium sulphate heptahydrate ($MgSO_4.7H_2O$)	0.12
Anhydrous dipotassium hydrogen orthophosphate (K_2HPO_4)	1.68

As the wastewater to be passed through the column contained no microorganisms that are usually encountered in wastewater treatment plants, it was found essential to initially seed the influent wastewater with microorganisms. A non-pathogenic

microbial seeding solution prepared from capsules containing a blend of microorganisms normally found in wastewater and used for biochemical oxygen demand (BOD) determination in wastewater analysis was used for this purpose. These capsules were obtained from Cole-Parmer, UK. To prepare the seed solution, the contents of one capsule was emptied into a conical flask containing 500 mL dilution water as used for BOD tests and aerated for one hour. The seed solution was introduced regularly into the influent line via the injection port (see Figure 3.1) at a volume of 5 mL for every 500 mL of synthetic wastewater diluted to obtain a chemical oxygen demand (COD) of 135 mg L^{-1}. Wastewater was supplied to the column at a rate of 10 mL min^{-1} during seeding. Seeding was stopped after about twice the volume of voids of wastewater had been passed through the column and only the synthetic wastewater fed to the column afterwards at a rate of 5 mL min^{-1}. The soil column was fed from the bottom to top throughout the experiments to maintain fully saturated conditions. Three months were allowed for growth of microorganisms in the soil and the establishment of steady state conditions as evidenced by near constant concentrations of wastewater parameters in column wastewater samples.

Routine cleaning and sterilizing of the tubing and flow meter was carried out twice a week with chlorine based sterilizing tablets. It was found that less frequent cleaning led to an appreciable reduction in the dissolved oxygen available in the influent, especially in the case where the high concentration wastewater was fed to the column.

3.2.3 Residence Time Distribution Studies

Residence time distribution tests were carried out at three hydraulic loading rates (HLR) being 44 cm d^{-1}, 88 cm d^{-1} and 169 cm d^{-1}, using 25 g L^{-1} fluorescein sodium salt purchased from Sigma-Aldrich, UK as a tracer. The tracer was prepared by dissolving 2.5 g of the salt in 100 mL of deionised water. Fluorescein concentrations were measured with an Ultraviolet-Visible spectrophotometer commonly referred to as UV/Vis spectrophotometer which is able to measure the intensity of light passing through a sample. During the test, the spectrophotometer was connected to a data logger and a flow through cell used in order to obtain continuous readings.

The spectrophotometer was calibrated before use so that absorbance readings obtained from the residence time distribution tests could be converted to fluorescein concentrations. The spectra of fluorescein was first developed to determine the wavelength at which maximum absorbance of the tracer occurs. This wavelength was found to be 489 nm and thus the calibration of the UV/Vis spectrophotometer was carried out at that wavelength. This figure compares closely with 490 nm measured elsewhere (Sjoback et al., 1995; Doughty, 2010). For the calibration, eight solutions of different concentrations of fluorescein were prepared by dissolving the salt in deionised water. Each solution was placed in a cuvette and the absorbance read at 489 nm and recorded. The cuvette was washed out with deionised water and a portion of the new sample before being read. A calibration curve was developed by plotting the data logger signal (mV) against the fluorescein concentration (mg L^{-1}). This curve is shown in Figure 3.2.

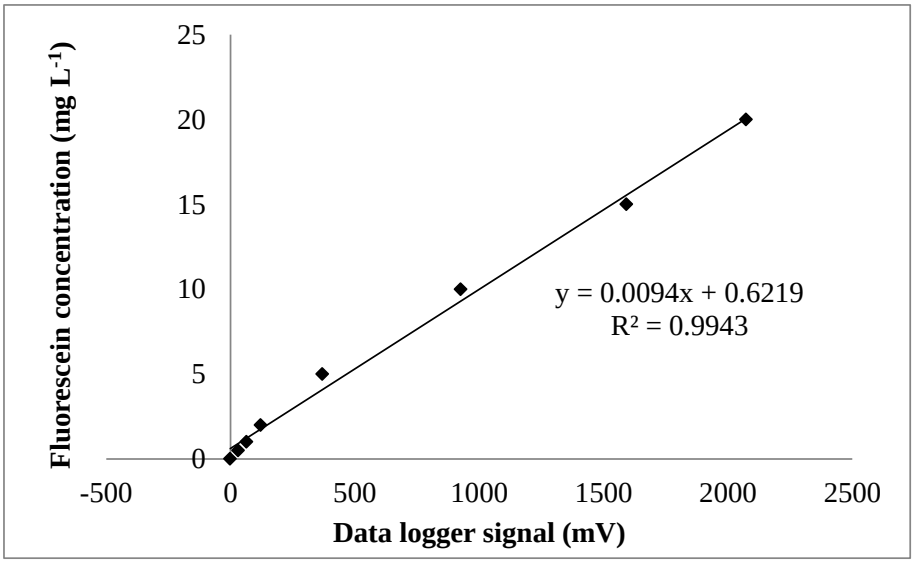

Figure 3.2 Fluorescein calibration curve

To develop the tracer concentration curve for the soil column, the effluent tube from the column was connected to the entry port of the flow-through cell of the UV/VIS spectrophotometer, and another tube connected to the exit end and allowed to discharge into the funnel provided for discharge of column effluent. It was ensured than no air bubbles were trapped within the flow-through cell and the flow was steady. The spectrophotometer was connected to a PICO ADC-16 data logger linked to a desktop computer for data acquisition and storage. The Picolog recorder (PICO software) was set at a sampling rate of 1 sample per minute. The spectrophotometer was set to a wavelength of 489 nm, which was chosen based on the result of the preliminary spectra test showing that maximum absorbance for fluorescein occurred at this wavelength. The instrument was then zeroed and 2 mL of the tracer solution rapidly injected as a pulse input through the injection port using a syringe. At the same time, the data collection by the Picolog recorder was started and the absorbance data at the effluent end as measured by the spectrophotometer acquired on the computer. After the tracer had passed through the column, indicated by the

development of the full development of the output tracer response curve and a return in spectrophotometer absorbance readings to the initial, the data collection was ended and the data downloaded for further processing. The absorbance readings were converted to tracer concentrations using the calibration curve previously developed (Figure 3.2). The tracer response curve was then analysed to obtain the mean residence time, τ (T; min) in the column at the hydraulic loading rate applied using Equation 3.1 (Levenspiel, 1999).

$$\tau = \frac{\int_0^\infty tC(t)dt}{\int_0^\infty C(t)dt} \quad \text{.....[3.1]}$$

where *C(t)* is the fluorescein concentration measured at time *t*.

The residence time was used to determine the appropriate period between the time of wastewater application and the time for obtaining wastewaters samples from the soil column during the SAT simulations.

3.2.4 SAT Simulations

The column experiments were run at three hydraulic loading rates and three COD concentrations. The wastewaters have been classified according to strength as high concentration (HC), medium concentration (MC) and low concentration (LC). Table 3.3 gives the average characteristics of the wastewater applied. pH of the influent was about 7.2. The experimental conditions are shown in Table 3.4.

Table 3.3 Influent characteristics

Parameter	**Average Concentration (mg L^{-1})**		
	HC	**MC**	**LC**
Chemical oxygen demand (COD)	135	61	42
Biochemical oxygen demand(BOD)	88	43	26
Dissolved organic carbon (DOC)	50	26.6	16
Total kjeldahl nitrogen (TKN)	15	6.7	4.1
Ammonia nitrogen (NH_3-N)	4	1.7	1.4
Organic nitrogen (Org-N)	11	5	2.7
Nitrate nitrogen (NO_3-N)	2.5	2.3	2.4
Total nitrogen (TN)	17.5	9	6.5
Phosphate (PO_4)	6.7	4.4	4
Sulphate (SO_4)	50	56	50

Table 3.4 Experimental conditions

Experiment	**Number of experimental replicates**	**Hydraulic loading rate (cm d^{-1})**	**Wastewater concentration**
HC-5	9	44	High concentration
HC-10	6	88	High concentration
HC-20	6	169	High concentration
MC-20	3	169	Medium concentration
LC-20	3	169	Low concentration

For each SAT experiment, wastewater was sampled from water sampling ports provided at depths of 100 mm, 600 mm, 1100 mm and 1700 mm along the column (see, Figure 3.1). Samples were not taken from all the ports provided as it was realized after initial analysis of test samples that the column wastewater quality did not vary much after the 100 mm sampling point. Influent samples were collected close to the column entry and final effluent from a column sampling port Teed from the discharge tube at a position very close to the exit point. The experiments were replicated under all experimental conditions to verify the results obtained. These are shown in Table 3.4. Replications involved sampling influent wastewater and collecting samples from each point along the soil column on another day. All collected samples were analyzed for BOD, COD, DOC, TKN, total nitrogen, organic nitrogen, ammonia nitrogen, nitrate, nitrite, phosphate and sulphate according to established methods, which are later described. Total nitrogen was determined by calculation as the sum of the TKN, nitrate and nitrite. Organic nitrogen was obtained by subtraction of ammonia nitrogen of the sample from the TKN. During the period of acclimation of the soil column, each soil column sample collected was analysed twice to verify the reproducibility of the wastewater analysis. The results of technical replicates were identical and so samples collected during the experimental stages were analysed once.

A water bath was used to raise the temperature of the influent wastewater to 20 °C when wastewater was being fed to the column at a hydraulic loading rate of 169 cm d^{-1}. This was achieved by immersing a short portion of the influent tubing in the bath. Regular maintenance of the soil column influent line and all accessories in contact with the influent wastewater was carried out to eliminate growth of

microorganisms. Growth of microorganisms in influent tubing led to decreases in influent wastewater parameters such as a COD and dissolved oxygen. This effect was especially pronounced when wastewater of high concentration was being applied to the column. The column was isolated during the cleaning operation with the influent sampling line being used as the waste line. Tubing and the flow meter were cleaned by squeezing the tubing to dislodge attached growth and flushing them with a double strength of sterilization solution prepared from Milton sterilization tablets. The pump was allowed to run dry to strip off any biological attachments developed in the flow meter. Tap water was then passed through the sterilised tubing and flow meter before being put back in line with the column.

3.2.5 Soil Column Soil Biomass Measurements

To compare the removal profiles obtained from the experiments with the soil column microbial profile, sand was sampled from the soil column at 100 mm, 300 mm, 600 mm, 1050 mm, 1400 mm and 1700 mm for phospholipid fatty acid analysis. The sand samples were freeze dried and 3 g weighed out into large test tubes. 28.5 mL of a one phase extraction mixture consisting of chloroform, methanol and 50 mM phosphate buffer at pH 7.4, in the ratio 1: 2: 0.8 was added to each tube, shaken and allowed to extract for 2 hours in the dark. The buffer was prepared by dissolving 8.7 g dipotassium hydrogen phosphate (K_2HPO_4) in water to make a total volume of 1 L and neutralising with 1 N hydrochloric acid (HCl) to a pH of 7.4. After the extraction period the solvents were partitioned from the aqueous phase by the addition of 7.5 mL chloroform and 7.5 mL deionised water. The tubes were shaken, centrifuged for 10 minutes at 2500 rpm and allowed to separate overnight. The surface layer was pipetted off and the chloroform layer containing the lipids filtered through

Whatmans 2E filter paper. 2 mL of filtrate was transferred to digestion tubes, dried under a stream of nitrogen and the phosphate liberated by potassium persulphate digestion. The digestion step involved the addition of 0.45 mL of saturated potassium persulphate solution to the dry sample and overnight incubation at 95°C. Saturated potassium persulphate solution was prepared by dissolving 5 g potassium persulphate in 0.36 N H_2SO_4 to a final volume of 1 L. 0.1 mL of 2.5 % ammonium molybdate ($(NH_4)_6Mo_7O_{24}.4H_2O$) in 5.72 N H_2SO_4 was added to the digested sample and a 10 minutes reaction time allowed. 0.45 mL of a solution containing 0.011 % malachite green and 0.111 % polyvinyl alcohol in water was added and left to stand for a further 30 minutes. The absorbance was then read at a wavelength 610 nm in a UV/Vis spectrophotometer. The instrument was zeroed with deionised water (Findlay et al., 1989).

A calibration line (Figure 3.3) was developed by digesting known concentrations of glycerol phosphate calcium salt and determining the absorbance. Absorbance readings obtained from sand samples were converted to phosphate concentrations using the regression line. The phosphate concentrations were converted to cell numbers by equating 0.1 nmol phosphate to approximately 3.4×10^6 cells (Findlay et al., 1989).

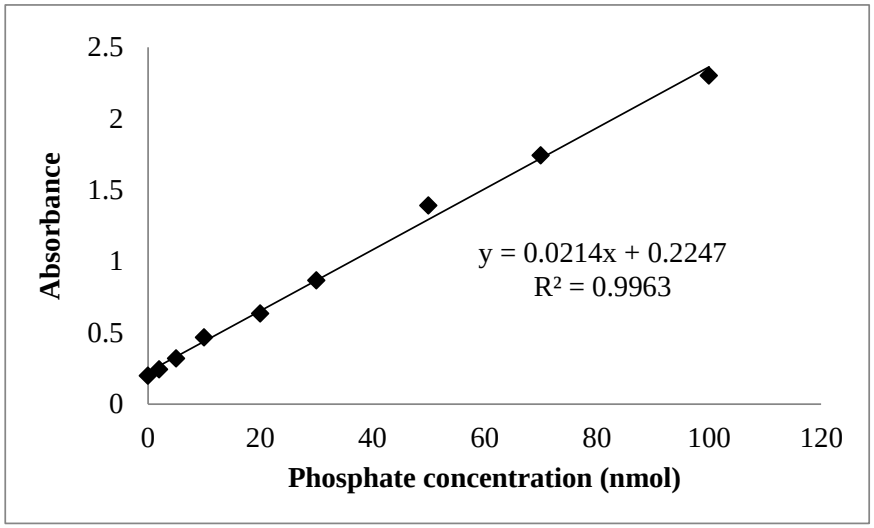

Figure 3.3 Phosphate calibration curve

3.2.6 Abiotic Soil Column Experiments

To evaluate removal of contaminants by processes other than biodegradation such as sorption, the soil column experiments were repeated under abiotic conditions. To achieve this, the soil column was sterilised and flushed well with tap water. LC wastewater was applied to it at a hydraulic loading rate of 169 cm d^{-1} and samples collected from the same points as done previously and analysed for COD, DOC, SO_4, PO_4, NO_3, TKN and NH_4-N.

3.3 Studies on the Removal of Estrogens under Saturated and Unsaturated Soil Conditions

Experiments on the removal of the estrogens estrone (E1), 17β-estradiol (E2), and 17α-ethinylestradiol (EE2) were undertaken using three 1 m long soil columns, two of which were saturated denoted by SC2 and SC3, and the other unsaturated namely SC1. All the soil columns were operated under aerobic conditions.

3.3.1 Soil Column Description and Setup

Each of the soil columns was fabricated from opaque PVC tubing of inner diameter 150 mm. Figure 3.4 shows a schematic diagram of the experimental setup. Water sampling ports were provided at 100 mm intervals from 150 mm to 850 mm along the height of the column. However a number of points were selected from these for sampling as shown in Figure 3.4. The water sampling ports were made of 6 mm outer diameter stainless steel tubes and covered internally by a stainless steel mesh to allow only for water flow. The end protruding out of the column was fitted with tygon tubing and closed with 3 mL syringes. Soil sampling ports made of plastic ball valves were provided at the same depth as the water sampling ports. The bottom of the column was fitted into a PVC flange and closed with a plate of the same material on which a distributor cut out in the form of concentric circles was mounted. Two gutters were cut across the circles to allow water flow over the whole cross section of the distributor. This distributor was to facilitate even distribution of water over the entire cross section of the saturated column and draining of the unsaturated column.

The top cap of the saturated columns was a 20 mm thick PVC plate. A shallow cone was cut out of the inner surface of the plate to allow easy removal through the outlet, of any air that may be trapped in the column. The column outlet comprised a 6 mm hose adaptor screwed into a threaded hole in the centre of the top cap. The top and bottom caps were secured onto the columns with bolts. Gaskets were placed between the caps and the column before closure to ensure a water tight seal. Each soil column was connected to a peristaltic pump, and a flow meter connected between the pump and the inlet to the column to accurately measure the wastewater flow rate.

CONMARK 314 water proof pocket thermometers were inserted midway of all three columns to monitor their internal temperature.

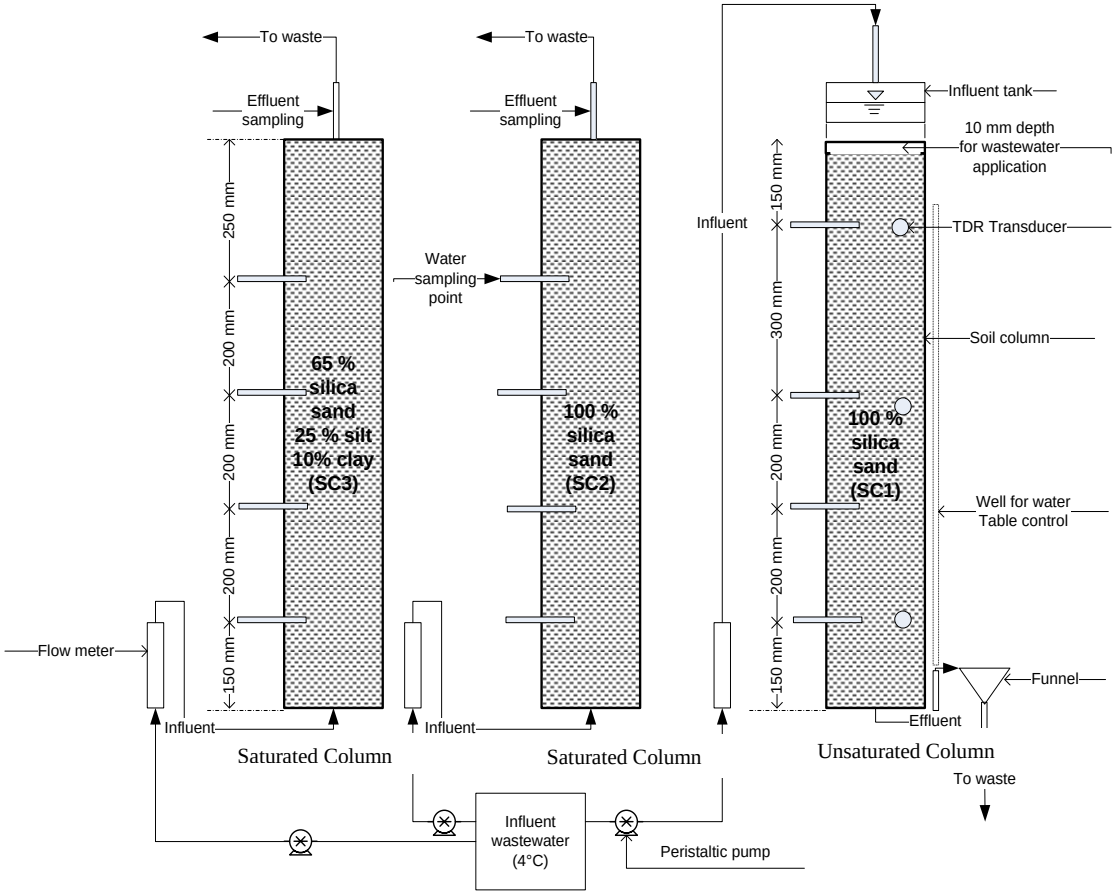

Figure 3.4 1-meter soil column setup

On the unsaturated soil column, access holes were provided at 150 mm, 500 mm and 850 mm for the insertion of SWT5 mini tensiometers for the measurement of soil water potential. The tensiometers were calibrated and secured into the column using M25 cable glands. Ports were also provided at the same level but on opposite sides to the tensiometers for insertion of Theta probes to monitor volumetric water content/degree of saturation in the soil. Volumetric water content (θ_v, $m^3.m^{-3}$) is the ratio between the volume of water present in a soil sample and the total volume of

the sample. These instruments were connected to an Agilent datalogger and a voltage stabiliser delivering a stable voltage of 10.6 V required by the tensiometers. The tensiometers and soil moisture sensors are described in the next subsection and their calibration curves presented therein.

The unsaturated soil column was left open at the top. A small PVC container fitted on the top of the unsaturated soil column served as a distribution tank. Holes were evenly distributed into the bottom of the container and hypodermic needles inserted into them for water distribution onto the sand surface. Four short rods were fitted at the bottom of the container so it could sit directly on top of the column without obstructing air flow into the column, thus maintaining a continuous air phase in the soil column with the ambient air. The container was closed with a 20 mm thick PVC plate. A hose adaptor was fitted into the centre of the cover plate and served as the entry port. Screwing down the lid of the SC1 distribution tank ensured that no wastewater could flow out until the pump was turned on. The wastewater hydraulic loading rate to the column could thus be solely controlled by the pump. A well was connected to the outlet of the soil column for accurate control of the water level inside the soil column. The end of the tube was attached to a funnel for discharge of wastewater from the column. Varying the level of the well outlet controlled the thickness of the unsaturated zone and maintained the level of water throughout the test at predetermined heights.

All three soil columns were mounted on a wooden platform, raised off the ground to allow access to the bottom of the columns. All the soil columns were prepared under fully saturated conditions by pouring soil into partially water-filled columns as

described previously for the 2 meter soil column. SC1 and SC2 were filled with silica sand. After filling, water in SC1 was drained from the base down to a predetermined level to create an unsaturated sand column. SC3 was filled with a soil mixture comprising 65 % silica sand, 25 % silt and 10 % clay. The three materials were mixed together in a tray together with some water to help the silt and clay stick to the grains of silica sand before the homogeneous mixture was poured into the column. Since low plasticity clay and silt were used, the mix did not exhibit any cohesive characteristics. After the filling process, the soil columns were seeded with the BOD capsules using the same method as employed during the seeding stage of the 2000 mm long soil column.

3.3.1.1 Description and Calibration of SWT5 Tensiometers

The SWT5 (Figure 3.5) is a miniature tensiometer designed for point measurements of soil water tension and creates minimal disturbance of the soil into which it is inserted. It consists of a water tight sensor body which houses the pressure transducer and all electronic parts, a transparent acrylic glass shaft and a high grade porous sintered Al_2O_3 ceramic cup of diameter 5 mm and length 5 mm. The length of tensiometer shaft used was 100 mm. The measurement range of the instrument is +100 kPa of water pressure down to -85 kPa of soil water tension. The tensiometers were obtained from Delta-T Devices Ltd., UK. The tensiometers were powered by a stabilized voltage of 10.6 V DC through an Agilent 34970A Data Acquisition / Data Logger Switch Unit and kept constant by a voltage stabilizer. The instrument's signals were recorded on the data logger and downloaded onto a computer.

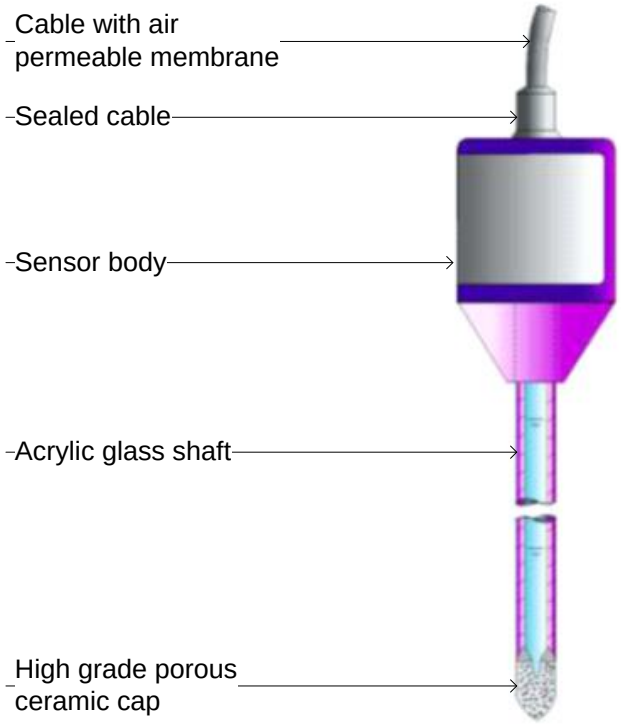

Figure 3.5 SWT5 Tensiometer

Principle of Operation

The movement of water through soils depends directly on the soil water tension, with the water moving from a point of higher potential to a point of lower potential. The majority of soil water flows take place in response to small water tensions which can be measured precisely and directly by the tensiometer. When the tensiometer is inserted into the soil, the soil water tension is transferred as a negative pressure through the ceramic cup to the pressure sensor. The piezoelectric pressure sensor of the instrument then measures the soil water tension against the atmospheric pressure, which is conducted through an air-permeable membrane on the cable to the reference side of the sensor. The pressure transducer presents the soil water tension as a linear

output signal which is captured by the datalogger and saved on a personal computer (PC).

Calibration of SWT5 Tensiometers

The tensiometers purchased were already factory calibrated. They were however recalibrated in order to develop individual calibration lines for the conversion of the analogue output signal from each tensiometer (mV) to pressure head (cm) and improve on the accuracy of the calibration curve given by the manufacturer. The tensiometers are identified as SWT5-165, SWT5-166 and SWT5-167. Figure 3.6 shows the setup used for the calibration of the tensiometers. The setup consisted of a 10 mm diameter glass tube (calibration tube) of 1.8 m to which was connected a 150 mm long perspex tube of inner diameter 50 mm. Each end of the perspex tube was closed with a solid PVC plate. A threaded hole was made on one end for the insertion of a PG7 cable gland through which the tensiometer would be inserted during the calibration. At the other end of the tube, another hole was drilled and a short 6 mm rigid tube inserted for attachment to the glass tube which would be filled with water to serve as the water head against which the calibration would be done. The calibration tube was fitted with a T-junction and a tap for lowering the water level in it during the calibration. The tube was then fitted with clips onto a vertically mounted graduated board.

All three tensiometers were calibrated in a controlled temperature room using the following procedure. Room temperature was 20 ± 0.5 °C. The perspex tube to house the tensiometer was first filled with water. The whole length of shaft of the tensiometer was inserted through the cable gland ensuring that no bubble was

trapped in the tube and the gland tightened just enough to prevent leakage of water from the tube. The perspex tube containing the tensiometer was then fitted horizontally into clips mounted towards the bottom of the graduated board to calibrate for positive pressure and hence saturated flow. A spirit level was used to check that the tensiometer was horizontal. The tensiometer was then connected to a data logger which was set to scan once every minute. A voltage stabilizer was connected to the data logger to maintain a steady voltage of 10.6 V.

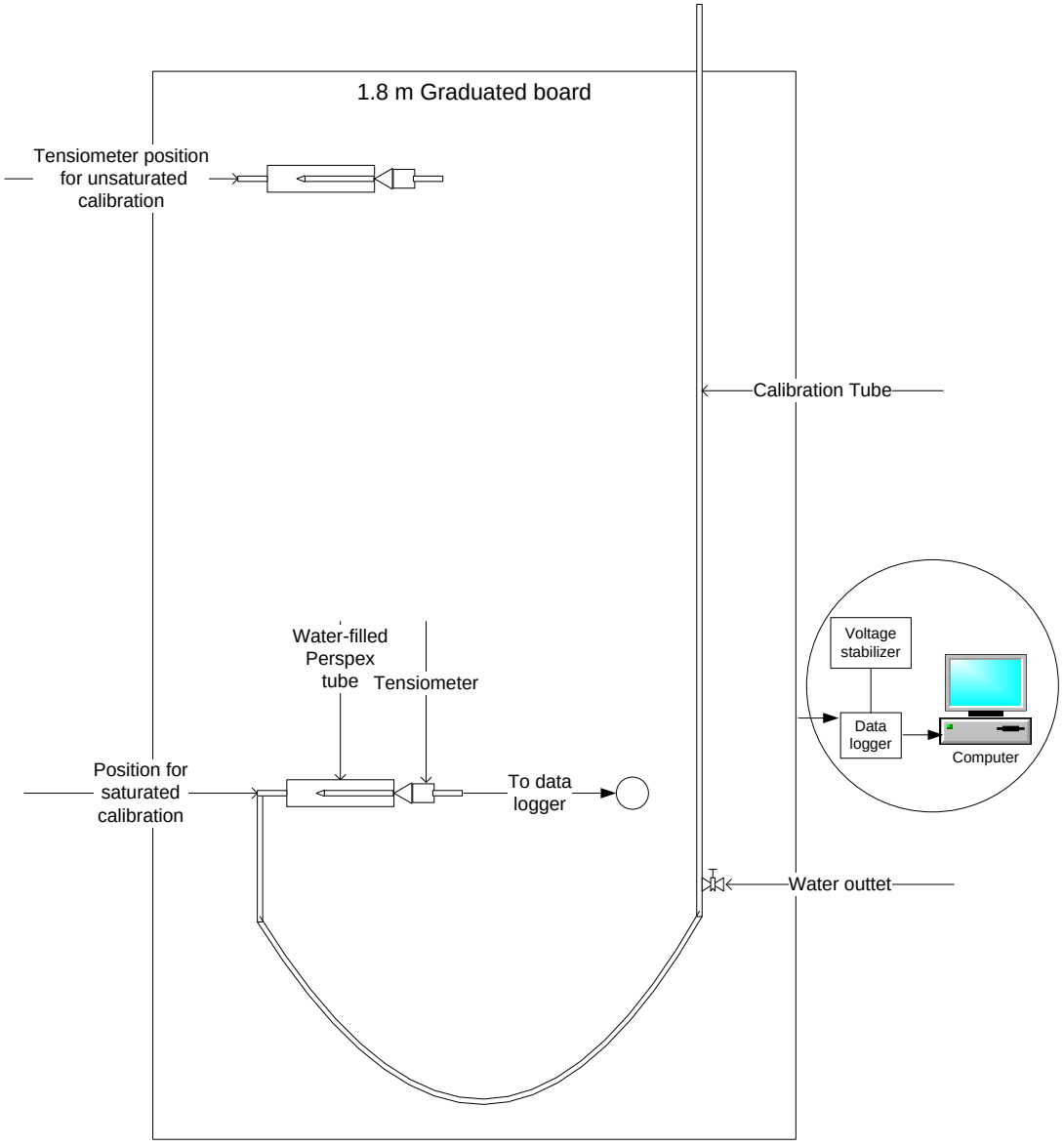

Figure 3.6 Calibration setup for tensiometers

The calibration tube was filled with water to a height of 180 cm on the graduated board and the corresponding tensiometer readings recorded over a time interval of at least 20 minutes. The water level was dropped in steps of 10 cm and tensiometer readings taken each time until the water level was at 15 cm. The pressure head was determined as the difference between level of the centre line of the tensiometer and the water level in the calibration tube for each measurement taken. To calibrate for negative pressure and thus unsaturated situations, the perspex tube housing the tensiometer was mounted towards the upper half of the board so that the water level in the calibration tube was always below the tensiometer. The water level was again lowered in steps of 10 cm and tensiometer readings recorded. The pressure head was determined as before. The calibration curve was developed by plotting the positive and negative pressures against the average of the corresponding tensiometer reading and the points fitted by a linear curve. The curves obtained are shown in Figure 3.7. R^2 obtained in all cases was 1.

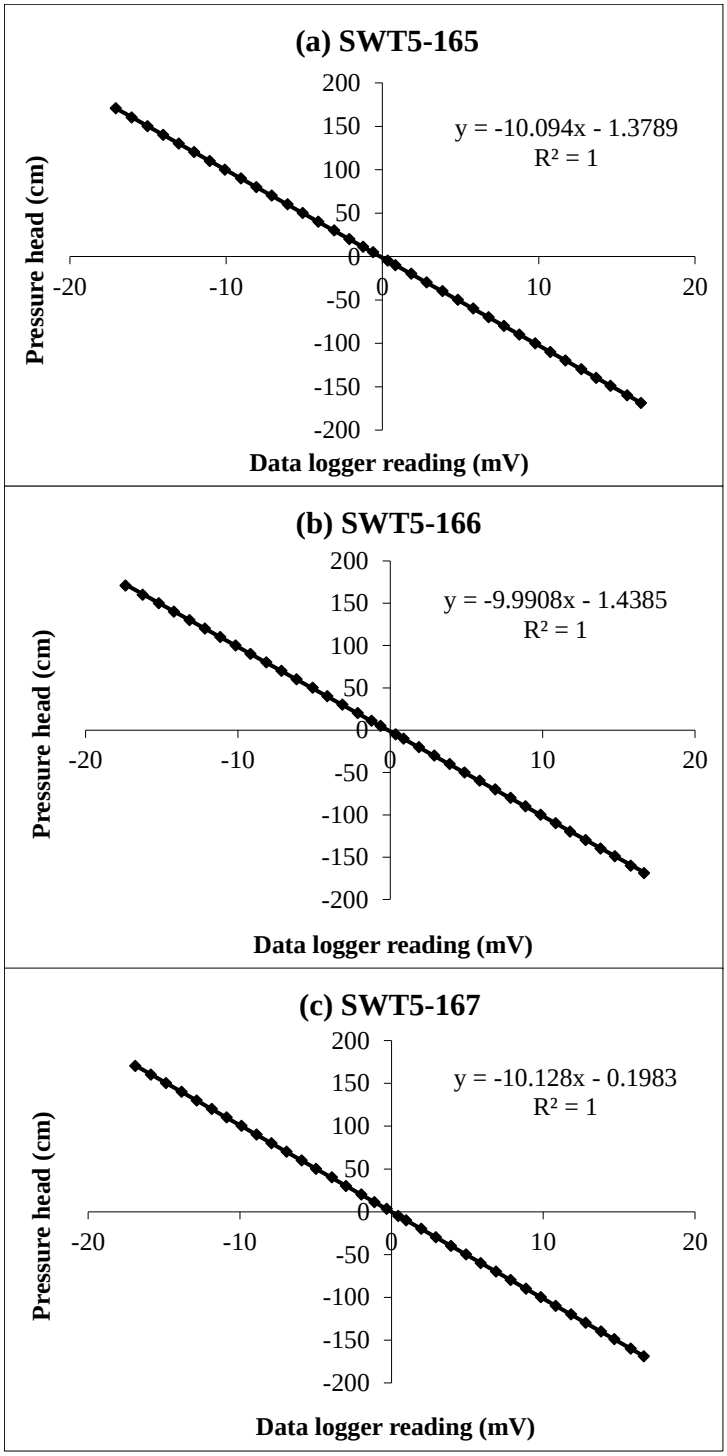

Figure 3.7 Calibration curves for SWT5 tensiometers

3.3.1.2 Description and Calibration of Soil Moisture Sensors

The *ThetaProbe* (Figure 3.8), used to measure volumetric soil moisture content in the unsaturated soil column, consists of a waterproof housing containing the

electronic components with four sharpened stainless steel rods protruding from the housing. These rods are inserted into the soil when measurements are to be made. It operates by responding to changes in the apparent dielectric constant of the soil, which are then converted into a DC voltage. This voltage is proportional to the moisture content of the soil over a wide working range.

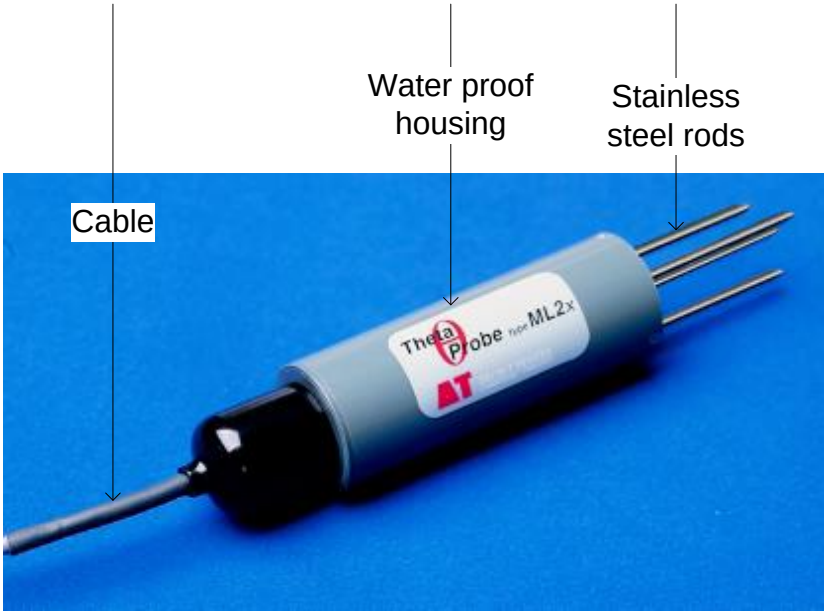

Figure 3.8 ThetaProbe soil moisture sensor

Principle of Operation

During operation, the ThetaProbe generates a 100 MHz sinusoidal signal which is applied to an internal transmission line that extends into the soil by means of the four stainless steel rods. The impedance of the array of rods varies with the impedance of the soil, composed of the ionic conductivity and the apparent dielectric constant. The 100 MHz signal frequency minimizes the effect of ionic conductivity thus making changes in the transmission line impedance dependent almost entirely on the soil's apparent dielectric constant. As the dielectric constant of water, which is about 81,

far exceeds that of soil, which typically ranges from 3 to 5, and air which has a value of 1, the dielectric constant of the soil is determined mainly by its water content. The impedance of the rod array affects the reflection of the 100 MHz signal. A combination of these reflections with the applied signal, form a voltage standing wave along the transmission line. The output is an analogue voltage that is proportional to the difference in amplitude of this standing wave at two points, thus giving rise to a sensitive and precise measure of the soil water content.

Calibration of Thetaprobe Soil Moisture Sensors

In all, three soil moisture sensors were calibrated. These are TDR-061, TDR-064 and TDR-065. The ThetaProbe soil moisture sensors were connected to a data logger and a voltage source through a connector. Three pre-weighed 1 litre containers were packed with dry silica sand in three layers ensuring that each layer was tamped equally. The packed container was weighed once again and the reading noted. One probe was inserted vertically in each container and a scan of the output signal voltage of each probe taken every 15 seconds over 5 minutes and the readings noted. Sand was sampled from each container at the points where the probes were inserted into pre-weighed containers, weighed and placed in the oven at 105 °C to be reweighed after 24 hrs. The dry sand was poured out into separate trays and each batch thoroughly mixed with some water to achieve about 2 % moisture content. The containers were then repacked with all the moist sand in the same way as the dry sand and weighed. The probes of the soil moisture sensor were inserted once again into the containers and the output voltage recorded. This procedure was repeated with increasing amounts of water, each time taking samples for moisture content determination until the probe readings did not increase anymore. To maintain a

constant dry density for each test, the moist sand was discarded, an equal weight of dry sand taken, the required amount of water added to approach the target moisture content and all the sand packed into the container. The average of the probe output signal for each test was plotted against the volumetric water content calculated from results of the moisture content test and the best curve fitted. The relevant equations used are shown by Equations 3.2 and 3.3.

$$Moisture\ content = \frac{(mass\ of\ wet\ sand - mass\ of\ dry\ sand)}{mass\ of\ dry\ sand} \quad \text{.....[3.2]}$$

$$Volumetric\ water\ content\ (\%) = \frac{moisture\ content \times mass\ of\ dry\ sand\ (g)}{volume\ of\ sand\ (cm^3) \times density\ of\ water\ (g\ cm^{-3})} \times 100 \quad \text{....[3.3]}$$

A fourth degree polynomial was fitted to the data points obtained. The calibration curves are shown in Figure 3.9.

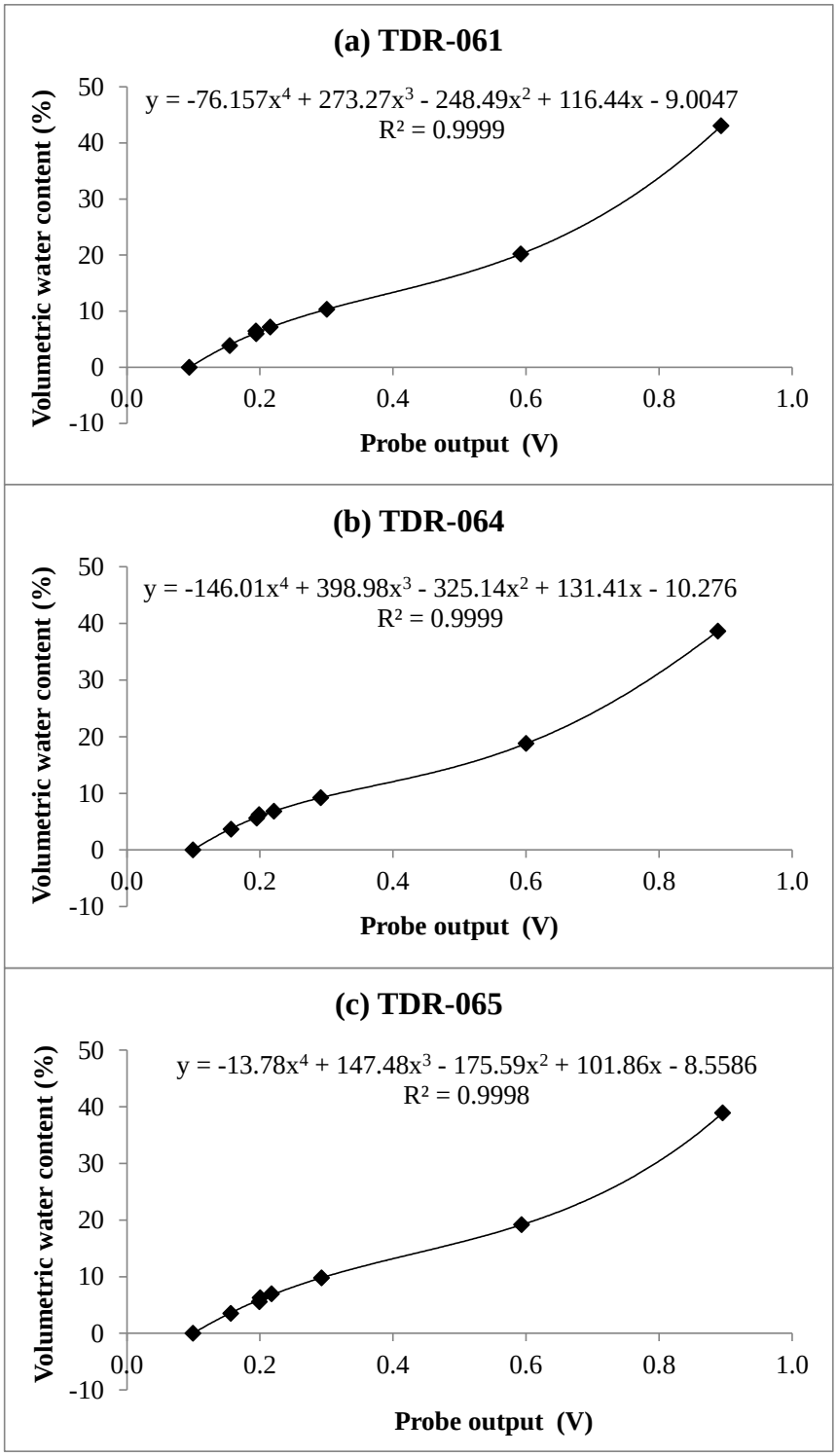

Figure 3.9 Calibration curves for soil moisture sensors

3.3.2 Soil Characterisation

The properties of the soil column packing materials were determined before use. Characteristics determined were the grain size distribution, Atterberg limits (plastic, liquid and shrinkage limits for clay and silt) and permeability. The permeability test was carried out using the constant head method. All tests were carried out according to standard methods developed for soil classification (Head, 1992). The determined characteristics of the silica sand, silt and clay in the soil columns are summarised in Table 3.5.

3.3.2.1 Grain Size Distribution

200 g of sand and BS sieves ranging from 2 mm to 63 µm were used for the sieve analysis. The mass of sand passing each sieve was determined after shaking and a plot of percentage passing against sieve size (mm) developed on a log – normal scale to obtain the grain size distribution curve as shown in Figure 3.10. The $d_{10,}$ d_{30}, d_{50} and d_{60} of the sand were read off the curve as the sand size (mm) on the x-axis corresponding to 10 %, 30 %, 50 % and 60 % passing respectively. The effective and average diameters of the sand are therefore 0.49 mm and 0.65 mm respectively. The coefficients of uniformity (C_u) and curvature (C_c) and were also determined as 1.38 and 1.08 respectively using Equations 3.4 and 3.5. A C_u value less than 5 indicates very uniform sand.

$$C_u = \frac{d_{60}}{d_{10}} \quad \text{.....[3.4]}$$

$$C_c = \frac{{d_{30}}^2}{d_{10} \times d_{60}} \quad \text{.....[3.5]}$$

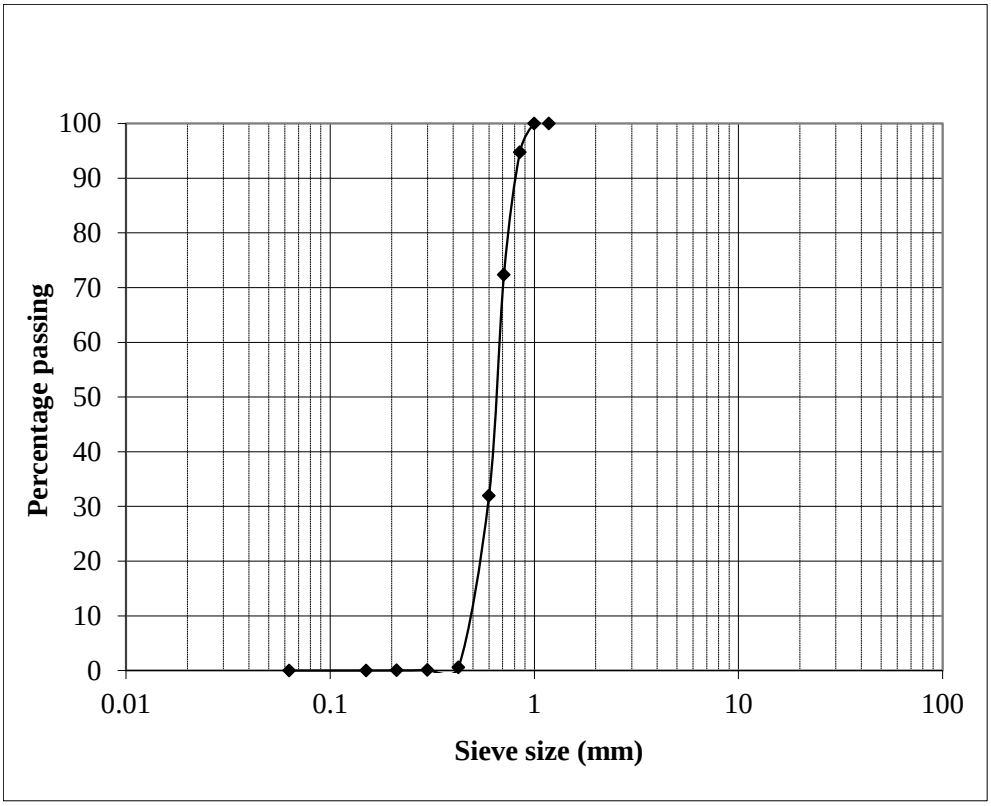

Figure 3.10 Silica sand grading curve

3.3.2.2 Atterberg Limits

The Atterberg limits tests (liquid, plastic and shrinkage limits) were performed according to standard methods for soil analysis (Head, 1992). Silt and clay samples in the form of dry powders were mixed with just enough water to obtain a workable consistency and stored in sealed plastic bags at least 24 hours before use in the tests.

Liquid Limit Test

The Cone Penetrometer Method (BS1377: Part 2: 1990:4.3) was used for the liquid limit test. The test was carried out at six different soil moisture contents to obtain penetrations between 10 mm and 25 mm. The test was repeated for each soil moisture content until two of the dial gauge readings were not more than 0.5 mm

apart. Moisture content determination involved drying the weighed sample in an oven at 105 °C for 24 hours. The average of the moisture content was plotted against the average penetration and the liquid limit of the sample read off the graph as the moisture content giving a 20 mm penetration.

Plastic Limit Test

The plastic limit was determined according to BS1377: Part 2:1990:5.3. Clay and silt samples were rolled into 3 mm threads until cracks begun to appear and the moisture content of the cracked threads determined. The plastic limit was calculated as the average of the moisture contents of the threads that differed by no more than 0.5 %.

Shrinkage Limit Test

Water was added to the sample to obtain a slightly wetter consistency than the liquid limit. A pre-weighed dish was filled with the sample ensuring no air bubbles were trapped. The filled dish was weighed and left to air dry for about 8 hours and then oven dried to constant mass at a temperature of 105 °C after which the mass was determined. The sample was then coated in paraffin wax and reweighed both in air and in water. The volume of the sample, V_d (L^3; cm^3) was determined by Archimedes principle from the weight in water and air (Head, 1992). The volume of the dish was also determined and the shrinkage limit, w_s, (%) calculated. The relevant equations are given in Equations 3.6 and 3.7.

$$V_d = (m_w - m_g) - \left(\frac{m_w - m_d}{\rho_P}\right) \quad \text{..... [3.6]}$$

$$w_s = w_1 - \left(\frac{V_1 - V_d}{m_d}\right) \times 100\,\% \quad \text{.....[3.7]}$$

where:

V_d = volume of dry soil pat (L^3; cm^3)

m_w = mass of wax-coated sample in air (M; g)

m_g = mass of wax-coated sample in water (M; g)

m_d = mass of dry soil pat (M; g)

ρ_p = density of paraffin wax (ML^{-3}; g cm^{-3})

w_1 = moisture content of soil (%)

V_1 = volume of wet soil pat (L^3; cm^3)

Table 3.5 Properties of silica sand, silt and clay used in 1 meter soil columns

Soil property	**Silica sand**	**Silt**	**Clay**
Effective diameter of (D_{10}), mm	0.49		
Average diameter (D_{50}), mm	0.65		
Coefficient of Uniformity (C_u)	1.38		
Coefficient of curvature (C_c)	1.08		
Liquid Limit (*LL*), %		34	41
Plastic Limit (*PL*), %		23	19
Plasticity Index (*PI*), %		11	22
Shrinkage Limit (*SL*), %		-	15

3.3.2.3 Hydraulic Conductivity

The saturated and unsaturated hydraulic conductivity of the silica sand were determined as described. Permeability tests, using the constant head method was carried out on the silica sand before use in the soil columns. The test setup comprised a Perspex cylinder of inner diameter 7.5 cm and length 30 cm. Manometers were

connected to three tapping points, h_1, h_2 and h_3. The difference between the outermost tapping points, h_1 and h_3, and thus length of sample (l, cm) considered for the test was 16.5 cm. The soil column was filled with the sand sample under saturated conditions as previously described and the permeability test carried out at four different head differences, Δh (L; cm), each time measuring the volume of water, V (L^3; cm^3) passing through the sample over a time, t (T; sec). Each test was repeated before change in flow conditions to ensure the accuracy of the results obtained. The coefficient of permeability or saturated hydraulic conductivity, K_s (LT^{-1}; cm s^{-1}) for each test was calculated from Equation 3.8. The coefficient of permeability of the sand was determined as the average permeability obtained from the four tests.

$$K_s = \frac{V \times l}{A \times \Delta h \times t} \quad \text{.....[3.8]}$$

where A, (L^2; cm^2) is the cross-sectional area of the soil column.

The unsaturated hydraulic conductivity was determined from the moisture retention curve of the silica sand. The relationship between matric potential and moisture content was determined using a Buchner funnel arrangement (Sharma and Mohamed, 2003). The experimental setup is shown in Figure 3.11.

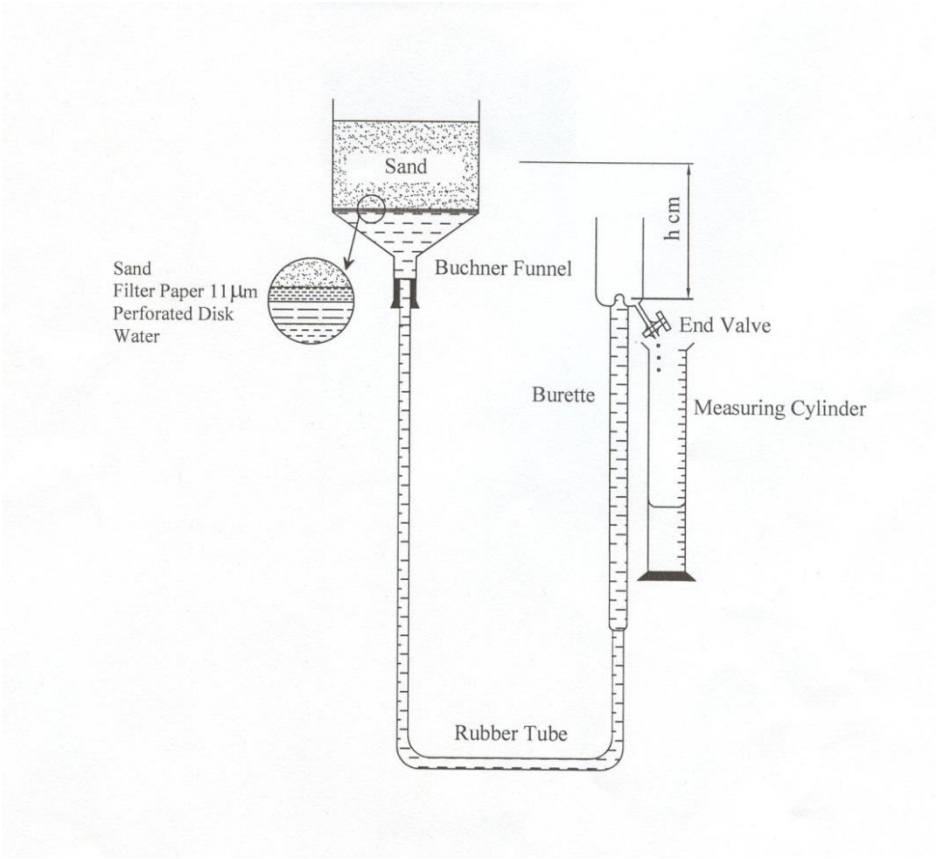

Figure 3.11 Experimental setup for the development of soil moisture retention curve

[Reproduced from Sharma and Mohamed, 2003]

The funnel, having a diameter of 130 mm and depth 60 mm, was first filled to a height of 40 mm with water and then the sand poured in up to the same height, taking note of the mass of sand used. The water displaced by the sand was removed from the surface of the packed sand and its volume determined. This was used to calculate the volume of the pores in the packed sand by deducting it from the volume of water in the funnel before the sand was poured in. The attached burette was then lowered in small incremental steps and the volume of water draining out of the sample collected and measured for each drop in the height of the burette until water no longer drained out of the sample. The volume of water drained out of the sample at each step was deducted from the water originally in the sample to obtain the water

remaining in and then further divided by the volume of water originally in the sample to obtain the degree of saturation. The matric suction head for each level of burette was also determined by subtracting the outflow level of the burette from the average level of water in the sample (Sharma and Mohamed, 2003). The matric suction head was plotted against the degree of water saturation to obtain the moisture retention curve for the sand as shown in Figure 3.12. The bubbling pressure, h_b (L; cm), is the matric potential at which water begins to drain from the soil.

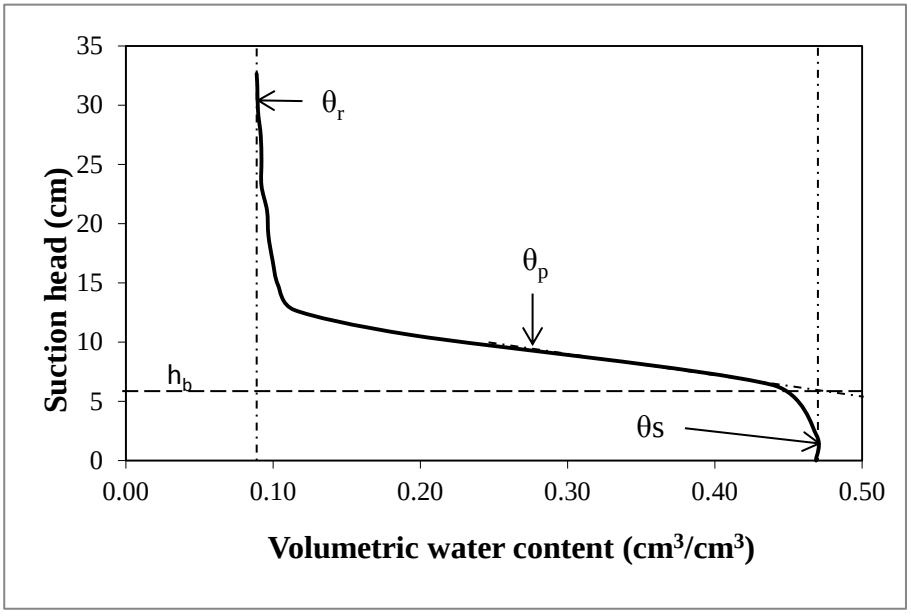

Figure 3.12 Silica sand moisture retention curve

The unsaturated hydraulic conductivity was then deduced from the moisture retention curve and the saturated hydraulic conductivity using the relationship developed by Van Genuchten (Van Genuchten, 1980). This is given by Equation 3.9 as:

$$K(\theta) = K_s S_e^{1/2} \left[1-(1-S_e^{1/m})^m\right]^2 \quad \text{.....[3.9]}$$

where:

$K(\theta)$ = unsaturated hydraulic conductivity at water content θ (LT^{-1}; cm d^{-1})

K_s = saturated hydraulic conductivity (LT^{-1}; cm d^{-1})

m = van Genuchten soil parameter

S_e = effective saturation defined as:

$$S_e = \frac{\theta - \theta_r}{\theta_s - \theta_r} \quad \text{……[3.10 a]}$$

where:

θ = volumetric water content (L^3L^{-3}; $cm^3\,cm^{-3}$)

θ_s = volumetric water content at saturation (L^3L^{-3}; $cm^3\,cm^{-3}$)

θ_r = irreducible minimum water content (L^3L^{-3}; $cm^3\,cm^{-3}$)

To obtain the van Genuchten soil parameter m, the slope S at a point P, corresponding to θ_p defined by Equation 3.10 b on the moisture retention curve was first determined. A dimensionless slope S_p was then determined from Equation 3.10 c and then m obtained using Equation 3.10 d.

$$\theta_p = \frac{\theta_s + \theta_r}{2} \quad \text{……[3.10 b]}$$

$$S_p = \frac{S}{\theta_s - \theta_r} \quad \text{……..……[3.10 c]}$$

$$m = 1 - \frac{0.5755}{S_p} + \frac{0.1}{S_p^2} + \frac{0.025}{S_p^3} \quad \text{…….…..……...[3.10 d]}$$

3.3.3 Soil Column Experiments

The studies carried out with the 1 m soil columns are described in this section. Synthetic wastewater was prepared from the stock solution and kept in the fridge with continuous aeration. To maintain saturated conditions in SC2 and SC3, wastewater flow was from the bottom of the column towards the top. In SC1

wastewater flow was from the top of the column and towards the bottom. The wastewater was applied continuously to the soil columns with periodic monitoring of samples collected from the columns to monitor the treatment occurring. All soil column wastewater samples collected were analysed for DOC, COD, TKN, NH_3-N, NO_2-N, NO_3-N, PO_4 and SO_4. The average characteristics of the wastewater applied are given in Table 3.6.

Table 3.6 Influent characteristics to 1 meter soil column

Parameter	**Average concentration (mg L^{-1})**
Chemical oxygen demand (COD)	40
Dissolved organic carbon (DOC)	17
Ammonia nitrogen (NH_3-N)	1.4
Organic nitrogen (Org-N)	2.8
Nitrate nitrogen (NO_3-N)	3.0
Total nitrogen (TN)	7.2
Phosphate (PO_4)	2.9
Sulphate (SO_4)	50

Synthetic estrogens were added to the synthetic wastewater being fed to the soil columns after steady state conditions had been attained with respect to reduction in concentrations of the wastewater parameters. This was achieved after about 3 months of continuous wastewater infiltration. The estrogen mix fed to the soil columns was prepared as follows. 1 mg L^{-1} concentrations of the estrogens E1, E2 and EE2 were prepared in methanol. Equal volumes of the three estrogen were mixed together to form the estrogen mix that was used in the experiments. During the experiments, a

small volume of the estrogen mix was added to synthetic wastewater and fed to the three columns. Average influent concentrations of E1, E2 and EE2 to SC1 were respectively 138 ± 6.7 ng L^{-1}, 206.3 ± 14.7 ng L^{-1} and 148.2 ± 9.6 ng L^{-1}. SC2 and SC3 concentrations were 120 ± 11.9 ng L^{-1}, 139 ± 18.3 ng L^{-1} and 124.7 ± 16.4 ng L^{-1}.

3.3.3.1 Experimental Conditions and Wastewater Sampling

In these experiments, hydraulic loading rates and DOC concentration in the saturated soil columns and the depth of water table in the unsaturated column were the parameters varied to determine their effects on the removal of the estrogens. Removal of E1, E2 and EE2 were studied at three different water table levels to quantify the effect of unsaturated zone thickness on removal efficiencies. The experimental stages are summarised in Figure 3.13. In all the columns about 500 mL of wastewater was sampled from specific depths along the soil columns into clean amber glass bottles. Influent and effluent from the columns were also sampled.

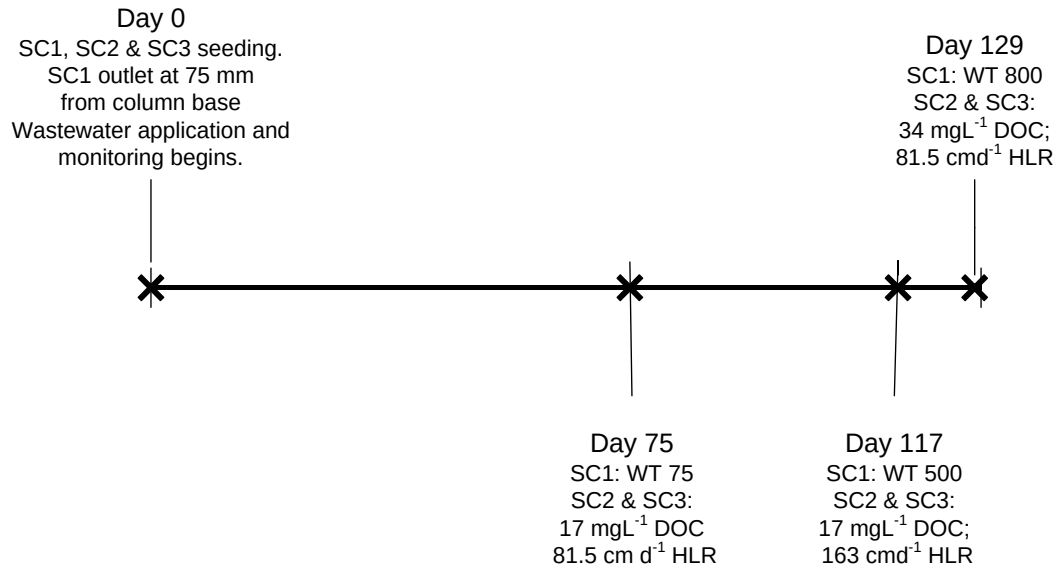

Figure 3.13 Experimental stages for estrogen studies

Unsaturated Soil Column (SC1) Experiments

HLR to SC1 was 49 cm d^{-1} throughout the experiments. The datalogger was programmed to scan all tensiometer and soil moisture readings every two minutes. In the first experiment, the outlet of the water well was adjusted so as to maintain the water table at 75 mm above the base of the column (WT75). Wastewater was sampled from the soil column for estrogen analysis. The water table was then raised to 500 mm (WT500) after six weeks and then to 800 mm (WT800) after a further two weeks. The sampling points for the unsaturated column were dependent on the level of the water table being considered (Table 3.7). It should be noted that as the water table was raised, wastewater could be sampled from an increasing number of points along the soil column since it was practically difficult to extract wastewater samples from the unsaturated zone due to the suction pressure. Each experiment was repeated prior to any change in the water table depth.

Table 3.7 SC1 sampling locations

Experiment	**Level of water table**	**Sampling points measured from bottom of soil column (mm)**	**Number of replicates for estrogens**
1	WT75	0, 150, 1000 (Influent)	6
2	WT500	0, 150, 350, 550, 1000	4
3	WT800	0, 150, 350, 550, 850, 1000	2

Saturated Soil Columns (SC2 and SC3) Experiments

The saturated soil columns were run at HLRs of 81.5 cm d^{-1} and 163 cm d^{-1}, and at 17 mg L^{-1} and 34 mg L^{-1} DOC. Wastewater at a DOC of 17 mg L^{-1} containing the estrogens was first applied to the soil columns at a hydraulic loading rate of 81.5 cm d^{-1}. Wastewater was sampled at 0 mm (influent), 150 mm, 350 mm, 550 mm, 750 mm, 1000 mm (effluent) from both columns for analysis. The wastewater concentration was then doubled with no change in the hydraulic loading rate and wastewater sampled once more from the same points along the column. After this, the wastewater concentration was reduced to that applied initially and the hydraulic loading rate doubled. Samples were then taken for analysis. The soil column experimental conditions are summarised in Table 3.8. The procedures employed for the preparation of collected samples and their analysis by LCMS are later described in Section 3.5.7. Each soil column sample was analysed twice.

Table 3.8 SC2 and SC3 experimental conditions

Soil column	**Hydraulic loading rate (cm d^{-1})**	**Influent DOC (mg L-1)**	**Number of replicates for estrogens**
SC2	81.5	17	6
SC2	81.5	34	2
SC2	163	17	2
SC3	81.5	17	6
SC3	81.5	34	2
SC3	163	17	2

3.3.3.2 Soil Sampling

At the end of the experiments, sand was sampled from various depths (150, 250, 350, 450, 550 and 750 mm measured from the bottom of the soil column) along SC2 and SC3 to determine the microbial structure within the soil columns. Difficulties were encountered in obtaining the samples from the soil sampling ports provided in SC3. Thus the soil was sampled by draining the soil columns, scooping out the sand and obtaining representative samples at the selected depths. The soil samples were analysed for phospholipids by extraction of the bacterial lipids and their subsequent identification by GC-MS analysis. The procedure adopted is described in Section 3.5.8.

3.4 Studies on Triclocarban (TCC) Removal

The removal of TCC was studied in a short column of length 300 mm infiltrated with synthetic wastewater.

3.4.1 Description of Setup

The soil column consists of a transparent perspex tube of inner diameter 7.8 cm and length 30 cm. Figure 3.14 shows a schematic diagram of the soil column setup. Three threaded rods projected vertically from the column base to serve as a means of securing the cover plate onto the column with butterfly screws. The cover plate comprised a perspex plate with a hose adapter screwed into its centre to serve as the column inlet. An o-ring fitted into the inner face of the plate ensured a good water seal could be obtained when the column is closed. Water and soil sampling ports were located at 8 and 19 cm from the top of the column. The water sampling ports were made of 3.2 mm stainless steel tubes extending to the centre of the column. Soil

sampling ports consisted of 12 mm plastic ball valves. Extra water sampling points for the influent and effluent were provided at the entry to the column and at its exit respectively. A perforated perspex plate was placed at the base of the column on top of which sat an inert and hydrophobic synthetic fibre mesh to allow draining of the column and prevent washout of sand from the column. During the experiments water was delivered to the column from the top by means of a peristaltic pump through tygon tubing and a variable area flow meter. The column and tubing were wrapped with aluminium foil to exclude light, thus discouraging the growth of algae in the system.

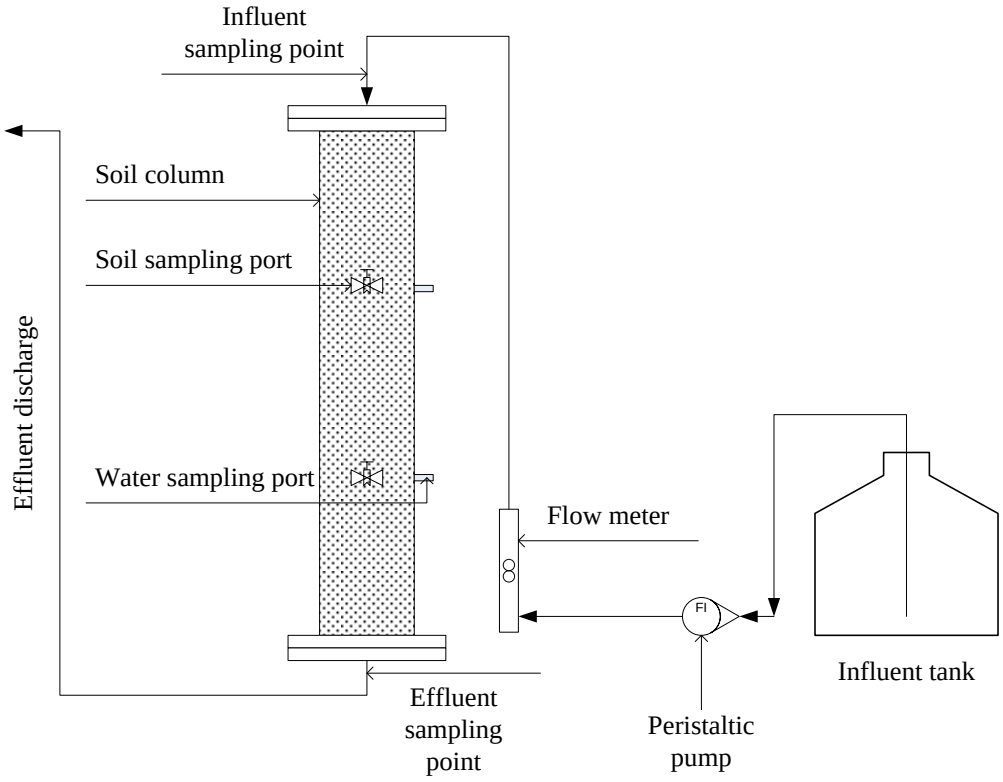

Figure 3.14 Schematic diagram of 300 mm soil column setup

3.4.2 Soil Column Start-Up and Operation

The soil column was packed under saturated conditions with uniform silica sand of average particle size 0.52 mm obtained from WBB Minerals, UK. Sand density in the column after packing was 1.55 g cm^{-3} and porosity 0.42. To ensure completely saturated conditions, the column was fed with water from the bottom during filling with sand, always keeping the water level in the column above the surface of the sand. The soil column was seeded with commercial microbial BOD seed solution and infiltrated with synthetic wastewater diluted with tap water to obtain a COD of about 67 mg L^{-1}.

The soil column was operated in down flow mode at a hydraulic loading rate of 150 cm d^{-1}. The outlet of the exit tube was elevated to a height corresponding with the top water level in the column to maintain saturated flow. The experiments were carried out at room temperature under aerobic conditions. Influent and effluent samples were collected for COD analysis to ascertain bioacclimation of the column. The COD of the column was monitored for 36 days prior to introduction of TCC into the influent. Wastewater containing TCC at different concentrations was applied to the column, and influent and effluent samples as well as water samples from the ports were taken at approximately 3 day intervals for analysis of COD and TCC using methods described in Sections 3.5.3 and 3.5.7.4 respectively.

Sorption of TCC onto the sand was also determined on sand sampled from the ports provided on the column. The sand samples were air dried and the TCC extracted with acetone. The extracts were then evaporated, the residue reconstituted in 1mL of

50:50 methanol and acetone and the resulting solutions filtered through 0.2 mm syringe filters before analysis by LCMS.

3.5 Instruments and Analytical Methods for Wastewater Characterisation

The instruments, analytical methods and reagents used for the characterisation of the soil column wastewater samples are briefly described in this subsection. For instruments requiring calibration, the calibration was done before soil column samples were analysed. Calibration standards and soil column wastewater samples were treated and analysed using the same procedure.

3.5.1 Dissolved Oxygen and pH Measurement

Dissolved oxygen (DO) was measured with a Hach Sension 6 dissolved oxygen meter. About 50 mL of freshly collected sample was poured into a glass beaker and placed on a magnetic stirrer. The magnetic attachment from the BOD accessory kit was fitted onto the probe and inserted in the sample. The DO was read off the meter in mg L^{-1}.

To measure the pH, the probe of an Oakton pH/mV/°C pH 11 series meter was inserted in the same sample and the reading on the display screen of the instrument recorded.

3.5.2 Dissolved Organic Carbon (DOC) Analysis

DOC was determined on filtered samples by low temperature oxidation using the ISCO Total Organic Carbon (TOC) analyser. The TOC analyser uses low temperature, UV assisted oxidation to analyse for organic carbon in water samples. The instrument consists of a display panel, an ultraviolet (UV) reactor, a condenser, two flow meters (inorganic carbon gas flow and reactor gas flow), an inorganic carbon scrubber (gas-liquid separator), four low revolutions per minute peristaltic-type pumps (source, acid, oxidation and organic sample pumps), sample inlet and outlets ports, valves and an infrared (IR) detector. Reagents required for the analysis are 10 % phosphoric acid (H_3PO_4) and 1.5 M sodium persulphate ($Na_2S_2O_8$) for the oxidation process. A source of carbon dioxide-free air is required as a purging gas to drive off carbon dioxide from the sample during the analysis.

3.5.2.1 Principle of Operation of TOC Analyser

The sample whose TOC is required is drawn by the source pump into the analyser. A portion of the sample is combined with phosphoric acid delivered by the acid pump, to lower the pH of the sample in order to cause the conversion of carbon contained in carbonates into carbon dioxide. This inorganic carbon, together with any other carbon dioxide dissolved in the sample, is driven off with the purging gas so that the organic carbon readings are not affected. The sample, now containing carbon only in the organic form, is mixed with $Na_2S_2O_8$ delivered by the oxidation pump and pumped into the UV reactor. In the reactor, the sample circulates close to the UV lamp and the radiation from the lamp together with the added $Na_2S_2O_8$ oxidise the organic carbon in the sample into carbon dioxide. The carbon dioxide then passes through the IR detector where the gas traps specific infrared wavelengths. The

attenuation of the IR beam through the IR analyser gives a precise measurement of the carbon dioxide, which is further correlated by the microprocessor to the value of carbon in the sample using the calibration of the analyser. The amount of organic carbon in the sample is then displayed on the display panel in mg L^{-1}.

3.5.2.2 Calibration of TOC Analyser

A re-calibration of the TOC analyser was carried out with potassium hydrogen phthalate (KHP) in order to check the calibration previously carried out on the instrument. A 100 mg L^{-1} solution of KHP was prepared by dissolving 0.21281 g of the powdered chemical, which had been dried in the oven at 105 °C for one hour, in 700 mL of deionised water and then making up to 1 L. Solutions of known concentration (0, 10, 20, 30, 40 and 50 mg L^{-1}) were prepared from the 100 mg L^{-1} stock solution by dilution in deionised water. The organic carbon was then determined on the TOC analyser and the readings given by the instrument plotted against the known concentrations of the prepared solutions to obtain the calibration curve. This curve was used to correct subsequent sample DOC readings from the instrument. Figure 3.15 shows the calibration curve.

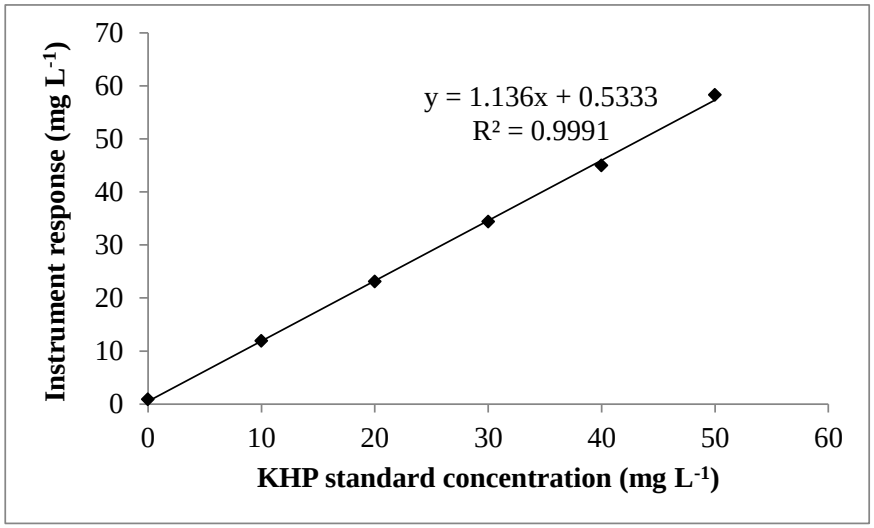

Figure 3.15 Dissolved organic carbon calibration curve

3.5.2.3 Sample Analysis

1.5 M sodium persulphate was prepared by first dissolving 350 g of the powdered chemical in about 800 mL deionised water and then diluting it to a volume of 1 L. The oxidising reagent was allowed to age for a minimum of 24 hours before use. A fresh batch was prepared every three to four weeks and whatever remained of the previous batch discarded. 10 % phosphoric acid was prepared by adding 100 mL of 85 % phosphoric acid to 900 mL deionised water. A source of pressurized synthetic air, regulated to 150 – 200 kPa (1.5 - 2 bar) was used as the purging gas to drive off the inorganic carbon during the analysis.

All samples were processed by vacuum filtration prior to analysis through 0.45 µm cellulose nitrate filters from Cole Parmer, UK. The filters were pre-washed before use on the samples by passing about 100 mL of deionised water through them. This was done to leach out any DOC that may be in them. One filter was used per sample. The filtered samples were then introduced into the analyser through the manual

sample port of the instrument and allowed to flow through the instrument for 20 minutes to ensure steady readings.

3.5.3 Chemical Oxygen Demand Analysis

Chemical Oxygen Demand (COD) analysis was carried out by the addition of 2 mL of sample to COD vials (range: 0 – 150 mg L^{-1}) from Hach Lange Limited. The vials were shaken and heated at 150 °C for two hours in a Hach COD reactor, allowed to cool for about 20 minutes in the reactor, taken out and shaken again and allowed to cool to temperature in a cooling rack. The COD was then determined colorimetrically on a DR/2400 spectrophotometer. A blank prepared in the same manner as the samples but using 2 mL deionised water in place of the sample was used to zero the instrument.

3.5.4 Biochemical Oxygen Demand Analysis

Biochemical Oxygen Demand (BOD) was measured according to the Standard Methods for the Examination of Water and Wastewater (Clesceri et al., 1998). Dilution water was first prepared by aerating 3 L of deionised water with an aquarium pump for about two hours and then adding 1 mL each of 27.5g L^{-1} $CaCl_2.2H_2O$, 22.5g L^{-1} $MgSO_4.7H_2O$, 250mg L^{-1} $FeCl_3$ and 54.3g L^{-1} K_2HPO_4 for every litre of water. 600 mL of the prepared dilution water was seeded with 4 mL of seed solution prepared as previously described for use on the influent sample. The remaining seed solution was discarded and fresh one prepared each time BOD tests were to be carried out. Samples that had passed through the soil column were not seeded. The wastewater samples were diluted with the dilution water according to

the expected BOD using recommended values (Clesceri et al., 1998). Clean BOD bottles were filled with the samples and the dissolved oxygen determined immediately. The bottles were then topped up with the sample to overflowing and closed, ensuring that no air was trapped in them. Seeded and unseeded blanks were also prepared. These blanks only contained seeded dilution water and dilution water with no seeding material respectively. The bottles were then incubated at 20 ºC for five days. After 5 days the dissolved oxygen in the bottles were again measured and the BOD determined as:

$$BOD = \frac{(D_1 - D_2) - (B_1 - B_2) \times f}{P} \quad \text{.....[3.11]}$$

where:

D_1 = dissolved oxygen of diluted sample immediately after preparation, (ML^{-3}; mg L^{-1})

D_2 = dissolved oxygen of diluted sample after 5-day incubation at 20 ºC, (ML^{-3}; mg L^{-1})

B_1 = dissolved oxygen of seed control before incubation (ML^{-3}; mg L^{-1})

B_2 = dissolved oxygen of seed control after incubation (ML^{-3}; mg L^{-1})

f = fraction of seeded dilution water volume in sample to volume of seeded dilution water in seed control

P = fraction of wastewater sample volume to total combined volume

f and P are determined as:

$$f = \frac{(V_B - V_{SP})}{V_B} \quad \text{.....[3.12]}$$

and

$$P = \frac{V_{SP}}{V_B} \quad \text{.....[3.13]}$$

where:

V_B = volume of the BOD bottle (L^3; mL)

V_{SP} = volume of the sample (L^3; mL)

3.5.5 Total Kjeldahl Nitrogen and Ammonia Nitrogen Analysis

Total Kjeldahl Nitrogen (TKN) was carried out using the digestion method developed by FOSS (FOSS, 2009) with some modification to the distillation step, which was carried out using indicating boric acid as specified in Standard Methods for the Examination of Water and Wastewater (Clesceri et al., 1998). The procedure was first tested on a peptone solution prepared to a known concentration. The results obtained from the digestion and distillation agreed closely with the TKN content of the prepared solution as obtained from calculations based on manufacturer's information. For the digestion, 100 mL of sample was placed into digestion tubes together with two kjeldahl tablets each containing 3.5 g selenium and 3.5 g potassium sulphate. 12 mL of concentrated sulphuric acid was added and the sample digested in a Tecator 2006 digestor for 70 minutes in a fume cupboard. After cooling the samples to room temperature, 75 mL deionised water was added and distilled in a Tecator Kjeltec System 1002 distilling unit after the addition of one full stroke of 40 % sodium hydroxide solution (FOSS, 2009). The sodium hydroxide was of analytical grade and purchased from VWR International. 200 mL of the distillate was collected in 50 mL of indicating boric acid and back titration done with 0.25 N sulphuric acid as the titrant (Clesceri et al., 1998). Ammonia Nitrogen (NH_3-N) analysis involved distilling 100 mL of sample in the same manner as for the TKN but without the digestion step and the addition of a smaller volume of sodium hydroxide to raise the pH up to 11. A blank was carried out with each batch of

samples for TKN and NH_3-N analysis. The concentration of NH_3-N or TKN in the sample was calculated from the volume of acid used for the titration in the appropriate test as:

$$C = \left(\frac{VA_s - VA_b}{V_{SP}}\right) \times 280 \quad \text{.....[3.14]}$$

where C is the concentration of NH_3-N or TKN (ML^{-3}; mg L^{-1}), VA_s and VA_b are the volumes of acid (L^3; mL) used for the sample and blank respectively and V_{SP} is the volume of sample (L^3; mL) used in the test.

3.5.6 Anions Analysis

Nitrate, phosphate and sulphate were determined by ion chromatography on a 4000*i* Dionex Ion Chromatograph. The ion chromatography setup consists of a basic chromatography module containing two high-pressure valves (an injection valve with a 50 µL sample loop and a column select valve), a conductivity detector, a gradient pump and an Advanced Computer Interface (ACI) module. A sample port located on the front panel provides access for loading the sample loop of the injection valve. The column selection valve serves as a means of switching between two sets of columns, for anion or cation analysis. The anion column set, which was used for the analysis comprised a membrane suppressor and an IonPac AG4A-SC 4-mm analytical column with an IonPac AS4A-SC 4-mm guard column installed in front of it to shield it from contamination. Waste lines from the injection valve, membrane suppressor and conductivity detector cell exit the module through the waste port at the rear of the instrument.

The system is controlled by the ACI module, which serves as a means of setting up the method for the analysis and also as the communications link between a computer and the analytical instrument. The ACI is connected to a computer via a RS-232 interface cable.

3.5.6.1 Principle of Operation

The gradient pump controls the injection and column select valves and delivers an eluent (1.8 mM sodium carbonate/1.7 mM sodium bicarbonate) to the injection valve through the eluant grommet on the front panel of the module. A regulated compressed cylinder of nitrogen provides 552 kPa of air pressure required by the air-operated high-pressure valves. When a sample is injected into the sample port of the IC and the analytical run commenced, the sample flows through the injection valve where it combines with the eluent. It then flows through the column select valve, the guard column and then to the analytical column. The sample exits the column, and flows through the membrane suppressor where the conductivity of the eluent is reduced. The membrane suppressor is continuously regenerated by a 0.025N sulphuric acid (H_2SO_4) regenerant which is driven through it by helium gas at a pressure of 35 kPa. From the suppressor the sample flows to the conductivity detector via the column select valve. The conductivity of the sample is continuously shown on the display panel of the conductivity detector during the analysis and the chromatogram displayed on the connected computer.

3.5.6.2 Instrument Calibration

The ion chromatograph was calibrated for the anions chloride, nitrite, nitrate, bromide, phosphate and sulphate. 1000 mg L^{-1} standards of the anions were prepared by dissolving the salts of the anions in deionised water. The mass of salt dissolved are given in Table 3.9. An example of calculation of the required mass of sodium chloride (NaCl) to prepare 1000 mg L^{-1} Cl^- is shown below.

$$Molar\ mass\ of\ NaCl = 58.44\ g$$

$$Molar\ mass\ of\ Cl^- = 35.45\ g$$

Therefore the mass of NaCl required in 1 L of deionised water to obtain a concentration of 1000 mg L^{-1} of chloride is:

$$\frac{Molar\ mass\ of\ NaCl}{Molar\ mass\ of\ Cl^-} \times Mass\ of\ chloride\ in\ 1\ L\ solution$$

$$= \frac{58.44 \times 1000}{35.45} = 1.648\ g \ldots\ldots\ldots [3.15]$$

Equal volumes of the 1000 mg L^{-1} standard solution of each anion were taken, combined and diluted with deionised water to give new lower concentrations ranging from 1 mg L^{-1} to 20 mg L^{-1}, which were used as the calibration standard. 0.5 mL of each standard was drawn into a 10 mL syringe, fitted with a 0.2 µm syringe filter and injected into the ion chromatograph. The identified peaks were integrated and the resulting area for each anion plotted against the concentration and fitted with a linear curve. The calibration curves for nitrate, nitrite, sulphate and phosphate are shown in Figure 3.16. The chloride calibration curves is presented in Appendix B. R^2 obtained for all curves was better than 0.999.

Table 3.9 Masses of compounds in 1 L of 1000 mg L^{-1} anion standards

Anion	**Compound**	**Mass (g)**
Chloride	Sodium chloride (NaCl)	1.648
Nitrite	Sodium nitrite ($NaNO_2$)	1.499
Bromide	Sodium bromide (NaBr)	1.288
Nitrate	Sodium nitrate ($NaNO_3$)	1.371
Ortho-phosphate	Potassium phosphate, monobasic (KH_2PO_4)	1.433
Sulphate	Sodium sulfate (Na_2SO_4)	1.479

(Dionex, 2001)

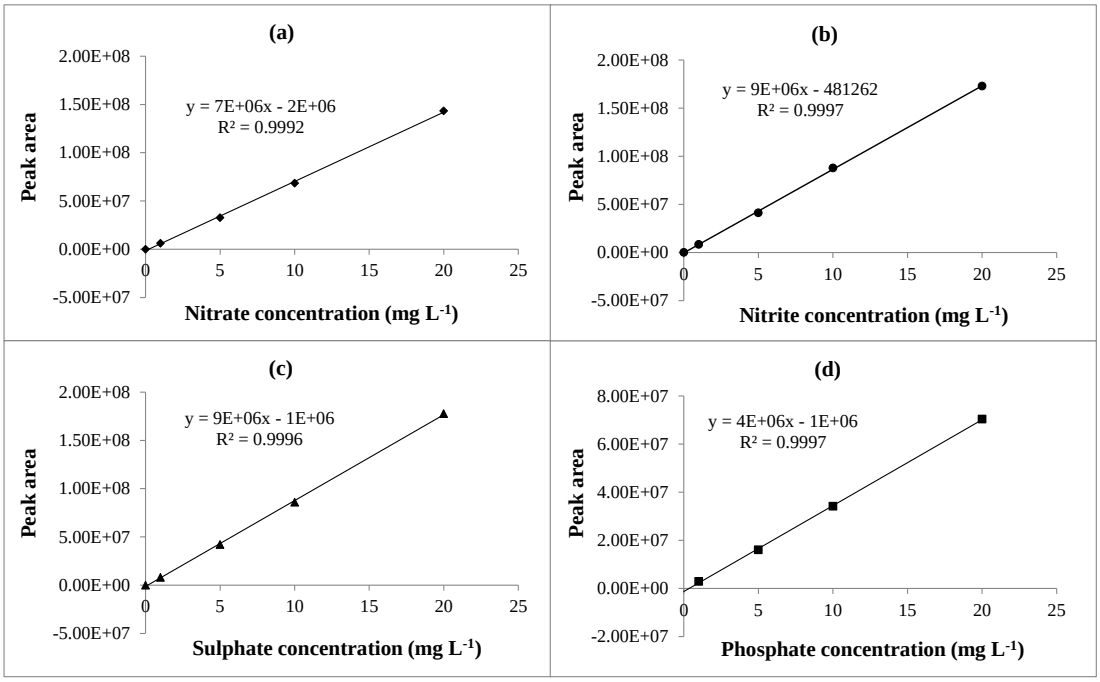

Figure 3.16 Anion calibration curves

(a) nitrate, (b) nitrite, (c) sulphate and (d) phosphate

3.5.6.3 Sample Analysis

The eluent of 1.8 mM sodium carbonate and 1.7 mM sodium bicarbonate was prepared by dissolving 0.1908 g of Na_2CO_3 and 0.1428 g of $NaHCO_3$ in deionised water and diluting to 1 L. It was ensured that the deionised water used for the preparation of all reagents was of 18 MΩ-cm resistance or better. The 0.025 N H_2SO_4 regenerant was also prepared by adding 0.7 mL of concentrated H_2SO_4 to about 800 mL of deionised water and then diluting to 1 L. All reagents were vacuum degassed before use in the analysis. The eluent and regenerant were placed in special glass bottles manufactured to withstand pressures of -100 kPa to + 150 kPa (-1 to +1.5 bar), connected to the instrument and pressurised to 35 kPa (5 psi) with helium gas. An inline filter was fitted on the ends of the delivery tubing in each bottle. The method for the analysis was loaded from the computer and the column allowed to equilibrate for about one hour. After equilibration, 0.5 mL of the sample to be analysed was injected into the instrument through 0.2 µm syringe filters using 10 mL syringes. The sample loop was flushed with deionised water between samples.

3.5.7 Analysis of Estrogens and Triclocarban

The estrogens E1, E2 and EE2 as well as triclocarban (TCC) were analysed by high performance liquid chromatography-mass spectrometry (LCMS). The LCMS setup for the analysis comprised a Waters Alliance 2695 separation module with an autosampler coupled to a Waters 2487 dual absorbance detector and a Micromass ZMD quadrupole mass spectrometer. The system was controlled by Masslynx 4.1 software.

3.5.7.1 Principle of Operation of LCMS

LCMS systems consists of a sample delivery system, a mobile phase delivery system, an analytical column usually fitted with a guard column to protect it from contamination, and a detection system, which is the mass spectrometer. Samples are injected by an auto sampler into the separation module and the analyte identified by the detector module.

The principle of chromatography is common to both the gas chromatograph (GC) and the liquid chromatograph (LC). During GC and HPLC analysis, the sample is dissolved in a gas or a liquid respectively, which serves as the mobile phase. The mobile phase is allowed to flow through an immiscible stationary phase. The various components of the sample are partitioned to varying extents between the stationary phase and the mobile phase. These differences in partitioning give rise to different speeds of movement of the sample components through the stationary phase. This results in weakly retained components travelling quickly and therefore being eluted first, whilst strongly retained ones move more slowly. The sample therefore becomes separated into peaks or bands and moves onward to the mass spectrometer where the components are ionised, analysed based on their mass to charge ratio (*m/z*) and detected (Lavagnini et al., 2006). To quantify the components in the sample, the peaks are integrated to obtain the area. The resulting peak areas can be converted to concentrations using calibration curves developed by analysing samples of known concentrations under the same instrument settings and conditions.

3.5.7.2 Optimisation and Calibration of LCMS

The sensitivity of the LCMS was optimised for the analysis of TCC and the estrogens E1, E2 and EE2, by tuning the mass spectrometer for optimum performance using prepared standards of the analytes (10 µg mL^{-1}). During the optimisation, the line from the HPLC to the mass spectrometer was teed into and the analytes infused directly into the mass spectrometer at a rate of 10 µL min^{-1}, using a Harvard Syringe Pump. The MS parameters, such as the cone voltage, source block and desolvation temperatures and gas flow rate, were then tuned to obtain the highest sensitivity.

After optimisation, the LCMS was calibrated for use on the analysis of TCC and for the estrogens. The optimisation and calibration for the two groups of EDCs were carried out on separate occasions, when the analyses of soil column samples were required. To develop the calibration curve for the estrogens 5, 10, 20, 50, 100, 200, 500 and 1000 ng mL^{-1} standard solutions were prepared from a mixture of the three estrogens in methanol each at a concentration of a 1 mg L^{-1}. For TCC, eight standard solutions (20, 50, 100, 500, 1000, 1500, 2500 and 3000 ng mL^{-1}) were prepared from a 1 g L^{-1} stock solution of TCC in 50/50 acetone/methanol. The standards were placed in HPLC vials and analysed on the LCMS. Blanks were analysed together with the standards in both cases. The resulting peaks were integrated and calibration curves developed from the concentrations and the corresponding peak areas obtained. The use of internal standards was not deemed essential to the analysis because the measured estrogen concentrations in the soil column would be expressed as a fraction of the influent concentration. Figure 3.17 and Figure 3.18 show the

calibration curves for the estrogens and TCC respectively. R^2 values obtained for all three estrogens were greater than 0.999 and was 0.9633 for TCC.

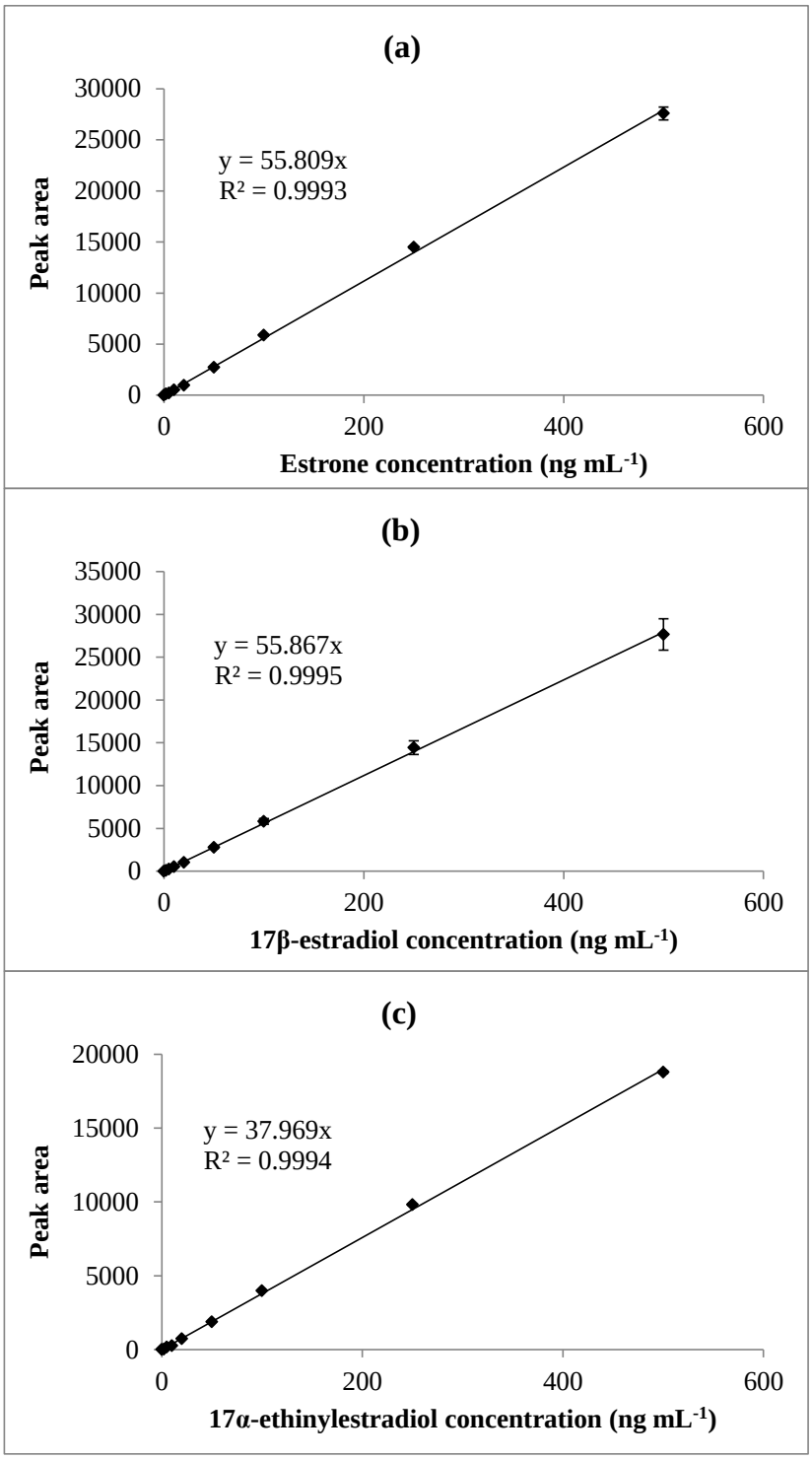

Figure 3.17 Estrogen calibration curves

(a) estrone, (b) 17β-estradiol and (c) 17α-ethinylestradiol

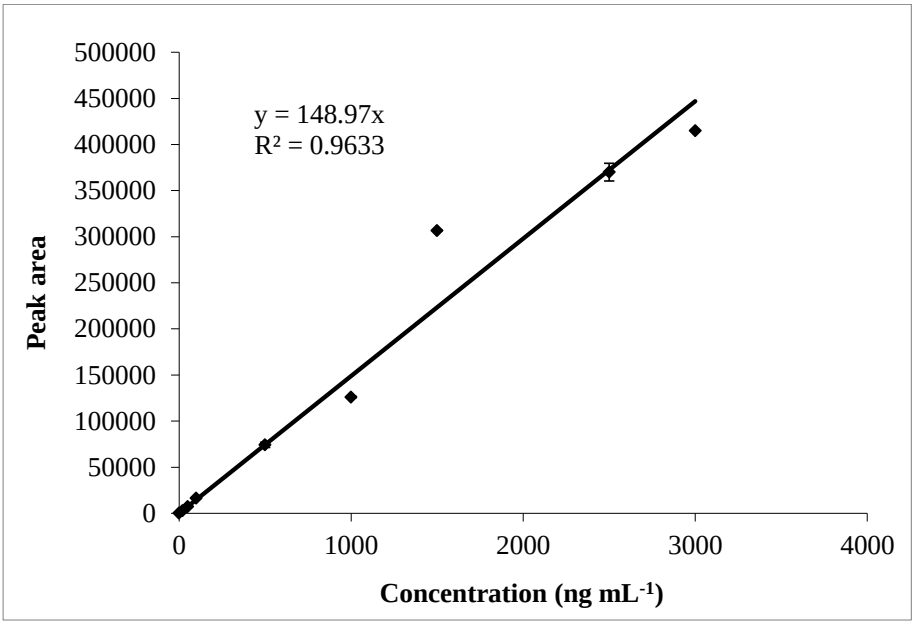

Figure 3.18 Triclocarban calibration curve

3.5.7.3 Wastewater Sample Preparation and Estrogen Analysis

All soil column wastewater samples were extracted and concentrated by solid phase extraction (SPE) before analysis because the concentrations were expected to be low due to the low levels of estrogens in the influent. Oasis ® HLB 3 cc /60 mg cartridges obtained from Waters UK was used for this purpose. The recovery of the cartridges was determined before use on the samples. This was done by extracting aqueous solutions containing known concentrations of the estrogens through the cartridges and comparing the results to solutions of the same concentrations prepared by dilution of the 1 mg L^{-1} estrogen mix stock solution in methanol.

For the extraction process, the cartridges were fitted onto a 12-port disposable liner SUPELCO Visiprep ^{TM} SPE vacuum manifold. Each cartridge was conditioned with 3 mL methanol followed by 3 mL deionised water. After conditioning, 500 mL of soil column water sample collected was connected to the cartridges through adaptors

and PTFE tubing. The vacuum on the manifold was maintained at about 103 kPa (15 psi) and the valves adjusted to allow a flow not exceeding 5 mL min^{-1} through the cartridges. After the entire volume of sample had passed through the cartridges, a Visidry ^{TM} drying attachment was fixed onto the manifold and the cartridges dried under a gentle stream of nitrogen. The estrogens were then eluted from the cartridges using 5 mL of acetone in 2 mL and 3 mL aliquots, the eluant collected in glass test tubes and dried under nitrogen. The dried extract was then redissolved in 1 mL methanol and analysed by LCMS.

During the LCMS analysis, source block and desolvation temperatures of the instrument were set at 80 °C and 150 °C respectively and nitrogen gas was flowing at 221 L min^{-1}. The separation of the estrogens was carried out using a Gemini-NX 3u C18 110A analytical column of size 150 mm x 2.00 mm (Phenomenex, UK). The mobile phase for the analysis consisted of acetonitrile (ACN) and 0.1 % ammonia (NH_3) in deionised water to aid ionization. A gradient elution was used for the HPLC with the flow rate set at 0.2 mL min^{-1}. The program at the start of the analytical run was 70 % NH_3 and 30 % ACN, changing to 30 % NH_3 and 70 % ACN at 4 minutes, 3 % NH_3 and 97 % ACN at 7 minutes and back to 70 % NH_3 and 30 % ACN at 12.20 minutes until the end of the 15 minute run. Estrogen quantification was performed by selective ion monitoring (SIM), with the instrument set for a single ion recording (SIR) of the masses 269.00, 271.00, 295.00 representing E1, E2 and EE2 respectively. A negative electrospray ionisation (ESI^-) mode was used for the analysis. Sample volume injected by the auto sampler after an hour of column equilibration was 10 µL. On the average, E1, E2 and EE2 eluted at 10 minutes, 9.2 minutes and 9.8 minutes respectively.

3.5.7.4 Sample Preparation and TCC Analysis

TCC was determined by liquid chromatography mass spectrometry in negative electrospray ionization mode (LC/ESI/MS) according to the method developed by Halden & Paull (2004). 6 cm^3 Envi-chrom P solid phase extraction (SPE) cartridges from Supelco were used to concentrate samples before analysis. The cartridges were tested for their recovery of the analyte TCC before use on the samples. They were first conditioned with 2 mL of methanol followed by 2 mL of a 50:50 by volume mixture of acetone and methanol and then 6 mL of deionised water. 500 mL of known concentrations of TCC solutions were then passed slowly through the cartridges at a flow rate not exceeding 5 mL min^{-1}, using the vacuum manifold. The cartridges were dried under vacuum and eluted with 4 mL of 50:50 acetone and methanol containing 10 mM acetic acid. The extracts were dried under vacuum, reconstituted in 1mL 50:50 acetone and methanol and stored in the freezer prior to analysis by LC/ESI/MS. Water samples obtained from the soil column were treated in a similar manner before analysis.

Analysis of TCC was carried out on a Gemini-NX 3u C18 110A analytical column of size 150 mm x 2.00 mm (Phenomenex, UK). 70 % acetonitrile and 30 % 10 mM acetic acid was used as the mobile phase running at a flow rate of 0.2 mL min^{-1}. An isocratic method of elution was used for the analysis. Source block and desolvation temperatures were set at 120 °C and 360 °C respectively. Nitrogen gas was flowing at 221 L min^{-1}. TCC quantification was performed by selective ion monitoring (SIM). The instrument was set for a single ion recording (SIR) scan of four channels to detect the characteristic molecular ion ($[M-H]^-$) of TCC at *m/z* 313, its molecular isotopes, chlorine 37 at *m/z* 315 and *m/z* 317 and also the TCC acetic adduct formed

at *m/z* 373. After equilibration of the column for 1 hour, the samples were injected. The autosampler was programmed to inject 10 mL of sample per analysis. Each soil column sample was analysed twice. An eight point calibration curve spanning a concentration range of 20 to 3,000 ng mL^{-1} was developed for conversion of peak areas to TCC concentration. TCC eluted at 6 minutes on the average as analysed by the mass spectrometer. No detectable peaks were observed by UV detection at wavelengths of 254 and 265 nm for the samples at the low levels of concentration used in this study.

3.5.8 Phospholipid Fatty Acid Analysis of Soil Column Packing Material

Sand sampled from the saturated 1 meter soil columns were analysed for their phospholipid fatty acids (PLFA) by gas chromatograph-mass spectrometry (GCMS). GCMS systems consist of a gas source, usually hydrogen or helium which serves as the mobile phase, a sample injection system, which could be automated or manual, an analytical column, a detector which is the mass spectrometer and a data control and analysis package. A guard column is usually used to prevent contamination of the analytical column.

3.5.8.1 Principle of Operation of GCMS

To perform an analysis, the dissolved sample is injected into the injection port. The sample is vapourised due to the high temperature at which the injector is operated, and is conveyed to the column for separation to take place. Sample injection may be carried out in split or splitless mode, the latter being used for detections in trace

quantities in liquid samples that are dilute. Where concentrations are high, a split mode, in which most of the injected sample is vented, is used to prevent overloading of the column. The sample components are detected by the mass spectrometer after elution from the column and the peaks recorded by the data analysis system.

3.5.8.2 Calibration of GCMS

The GCMS was calibrated using eight standard solutions prepared by dilution of a Bacterial Acid Methyl Ester (BAME) CP mix (10 mg mL^{-1} total concentration in methyl caproate), obtained from Sigma Aldrich UK. This mix contained twenty five different BAMEs as given in Table 3.10. The resulting peaks from the analysis were integrated and plotted against the known concentrations to obtain the calibration curves shown in Figure 3.19. Due to the large number of BAMEs in the mix, only a selection of the calibration curves is presented here. The rest of the curves can be found in Appendix B.

Table 3.10 Composition of BAME mix

Methyl ester	**Formula/structure**	**Shorthand designation**
Methyl undecanoate	$C_{12}H_{24}O_2$ 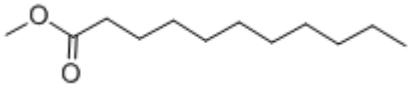	11:0
Methyl (±)-2-hydroxydecanoate	$C_{11}H_{22}O_3$ 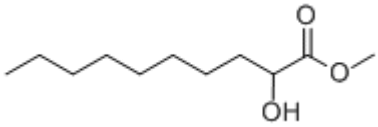	2-OH 10:0
Methyl dodecanoate	$C_{13}H_{26}O_2$ 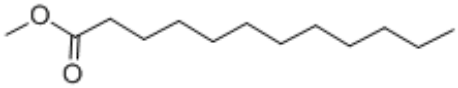	12:0
Methyl tridecanoate	$C_{14}H_{28}O_2$ 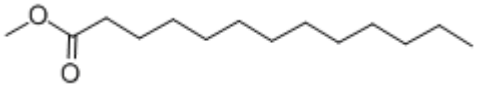	13:0
Methyl 2-hydroxydodecanoate	$C_{13}H_{26}O_3$ 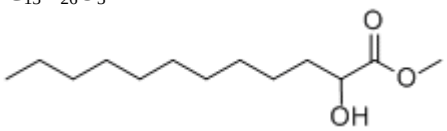	2-OH 12:0
Methyl (±)-3-hydroxydodecanoate	$C_{13}H_{26}O_3$ 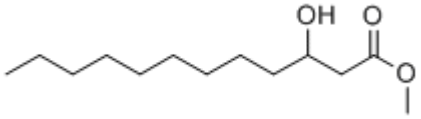	3-OH 12:0
Methyl myristate	$C_{15}H_{30}O_2$ 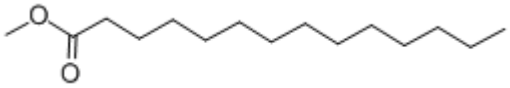	14:0
Methyl 13-methyltetradecanoate	$C_{16}H_{32}O_2$ 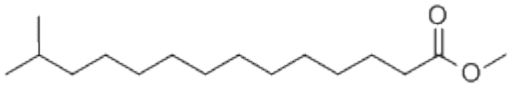	i-15:0
Methyl 12-methyltetradecanoate	$C_{16}H_{32}O_2$ 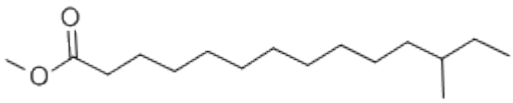	α-15:0
Methyl pentadecanoate	$C_{16}H_{32}O_2$ 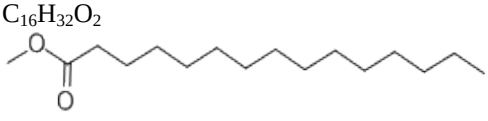	15:0

Methyl ester	**Formula/structure**	**Shorthand designation**
Methyl 2-hydroxytetradecanoate	$C_{15}H_{30}O_3$ 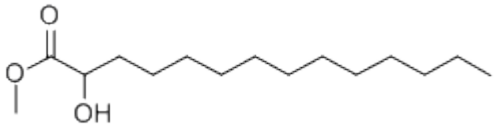	2-OH 14:0
Methyl 3-hydroxytetradecanoate	$C_{15}H_{30}O_3$ 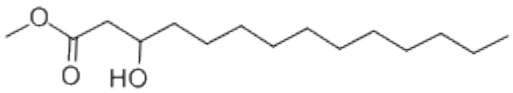	3-OH 14:0
Methyl 14-methylpentadecanoate	$C_{17}H_{34}O_2$ 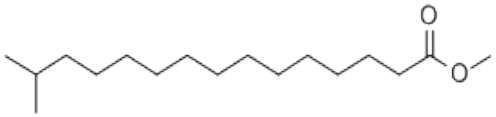	i-16:0
Methyl cis-9-hexadecenoate	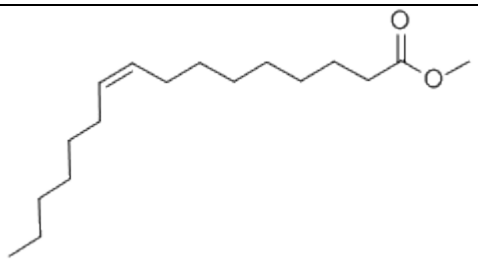 $C_{17}H_{32}O_2$	$16:1^{9}$
Methyl palmitate Methyl hexadecanoate	$C_{17}H_{34}O_2$ 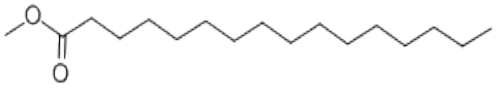	16:0
Methyl 15-methylhexadecanoate	$C_{18}H_{36}O_2$ 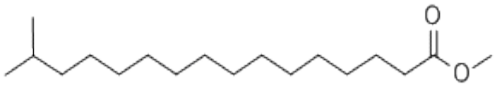	i-17:0
Methyl *cis*-9,10-methylenehexadecanoate	$C_{18}H_{34}O_2$ 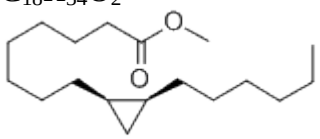	$17:0^{\Delta}$
Methyl heptadecanoate	$C_{18}H_{36}O_2$ 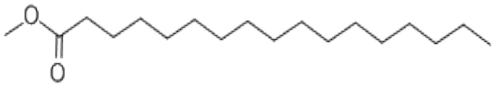	17:0
Methyl 2-hydroxyhexadecanoate	$C_{17}H_{34}O_3$ 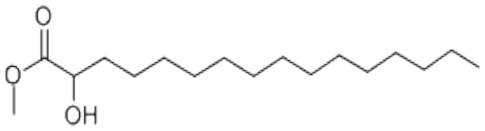	2-OH 16:0

Methyl ester	**Formula/structure**	**Shorthand designation**
Methyl linoleate	$C_{19}H_{34}O_2$ 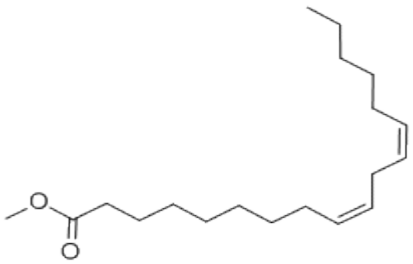	$18:2^{9,12}$
Methyl oleate	$C_{19}H_{36}O_2$ 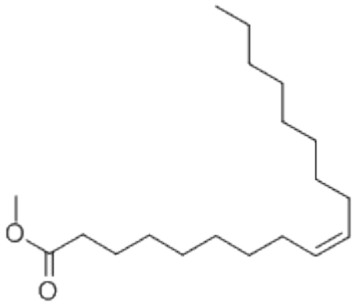	$C18:1^{9}$
Methyl trans-9-octadecenoate	$C_{19}H_{36}O_2$ 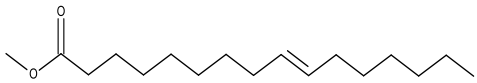	$C18:1^{9}$
Methyl stearate	$C_{19}H_{38}O_2$ 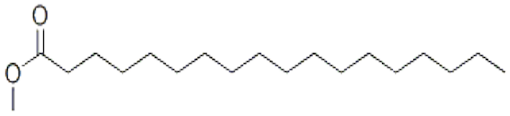	C18:0
Methyl cis-9,10-methyleneoctadecanoate	$C_{20}H_{38}O_2$ 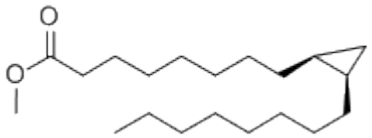	$C19:0^{\Delta}$
Methyl nonadecanoate	$C_{20}H_{40}O_2$ 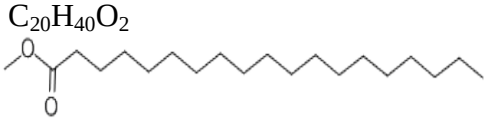	C19:0
Methyl eicosanoate	$C_{21}H_{42}O_2$ 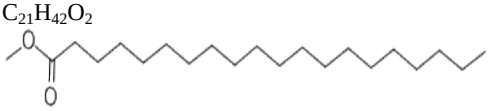	C20:0

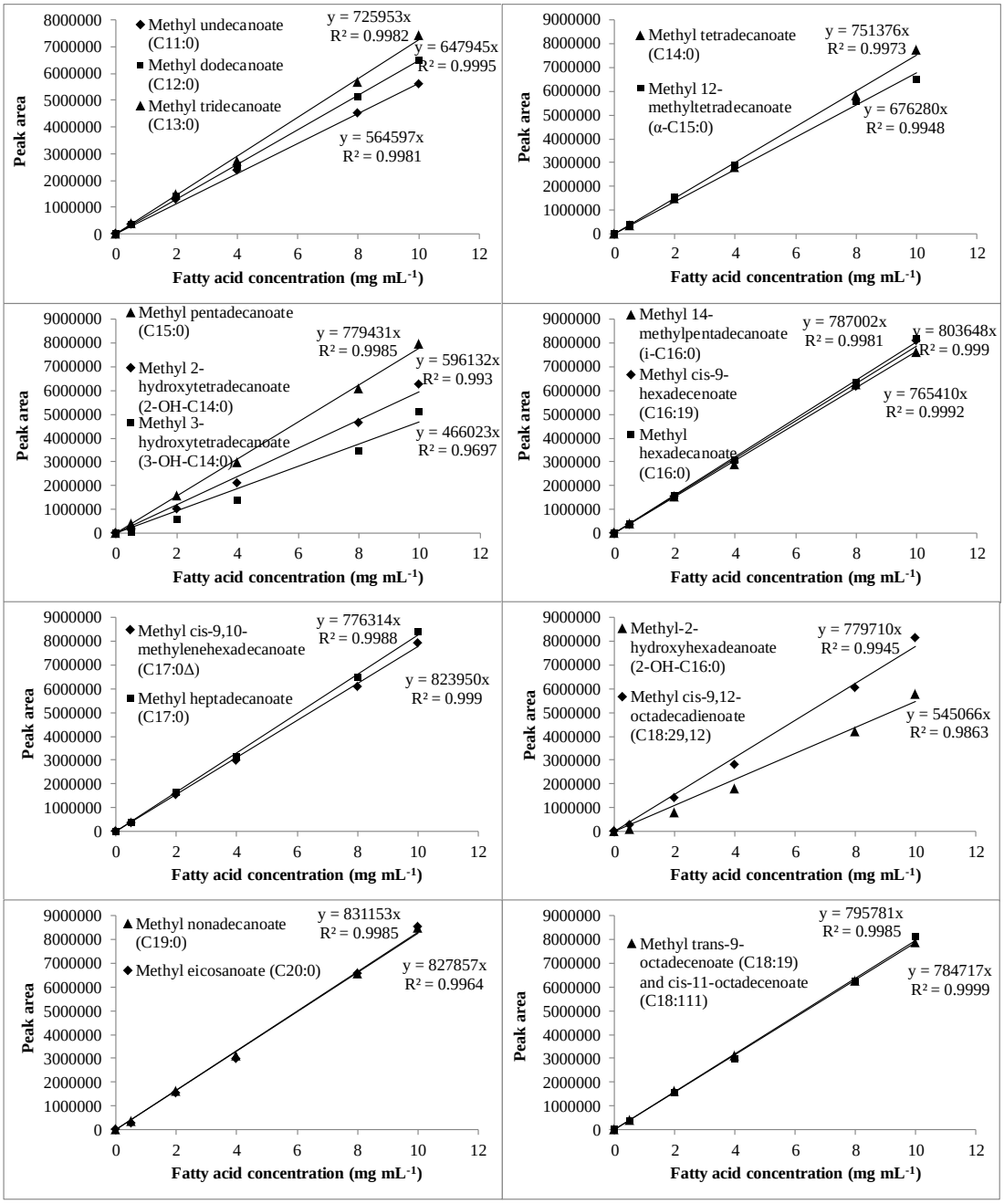

Figure 3.19 Calibration curves of bacterial acids methyl esters

3.5.8.3 Sample Preparation

The sample preparation involved extracting the lipids with solvents and methylation of the lipids to form fatty acid methyl esters (FAMEs) (White et al., 1979). 5 g of freeze dried sample were placed in 250 mL separating funnels, which had been

prewashed with DECON (phosphate free detergent), dried, rinsed with chloroform and allowed to dry. 30 mL phosphate buffer (prepared from 8.75 g K_2HPO_4 in 1 L of deionised water and the pH corrected to 7.4 with HCl) was added followed by 75 mL methanol and 37.5 mL chloroform. The funnels were shaken vigorously and the lipids allowed to extract for two hours. The separating funnel was covered with aluminium foil to exclude light as lipids are photosensitive. After two hours of extraction 37.5 mL chloroform and 37.5 mL water were added to break the liquid phases and the funnel shaken once more. The samples were left to separate into the aqueous and organic phases for 24 hours. The chloroform layer, which was at the bottom, was withdrawn from the funnel and filtered through Whatman No. 2 filter paper into glass vials. 20 mL of the lipid containing solvent was dried under a stream of nitrogen using a Techne sample concentrator. The samples were placed in a Techne dri-block set to a temperature of 30 °C during nitrogen blow down to aid evaporation of the solvent.

After the samples were dry, 1 mL of a 1:1 methanol: toluene mixture was added to them followed by 1 mL of freshly prepared 0.2 N methanolic potassium hydroxide solution (0.28 g KOH dissolved in 25 mL methanol). The vials were heated at 37 °C for 15 minutes and allowed to cool to room temperature. 1 mL of 1 M acetic acid was then added to lower the pH to 6 after which 2 mL chloroform followed by 2 mL water were added. The vials were shaken vigorously in a flask shaker for 5 minutes and then centrifuged at 2000 rpm for 5 minutes. The bottom layer of chloroform was withdrawn using glass Pasteur pipettes ensuring that none of the upper aqueous layer was withdrawn with it, placed into another vial and dried under nitrogen blow down. The dried lipids were resuspended in 300 µL of hexane. 150 µL was placed in GC

vials and 5 µL of bacterial acid methyl ester (BAME) CP mix (10 mg mL^{-1} total concentration in methyl caproate), obtained from Sigma Aldrich UK, added as an internal standard. The samples were then ready for GCMS analysis.

3.5.8.4 GCMS Analysis

The FAMEs were separated on the GCMS. The GC column was 15 m x 250 µm x 0.25 µm. The instrument was programmed to run at an initial temperature of 80 °C for the first minute and increasing at a rate of 20 °C min^{-1} up to 160 °C. It was then increased at 5 °C min^{-1} from 160 °C up to 270 °C. Total run time was 32 minutes. The carrier gas was helium and electron energy in electron impact was 70 eV. Injections were carried out in splitless mode (Frostegard et al., 1993). The lipids were identified by comparing their retention times to a lipids library suite in the analytical software and to the retention time of the BAME mix. Lipid quantification was by comparison of peak areas from samples to peak areas from BAME standards of known concentration.

3.6 Summary of Experiments

A summary of the soil column experiments carried out and the corresponding operating conditions are given in Tables 3.11 to 3.14.

Table 3.11 Summary of experiments and operating conditions for 2 meter soil column

Exper-iment number	Exper-iment ID	Duration of experiment (days)	Soil column length (mm)	Soil column inner diameter (mm)	Packing material	Water saturation	Parameter studied	Experimental condition	
								Influent concentration (mg L^{-1})	HLR (cm d^{-1})
1	HC-5	62	2000	140	Silica sand	Saturated	BOD, COD, DOC, DO, SO_4, NO_3, NH_3, Organic-N, phosphate, pH, temperature	135 (COD)	44
2	HC-10	18	2000	140	Silica sand	Saturated	BOD, COD, DOC, DO, SO_4, NO_3, NH_3, Organic-N, phosphate, pH, temperature	135 (COD)	88
3	HC-20	15	2000	140	Silica sand	Saturated	BOD, COD, DOC, DO, SO_4, NO_3, NH_3, Organic-N, phosphate, pH, temperature	135 (COD)	169
4	MC-20	8	2000	140	Silica sand	Saturated	BOD, COD, DOC, DO, SO_4, NO_3, NH_3, Organic-N, phosphate, pH, temperature	61 (COD)	169
5	LC-20	8	2000	140	Silica sand	Saturated	BOD, COD, DOC, DO, SO_4, NO_3, NH_3, Organic-N, phosphate, pH, temperature	42 (COD)	169

Table 3.12 Summary of experiments and operating conditions for unsaturated soil column

Exper-iment number	Exper-iment ID	Duration of experiment (days)	Soil column length (mm)	Soil column inner diameter (mm)	Packing material	Water saturation	Parameters studied	Experimental condition	
								Influent concentration (mg L^{-1})	HLR (cm d^{-1})
1	WT75 (SC1)	42	1000	150	Silica sand	Unsaturated – water table at 75 mm from column base	E1, E2, EE2, DOC, DO, SO_4, NO_3, NH_3, Organic-N, temperature, pressure head, water content	17 (DOC)	49
2	WT500 (SC1)	12	1000	150	Silica sand	Unsaturated – water table at 500 mm from column base	E1, E2, EE2, DOC, DO, SO_4, NO_3, NH_3, Organic-N, temperature, pressure head, water content	17 (DOC)	49
3	WT800 (SC1)	12	1000	150	Silica sand	Unsaturated – water table at 800 mm from column base	E1, E2, EE2, DOC, DO, SO_4, NO_3, NH_3, Organic-N, temperature, pressure head, water content	17 (DOC)	49

Table 3.13 Summary of experiments and operating conditions for 1 meter silica sand and silica sand/silt/clay columns

Exper-iment number	**Exper-iment ID**	**Duration of experiment (days)**	**Soil column length (mm)**	**Soil column inner diameter (mm)**	**Packing material**	**Water saturation**	**Parameter studied**	**Experimental condition**	
								Influent concentration (mg L^{-1})	**HLR (cm d^{-1})**
1	SC2	42	1000	150	Silica sand	Saturated	E1, E2, EE2, DOC, DO, SO_4, NO_3, temperature	17 (DOC)	81.5
2	SC2	12	1000	150	Silica sand	Saturated	E1, E2, EE2, DOC, DO, SO_4, NO_3, temperature	17 (DOC)	163
3	SC2	12	1000	150	Silica sand	Saturated	E1, E2, EE2, DOC, DO, SO_4, NO_3, temperature	34 (DOC)	81.5
4	SC3	42	1000	150	65% silica sand/ 25% silt/10% clay	Saturated	E1, E2, EE2, DOC, DO, SO_4, NO_3, temperature	17 (DOC)	81.5
5	SC3	12	1000	150	65% silica sand/ 25% silt/10% clay	Saturated	E1, E2, EE2, DOC, DO, SO_4, NO_3, temperature	17 (DOC)	163
6	SC3	12	1000	150	65% silica sand/ 25% silt/10% clay	Saturated	E1, E2, EE2 DOC, DO, SO_4, NO_3, temperature,	34 (DOC)	81.5

Table 3.14 Summary of experiments and operating conditions for 300 mm soil column

Exper-iment number	**Exper-iment ID**	**Duration of experiment (days)**	**Soil column length (mm)**	**Soil column inner diameter (mm)**	**Packing material**	**Water saturation**	**Parameter studied**	**Experimental condition**	
								Influent concentration (mg L^{-1})	**HLR (cm d^{-1})**
1	Small column	3	300	75	Silica sand	Saturated	TCC, COD	67 (COD)/ 7.830 x 10^{-4} (TCC)	150
2	Small column	4	300	75	Silica sand	Saturated	TCC, COD	67 (COD)/ 1.112 x 10^{-3} (TCC)	150
3	Small column	3	300	75	Silica sand	Saturated	TCC, COD	67 (COD)/ 2.130 x 10^{-3} (TCC)	150
4	Small column	3	300	75	Silica sand	Saturated	TCC, COD	67 (COD)/ 3.501 x 10^{-3} (TCC)	150
5	Small column	1	300	75	Silica sand	Saturated	TCC, COD	67 (COD)/ 2.372 x 10^{-3} (TCC)	150

CHAPTER 4

4 RESULTS AND DISCUSSIONS

4.1 Introduction

This chapter presents the results and discussions on all the experiments carried out as detailed in Chapter 3. These are:

i. Simulations carried out in the 2 meter long saturated soil column for the removal of common wastewater parameters;
ii. Investigations carried out on the removal of estrogens in the set of three 1 meter long soil columns under saturated and unsaturated soil conditions;
iii. Studies undertaken on the removal of triclocarban using a saturated 300 mm long soil column.

4.2 Removal of Synthetic Wastewater Parameters under Varying Hydraulic Loading Rates and Chemical Oxygen Demand

Investigations conducted to assess the removal of chemical oxygen demand (COD), biochemical oxygen demand (BOD), dissolved organic carbon (DOC), nitrogen and phosphate under variable hydraulic loading rates (HLRs) and influent COD concentration in the 2 meter saturated soil column are herein discussed. These saturated zone simulations may be likened to wastewater flow through shallow sandy aquifers where there is high likelihood of hydraulic continuity of the ponded wastewater in the SAT infiltration basin with the saturated zone of the aquifer. The hydraulic characteristics of the soil column obtained from residence time distribution studies carried out are presented. The soil column was packed at a density of 1.55 g

cm^{-3} and porosity of 0.41 using medium sand with median grain diameter of 750 microns.

4.2.1 2-meter Soil Column Hydraulic Properties

The hydraulic characteristics of the soil column at the different applied hydraulic loading rates were assessed from the tracer response curves obtained from residence time distribution studies. Figures 4.1 a – c show the concentration versus time tracer response curves for HLRs of 44, 88 and 169 cm d^{-1} respectively. At all three hydraulic loading rates, consistency checks carried out showed that 97 % or more of the tracer was recovered at the effluent end of the soil column. The consistency check involved comparing the sum of all fluorescein concentrations (C) measured at the effluent end within the test interval (t), that is, the area under the tracer response curve ($\int_0^\infty C(t)dt$) to the mass of tracer applied divided by the flow rate. Deviations of the measured value of $\int_0^\infty C(t)dt$ from the mass applied was in the range 2 to 3 % in all cases, meaning a tracer recovery of at least 97 % was achieved, which is acceptable (Crittenden et al., 2005).

The mean residence time, τ (T; min) from the tracer studies agreed closely with the theoretical value (τ_t) based on the soil column dimensions. The calculated (theoretical) value of the mean residence time included a correction for the 5 cm head of water present above the sand i.e.

$$\tau_t = \frac{A\left(\left(n \times (L - 5)\right) + 5\right)}{Q} \quad \text{.....[4.1]}$$

where A is the cross sectional area of the soil column (L^2; cm^2), L is the length (L; cm), n is the porosity of the sand and Q (L^3T^{-1}; $cm^3\ min^{-1}$) is the flow rate.

Theoretical residence times calculated were respectively 726 minutes (12.1 hrs), 1397 minutes (23.2 hrs) and 2539 minutes (1 day and 18.3 hrs) for HLRs of 169 cm d^{-1} (denoted by HF), 88 cm d^{-1} (denoted by MF) and 44 cm d^{-1} (denoted by LF). Hydraulic residence times obtained from the tracer tests at HLRs conditions of HF, MF and LF were respectively 730 minutes (12.2 hrs), 1427 minutes (23.8 hrs) and 3106 minutes (2 days and 3.8 hrs). Although the experimental residence times exceeded the theoretical, the deviations were only 0.5 % at 169 cm d^{-1} and 2 % at 88 cm d^{-1}. At 44 cm d^{-1} however, the experimental value exceeded the theoretical by 22 %. This large deviation could have occurred because of the low flow rate which was unable to properly transport the tracer allowing it to be retarded slightly by the sand. The soil column hydraulic properties derived from the tracer studies are summarised in Table 4.1.

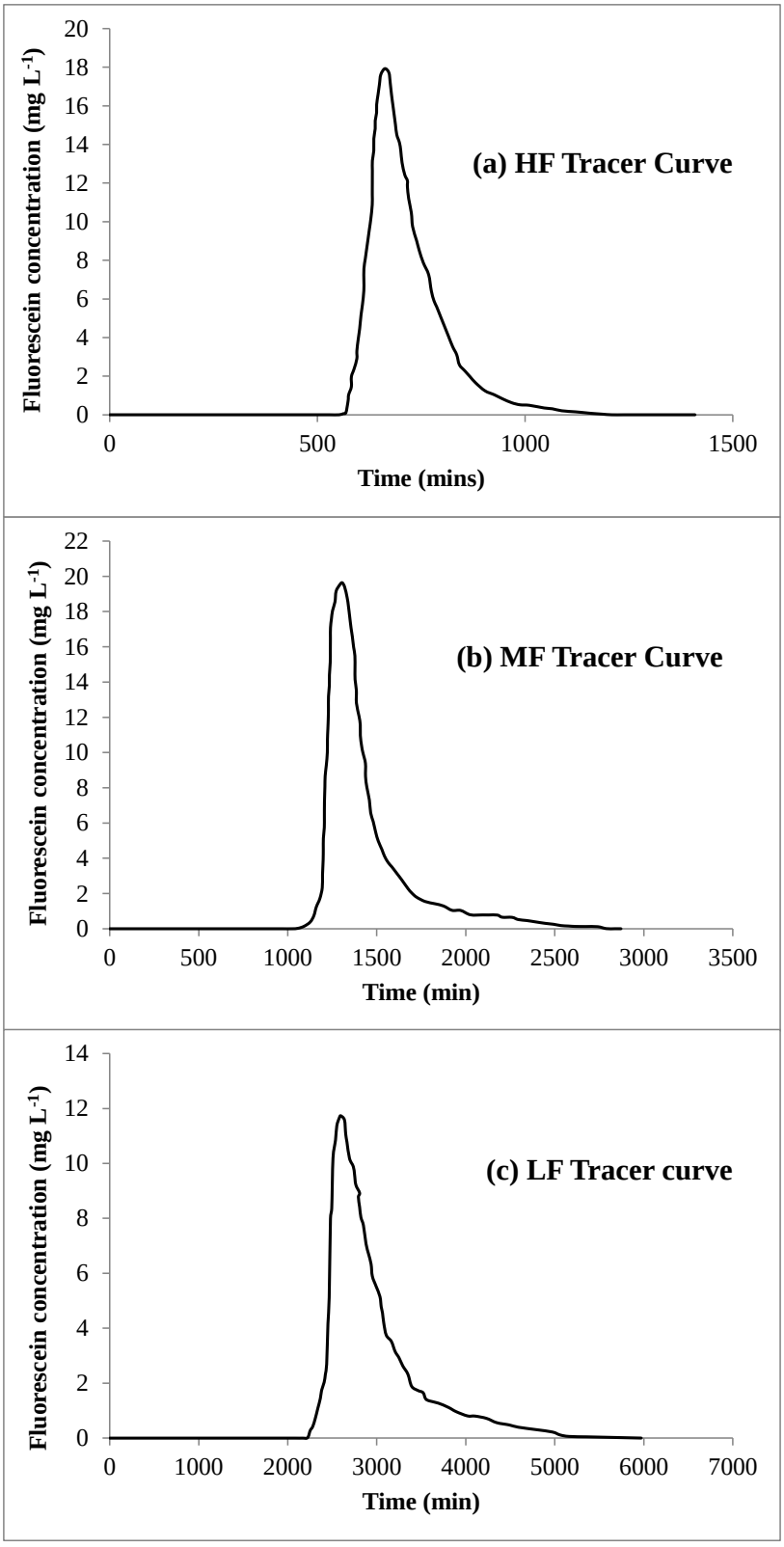

Figure 4.1 Concentration versus time tracer response at varying hydraulic loading rates using 50 mg pulse input of fluorescein tracer

(a) 169 cm d^{-1} HLR, (b) 88 cm d^{-1} HLR and, (c) 44 cm d^{-1} HLR

Table 4.1 Summary of soil column hydraulic characteristics

Parameter	**HF**	**MF**	**LF**
Residence time (minutes)			
Experimental, τ	730	1427	3106
Theoretical, τ_t	726	1397	2539
Coefficient of axial dispersion, D ($cm^2\ min^{-1}$)	0.68	0.58	0.53
Dispersion number, d	0.012	0.02	0.032
Peclet number of longitudinal dispersion, Pe	84	51	31
Variance, σ^2 (min^2)	12842	81743	641852
Number of complete-mix reactors in series, N_r	42	25	15

HF, MF and LF indicate HLRs of 169 cm d^{-1}, 88 cm d^{-1} and 44 cm d^{-1} respectively.

The relevant equations used to determine the values of the parameters in Table 4.1 are given in Equations 4.2 to 4.7 (Levenspiel, 1999):

$$\tau = \frac{\int_0^\infty tC(t)dt}{\int_0^\infty C(t)dt} \quad \text{.....[4.2]}$$

$$\sigma^2 = \frac{\int_0^\infty t^2C(t)dt}{\int_0^\infty C(t)dt} - \tau^2 \quad \text{.....[4.3]}$$

$$\sigma_\theta^2 = \frac{\sigma^2}{\tau^2} = 2\left(\frac{D}{uL}\right) - 2\left(\frac{D}{uL}\right)^2 \left[1 - e^{-uL/D}\right] \quad \text{.....[4.4]}$$

The peclet number, Pe is given by:

$$Pe = \frac{uL}{D} \quad \text{.....[4.5]}$$

Simplifying Equation 4.4 by substituting Equation 4.5, the resulting equation was solved for *Pe*. The coefficient of axial dispersion, *D*, and the dispersion number, *d*, were then obtained from

$$D = \frac{uL}{Pe} \quad \text{.....[4.6]}$$

and

$$d = \frac{D}{uL} = \frac{1}{Pe} \quad \text{.....[4.7]}$$

The increase in the coefficient of dispersion with increase in pore water velocity, *u*, is consistent with literature where positive correlations are reported to exist between *D* and *u* (Perfect et al., 2002; Miretzky et al., 2006). The Peclet number of longitudinal dispersion, which signifies the ratio of mass transport by advection and that generated by dispersion, was found to be greater than 5 under all HLRs applied indicating that the mass transport of organic and inorganic substances in the soil column is facilitated mainly by the advective transport process (Bear, 1972; Tchobanoglous et al., 2003). At all the hydraulic loading rates, the dispersion number *d* was less than 0.05, indicating low dispersion and a small deviation from plug flow. A *d* value of zero indicates ideal plug flow whilst greater than 0.25 would mean high dispersion. Complete-mix reactors have dispersion numbers approaching infinity (Tchobanoglous et al., 2003). In the soil column used, forty one complete-mix reactors, given by half the Peclet number (Tchobanoglous et al., 2003), would be required to simulate plug flow with axial dispersion at a HLR of 169 cm d^{-1}. The number of reactors required reduces as the flow rate and thus velocity is also reduced.

4.2.2 Soil Column Experiments

This section presents findings from the experiments performed in the 2 meter soil column at constant HLR but varying wastewater COD and at constant COD but variable hydraulic loading rates. The removal of COD, BOD, DOC, nitrogen (nitrate, ammonia, organic) and phosphate in the soil column were studied at an influent COD of 135 mg L^{-1} applied at HLRs of 44 cm d^{-1}, 88 cm d^{-1} and 169 cm d^{-1} and also at influent COD of 61 mg L^{-1} and 42 mg L^{-1} applied at a HLR of 169 cm d^{-1}. Biodegradation and adsorption processes for the removal of organic material and nitrogen and phosphate in the soil column were evaluated due to them being the important removal mechanisms in SAT systems (Idelovitch and Michail, 1984). Samples were collected at 6 points along the soil column profile (0 mm, 100 mm, 600 mm, 1100 mm, 1700 mm and 2000 mm). 0 mm and 2000 mm respectively represent the influent and effluent samples. For each experiment, sampling was carried out from all points on at least three different occasions to confirm the results obtained. In addition to the previously mentioned wastewater quality parameters, dissolved oxygen and sulphate and pH were measured at all sampling depths. Changes in dissolved oxygen, nitrate and sulphate concentrations were used to determine the biochemical oxidation processes occurring in the soil column for the removal of COD, BOD and DOC.

4.2.2.1 Mass Loading Rates on the Soil Column

Average wastewater characteristics for each experiment are given in Table 4.2. HC, MC and LC represent high concentration, medium concentration and low concentration respectively. The notations allocated to each experiment and mass loadings to the soil column are given in Table 4.3.

Table 4.2 Influent characteristics

Parameter	**Average concentration (mg L^{-1})**		
	HC	**MC**	**LC**
Chemical Oxygen Demand (COD)	135	61	42
Biochemical Oxygen Demand(BOD)	88	43	26
Dissolved Organic Carbon (DOC)	50	26.6	16
Total Kjeldahl Nitrogen (TKN)	15	6.7	4.1
Ammonia nitrogen (NH_3-N)	4	1.7	1.4
Organic nitrogen (Org-N)	11	5	2.7
Nitrate nitrogen (NO_3-N)	2.5	2.3	2.4
Total nitrogen (TN)	17.5	9	6.5
Phosphate (PO_4)	6.7	4.4	4
Sulphate (SO_4)	50	56	50

Table 4.3 Experimental conditions

Exper-iment	**Wastewater concentration**	**Hydraulic loading rate (cm d^{-1})**	**Hydraulic residence time (hours)**	**Average COD mass loading rate (mg d^{-1})**	**Number of replicates**	**Standard error (mg d^{-1})**
HC-5	High concentration[a]	44	51.8	911	9	30.8
HC-10	High concentration[a]	88	23.8	1781	6	42.5
HC-20	High concentration[a]	169	12.2	3553	6	18.3
MC-20	Medium concentration[b]	169	12.2	1586	3	31.8
LC-20	Low concentration[c]	169	12.2	1084	3	31.2

[a] HC concentrations, [b] MC concentrations, [c] LC concentrations are as given in Table 4.2.

The mass loadings of dissolved oxygen, nitrate, sulphate, COD, DOC, BOD, nitrogen and phosphate on the soil column under the different conditions simulated are shown in Figures 4.2 a - c. Error bars in all figures are based on the standard error. These loadings (mg d^{-1}) were determined for each experiment by taking the product of the influent concentration (mg L^{-1}), the HLR (cm d^{-1}) and the cross sectional area (cm^2) of the soil in the column. The mass of the parameters existing at all the sampling points along the soil column was also determined in a similar fashion. The COD, DOC and BOD mass loadings to the soil column increased with an increase in HLR, with HC-20 having the highest loading. Mass loadings for HC-5 were close to LC-20 and that for HC-10 comparable to MC-20. The differences were less than 20 % in the former and 10 % for the latter.

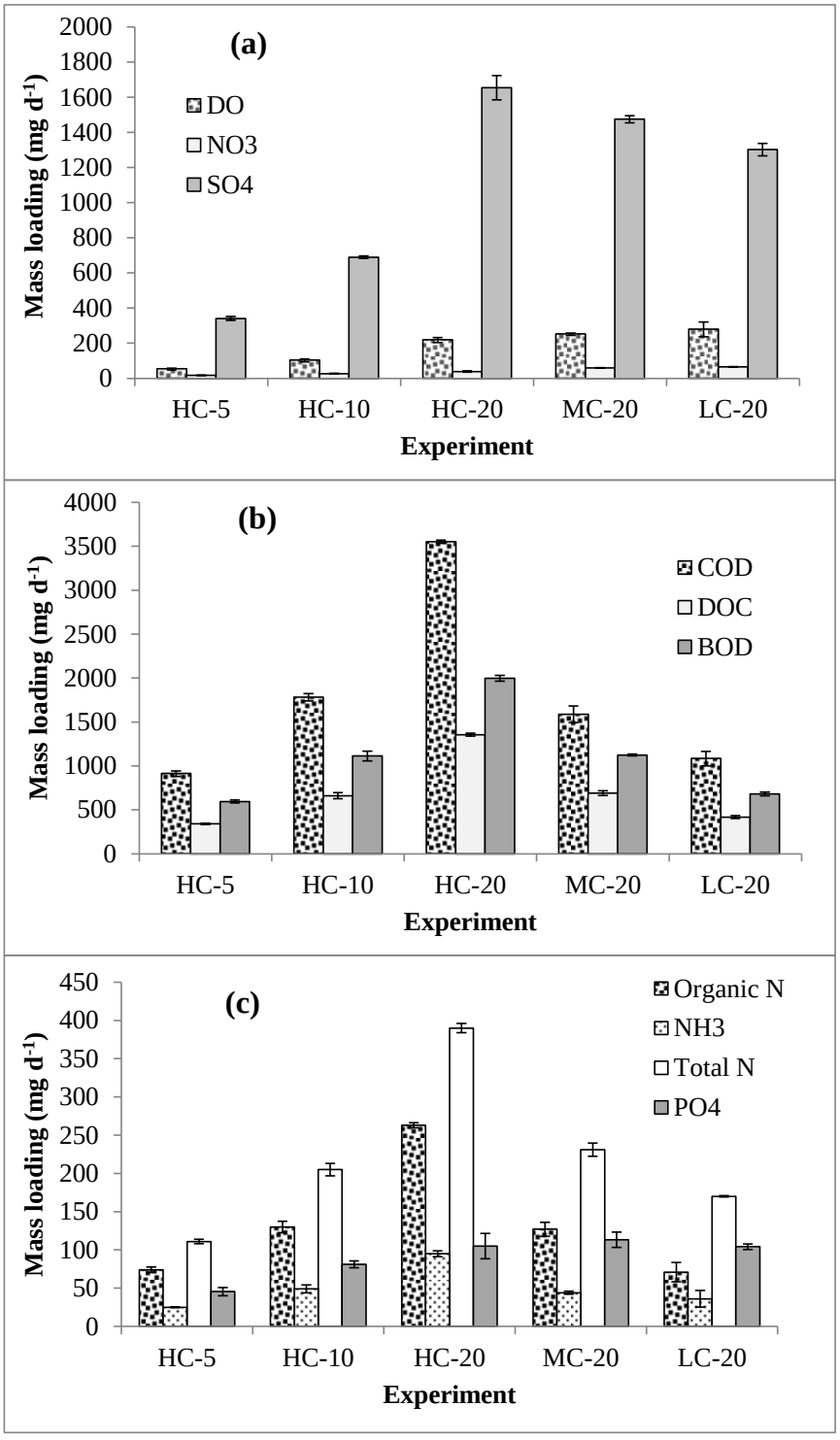

Figure 4.2 Mass loadings of wastewater parameters to the soil column

(a) Dissolved oxygen, nitrate and sulphate (b) COD, DOC and BOD (c) Organic nitrogen, ammonia nitrogen, total nitrogen and phosphate.

The same ratios of dissolved oxygen to COD, BOD and DOC were maintained when the HLR was changed and were 0.06, 0.09 and 0.16 respectively. MC-20 and LC-20 had ratios of 0.16 and 0.26 for COD, 0.22 and 0.41 for BOD and 0.36 and 0.67 for DOC. Higher dissolved oxygen to COD, BOD and DOC ratios resulting from decrease in substrate concentration means that there is greater dissolved oxygen availability per gram of substrate for aerobic degradation processes. The ratios of nitrate to COD, BOD and DOC were respectively 0.02, 0.02 and 0.05 during infiltration of HC wastewater and sulphate 0.4, 0.6 and 1.0.

4.2.2.2 Redox Conditions in the Soil Column

The redox conditions pertaining in the soil column were assessed by the consumption of dissolved oxygen, nitrate and sulphate in the soil column. The profiles for the mass of dissolved oxygen, nitrate and sulphate consumed per day using HC influent at the three different HLRs of 44 cm d^{-1}, 88 cm d^{-1} and 169 cm d^{-1} and the mass removed when the COD was varied while maintaining the HLR at 169 cm d^{-1} are respectively shown in the following subsections as Figures 4.3 through to 4.5. At the HLRs applied, hydraulic residence times in the soil column were 51.8 hours (2.15 days), 23.8 hours (0.99 days) and 12.2 hours (0.5 days). The removal profiles showed that dissolved oxygen, nitrate and sulphate were all consumed within the soil column. Microbial respiration mechanisms identified to have occurred in the soil column for the removal of organic carbon are therefore aerobic respiration involving the use of dissolved oxygen as the final electron acceptor and anaerobic respiration with nitrate (denitrification) and sulphate (sulphate reduction) as other terminal electron acceptors.

Dissolved Oxygen Utilisation

At all the HLRs applied, mass removal rates of dissolved oxygen in the soil column increased with an increase in HLR (Figure 4.3 a) due to higher organic mass loadings. Oxygen utilisation rates were thus highest in HC-20.

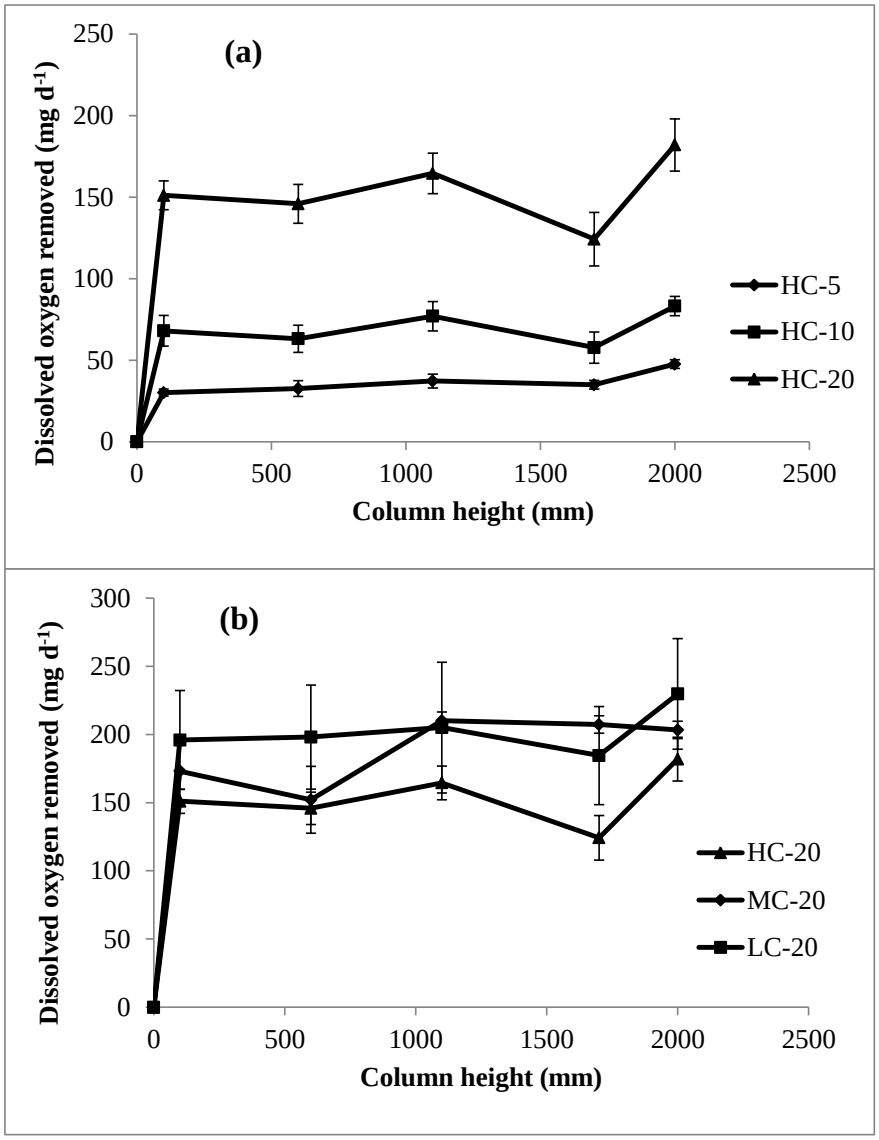

Figure 4.3 Dissolved oxygen mass removal rate against soil column depth (a) at constant COD of 135 mg L^{-1} and HLR of 44, 88 and 169 cm d^{-1} and (b) at constant HLR of 169 cm d^{-1} and 135, 61 and 42 mg L^{-1} COD (T = 20 °C)

At 100 mm, dissolved oxygen consumption as a function of the amount available initially increased with corresponding increase in COD mass loading. 57 %, 67 % and 69 % dissolved oxygen was already consumed by 100 mm for HC-5, HC-10 and HC-20 respectively. Beyond that depth, as most of the oxygen had already been consumed and concentrations in the wastewater were only 3 mg L^{-1}, removals measured were not found to reduce consistently and in some cases, increased concentrations were measured. The inconsistencies in measured concentrations may be due to some entrainment of oxygen during sample collection and as the concentrations were already low, any little addition would not be buffered and would be obvious. Over all oxygen was utilised at 48 mg d^{-1}, 83 mg d^{-1} and 182 mg d^{-1} for HC-5, HC-10 and HC-20 respectively.

Figure 4.3 b depicts the mass removal profiles of dissolved oxygen along the soil column at a constant HLR of 169 cm d^{-1} and varying wastewater COD concentrations. Again, at 100 mm, dissolved oxygen concentrations in samples were 3 mg L^{-1} on the average, representing a significant utilization of about 70 %. In all samples, overall, greater than 80 % of available dissolved oxygen was utilised. Oxygen utilization rates for MC-20 and LC-20 were respectively 203 mg d^{-1} and 230 mg d^{-1}.

The utilisation of dissolved oxygen by microorganisms for the oxidation of organic material in the soil column can be represented by the reaction below (Gray, 2004):

$$Organics + O_2 \xrightarrow[organisms]{aerobic\ micro} Aerobic\ microorganisms + CO_2 + H_2O + energy$$

Some of the energy released from this reaction is used by the soil column microorganisms for cell maintenance and synthesis and growth of new microbial cells (Bitton, 1999). Due to the slow rate of oxygen replenishment to the soil column at reduced HLR, the other electron acceptors being nitrate and sulphate were increasingly relied on when HLR and thus mass loadings were increased. This occurred especially within the first 100 mm of the soil column where highest organic loading pertains. Biodegradation involving these electron acceptors is much slower and often produces malodourous chemically complex by-products especially in the case of sulphate (Gray, 2004), and this was evident in the soil column.

Nitrate Utilisation

The results shown in Figures 4.4 a and b show reductions in nitrate concentrations occurred simultaneously with dissolved oxygen removal within the soil column. When the wastewater of high concentration was applied, nitrate concentrations reduced by 87 % to 93 % within the first 100 mm of the soil column. Although the rate of nitrate removal within the first 100 mm of the sand column was highest (93 %) at the lowest loading rate (HC-5), the removal proceeded slowest beyond that point compared to the other HLRs, for which 100 % nitrate removal was achieved by the 600 mm depth. No nitrate was therefore detected at 600 mm in HC-10 and HC-20 soil column samples. At a HLR of 44 cm d^{-1}, there was complete removal of nitrate after a distance of 1100 mm. Within the whole column depth, nitrate consumption occurred at a rate of 17 mg d^{-1}, 27 mg d^{-1} and 39 mg d^{-1} for HC-5, HC-10 and HC-20 respectively. At very low nitrate-N concentrations (0.1 mg L^{-1}), the kinetics of utilization of substrate in the soil column would be influenced by the nitrate concentration (Tchobanoglous et al., 2003). Due to nitrate serving as an

electron acceptor, the rate of denitrification would be proportional to the rate of substrate utilization (Tchobanoglous et al., 2003). Thus it is expected that nitrate depletion would contribute to a drop in the removal of organic substances in the soil column, as would occur in the case of oxygen.

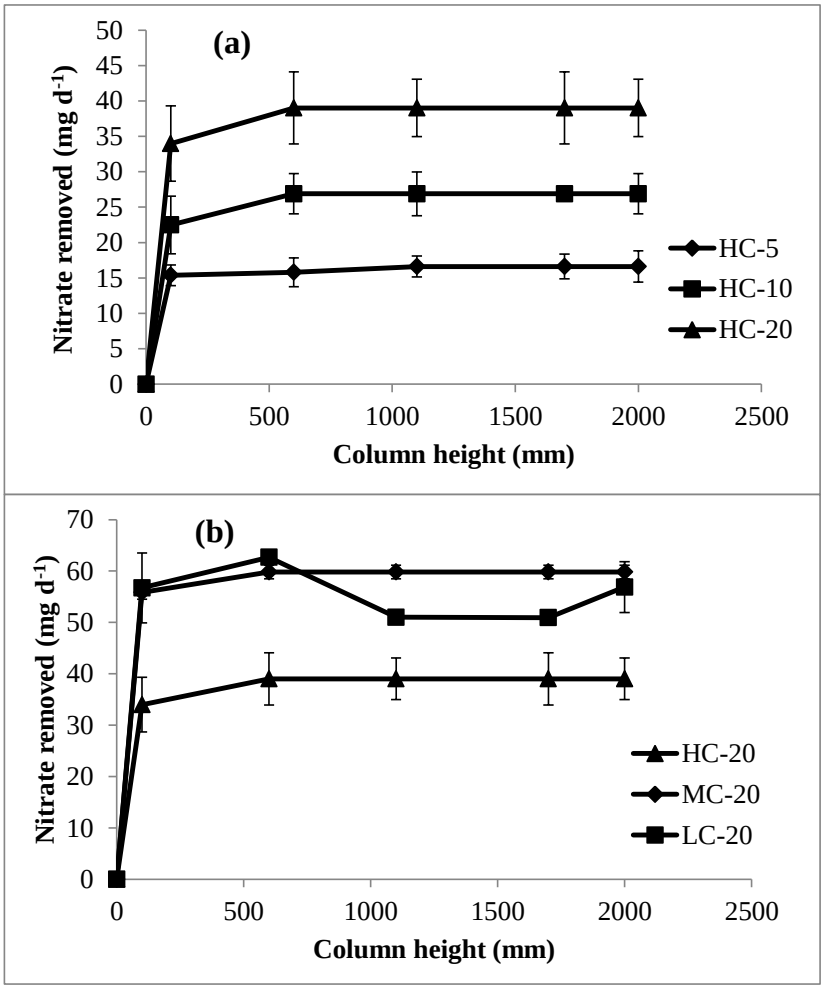

Figure 4.4 Nitrate mass removal rate against soil column depth at 20 °C for (a) constant COD of 135 mg L^{-1} and HLR of 44, 88 and 169 cm d^{-1} (b) constant HLR of 169 cm d^{-1} and 135, 61 and 42 mg L^{-1} COD.

In the experiments where the wastewater concentration was varied at constant HLR (Figure 4.4 b), nitrate was completely depleted in all samples by the 600 mm depth

of the soil column. In the LC influent, nitrate was again detected at the 1100 mm depth. This may be due to nitrification of ammonia taking place as a result of the low wastewater concentration and therefore higher dissolved oxygen concentrations pertaining within deeper layers of the soil column. A corresponding reduction in ammonia was not detected probably due to the continued degradation of organic nitrogen in the infiltrating wastewater. Any remaining nitrate was once again consumed further along the soil column.

Even though the removal of nitrate by microorganisms could occur through a dissimilatory (denitrification) or an assimilatory (conversion of NO_3 to NH_3) route (Bitton, 1999), the presence of ammonium nitrogen in the soil column influent and wastewater samples rules out the occurrence of assimilatory nitrate reduction and confirms the occurrence of denitrification in the soil column. This is because assimilatory nitrate reduction takes place when ammonium nitrogen, which serves as a nutrient source for microbial cell synthesis is unavailable thereby necessitating the biological breakdown of nitrate for the release of ammonia (Tchobanoglous et al., 2003). Denitrification occurred in the soil column by the reduction of nitrate to nitrogen gas through nitrite, nitric and nitrous oxide intermediaries as shown below (Bitton, 1999).

$$NO_3 \xrightarrow{\text{Nitrate reductase}} NO_2 \xrightarrow{\text{Nitrite reductase}} NO \xrightarrow{\text{Nitric oxide reductase}} N_2O \xrightarrow{\text{Nitrous oxide reductase}} N_2$$

The reaction of nitrate with organic material in the soil column is therefore as shown (Gray, 2004):

$$Organics + NO_3 \xrightarrow{\text{anaerobic micro organisms}} Anaerobic\ microorganisms + CO_2 + N_2 + energy$$

It was expected that in the soil column environment, consisting of a mixed culture of bacteria, the microorganisms would pursue the route with the highest energy yield so as to attain maximum cell synthesis (Gray, 2004). The order of preference of use of electron acceptor would therefore be in the descending order of oxygen, nitrate and sulphate, which respectively release -78.14, -71.67 and 21.27 kJ of free energy per electron equivalent (Tchobanoglous et al., 2003; Gray, 2004). This was however found not to be the case and oxygen was not completely depleted before nitrate consumption begun. Neither was nitrate completely depleted before the consumption of sulphate. The hierarchy for utilization of TEAs (based on their respective redox potentials) therefore does not preclude the occurrence of denitrification and sulphate reduction in cases where there are relatively high oxygen concentrations existing in the bulk wastewater. Denitrification in the aerobic environment is hypothesised to have been facilitated by active nitrate reductase sites within the periplasmic parts of the soil column bacteria (Carter et al., 1995). These results are confirmed by other studies where denitrification was observed to occur in aerobic environments (Lloyd et al., 1987; Bengtsson and Annadotter, 1989; Bateman and Baggs, 2005; Rao et al., 2007; Gao et al., 2010) even at concentrations close to or greater that air oxygen saturation values (8.6 mg L^{-1}). Specific bacteria (Carter et al., 1995; Patureau et al., 2000; Kim et al., 2008) as well as some fungi (Hayatsu et al., 2008) have also been isolated that are able to carry out denitrification under aerobic conditions.

Sulphate Utilisation

As shown in Figures 4.5 a and b, reductions in sulphate concentrations also occurred simultaneously with dissolved oxygen and nitrate removal within the soil column. Sulphate consumption occurred in the soil column at all mass loading rates.

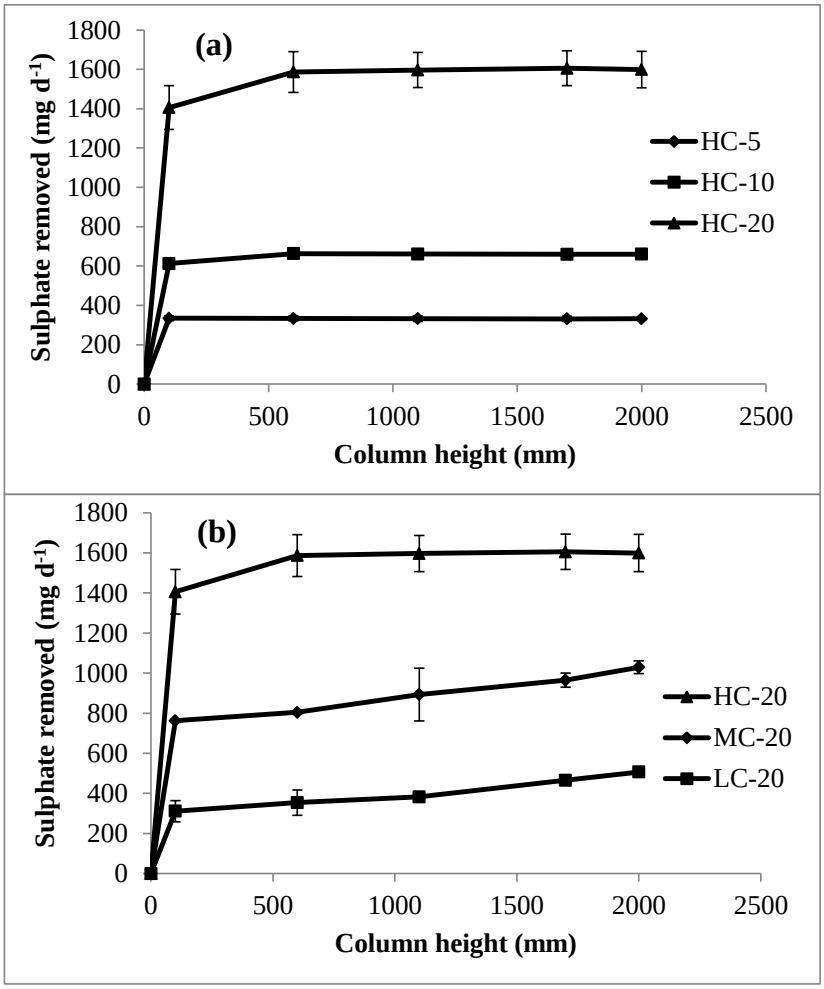

Figure 4.5 Sulphate mass removal rate against soil column depth at 20 °C for (a) constant COD of 135 mg L^{-1} and HLR of 44, 88 and 169 cm d^{-1} and (b) constant HLR of 169 cm d^{-1} and 135, 61 and 42 mg L^{-1} COD.

The characteristic rotten egg smell of hydrogen sulphide emanated from all column samples, with it being strongest in the HC wastewater and lowest in the LC wastewater. Sulphate reduction can therefore be represented by the reaction below (Gray, 2004):

$$Organics + SO_4^{2-} \xrightarrow{\substack{anaerobic\\micro\\organisms}} Anaerobic\ microorganisms + CO_2 + H_2S + energy$$

As HLR and thus the mass loadings increased, the mass of sulphate removed also increased. During infiltration of HC wastewater, almost all the sulphate was broken down due to a high demand for oxygen for the degradation of organic carbon. Sulphate utilization rates at HLR of 44 cm d^{-1}, 88 cm d^{-1} and 169 cm d^{-1} were respectively 334 mg d^{-1}, 613 mg d^{-1} and 1406 mg d^{-1}, representing 98 %, 89 % and 85 % reduction within the first 100 mm of the column. By the column exit, sulphate utilization had reached 660 mg d^{-1} and 1599 mg d^{-1} for HC-10 and HC-20. No further increase in sulphate removed occurred for HC-5 since most of the sulphate had already been consumed. The percentage reduction thus did not change much beyond this depth.

Sulphate reduction occurred in the soil column at all applied wastewater COD concentrations (Figures 4.5 b). However, reducing the mass loading by applying wastewater of lower COD while keeping the HLR at 169 cm d^{-1} resulted in a decrease in sulphate consumption in the soil column. Removal rates dropped from 1599 mg d^{-1} in HC wastewater to 1029 mg d^{-1} and 507 mg d^{-1} in MC and LC wastewaters respectively. Less than 40 % of influent sulphate was therefore consumed in LC wastewater compared to 98 % in the high COD wastewater. Even though sulphate reducing bacteria, which are responsible for sulphate reduction, are thought to be strict anaerobes their presence in the soil column, confirmed by the occurrence of sulphate reduction indicates that they are also able to tolerate oxygen in their environment. These results are consistent with other studies where sulphate reducing bacteria were found to exist in activated sludge flocs as well as in biofilms of rotating biological contactors and trickling filters (Lens et al., 1995). Besides sulphate reduction has been observed to occur consistently in well-oxygenated

biomats (Canfield and Des Marais, 1991). The occurrence of sulphate reduction in the aerobic environment of the soil column could be attributed to the development of anoxic microsites and physiological adaptability of the anaerobic microorganisms (Lens et al., 1995). It is hypothesised that oxygen concentration gradients across the thickness of biofilms coating the sand grains could have contributed to the formation of anoxic and anaerobic zones in the deeper layers of the biofilm (Tchobanoglous et al., 2003).

The results obtained clearly showed that at constant hydraulic loading rate, sulphate reduction was dependent on the COD mass loading with its breakdown reducing with a corresponding reduction in COD loading. Sulphate reduction was also found to be affected by changes in HLR with its rate of reduction decreasing with the increase in the loading rate, though not to as much extent as changes in COD concentrations.

4.2.2.3 Dissolved Organic Carbon, Biochemical and Chemical Oxygen Demand Removal under Constant Chemical Oxygen Demand and Variable Hydraulic Loading Rates

Figures 4.6 a - c show the mass removal of DOC, BOD and COD in the column at constant COD and variable HLR. There was a corresponding increase in mass removed with mass loading rate. This is because aerobic bacteria conversion of organic material, assessed by BOD, is typically a first order reaction and is a function of the substrate concentration remaining at any time (Tchobanoglous et al., 2003). At HC-5, HC-10 and HC-20, COD, DOC and BOD mass removal rates after

2000 mm travel through the soil column were respectively 249, 568 and 1024 mg d^{-1}, 172, 321 and 716 mg d^{-1}, and 247, 475 and 555 mg d^{-1}.

Even though more mass was removed as the mass loading was increased, it did not necessarily translate into improved removal efficiencies for BOD and COD. These respectively give overall removal efficiencies at HC-5, HC-10 and HC-20 of 27, 32 and 29 % for COD, 50, 49 and 53 % for DOC and 41, 42 and 28 % for BOD. As occurred with dissolved oxygen, sulphate and nitrate most of the removal attained after travel through the whole length of the soil column occurred within the first 100 mm of the soil column. In most cases removal within this depth amounted to 80 % or greater of the overall removal achieved. Most of the available dissolved oxygen was consumed here and on the average only 3 mg L^{-1} remained after 100 mm. Nitrate and sulphate were also considerably used up within the first 100 mm with less than 0.5 mg L^{-1} nitrate and 2 mg L^{-1} sulphate remaining.

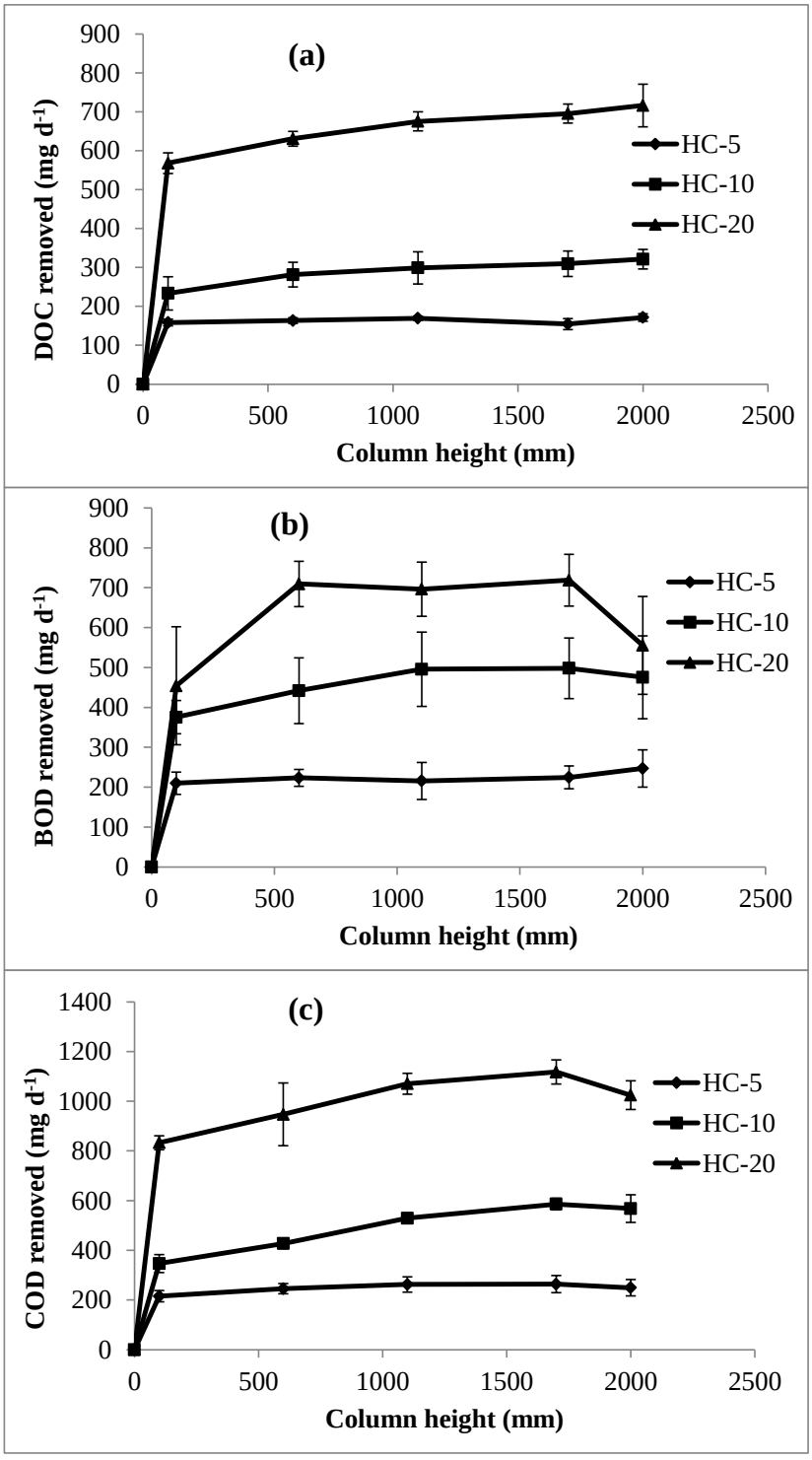

Figure 4.6 Mass removal rate of DOC, BOD and COD with soil column depth at 135 mg L^{-1} COD and variable HLRs of 44 cm d^{-1}, 88 cm d^{-1} and 169 cm d^{-1}

(a) DOC (b) BOD (c) COD

Similar patterns of removal between COD, DOC, BOD and DO, NO_3 and SO_4 are expected because during biological oxidation energy stored in organic matter is released by dehydrogenation of the substrate leading to the donation of electrons. The electrons given up by the electron donor are then carried through a series of complex biochemical pathways to oxygen, nitrate and sulphate which are the terminal electron acceptors (TEAs) (Bitton, 1999; Gray, 2004). This electron transport is facilitated through the electron transport system (ETS) of the bacteria proliferating in the soil column (Bitton, 1999). The degree of biodegradation that would take place would therefore be dependent on the type and quantity of TEAs present which would determine the electron accepting capacity.

For DOC, COD and BOD the lowest loading rate performed very well initially, in terms of its efficiency of removal, it however did not give the best overall removal due to its slower rate of removal beyond the 100 mm depth. This may have been contributed by the high retention time in the column, necessitating high oxygen replenishment for aerobic processes and limitations on the availability of the other electron acceptors. Within the first 100 mm as dissolved oxygen levels were high, longer residence times allowed sufficient time for effective aerobic degradation of the DOC, BOD and COD. However, as dissolved oxygen was being depleted, its low rate of replenishment from the influent wastewater became an important factor as removal could not be sustained deeper within the soil column. This is evident from the flattening of the curves beyond 100 mm as the HLR is reduced (Figures 4.6 a – c). The low oxygen concentrations and yet high oxygen demand of the wastewater therefore promoted the onset of anoxic and anaerobic degradation processes. Thus by the 600 mm depth, long residence time was no longer the most efficient operating

condition. Due to better oxygen replenishment upon increase of the HLR, DOC, BOD and COD removal could be sustained better within deeper layers of the soil column although the rate was considerably slowed down. A balance between residence times and the rate of replenishment of electron acceptors was thus found crucial to the efficiency of the removal process in the soil column. HC-10 therefore gave the highest and HC-5 the lowest overall removal of BOD and COD, with HC-20 being the most efficient condition for DOC. This behaviour suggests that a certain critical hydraulic loading rate may exist for efficient removal of each parameter based on the influent concentration and that long residence times do not necessarily improve performance.

4.2.2.4 Dissolved Organic Carbon, Biochemical and Chemical Oxygen Demand Removal under Variable Chemical Oxygen Demand and Constant Hydraulic Loading Rate

Figures 4.7 a - c show profiles of the mass reductions in COD, BOD and DOC at constant HLR of 169 cm d^{-1} and varying wastewater COD. At constant hydraulic loading rate, the mass loadings of COD, DOC and BOD applied to the soil column decrease with reduction in COD concentration. Mass of DOC, COD and BOD removed decreased with a corresponding decrease in mass applied. The removal efficiency however increased. COD mass removal rate was 1024 mg d^{-1} for HC-20, decreasing to 582 mg d^{-1} for LC-20. The corresponding increase in removal efficiency was from 29 % to 54 %. Increase in removal efficiency with reduction in COD under constant HLR has also been found to occur in horizontal flow constructed wetlands (Ojeda et al., 2008).

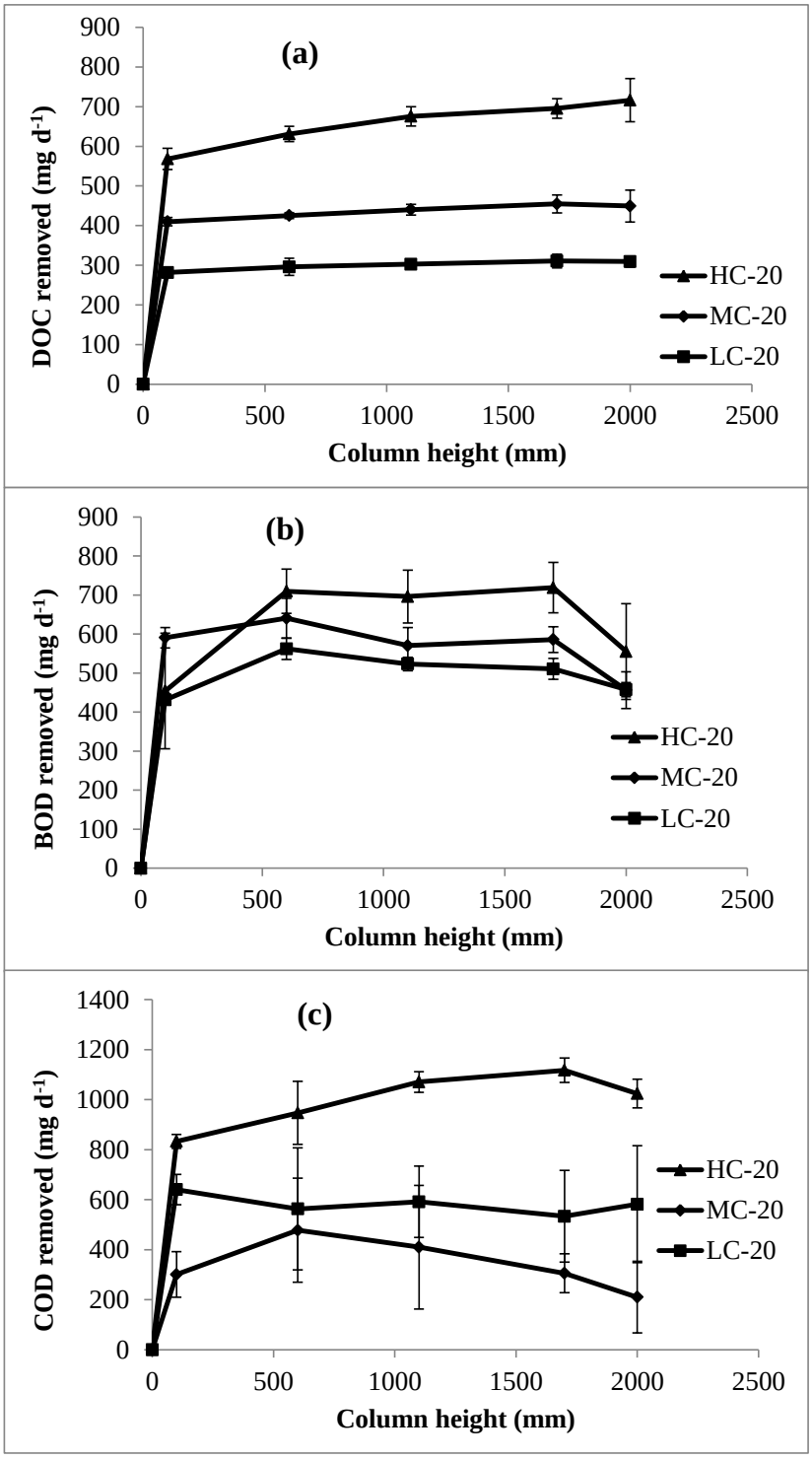

Figure 4.7 Mass removal rate of DOC, BOD and COD with soil column depth at HLR of 169 cm d^{-1} and variable COD of 135 mg L^{-1}, 81 mg L^{-1} and 42 mg L^{-1}

(a) DOC, (b) BOD and (c) COD

Regardless of the residence times or influent concentration the first 100 mm depth of the soil column accounted for a greater proportion of DOC, COD and BOD removal obtained. These results are in good agreement with published literature confirming the important role of the first few cm of the soil in the treatment process (Quanrud et al., 2003b; Cha et al., 2004; Grünheid et al., 2005). Bunsri et al's (2008) studies revealed that out of 83 % COD removal achieved after wastewater travel through 120 cm of a column of soil, 80 % removal was already attained after only 30 cm travel length. In field studies about 75 % of the DOC removal obtained after 37 m infiltration occurred within the first 1.5 m of soil (Quanrud et al., 2003b) and in unsaturated soil columns 44 % DOC removal was realised within the top 8 cm of the soil (Quanrud et al., 1996b). Rauch-Williams and Drewes (2006) also found from their study that removal of biodegradable organic carbon occurs within 30 cm of the soil depth. Removal is rapid near the soil/water interface in SAT systems because organic matter and dissolved oxygen are at their highest concentrations resulting in high biological activity (Fox et al., 2006). The prominence of the role of this depth was observed to increase with a decrease in influent concentration, accounting for 79 %, 91 % and then 92 % of the overall removal achieved respectively. These percentages have been determined by expressing the amount of DOC removed at the 100 mm depth as a percentage of the total amount removed in the whole 2000 mm depth of the column.

Overall DOC mass removals per day achieved over the 2000 mm column for HC-20, MC-20 and LC-20 were 716 mg (53 %), 449 mg (65 %) and 309 mg (74 %) respectively. Biodegradation as measured by the BOD (Figure 4.7 b) also followed a similar pattern of reduction as the DOC. BOD removed per day was 555 mg (28 %),

456 mg (41 %) and 458 mg (67 %). Increases in the values of BOD and COD within the sand profile were observed in some samples depicted by a drop in mass removed as shown in Figures 4.7 b and c respectively. The increases may be attributed to the generation of soluble extracellular by-products by the microorganisms in the column or desorption of organics from the sand as has been observed to occur for DOC (Drewes and Jekel, 1996; Reemtsma et al., 2000; Quanrud et al., 2003b). These soluble microbial products, comprising polysaccharides, proteins, nucleic and humic acids and lipids (Wu and Lee, 2011), are by-products of microbial substrate utilisation and are released into the soil column liquid phase during lysis of soil column microbial cells (de Silva and Rittmann, 2000). Soluble microbial products may increase in the soil column under stress conditions such as insufficient quantity of nutrients and low pH (Jarusutthirak and Amy, 2007), which was the condition prevailing especially towards the soil column outlet.

Even though higher mass loadings corresponded with larger mass removals, the percentage removal was better at lower mass loading rates due to higher dissolved oxygen to substrate mass loading ratios. The decrease in removal of COD, BOD and DOC with increase in influent concentration may be attributed to the corresponding increase in anaerobic conditions in the soil column. Maddoff et al (1974) found in their study on soil infiltration with septic tank effluent that COD removal decreased when the soil surface became permanently ponded due to encrustation and the subsequent onset of anaerobic conditions. The pattern of dissolved oxygen, nitrate and sulphate removal (Figures 4.3, 4.4 and 4.5) suggest the predominance of aerobic degradation during infiltration with LC wastewater. The percentage utilisation of dissolved oxygen was found to increase with a reduction in the mass loadings, whilst

the opposite effect occurred on sulphate. Consequently, sulphate reduction processes dropped from overall utilisation of 97 % for a COD loading of 3552 mg d^{-1} down to 70 % at 1586 mg d^{-1} and a further reduction to 40 % when a COD loading of 1084 mg d^{-1} was applied. Aerobic degradation which proceeds more rapidly and has much higher biochemical efficiency than anoxic processes and anaerobic degradation (Gray, 2004) thus increasingly dominated the removal process resulting in improved removal efficiencies.

Using a COD of 135 mg L^{-1}, the range of removal efficiencies obtained for COD (27 – 32 %), DOC (49 – 53 %) and BOD (28 – 43%) are lower than reported in literature due to the much higher concentrations of the parameters in the influent coupled with saturated soil conditions in the column. COD removals reported include 80 – 85 % (Carre and Dufils, 1991) and almost 100 % (Bouwer et al., 1980). Even though 80 – 85 % COD removal was reported by Carré and Dufils (1991) the soluble COD removal was only 30 – 35 %. Chua et al., (2010) also measured lower DOC removal (31 %) compared to removals from other SAT field sites, when the unsaturated zone was by-passed and the wastewater directly injected into the saturated zone of the aquifer. DOC removal obtained by Chua et al., (2010) is still lower than in the current study due to the differences in characteristics of the infiltrating wastewater, which was ultra-filtered effluent and therefore has a low level of biodegradable DOC. With a reduction in COD concentrations, for example at influent wastewater COD of 42 mg L^{-1}, the removal of 54 % COD, 74 % DOC and 67 % BOD obtained compared more closely to those obtained from other studies. They are however in the lower range of removals obtainable due to the absence of an unsaturated zone, where replenishment of dissolved oxygen is easily achieved.

4.2.2.5 Organic Matter Removal by Adsorption in the Soil Column

Abiotic soil column data obtained from running the soil column at condition LC-20 after sterilisation showed only slight reductions in COD and DOC occurring within the first 100 mm of the soil column which in the biotic experiments was the most active removal zone. COD and DOC removal rates realised were only 52 mg d^{-1} and 2.3 mg d^{-1} respectively, representing 4 % COD and less than 1 % DOC removal. Abiotic removal such as physical adsorption thus represented only a small proportion of the removals obtained in the soil column. COD, DOC and BOD removal in the soil column could therefore be attributed primarily to biological removal which may occur through the mechanisms of biodegradation or biosorption onto biomass structures such as biofilms (Carlson and Silverstein, 1998) developed around the sand grains.

The identification of biodegradation as the primary removal mechanism for DOC agrees with findings from previous studies (Rauch-Williams and Drewes, 2006). In biotic soil columns studies carried out by Quanrud et al, (1996b) 54 % DOC removal occurred whilst only 10 % removal was achieved in sodium azide-inhibited columns under similar experimental conditions. Similar observations have been made in other studies where biotic soil columns achieved 70 % DOC removal. On the other hand, in soil columns where aerobic degradation was inhibited, DOC removal obtained was 27 % (Xue et al., 2009). Sodium azide inhibits only aerobic activity. Therefore the removals are attributed to a combination of sorption and anaerobic degradation (Xue et al., 2009). Besides the soil used to pack Xue et al.'s (2009) columns contained some silt and clay fractions which are expected to have better adsorption compared to silica sand. These factors could account for the higher removals

obtained compared to less than 1 % DOC removal obtained in the current experiments.

4.2.2.6 Nitrogen Removal under Constant Chemical Oxygen Demand and Variable Hydraulic Loading Rates

The production of ammonia nitrogen and organic nitrogen and total nitrogen removal rates are shown in Figures 4.8 a - c. There was a high conversion of organic nitrogen to ammonia at all the loading rates applied. Organic nitrogen in the wastewater was hydrolysed to ammonium. Proteins and amino acids from the meat extract and peptone were converted into inorganic forms by ammonification of the organic nitrogenous compounds. Mineralization of proteins into ammonium (NH_4^+) occurred by their conversion into peptides and amino acids by extracellular proteolytic enzymes, which were then transformed through oxidative or reductive deamination to ammonium (Bitton, 1999). Since the pH was kept at values in the range 6.2 to 6.7 (Figure 4.9), at all soil column depths ammonium was the main form of nitrogen pertaining in the wastewater samples. The acidic environment in the column retained ammonia in its ion (NH_4^+) form (Figure 4.10) (Tchobanoglous et al., 2003).

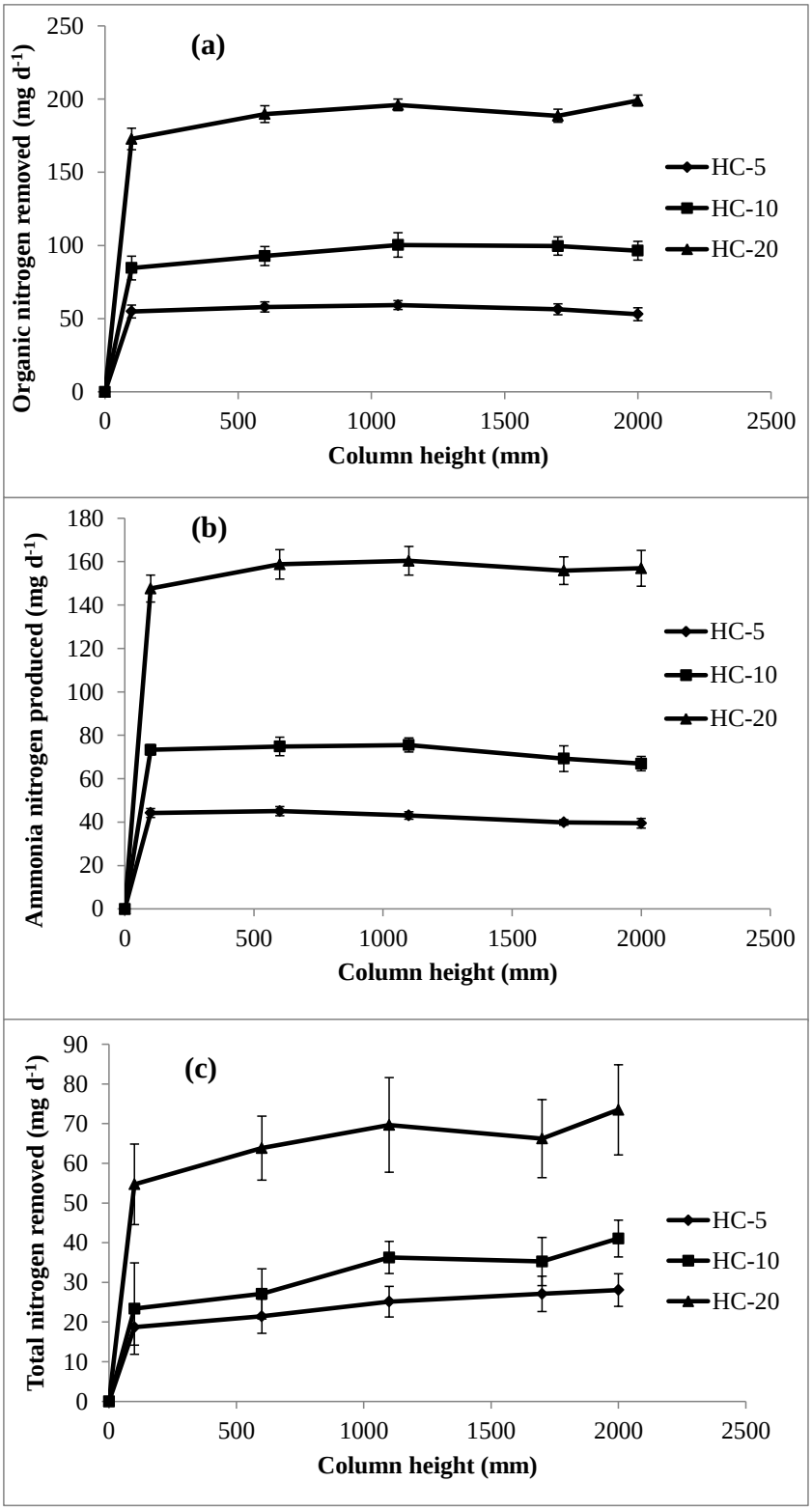

Figure 4.8 Nitrogen mass removal rate against column depth at constant COD of 135 mg L^{-1} and variable HLR of 44 cm d^{-1}, 88 cm d^{-1} and 169 cm d^{-1}

(a) organic nitrogen, (b) ammonia nitrogen, and (c) total nitrogen

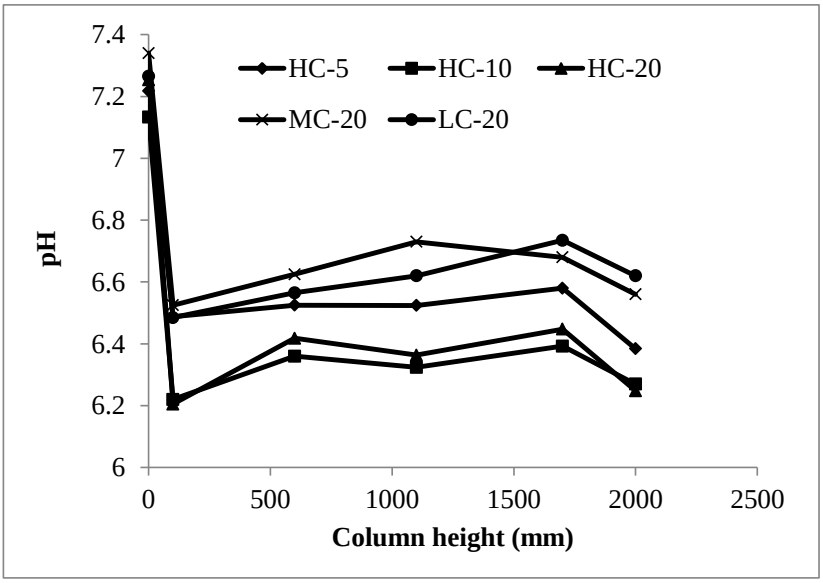

Figure 4.9 pH profile in soil column under experimental conditions HC-5, HC-10, HC-20, MC-20 and LC-20 at 20 °C

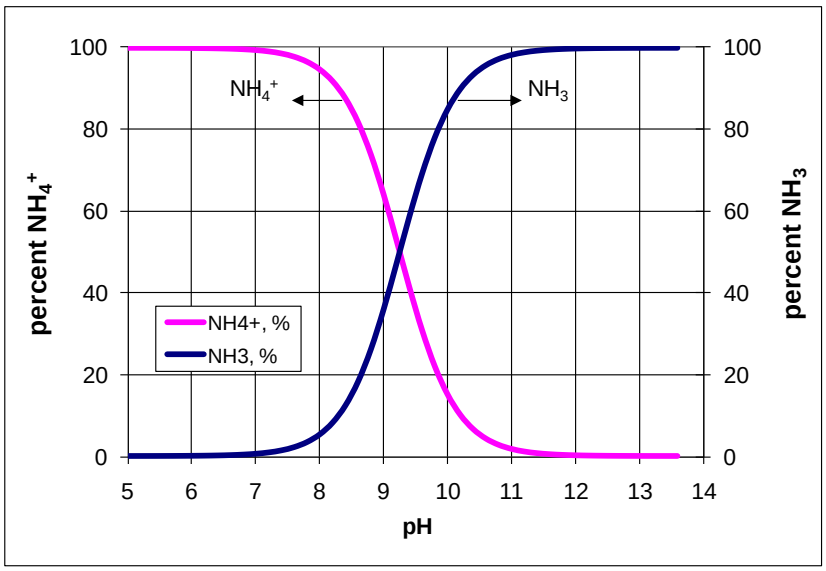

Figure 4.10 Influence of pH with oxidation states of ammonia-nitrogen

At a loading rate of 44 cm d^{-1}, 55 mg d^{-1} (representing 74 %) organic nitrogen was removed within the first 100 mm of the sand (Figure 4.8 a). When the mass loading was increased to 130 mg d^{-1}, the percentage removal dropped to 65 %. A further increase in loading rate up to 169 cm d^{-1} did not yield any difference in removal.

Overall organic nitrogen removal were 71 %, 74 % and 76 % for loadings of 74 mg d^{-1} (HC-5), 130 mg d^{-1} (HC-10) and 263 mg d^{-1} (HC-20). The rate of removal as shown by the slope of the graph after the first 100 mm was however lowest at loading rate 44 cm d^{-1} and some increases in concentration were observed after passage through 1100 mm of the sand. After the transformation of organic nitrogen to ammonia in the lower parts of the column, the hydraulic loading rate was observed to influence the amount of ammonia present further along the column (Figure 4.8 b). At 44 cm d^{-1}, a decrease in the mass of ammonia in the soil column began after the 600 mm depth. This behaviour was also observed after the 1100 mm depth at 88 cm d^{-1}, but at a slightly lower rate. The reduction in ammonia at the lower hydraulic loading rate could be attributed to biosorption onto the biofilms coating the sand grains. No decrease in ammonia concentration occurred at 169 cm d^{-1}. This may be due to the continued hydrolysis of organic nitrogen to ammonia and also insufficient time for sorption to occur.

Total nitrogen removal was most efficient at 44 cm d^{-1} (Figure 4.8 c). Overall however a removal rate of only 28 mg d^{-1} (25 % removal) was attained. This value is lower than the range for typical SAT systems reported in literature (60 – 92.5 %) (Crites et al., 2000), due to the accumulation of ammonia in the column. Lower removals, being 45.6 % using primary effluent and 28.5 % with secondary effluent, have also been reported by Lance et al., (1980). Bouwer et al., (1980) have also reported a range of removal of 30 – 65 %. Removal rates at HLR of 88 cm d^{-1} and 169 cm d^{-1} were 41 mg d^{-1} and 74 mg d^{-1} being 20 % and 19 % removal respectively. Although a higher removal rate is obtained at higher mass loadings, the efficiency of the removal process is lowered.

4.2.2.7 Nitrogen Removal under Variable Chemical Oxygen Demand and Constant Hydraulic Loading Rate

Figures 4.11 a - c show the production of ammonia nitrogen and organic nitrogen and total nitrogen removal rates when the HLR was held constant at 169 cm d^{-1} and the wastewater COD varied. A decrease in influent concentration resulted in a decrease in the nitrogen mass loadings to the soil column. There was a corresponding reduction in the organic nitrogen removal and the conversion rate to ammonia varied with wastewater concentration, with greater percentage reduction occurring at higher influent concentrations. Removal rates were 199 mg d^{-1} (achieving 76 % removal efficiency), 88 mg d^{-1} (69 % removal efficiency) and 41 mg d^{-1} (58 % removal efficiency) in HC, MC and LC wastewaters respectively. Ammonium production was thus lowest under LC experimental conditions (Figure 4.11 b). Resulting total nitrogen removal was therefore found to be dependent on influent concentration with highest removal occurring in the LC wastewater (Figure 4.11 c).

The removal of organic nitrogen under varying HLR and COD did not cause an equal increase in ammonia concentration. As nitrification hardly occurred in the soil column this difference could mainly be due to the use of ammonia as a nutrient source by microorganisms during cell synthesis (Gray, 2004) and also a result of adsorption, which is the main removal mechanism for ammonia during SAT (Fox et al., 2006). In the sterile column, no increase in ammonia occurred along the column. As opposed to the biotic soil column conditions, the concentration decreased along the soil column confirming the occurrence of adsorption. The removal rate obtained was 33 mg d^{-1}, representing a 69 % reduction.

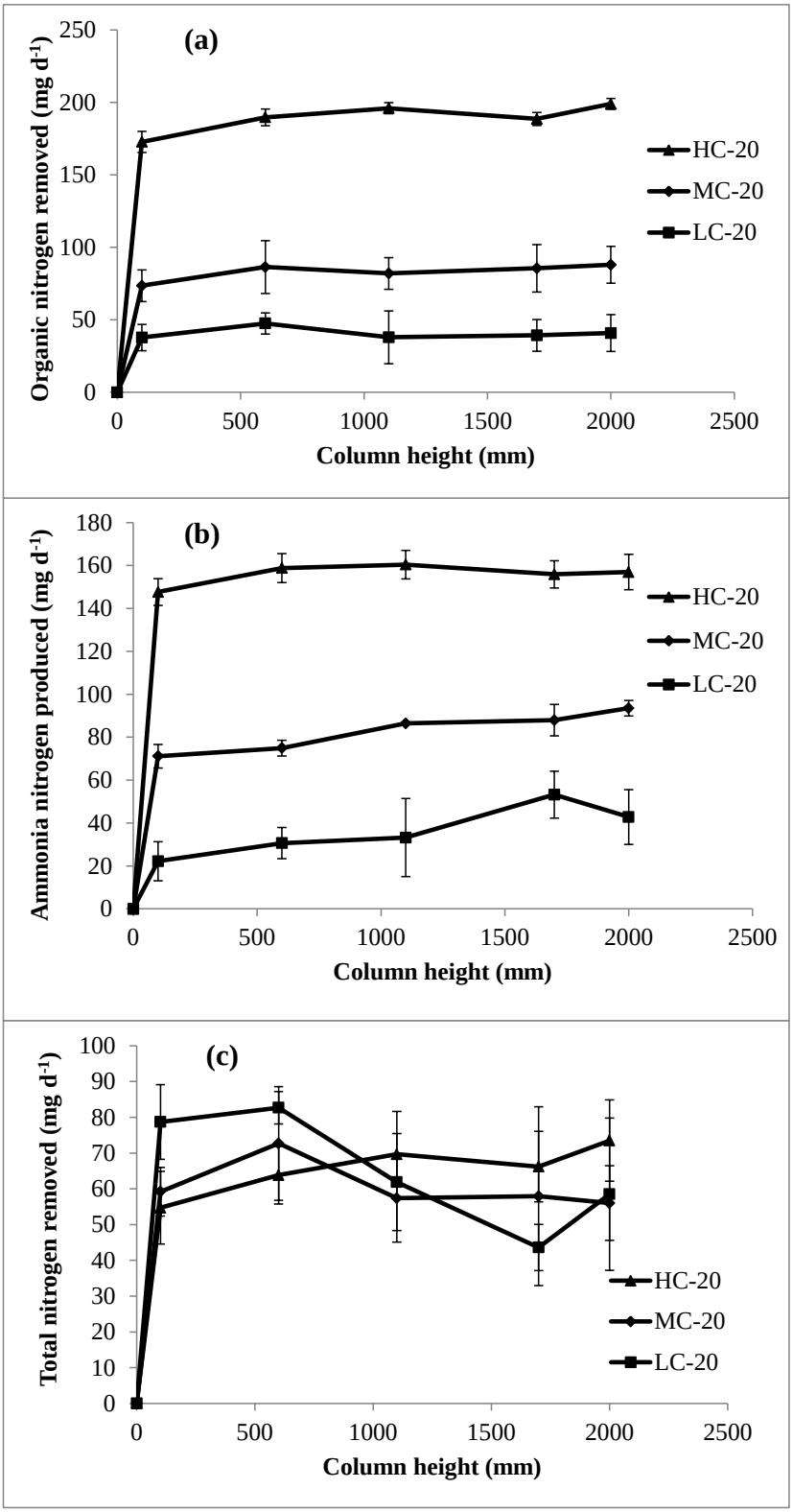

Figure 4.11 Nitrogen mass removal rate against column depth at constant HLR of 169 cm d^{-1} and variable COD of 135 mg L^{-1}, 81 mg L^{-1} and 42 mg L^{-1}

(a) organic nitrogen, (b) ammonia nitrogen, and (c) total nitrogen

4.2.2.8 Phosphate Removal

Phosphate was poorly removed in the soil column under all the experimental conditions. Figures 4.12 a and b show the mass removal rates in the soil column. Concentrations above the influent phosphate concentration were measured in most column samples especially at the 100 mm depth. Increases in phosphate amounts were respectively 4 mg d^{-1}, 13 mg d^{-1}, 58 mg d^{-1} for HC-5, HC-10, and HC-20 representing 109 %, 116 %, 156 % of the influent mass.

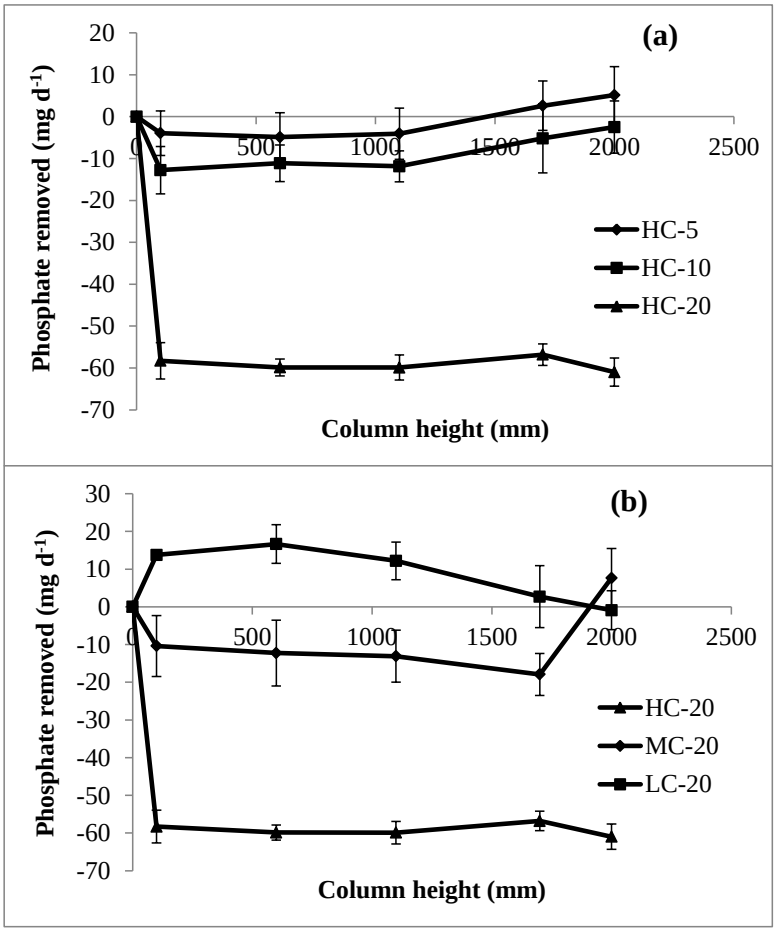

Figure 4.12 Phosphate removal rate against column height

at: (a) constant COD of 135 mg L^{-1} and variable HLR of 169 cm d^{-1}, 88 cm d^{-1} and 44 cm d^{-1} (b) constant HLR of 169 cm d^{-1} and variable COD of 135 mg L^{-1}, 81 mg L^{-1} and 42 mg L^{-1}

Some amount of removal begun beyond the 100 mm depth of the soil column and was observed to be dependent on the hydraulic loading rate. Poor phosphate removal in sandy soils as well as increasing concentrations of phosphate in the soil during infiltration has also been observed by other researchers (Stuyfzand, 1989; Reemtsma et al., 2000). Increase in phosphate concentrations in the soil column could be due to the release of phosphates previously assimilated by bacterial biofilms in the column solution following their death and subsequent degradation under anoxic conditions. Besides during oxidation-reduction reactions for the biodegradation of organic matter in the column, adenosine diphosphate (ADP) is transformed to adenosine triphosphate (ATP), with the energy produced stored in the phosphate bond. It is likely that the soil column bacteria stored up the phosphates in the form of energy-rich polyphosphates within their cells. Previously stored polyphosphates were then utilised as the source of energy, resulting in the production of intracellular polyhydroxybutyrate (PHB) storage products and releasing orthophosphate from the bacterial cells into the aqueous phase of the soil column in the process (Randall et al., 1992; Tchobanoglous et al., 2003). Under aerobic and anoxic conditions, the PHB storage products are metabolised, supplying energy for new cell synthesis and facilitating the formation of polyphosphate bonds in cell storage, which become sites for further integration of soluble orthophosphates removed from the aqueous phase of the soil column (Tchobanoglous et al., 2003). When the soil column became devoid of nitrates, the soil column bacteria could also have assimilated low weight fermentation products such as acetate into their cells. Although methane producers are not expected to thrive in the soil column, some genera of denitrifying bacteria able to carry out fermentation processes in anaerobic environments (Randall et al., 1992) may have been a source of acetate for the phosphorus assimilating organisms.

It is possible that anaerobic microsites existed within the soil column, say in deeper layers of biofilms thereby providing a suitable environment for fermentation.

The best phosphate removal occurred at the lowest HLRs (HC-5), where the mass loading was 45 mg d^{-1}. Here the removal occurred after an initial increase in concentration at the 100 mm depth. Overall removal rate achieved was only 5 mg d^{-1}. Increase in phosphate removal with a decrease in infiltration rate has also been observed in other studies (Lance et al., 1980). For a COD of 135 mg L^{-1}, an increase in HLR led to a drop in the overall removal, from 20 % to 12 % for a loading rate of 88 cm d^{-1} and then no removal is observed for a loading rate of 169 cm d^{-1}. These percentages represent removals occurring after the initial increase in concentration at 100 mm. At HLR of 169 cm d^{-1} no phosphate removal was observed to occur in the column except within the first 100 mm of the sand when the influent of low concentration was infiltrated. The concentration however rose again in the column by about 45 % after a travel distance of 600 mm. Under constant COD loading and therefore DO/COD ratios, the phosphate released would be influenced by the mass loading, since it is expected that more phosphate would be assimilated when there is more available and thus a greater amount would be released.

From the results it is observed that the redox conditions also had an influence on the removal of phosphate within the soil column. The percentage increases in phosphate concentration that occurred within the first 100 mm of the soil column were lower at higher DO/COD ratios. Increases in phosphate amounts were respectively 58 mg d^{-1} and 10 mg d^{-1} for HC-20 and MC-20, whilst 14 mg d^{-1} was removed for LC-20. Phosphates at 100 mm therefore represented 156 %, 109 %, and 87 % of the influent

mass loading. It is worth noting that even though there were slight differences in phosphate mass loadings due to errors introduced during wastewater preparation and sample analysis the variation was very small and the difference between phosphate mass loadings for HC and LC wastewater was negligible (105 mg d^{-1} against 104 mg d^{-1}). The higher mass increase when HC wastewater was applied cannot therefore be attributed to the slightly higher mass loading. Besides, despite the higher mass loading when MC wastewater was applied (113 mg d^{-1}), less mass increase occurred at 100 mm compared to when HC wastewater was infiltrated. It is also observed that as the soil column environment became more predominantly aerobic (indicated by less sulphate consumption), less phosphate was released. The mechanism of phosphate removal that occurred in the soil column can thus be deduced as biological phosphate removal. Although in SAT systems, phosphate is removed mainly by adsorption and chemical precipitation (Asano, 1985; NRC, 1994), the high wastewater concentration and low dissolved oxygen concentrations in the soil column could have provided a favourable environment for the growth of phosphorus accumulating organisms rendering biological phosphate removal an important removal mechanism in this case. Also chemical precipitation can be biologically mediated by microorganisms, whereby phosphate precipitation (in the form calcium phosphate precipitates) occurs within denitrifying biofilms due to pH increases caused by denitrification reactions (Arvin and Kristensen, 1983).

4.2.3 Chemical Oxygen Demand Balance in the Soil Column

The potential for the aerobic degradation of COD in the soil column was assessed to confirm that the removal did not occur solely by aerobic oxidation, but also by

anoxic and anaerobic degradation. Stoichiometric relations between COD and dissolved oxygen were used for the assessment.

Representing the soil column wastewater carbonaceous organic matter simply by glucose ($C_6H_{12}O_6$), 1 g of oxygen would be consumed per gram of COD removed in the soil column (Tchobanoglous et al., 2003), as shown in Chapter 2. It is therefore not expected that all the COD applied to the soil column would be removed by aerobic degradation processes alone as all the influent DO/COD ratios, which were respectively 0.06, 0.16 and 0.26 for HC, MC and HC wastewaters, were below the requirement. Denitrification and sulphate reduction processes were thus induced by bacteria in the soil column. Predicted COD removals calculated based on the oxygen available in the influent are 48, 83, 182, 203 and 230 mg d^{-1} for conditions HC-5, HC-10, HC-20, MC-20 and LC-20 respectively. COD removal attained in the soil column however exceeded these values, dissolved oxygen accounting for only 13 – 15 % for HC, 18 % for MC and 32 % for LC wastewaters, confirming that further COD removal occurred by some other removal mechanisms. The extra removal could not be attributed to sorption as abiotic soil column tests showed negligible COD removal efficiencies and has been attributed to denitrification and sulphate reduction processes.

Using stoichiometric relations (Sarfaraz et al., 2004; Henze et al., 2008; Velasco et al., 2008), expected COD removal based on consumption of electron acceptors was estimated. The oxygen equivalent of nitrate is 2.86 mg O_2 /mg NO_3-N. Therefore 1 mg NO_3-N denitrified to nitrogen gas would have the same electron accepting capacity as 2.86 mg of oxygen. Likewise, during COD oxidation, oxygen accepts 4

electrons whilst sulphate accepts 8. Thus 2 moles of oxygen is equivalent to 1 mole of sulphate and 1 g of sulphate would have the electron accepting capability of 0.67 g of oxygen. These factors were used to convert the respective masses of electron acceptors consumed in the soil column to the equivalent COD removed and summed up to obtain a predicted value for COD removal to occur in the soil column. Actual COD removal that occurred in the soil column was found to be less than the predicted value by about 20 %. HC-10 however gave only a 5 % deviation (Table 4.4). MC-20 gave inconsistent results and so has been omitted. Besides experimental errors, the deviation between actual and predicted COD removal could be attributed to incomplete denitrification to nitrogen gas. Although nitrite was not detected in any of the samples, some nitrate may have been converted to the other denitrification intermediaries being nitric and nitrous oxide. Also as the soil column environment was neither strictly aerobic, anoxic nor anaerobic, the stoichiometric conversion factors used to predict COD removal may not have been accurate.

Table 4.4 Comparison of predicted and actual COD removal in 2000 mm of the soil column

Experimental condition	**Dissolved Oxygen (mg d^{-1})**		**Nitrate (mg d^{-1})**		**Sulphate (mg d^{-1})**		**Total COD removed (mg d^{-1})**		**Difference b/w predicted and actual COD removal (%)**
	DO used	**Predicted COD removal**	**NO_3 used**	**Predicted COD removal**	**SO_4 used**	**Predicted COD removal**	**Predicted COD removed**	**Actual COD removed**	
HC-5	48	48	17	48	332	221	316	249 ± 33	21
HC-10	83	83	27	77	660	440	600	568 ± 55	5
HC-20	182	182	39	112	1599	1066	1360	1118 ± 58	18
LC-20	230	230	57	163	507	338	730	582 ± 234	20

4.2.4 Correlations between Electron Donor and Electron Acceptors

Dissolved oxygen mass removal rates were correlated with COD, DOC, nitrate and sulphate removal rates when the influent concentration was held constant and the HLR varied (Figure 4.13). In all cases there was a strong positive linear correlation between DO removal and the removal of all the parameters considered. Nitrate and sulphate removal also correlated well with COD removal. R^2 in all cases was greater than 0.9. Correlation of sulphate reduction with COD removal showed sulphate reduction occurred at a rate of approximately 1.47 mg/ mg of COD removed per day. It is deduced from these correlations that oxygen consumption in the soil column was 0.14 mg / mg of COD removed.

These correlations would be used later in Chapter 5 to model the removal of COD in the soil column.

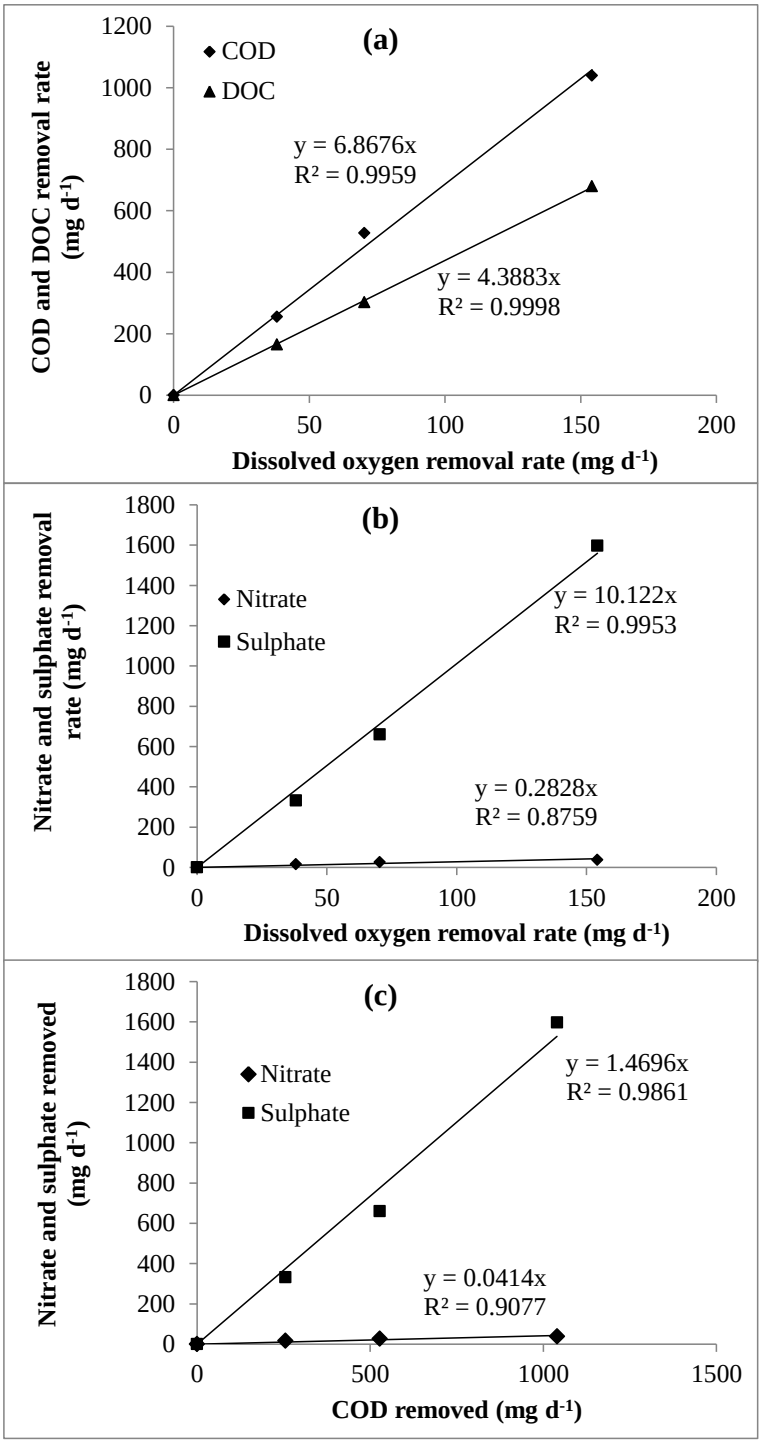

Figure 4.13 Correlations between wastewater parameters at constant COD of 135 mg L^{-1} COD and varying HLR at 20 °C

(a) COD and DOC against dissolved oxygen removal rate (b) nitrate and sulphate against dissolved oxygen removal rate (c) Nitrate and sulphate against COD mass removal rate

4.2.5 Microbial Concentration Profile in the Soil Column

The concentration profile of microorganisms in the soil column was determined using phospholipid fatty acid (PLFA) analysis (Findlay et al., 1989). Viable microorganisms have phospholipid fatty acids as a component of their cell walls (Zelles, 1999). Soil was sampled from 100 mm, 300 mm, 600 mm, 1100 mm and 1400 mm for PLFA analysis. Absorbance readings of processed samples were converted to phosphate concentrations using the calibration curve shown in Figure 3.13 of Chapter 3, and then converted to number of microbial cells using an approximation of 3.4 million cells per 0.1 n mol of phosphate (Findlay et al., 1989). Figure 4.14 shows the microbial concentration profile along the soil column.

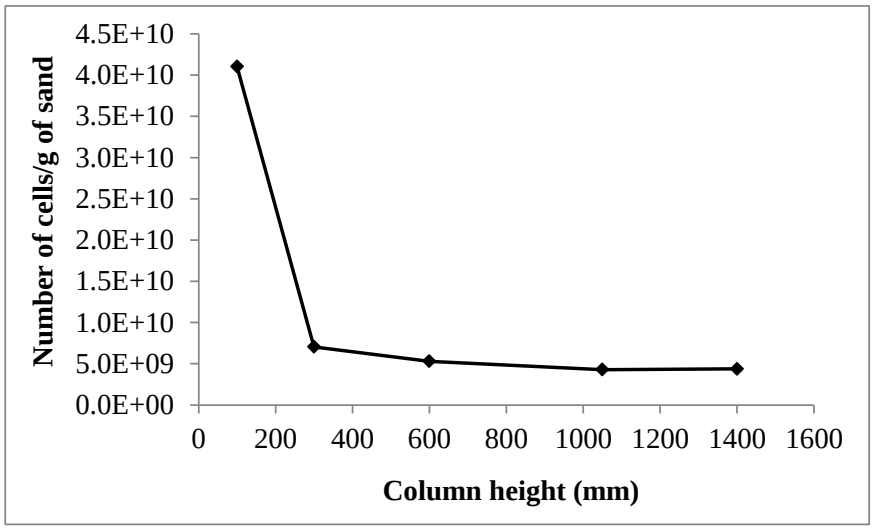

Figure 4.14 Soil column microbial profile

The results of PLFA analysis revealed that the soil column had a microbial concentration profile that correlated positively with the removal profile of COD, DOC, BOD, organic nitrogen, dissolved oxygen, nitrate and sulphate. Positive correlations of microbial biomass with concentrations of biodegradable organics during soil aquifer treatment have also been observed by other researchers (Rauch-

Williams and Drewes, 2006). The highest concentration of phospholipids (1207 n mol g^{-1} of sand) was measured at the first sampling point. This corresponds to 4.1 x 10^{10} cells g^{-1} of sand. There was a marked decrease in the concentration of phospholipids beyond that point. At 300 mm, the phospholipid concentration was only 17 % of that at 100 mm. The lowest concentration of 129 n mol g^{-1} of sand (4.37 x 10^9 cells g^{-1} of sand), being approximately 10 % of the concentration at 100 mm, was measured at 1400 mm. The profile of bacterial concentrations along the soil column showed an exponential decrease (R^2 of 0.5688) with depth, which depicts the kind of microbial concentration profile normally found in natural soils. In natural soils, there are about 10^7 to 10^8 bacteria in every 1 g of soil with the largest numbers being found in the surface layer and the numbers decreasing exponentially with depth of soil (Ishizawa and Toyoda, 1964). The bacterial cells, which are expected to be the most predominant microbial species involved in stabilisation of organic matter in the soil column (Gray, 2004), were higher than in natural soil because of substrate abundance.

Phospholipids were highest at the 100 mm point because from the column entry to this point, organic carbon, nutrients and electron acceptors were at their highest concentration. This bacterial profile is consistent with findings from other studies (Nema et al., 2001) in which a large percentage of the bacteria present are observed to remain near the infiltration surface. The microorganisms grow quickly and have high activity at the soil water interface due to abundance of biodegradable organic matter and dissolved oxygen (Fox et al., 2006). The removal profile correlated well with the amount of phospholipids in the soil column because biodegradation was the main removal mechanism in the soil column. Beyond the 100 mm depth of the

column, the bacterial consortium is likely to be composed mainly of facultative and anaerobic types, which grow more slowly than aerobes and are less biochemically efficient (Gray, 2004), contributing to lower removal of COD. Thus besides relatively lower availability of electron acceptors and less effective redox conditions pertaining beyond 100mm, the concentration and type of microorganisms limited the removal of COD, BOD and DOC within the deeper layers of the soil column (Charbeneau, 2000). Besides, it is possible that most or all of more readily biodegradable organic carbon was depleted within the first 100 mm leaving relatively slower biodegradable forms.

4.2.6 Soil Column Reaction Kinetics

The kinetic rate constants of COD, DOC and BOD and the electron acceptors dissolved oxygen, nitrate and sulphate were determined by assuming 1st order, 2nd order and mixed order reaction rates, using the concentration profiles along the 2 meter soil column and at the entry point. For the 1st order assumption, a plot of $-ln(C_o/C_t)$ against the soil column residence time (t, min) did not yield a straight line. A 2nd order reaction was then assumed and $1/C_t$ plotted against t, which again failed to give a straight line. A straight line as shown in Figures 4.15 and 4.16 was obtained for a plot of $1/t\ ln(C_o/C_t)$ against $(C_o-C_t)/t$ and thus the kinetic rate constant in the column concluded to be of mixed order. The rate equation for mixed order (Tchobanoglous et al., 2003) takes the general form:

$$r_c = \frac{dC}{dt} = \frac{kC}{K + C} \quad \text{.....[4.11]}$$

where:

r_c = constituent reaction rate ($ML^{-3}T^{-1}$)

C = constituent concentration (ML^{-3})

k = reaction rate coefficient (T^{-1})

K = saturation constant (ML^{-3})

t = time (T)

Integrating,

$$kt = K \ln \frac{C_o}{C_t} + (C_o - C_t) \quad \text{.....[4.12]}$$

where C_0 is the initial concentration and C_t is the concentration at time t. In the analysis made on the soil column data, the concentrations have been substituted with the mass loadings. The plot for nitrate could only be determined for LC-20 as nitrate was completely consumed within the first half of the soil column resulting in insufficient valid data points for the plot.

The reaction order in the soil column was confirmed by COD results obtained from preliminary tests carried out in 300 mm long soil column filled with silica sand of the same characteristics as for the long columns, seeded similarly and fed with synthetic wastewater prepared with the same recipe as used in the current experiments. The purpose of these preliminary tests was to assess the viability of the microbial seeding material in sand and the suitability of the synthetic wastewater before replication in larger soil columns.

Mixed order reaction is expected to prevail within the soil column as substrate travels across biofilm layers developed around the sand grains by diffusion. A portion of the substrate is consumed within each layer, leading to reductions in substrate concentrations with the depth of the biofilm (Tchobanoglous et al., 2003).

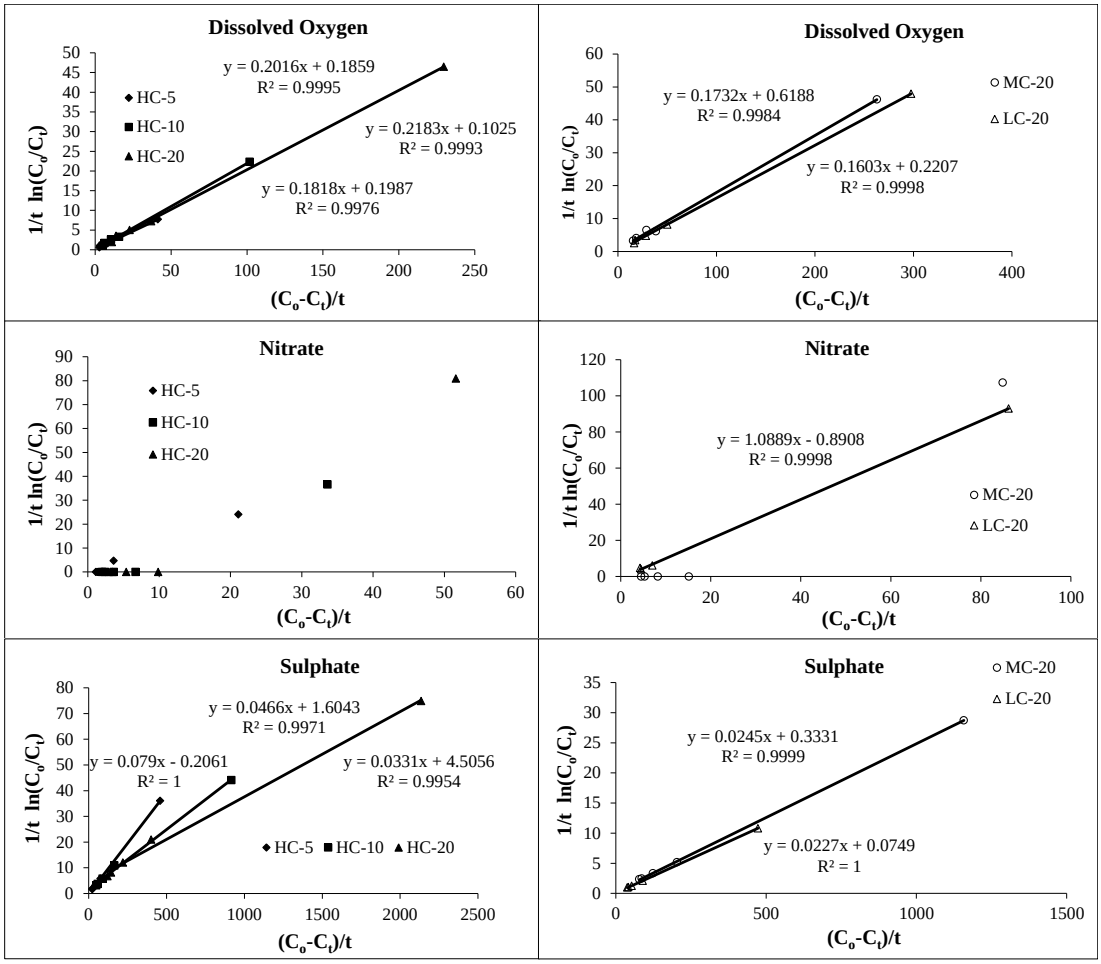

Figure 4.15 Test for mixed-order reaction rate for dissolved oxygen, nitrate and sulphate

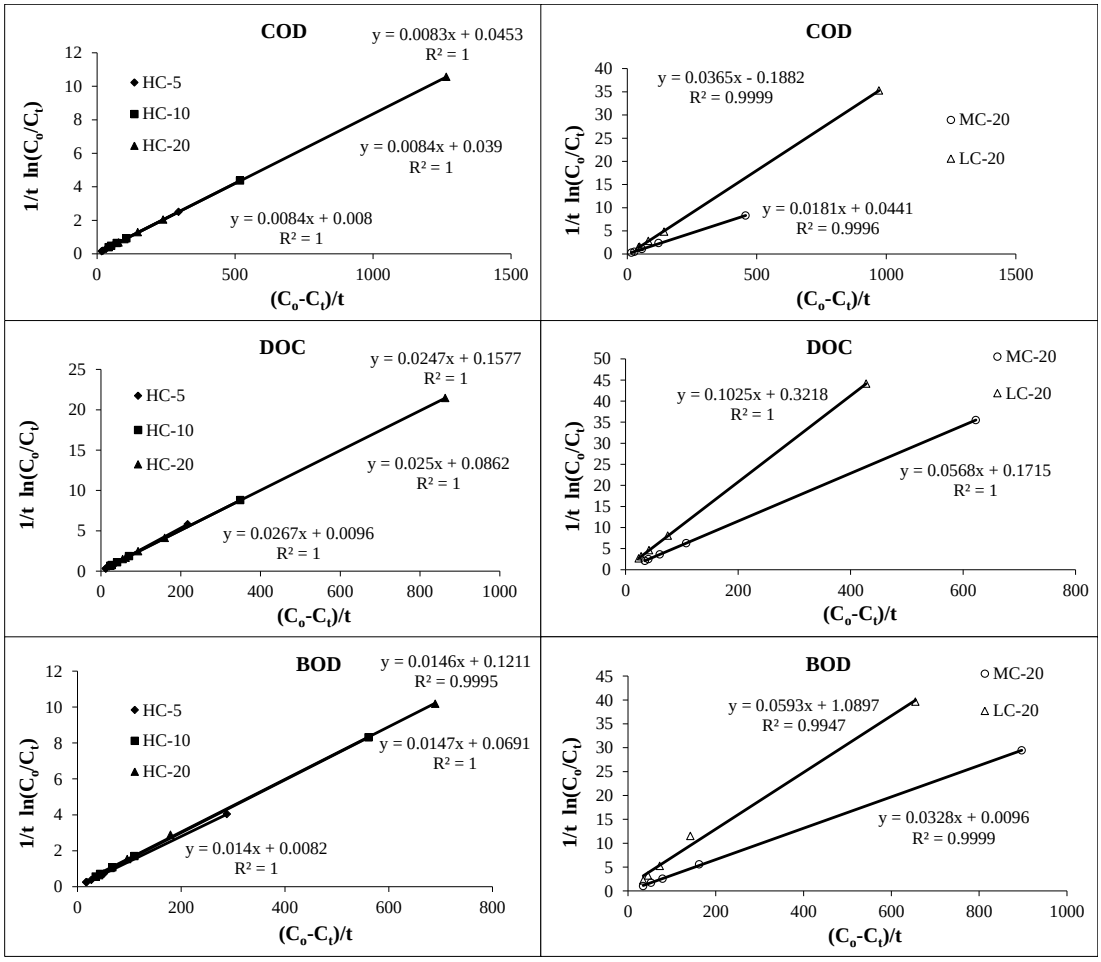

Figure 4.16 Test for mixed-order reaction rate for chemical oxygen demand, dissolved organic carbon and biochemical oxygen demand

4.2.7 Comparison of Removal Efficiencies under Varying Chemical Oxygen Demand and Hydraulic Loading Rates

The removal efficiencies of COD, BOD, DOC and organic nitrogen were compared under experimental conditions of HC-5 and HC-10 against LC-20 and MC-20 respectively. These conditions were chosen for comparison because the mass loadings applied for HC-5 compared closely to that of LC-20 and HC-10 to MC-20. Ratios of the dissolved oxygen, nitrate and sulphate with COD, DOC and BOD remained constant at no change in organic influent concentration (i.e. for HC-5, HC-

10 and HC-20). The ratios increased with a reduction in organic influent concentration meaning that more oxygen was available per gram of organics to be degraded. Figure 4.17 compares the mass removal rates.

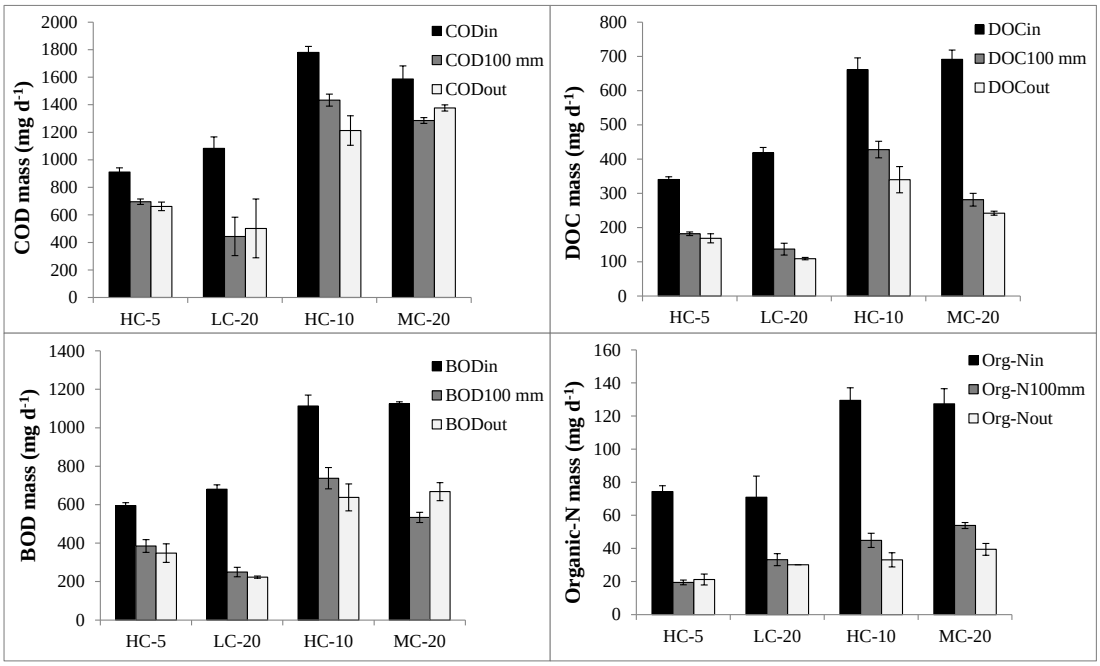

Figure 4.17 Comparison of mass removal under investigated experimental conditions

The removal at 100 mm has been included in the analysis because removals beyond that point sometimes did not decrease consistently. However it can be seen that generally LC-20 and MC-20 achieved higher removals than HC-5 and HC-10 respectively for approximately the same COD, BOD and DOC mass applied. These differences could be attributed to dissolved oxygen limitations in the wastewater of higher concentration. Dissolved oxygen limitation in the saturated zone is an important consideration as the provision of oxygen for degradation processes is only from the regional groundwater (Fox et al., 2006). The results suggest that application of a low concentration substrate at short residence time would be more effective in the removal process than applying the mass in the form of a more highly

concentrated substrate with long residence times. The opposite holds for organic nitrogen, where longer residence times improve its removal.

To determine the significance of varying HLR and influent COD on the removal efficiencies obtained for dissolved oxygen, sulphate, phosphate, nitrogen, COD, BOD, and DOC, the data were analysed using the analysis of variance (ANOVA) statistical test at a significance level, p of 0.05. The experimental conditions were to be deemed to have a significant effect if the p value obtained is less than 0.05. For all the wastewater parameters investigated, the p values were less than 0.05 and therefore the differences in removal efficiencies resulting from changes in HLR and influent COD were significant.

4.2.8 Conclusions

Under all experimental conditions investigated, the first 100 mm of the soil column was responsible for most of the removal or transformation of the wastewater parameters that occurred. Abiotic studies, in comparison with biotic studies, showed that the main removal mechanism occurring in the soil for the removal of the wastewater parameters was biodegradation. Dissolved oxygen availability and its rate of replenishment to the soil column played a key role in the removal process. Relatively high DO to DOC, COD and BOD mass loadings improved the efficiency of the removal process. Anoxic (denitrification) and anaerobic (sulphate reduction) processes occurred in the soil column in addition to aerobic degradation. At high mass loadings, they played a more active role as electron acceptors. Higher mass loadings achieved higher mass removal rates, however COD, DOC and BOD removal efficiency is better when the mass applied has lower COD concentration.

Comparison of removal efficiencies of HC-5 versus LC-20 and HC-10 against MC-20 suggests that within the range of mass loadings investigated, lowering influent COD concentrations, not increasing residence times would improve removal efficiencies of COD, BOD and DOC in the saturated zone of SAT systems while high concentrations and long residence times would improve nitrogen removal.

It is therefore expected that in cases where dissolved oxygen is a limiting factor, high permeability soils infiltrated with effluent of low concentration would achieve better removal efficiencies than infiltrating a relatively higher concentrated effluent through soils of low permeability allowing longer residence times. It should be noted however that the organic concentrations used in this study (even that classified as low concentration) exceed that normally applied in SAT systems.

4.3 Removal of Estrone, 17β-Estradiol and 17α-Ethinylestradiol under Saturated and Unsaturated Soil Conditions

This section presents the results and discusses the removal of natural and synthetic estrogens namely estrone (E1), 17β-estradiol (E2) and 17α-ethinylestradiol (EE2), through 1 m long unsaturated and saturated soil columns. Three soil columns were used, two being saturated and the third operated under unsaturated soil conditions. These soil columns are identified as SC1, SC2 and SC3. SC1 is the unsaturated Soil Column and contains silica sand as a packing material. The second Soil Column (SC2) also contains silica sand but is saturated whilst SC3 is a saturated Soil Column containing a mixture of silica sand, silt and clay in the proportion 65 %: 25 %: 10 % respectively. The soil columns are first investigated for their removal potential for dissolved organic carbon and nitrogen. Their efficiency for the removal of estrogens under different experimental conditions is then evaluated. The experimental conditions varied in the saturated soil columns were dissolved organic carbon concentration and hydraulic loading rate and in the unsaturated soil column the level of water table was varied. E1, E2 and EE2 removal under unsaturated conditions were studied at three water table heights by placing the soil column outlet at different elevations of 75 mm (WT 75), 500 mm (WT 500) and 800 mm (WT 800) from the column base.

4.3.1 Soil and Hydraulic Characteristics of 1-meter Soil Columns

The characteristics of the soil in the three soil columns have been presented in Section 3.3.2 of Chapter 3. The grading curve of the silica sand is also presented in Figure 3.10 of the same chapter. The silica sand was of uniform size with

coefficients of curvature and uniformity of 1.38 and 1.08 respectively. All three soil columns were packed with the same mass of material (24.97 kg) resulting in a bulk density of 1.57 g cm^{-3}. The hydraulic characteristics measured were the hydraulic residence times and the hydraulic conductivity under unsaturated conditions.

4.3.1.1 Hydraulic Residence Time

Figures 4.18 a - c show the fluorescein tracer breakthrough curves for SC1, SC2 and SC3. Mean hydraulic residence times in the soil columns were determined graphically from the breakthrough curves at the point corresponding to C/C_o = 0.5, where C is the effluent tracer concentration at any time, t and C_o is the influent tracer concentration. Mean hydraulic residence times in SC1, SC2 and SC3 were respectively 542, 630 and 238 minutes. These residence times are for the conditions WT75 in SC1 and HLR 81.5 cm d^{-1} in SC2 and SC3. Residence times for WT500 and WT800 were not determined but are expected to be shorter than that for WT75 since higher water tables would mean smaller zone of unsaturation and thus faster transmission of water through the column as a whole. This is because the hydraulic conductivity of unsaturated soil is lower than that under saturated conditions due to some of the pore spaces in the unsaturated soil being occupied by air (Fetter, 1999). The residence time in SC3 was much shorter than that in SC2 probably due to some short circuiting occurring in the soil column. The time for complete breakthrough were however close. A comparison between the influent tracer concentration and the measured concentration at the end of the tests showed tracer loss of 8 %, 4 % and 6 % in SC1, SC2 and SC3 respectively. The hydraulic properties of the three columns are summarised in Table 4.5.

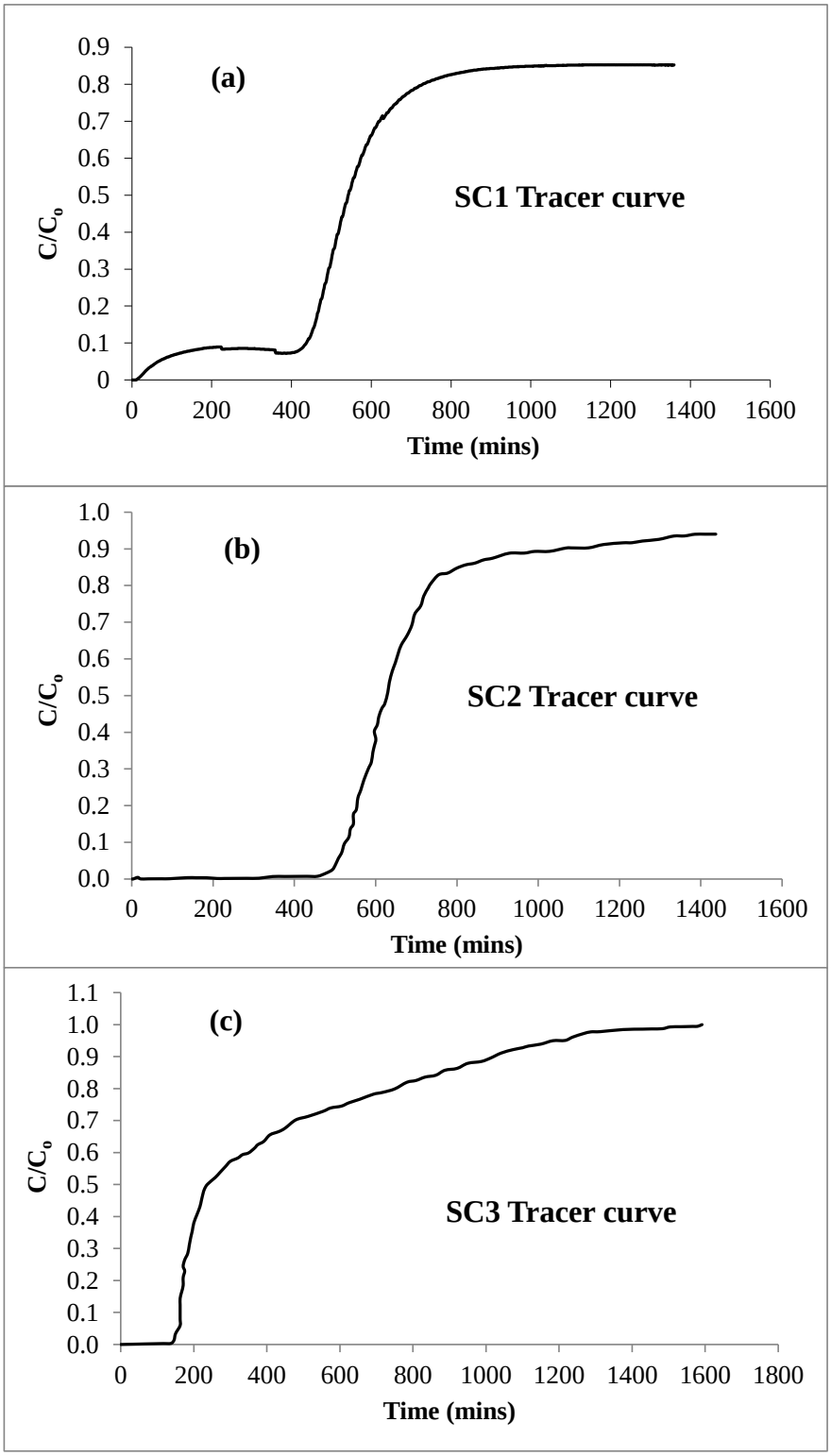

Figure 4.18 Hydraulic residence time distribution curves in 1 m soil columns (a) SC1 at WT75 and HLR of 49 cm d^{-1} (b) SC2 and (c) SC3 at HLR of 81.5 cm d^{-1}.

Table 4.5 1 meter soil column hydraulic properties

Parameter	**SC1**	**SC2**	**SC3**
Hydraulic loading rate (cm d^{-1})	49	81.5/163	81.5/163
Mean residence time (minutes)	542	630	238
Saturated hydraulic conductivity (cm s^{-1})	0.42	0.42	-

4.3.1.2 Unsaturated Hydraulic Conductivity

Soil parameters for the determination of the unsaturated hydraulic conductivity were obtained from the moisture retention curve developed for silica sand (Figure 4.19 a). The moisture retention curve was developed from experimental data obtained using a Buchner funnel setup (Sharma and Mohamed, 2003) as detailed in Section 3.3.8.3.2 of Chapter 3. From Figure 4.19 a the bubbling pressure, h_b, which is the matric potential at which water begins to drain from the soil, was found to be 6 cm. Figure 4.19 b shows the hydraulic conductivity variation with moisture content for silica sand. The relation developed by van Genuchten (1980) (Equation 3.9) was used to develop the curve relating the unsaturated hydraulic conductivity to the soil's water content as described in Section 3.3.2.3 of Chapter 3. The unsaturated hydraulic conductivity is lower than under saturated conditions, which was 0.42 cm s^{-1}, due to some of the pore spaces in the unsaturated soil being occupied by air (Fetter, 1999). It therefore reduces with a reduction in the degree of saturation until the irreducible water content is reached.

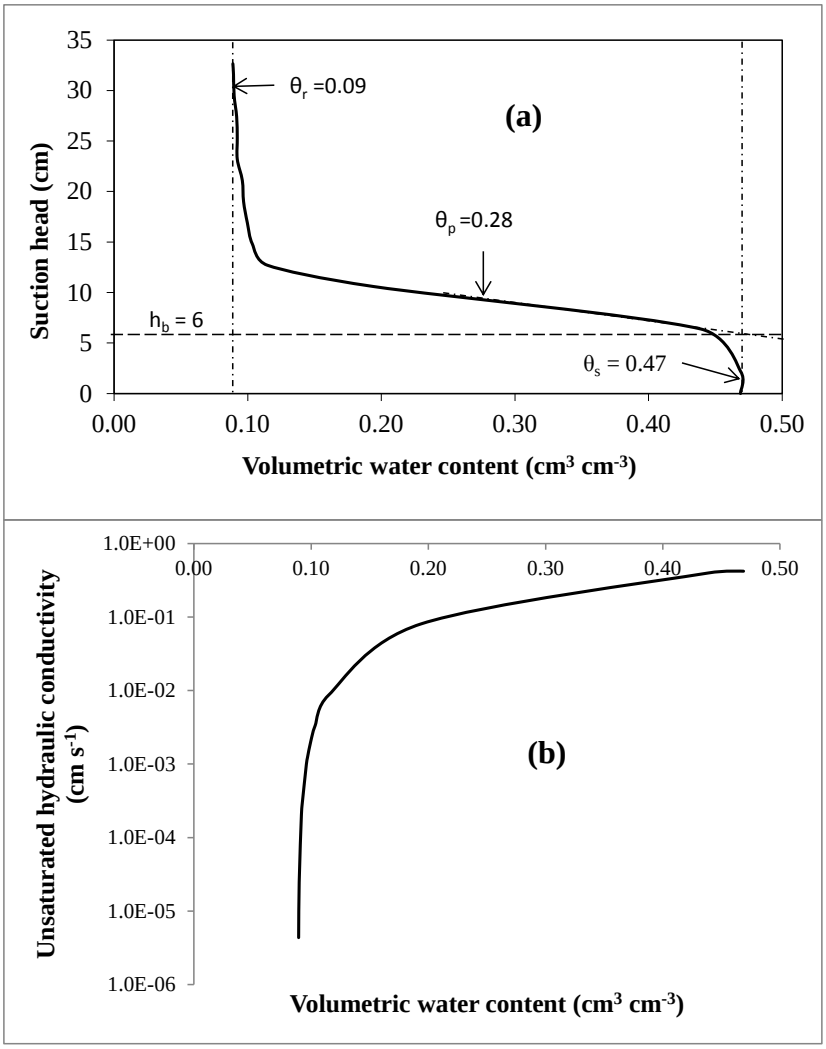

Figure 4.19 Moisture retention curve and unsaturated hydraulic conductivity of silica sand

(a) moisture retention curve and (b) unsaturated hydraulic conductivity

4.3.1.3 Soil Matric Potential and Water Content

Measurements taken from the tensiometers and the soil moisture probes under the different water table levels in the unsaturated soil column (SC1) were converted into pressure and soil water content respectively using the calibration curves shown in Figures 3.7 and 3.9 of Chapter 3. Frequency of data collection was one reading every 2 minutes. The average water content and pressure measurements together with the

standard deviations (enclosed in parentheses) are presented in Table 4.6. Sample graphs of the pressure and water content measurements are presented in Appendix B. The negative values of pressure indicate suction which shows the soil is unsaturated, whilst positive values indicate soil water saturation.

Table 4.6 Pressure and water content in 1 m unsaturated soil column

Experimental Condition	**Pressure (cm)**			**Water Content**		
	850 mm	**500 mm**	**150 mm**	**850 mm**	**500 mm**	**150 mm**
WT75[a]	-7.18 (3.2)	-9.67 (1.22)	11.32 (4.81)	7.88 (0.47)	7.21 (0.54)	35.43 (2.43)
WT75[b]	14.22 (9.6)		-3.16 (0.99)			
WT500	-10.79 (0.56)	1.92 (0.51)	30.06 (0.62)	7.56 (0.28)	28.37 (1.34)	35.69 (0.95)
WT800	-1.28 (0.47)	31.88 (0.6)	60.42 (0.57)	26.7 (0.41)	30.61 (0.33)	37.44 (0.13)

[a] *during unrestricted infiltration,* [b] *during clogging*

Due to transient flow, the difference in pressure head measured in the saturated zone for WT500 and WT800 was slightly less than the difference in water head between the two measurement points (i.e. 500 mm and 150 mm). The pressures at 850 mm and 150 mm fluctuated between negative and positive. These fluctuations coincided with surface clogging and ponding in the soil column. As the clogging layer developed, restricting infiltration, the pressure at 850 mm begun to rise from suction

to a positive pressure. At the same time, the pressure at 150 mm begun to drop from a positive pressure to suction due to a decrease in the amount of water infiltrating to that depth. Breaking up the surface clogging layer restored infiltration rates and caused the pressures at 850 mm and 150 mm to revert to suction and positive pressures respectively.

The maximum soil water saturation obtained in the soil column was less than that obtained for the drying tests curve obtained from the Buchner funnel tests (Figure 4.19) due to hysteresis. Draining the soil column before rewetting with wastewater application caused air bubbles to be trapped in the pores of the sand and therefore the volumetric water content could not equal the porosity (Charbeneau, 2000). Besides, the soil pores, which are not equally sized, do not drain and fill in the same way, the capillary pressure needed for draining being controlled by the minimum pore or (throat) radius whilst that for wetting is controlled by the maximum radius (Charbeneau, 2000). Besides these, drying and wetting angles also contribute to hysteresis (Bear, 1972).

4.3.2 Soil Column Dissolved Organic Carbon Removal and Nitrogen Transformation Processes

Monitoring tests on soil column wastewater samples from all three soil columns were carried out before the introduction of estrogens to confirm the occurrence of biological activity in the soil column environment and to determine their removal potential for wastewater treatment. In the saturated soil columns, wastewater was pumped into the column from the bottom. Flow direction was therefore upwards (from bottom to top) whilst in the unsaturated column, the influent was applied on

the sand surface at the top of the column and flow was by gravity. All lengths mentioned in the following sections are measured using the column base as the datum. The average influent wastewater concentrations to the soil columns are given in Table 4.7.

Table 4.7 Wastewater influent characteristics for SC1, SC2 and SC3

Parameter (mg L^{-1})	**Soil Column**		
	SC1	**SC2**	**SC3**
Chemical oxygen demand	40	40	39
Dissolved Organic Carbon	16.7	17.1	17
Ammonia nitrogen	1.5	1.4	1.3
Organic nitrogen	2.8	2.9	2.6
Nitrate	2.9	3.0	3.1
Total nitrogen	7.2	7.3	7.0
Sulphate	59	47.5	47.5
Dissolved oxygen	8.7	9.7	9.8

4.3.2.1 Saturated Soil Columns

Figures 4.20 a – d show the removal profiles of DOC, dissolved oxygen, nitrate and sulphate in the saturated soil columns at HLR 81.5 cm d^{-1} and influent DOC of 17 mg L^{-1}. These figures are based on at least two experimental replicates which

involved wastewater sampling from all the sampling points on a different occasion. The reduction of the synthetic wastewater quality parameters such as chemical oxygen demand, dissolved organic carbon and nitrogen under saturated conditions with varying hydraulic loading rates and COD concentrations has already been extensively discussed in Section 4.2. Therefore the scope of the discussion on the removal of these parameters in the 1-meter saturated soil columns (SC2 and SC3) would be an assessment of the treatment efficiency attainable in the soil column using dissolved organic carbon measurements as a surrogate parameter with the associated electron acceptor consumption.

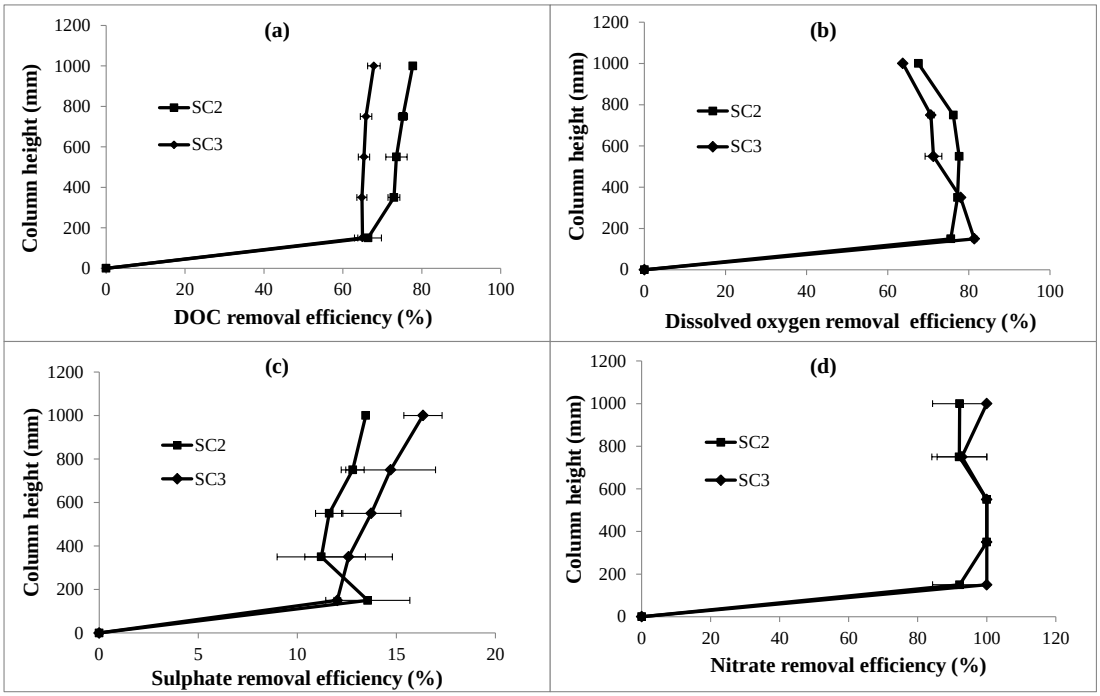

Figure 4.20 Dissolved organic carbon, oxygen, sulphate and nitrate removal efficiencies at 20°C in saturated soil columns, SC2 and SC3, at HLR of 81.5 cm d^{-1} (a) Dissolved organic carbon, (b) Dissolved oxygen, (c) Sulphate and (d) Nitrate

Dissolved oxygen, nitrate and sulphate were consumed in both soil columns. Influent dissolved oxygen was about 9.7 mg L^{-1} and on the average, 2.7 mg L^{-1} remained in

samples beyond 150 mm travel through the soil column. Nitrate was also almost completely consumed in both soil columns. Out of the 3 mg L^{-1} present in the influent, 93 - 100 % was consumed. Similar sulphate reduction rates also occurred in both soil columns up to 150 mm. Beyond this point, the reduction rate was slower in SC2 than SC3. This behaviour can be attributed to the better DOC removal that occurred in SC2. At 150 mm only 4.5 mg L^{-1} DOC remained in SC2 compared to 5.9 mg L^{-1} in SC3. Less sulphate was thus needed to serve as an electron acceptor for biodegradation of the resident organic carbon. Final effluent DOC concentrations in SC2 and SC3 were 3.8 mg L^{-1} and 5.5 mg L^{-1} respectively. DOC removal efficiencies achieved were thus 78 % and 68 % respectively.

It was expected that silt and clay would enhance DOC removal by providing adsorption sites and larger surface area for the development of biofilms. However the performance was poorer than in the soil column containing silica sand alone. The lower removal efficiency that occurred could be attributed to the shorter residence time of 238 minutes compared to 630 minutes in SC3, which was 2.6 times longer, or to the presence of lower concentrations of microorganisms. The effect of microbial concentrations was investigated using the results of the phospholipid fatty acid analysis carried out on soil samples from the columns. This is discussed in the following section.

4.3.2.2 Phospholipid Fatty Acid Analysis of Soil Samples

Phospholipid fatty acids were analysed in soil samples taken from a number of depths of each soil column to confirm the removal of wastewater constituents by an established presence of microorganisms. The identification of microorganisms in the

soil columns was carried out because the applied wastewater was initially seeded with a commercial microbial seeding material (i.e. BOD seed from Cole Parmer Ltd, UK). Besides, wastewater infiltrated to the soil column was synthetic. It was also performed to help explain any differences in performance efficiency of SC2 and SC3 which could not be attributed to physical processes related to the soil properties.

The inherent libraries suite for the GCMS analytical software was used to identify the fatty acid methyl esters corresponding to the peaks obtained from the GCMS analysis of the extracted soil samples. These peaks were then confirmed by comparing them to the chromatograms obtained for the analysis of the Bacterial Acid Methyl Ester (BAME) mix which was used as a standard. Even though the elution times of the fatty acids in the soil column samples did not exactly match that of the BAME mix, the order of elution of the fatty acids in both cases were the same. The libraries suite was thus found to accurately identify the fatty acids in the samples. In all 24 fatty acids were identified in SC2 and SC3 as shown in Table 4.8. Of these, 78 % had a quality of 97 % or better. The peak areas obtained were corrected by deducting the peak areas resulting from the addition of 5 µL of BAME mix to each sample before GCMS analysis. This peak area was determined from calibration curves developed, which have been presented in Figure 3.19 of Chapter 3. Resulting R^2 values for all the calibration curves developed for the BAME mix ranged from 0.9633 to 0.9999, 85 % of which exceeded 0.99. The structures of the fatty acids and their IUPAC names are presented in Table C1 of Appendix C. Sample chromatograms are also presented in Appendix C.

Table 4.8 Fatty acids identified in soil column samples by GCMS analysis

Type of Fatty Acid	**Shorthand designation**	**Quality**
Undecanoic acid, methyl ester ($C_{12}H_{24}O_2$)	11:0	97
Methyl 2-hydroxydecanoate	2-OH 10:0	95
Dodecanoic acid, methyl ester ($C_{13}H_{26}O_2$)	12:0	96
Tridecanoic acid, methyl ester ($C_{14}H_{28}O_2$)	13:0	97
Tetradecanoic acid, methyl ester ($C_{15}H_{30}O_2$)	14:0	97
Methyl 9-methyltetradecanoate ($C_{16}H_{32}O_2$)	9Me15:0	95
Tetradecanoic acid, 12-methyl-, methyl ester ($C_{16}H_{32}O_2$)	a15:0	90
Pentadecanoic acid, methyl ester ($C_{16}H_{32}O_2$)	15:0	98
Tetradecanoic acid, 2-hydroxy-, methyl ester ($C_{15}H_{30}O_3$)	2-OH 14:0	99
Methyl 3-hydroxytetradecanoate ($C_{15}H_{30}O_3$)	3-OH 14:0	91
Pentadecanoic acid, 14-methyl-, methyl ester ($C_{17}H_{34}O_2$)	i16:0	97
9-Hexadecenoic acid, methyl ester, (Z)- ($C_{17}H_{32}O_2$)	16:1ω7	99
Hexadecanoic acid, methyl ester ($C_{17}H_{34}O_2$)	16:0	98
Hexadecanoic acid, 14-methyl-, methyl ester ($C_{18}H_{36}O_2$)	a17:0	97
Cyclopropaneoctanoic acid, 2-hexyl-, methyl ester ($C_{18}H_{34}O_2$)	cy17:0	96
Heptadecanoic acid, methyl ester ($C_{18}H_{36}O_2$)	17:0	99
Hexadecanoic acid, 2-hydroxy-, methyl ester ($C_{17}H_{34}O_3$)	2-OH 16:0	94
9,12-Octadecadienoic acid, methyl ester, (E,E)- ($C_{19}H_{34}O_2$)	18:2ω6	99
8-Octadecenoic acid, methyl ester ($C_{19}H_{36}O_2$)	18:1ω10	99
9-Octadecenoic acid, methyl ester, (E) ($C_{19}H_{36}O_2$)	18:1ω9	99
Octadecanoic acid, methyl ester ($C_{19}H_{38}O_2$)	18:0	97
Cyclopropaneoctanoic acid, 2-octyl-, methyl ester ($C_{20}H_{38}O_2$)	cy19:0	99
Nonadecanoic acid, methyl ester ($C_{20}H_{40}O_2$)	19:0	98
Eicosanoic acid, methyl ester ($C_{21}H_{42}O_2$)	20:0	99

Similar kinds of PLFAs were identified in both soil columns except for methyl 2-hydroxydecanoate and hexadecanoic acid, 2-hydroxy-, methyl ester which was absent in SC2. The fatty acids 14:0, 15:0, 16:0, 17:0 and 18:0 which were identified are constituents of a diverse number of microorganisms (Findlay and Dobbs, 1993). Branched-chain (iso, anteiso and branched), cyclopropane and β-OH (3-OH) fatty acids which were also identified in the soil column are however more specific to bacteria as they do not usually occur in other organisms (Lechevalier, 1989). In general therefore, the saturated fatty acids 15:0, a15:0, 17:0 and a17:0 in the soil column indicate the presence of bacteria (Vestal and White, 1989). Gram positive bacteria are further identified by the presence of i16:0, a15:0, a17:0 and 16:1ω7 constituting less than 20 % of the monounsaturated fatty acids, and gram negative bacteria by cy17:0, cy19:0 and 3-OH 14:0. The presence of 16:1ω7 and the cyclo-fatty acids (cy17:0 and cy19:0) respectively show that the soil column environment is populated by bacteria of aerobic and anaerobic kinds (Vestal and White, 1989). Even though the soil column was mainly aerobic, confirmed by dissolved oxygen concentrations greater than 2 mg L^{-1} at all depths, anaerobic bacteria could still proliferate in anaerobic microsites within the soil column. The fatty acid 18:2ω6 identified in the soil samples is common to both plant cells and fungi (Zelles, 1999). In the absence of plant cells therefore, which is the case in the soil columns, the presence of 18:2ω6 in the soil samples indicates the presence of fungi. 18:1ω9 also indicates fungi (Vestal and White, 1989). Since bacteria and fungi are microorganisms found in wastewaters (Tchobanoglous et al., 2003), the soil column is representative of a biological wastewater treatment system.

The comparison of the microbial concentrations in SC2 and SC3 was carried out based on the peak areas from the GCMS analysis. The peak areas obtained for the SC2 and SC3 are shown in Figure 4.21. The peak areas were not converted to concentrations because standards were not available for all the fatty acids methyl esters detected as some of the fatty acids detected were not constituents of the BAME mix.

During the sample preparation stage for SC2, 10 mL of the lipid extract was dried and used for the formation of the methyl esters. In subsequent sample preparations however, this volume was doubled in order to amplify peaks during the GCMS analysis. Therefore 20 mL extract was used for the SC3 samples. Resulting GCMS peak areas for the chromatograms for SC2 have therefore been doubled after the correction for the addition of the BAME mix before the GCMS analysis and used in the plots of Figure 4.21. This approach was deemed valid since the peak area was found to be directly proportional to the concentration.

The results shown in Figure 4.21 indicate that generally there was a higher concentration of microorganisms in SC2. The lower concentrations in SC3 therefore could explain the poorer DOC removal that occurred. Lower hydraulic conductivity of the packing in SC3 due to the presence of clay is likely to have contributed to the smaller concentrations of microorganisms in the soil column. The wastewater may not have adequately penetrated the pores of the soil mix leading to relatively poorer growth or uneven distribution of microorganism around the soil grains.

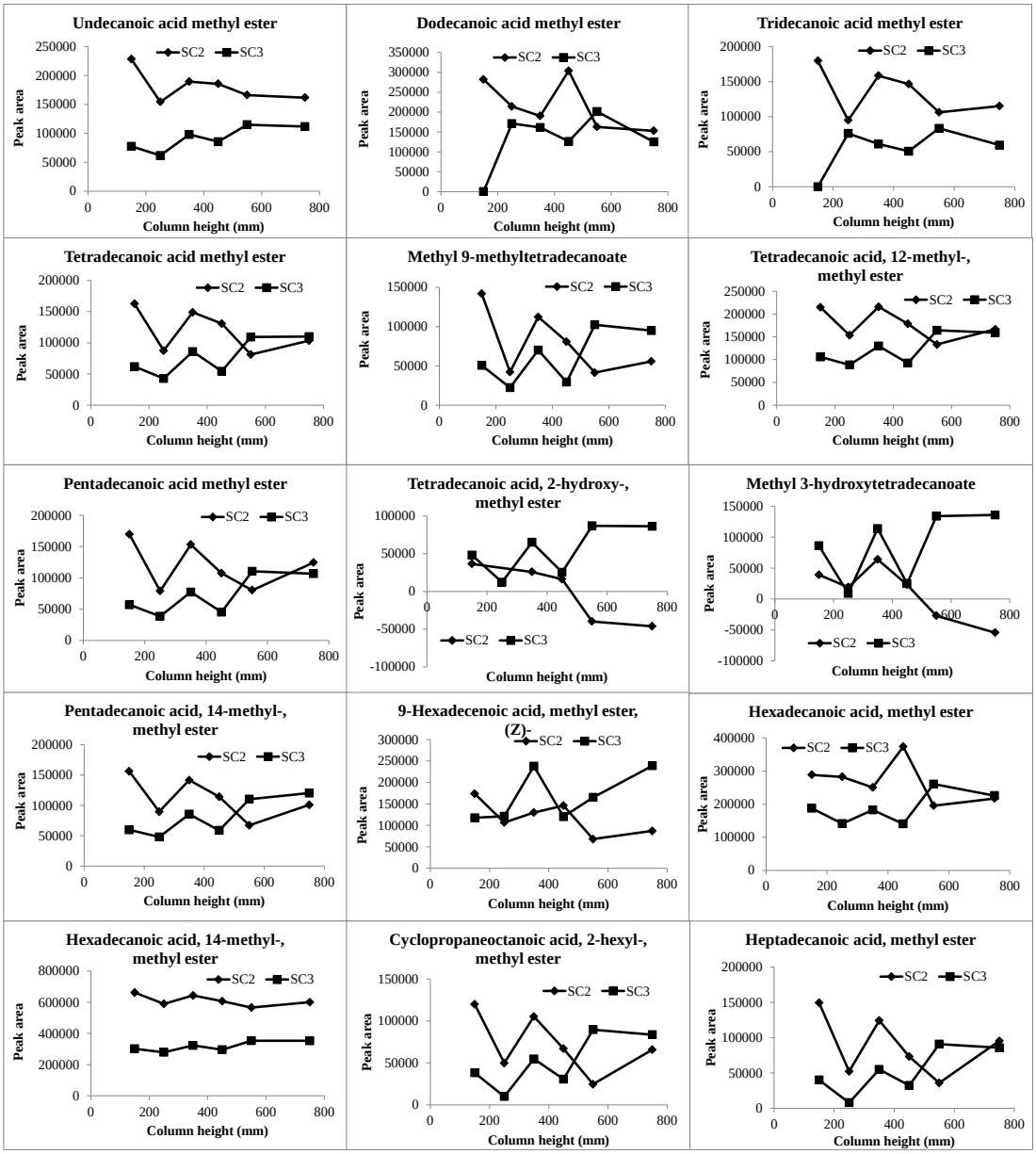

Figure 4.21 Peak areas against column height for depths for the various fatty acids identified in SC2 and SC3

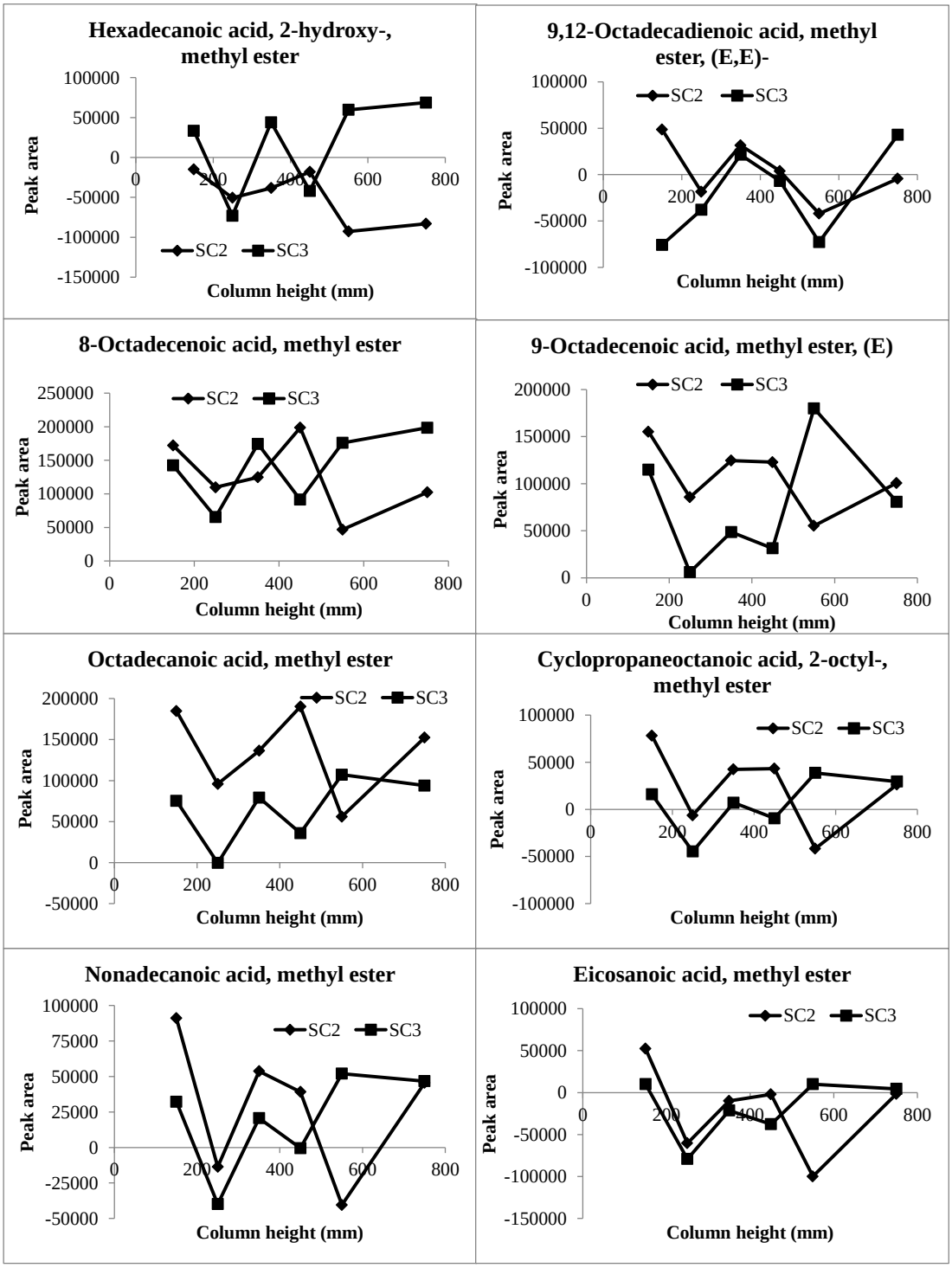

Figure 4.21 (cont'd) Peak areas against column height for depths for the various fatty acids identified in SC2 and SC3

4.3.2.3 Wastewater Treatment under Unsaturated Conditions

Figure 4.22 a shows the distribution of water in the unsaturated soil column for each level of water table (WT75, WT500 and WT800) and Figures 4.22 b and c, the removal of DOC and sulphate in the soil column for these experimental conditions.

Unsaturated zone thickness in the soil column was 850 mm, 425 mm and 125 mm corresponding to WT75, WT500 and WT800 respectively. Volumetric water content was 7 – 8 % in the unsaturated zone increasing as the water table was approached, and reached 28 % midway of the column for WT500. For WT75, volumetric water content measured at 500 mm was less than at 850 mm because water was infiltrated downwards from the top of the soil column. At WT800, water content for most of the column length exceeded 27 %. Highest water content measured was 37 % at 150 mm. The water content is less than the porosity because of air trapped in the pores of the sand during rewetting after the initial drying sequence after column packing. Not much difference existed between the water content at 150 mm for the three heights of water table. There was however a slight increase in the water content from WT75 through to WT 800 because with time, some of the trapped air dissolved. This also explains the lower volumetric water content of 30.6 % measured at 500 mm for WT 800 even though the water table was at a level almost 32 cm above that point. Trapped air in the soil pores in the saturated zone is advantageous in that it contributes to the oxygen supply for biodegradation in the saturated zone.

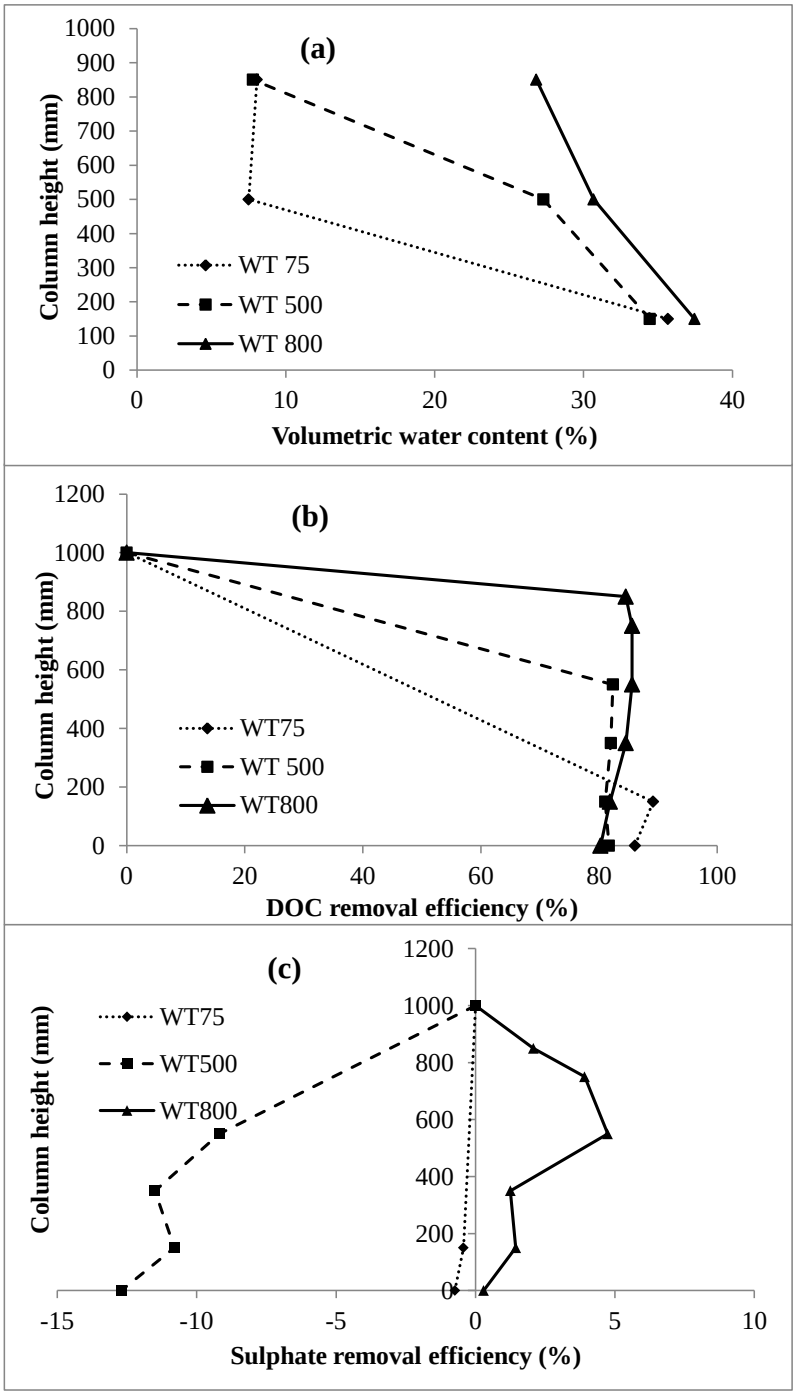

Figure 4.22 Volumetric water content profiles and DOC and sulphate removal efficiencies at differing water table levels in unsaturated silica sand column (SC1) (a) Volumetric water content (b) DOC removal efficiency (c) Sulphate removal efficiency

Dissolved Organic Carbon Removal

For a wastewater travel length of 850 mm through unsaturated zone (WT75), DOC removal in SC1 was 86 %. The removal dropped slightly to 80 % when the travel length was reduced to 425 mm (WT500). DOC removal of this magnitude has been reported in field studies (Idelovitch and Michail, 1984). There was not much difference in removal with further reduction in the travel length to 125 mm (Figure 4.22 b). Water content was thus found not to appreciably affect DOC removal. Cha et al. (2005) also observed in soil column experiments that except at the beginning of the flooding cycle, DOC removal was not dependent on the depth of the unsaturated zone. Van Cuyz (2001) also found no significant difference in BOD and COD removal efficiency with change in soil depth from 60 cm to 90 cm when septic tank effluent was infiltrated. Even though the depth of unsaturated zone to the groundwater table is expected to influence removal efficiency due to its influence on the hydraulic behaviour and soil water content and therefore hydraulic retention time and level of soil aeration (Van Cuyk et al., 2001), which are parameters that can affect biodegradation potential, the influence on removal of the travel length through the unsaturated zone may be minimal because a greater proportion of the removal that occurs in SAT occurs within the first few cm of the soil (Quanrud et al., 1996b). This is due to the large percentage of microorganisms that proliferate near the infiltration surface (Van Cuyk et al., 2001). Besides, there were no limitations on dissolved oxygen availability in the soil column under all water table conditions investigated.

Dissolved Oxygen and Sulphate Removal

The effluent from the soil column remained well oxygenated when it was operated at the lowest water table level even though about 14 mg L^{-1} had been removed. Dissolved oxygen concentration was 8.4 mg L^{-1} signifying only a 6 % decrease. Dissolved oxygen would have been consumed in the soil column for DOC degradation, but effectively replenished from the surrounding air due to the low water content of the sand. Even though the influent concentration remained the same the concentration of dissolved oxygen in the effluent reduced when the water table was raised. Dissolved oxygen concentration remaining in the soil column effluent was 6 mg L^{-1} for WT500 condition compared to 8.4 mg L^{-1} at the lower water table level. The lower concentrations at higher water table levels and therefore higher soil water contents could be attributed to the slow diffusion of oxygen through water.

Sulphate reduction though minimal occurred at WT800. Within the first 500 mm of the soil column up to 4 % of influent sulphate corresponding to 3 mg L^{-1} was removed. For WT75, WT500 and within the first 550 mm of the soil column when the outlet was placed at 800 mm, (i.e. WT800), sulphate concentrations were observed to increase in the soil column (Figure 4.22 c). These increases are due to the oxidation of sulphur to sulphate which occurs under aerobic conditions. The sulphur may have been be derived from proteins in the meat extract and peptone (which had the sulphur containing amino acid methionine as part of their constitution) included in the synthetic wastewater composition, or from the activities of sulphate reducing bacteria within the anaerobic zone of biofilms, which releases hydrogen sulphide. The production of hydrogen sulphide has been observed to occur within the clogging layer of infiltration ponds even at very low DOC concentrations

of 5 mg L^{-1} to 11 mg L^{-1} (Greskowiak et al., 2005), the levels of which suggests adequate dissolved oxygen to DOC ratios to sustain aerobic conditions. The proteins in the wastewater are converted into amino acids which are further degraded, with sulphur containing amino acids such as cysteine, cystine and methionine releasing sulphide during the degradation process (Gray, 2004). Sulphide can readily be used as an electron donor by bacteria such as *Beggiatoa* causing its oxidation to elemental sulphur (Bitton, 1999) which is further oxidised to sulphate (Wiessner et al., 2010). The breakdown of proteins in the soil column is confirmed by the reduction in organic nitrogen concentration as shown in Figure 4.24 c.

Nitrogen Transformation and Removal

Nitrogen transformation processes involving the conversion of organic nitrogen to ammonium nitrogen (ammonification), ammonium nitrogen to nitrate (nitrification) and some degree of denitrification at high water table levels were observed to occur within the soil column. A schematic diagram of the transformation processes within an imaginary boundary in the soil column, modified from van Haandel and van der Lubbe (2007), is shown in Figure 4.23. The percentage change in nitrate, ammonia and organic nitrogen concentrations in the soil column under the different water table conditions are also shown in Figures 4.24 a – c respectively.

Greater than 80 % organic nitrogen removal was achieved after 850 mm travel through the soil column at all three water table depths. Increases in organic nitrogen concentrations depicted by a drop in removal efficiencies occurred at some points within the soil profile. This may be due to the release of soluble microbial products, which contain proteins (Wu and Lee, 2011), into the liquid phase of the soil column

during microbial substrate utilisation (de Silva and Rittmann, 2000). Deamination of organic nitrogen to ammonia may have occurred through the action of extracellular proteolytic enzymes, which convert proteins to peptides and then to amino acids, which are further deaminated (Gray, 2004). Better conversion of organic nitrogen to ammonia seemed to occur at higher levels of water table (comparing WT500 and WT800) corresponding to higher soil water contents and shorter lengths of travel through the unsaturated zone. Nitrogen transformation processes involved in the removal of nitrogen are dynamic and complex due to the different oxidation states of nitrogen and the ease of transformation from one state to the other (Crites et al., 2000).

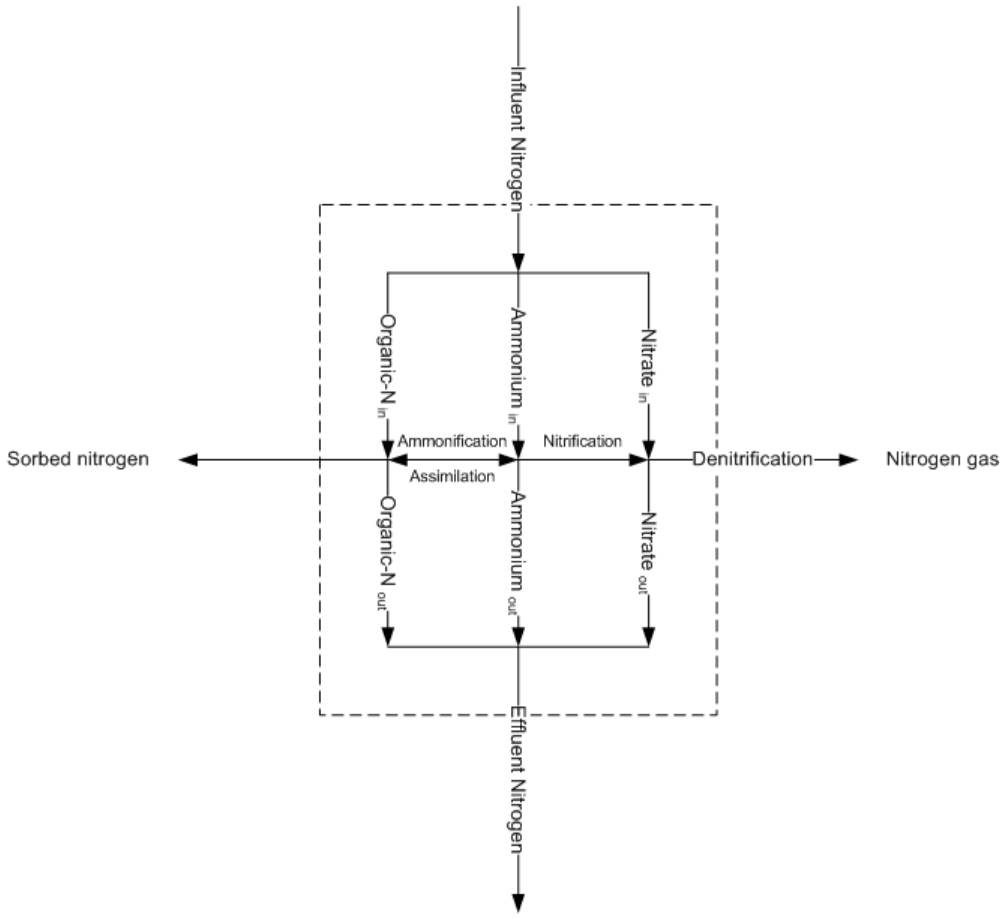

Figure 4.23 Schematic diagram of nitrogen transformation processes within the soil column

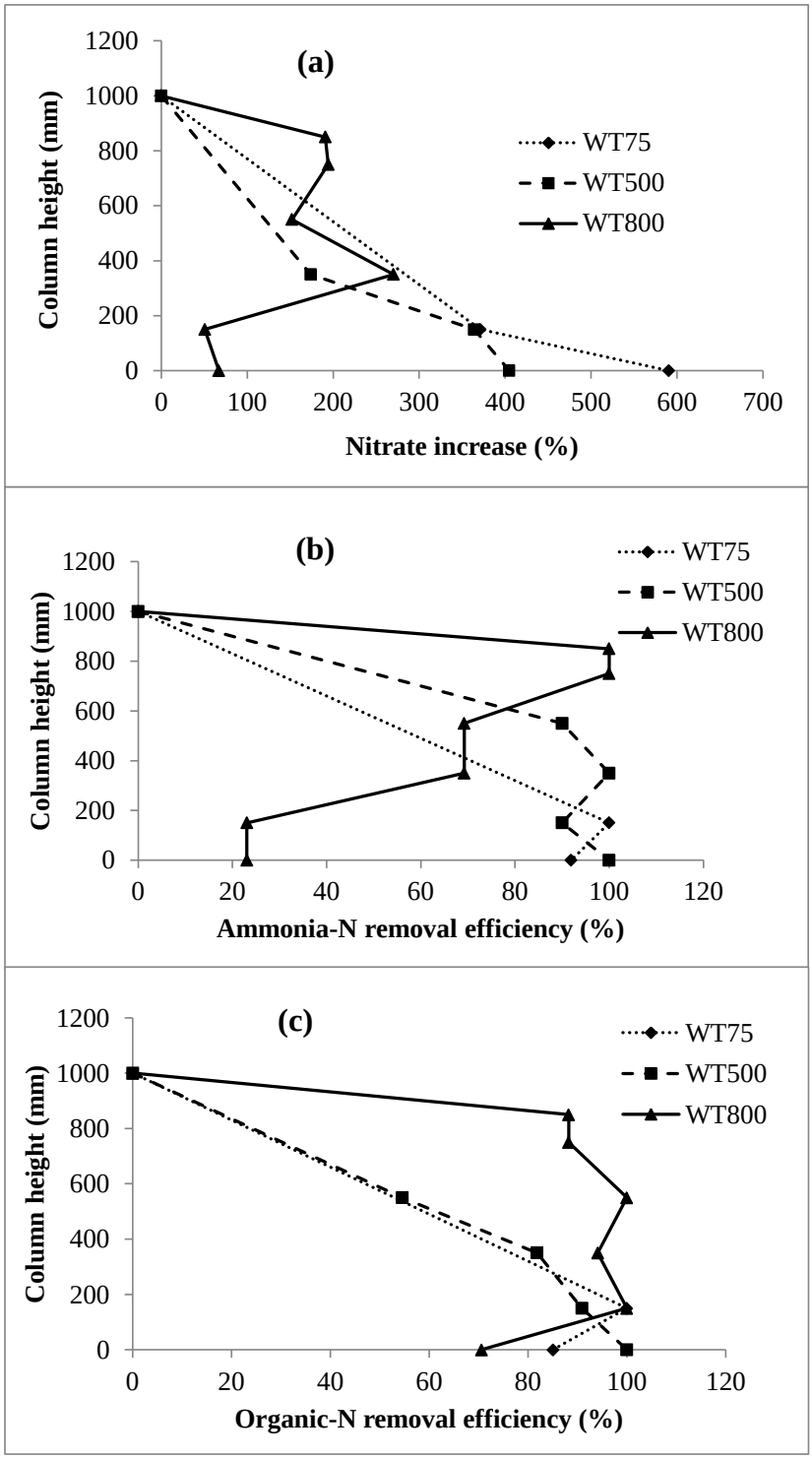

Figure 4.24 Nitrogen removal at differing water table levels in SC1

(a) Nitrate increase (b) ammonia removal efficiency (c) organic nitrogen removal efficiency

Ammonia was almost completely removed in the soil column. Ammonia could have been lost by a combination of volatilization and adsorption with subsequent nitrification (Crites et al., 2000), the latter removal mechanism yielding high concentrations of nitrate in the effluent. Some of the ammonia could also have been assimilated by the soil column microorganisms for growth and cell maintenance (Bitton, 1999). Average effluent nitrate concentration of 19.5 mg L^{-1} measured at WT75 was six times the initial concentration. This concentration exceeds the limit permitted in drinking water and the effluent would need to be denitrified for conversion into nitrogen gas. The discharge limit of nitrate is 10 mg L^{-1} due to the risk of methemoglobinemia occurring in infants less than 6 months old upon ingestion of high concentrations of nitrate (Crites et al., 2000). Nitrification for oxidation of ammonium ions in the soil column was facilitated by chemo-autotrophic nitrifying bacteria in the soil column and proceeds as follows (Gray, 2004):

$$NH_4^+ + 1.5O_2 \rightarrow NO_2 + 2H^+ + H_2O$$

$$NO_2 + 0.5O_2 \rightarrow NO_3^-$$

Nitrification reduced as the depth of the unsaturated zone was reduced due to a corresponding reduction in dissolved oxygen zones. Effluent nitrate concentrations for WT500 and WT800 were 13 mg L^{-1} and 4.6 mg L^{-1} respectively. Nitrification has high dissolved oxygen requirements, ammonia being used as the terminal electron acceptor by the microorganisms (Gray, 2004). From the stoichiometry of the overall nitrification reaction, 4.57 g of oxygen is consumed for each gram of ammonium nitrogen oxidised (Tchobanoglous et al., 2003). Nitrification is thus inhibited when dissolved oxygen concentrations are very low (Gray, 2004), such as could pertain under saturated conditions in the presence of organic matter. This was evident under water table condition WT800. Oxygen renewal in the soil column occurs through air

convection and molecular diffusion (Jellali et al., 2009) the latter of which is influenced by the soil water content. After the 150 mm depth, the rate of nitrification slowed down considerably. This coincided with a marked decrease in ammonia removal efficiency. Beyond 250 mm of wastewater travel, nitrification ceased completely as indicated by the accumulation ammonium nitrogen (decrease in removal efficiency of ammonium). At the same point, the onset of denitrification, which reduces nitrate to nitrogen gas through the intermediate compounds nitrite, nitric oxide and nitrous oxide (Gray, 2004) was apparent. The occurrence of denitrification is confirmed by the disappearance of nitrate in the presence of ammonium nitrogen (Tchobanoglous et al., 2003). The reactions involved in the denitrification process have already been discussed in Section 4.2 and would therefore not be repeated.

The nitrogen species in the soil column were balanced considering a batch of wastewater in the soil column, to determine if the total loss of organic nitrogen and ammonia nitrogen would translate into an equal or smaller rise in nitrate concentrations. Total nitrogen in the influent, which was determined as the sum of organic nitrogen, ammonia nitrogen and nitrate (nitrite was not detected in any soil column samples), was compared to the corresponding concentration in the effluent. In the effluent, 97 % of the total nitrogen concentration was in the form of nitrate. The mass balance analysis showed that the nitrate concentrations measured at the effluent end were not only as a result of nitrification processes occurring during that infiltration sequence alone but also included nitrate already accumulated in the soil column or nitrified adsorbed ammonium from previous wastewater infiltration cycles. This confirms the occurrence of ammonium sorption in the soil column. The

nitrate formed was dissolved in the infiltrating wastewater and carried along to the effluent end.

Summary of Soil Column Performance for Organic Matter and Nitrogen Removal under Unsaturated Conditions

From the results, the nitrification rate was found to be dependent on the length of unsaturated zone available for wastewater travel. Reduced oxygen availability in the soil profile due to increased water content therefore accounted for the reduction in nitrification as the water table was raised. As the soil column achieved greater than 80 % DOC and organic nitrogen removal and also substantial nitrification was evident, with 90 % nitrification or better occurring at the lower water table conditions, the soil column could be said to be performing well with respect to its degradation and transformation potential. Previous studies of SAT systems have shown that they are capable of achieving 5 to 50 mg L^{-1} nitrification per day and 92 % total nitrogen removal could occur (Crites et al., 2000). To assess total nitrogen removal efficiency in the current experiments, the wastewater would have to go through an anoxic soil zone for denitrification of formed nitrate to occur.

4.3.3 Investigation of Estrogens Removal

With the soil column environment verified to be suitable for the removal of organic matter and nitrogen, the removal of estrogens was investigated. This section presents the findings on the removal of the estrogens during travel through unsaturated sand as well as through the saturated silica sand and silica sand-silt-clay mixture soil columns. The calibration curves developed for E1, E2 and EE2 (Figures 3.17 a – c) were used to convert peak areas obtained from the LCMS analysis to estrogen

concentrations. The impacts of altering the height of the water table in the unsaturated soil column and the wastewater hydraulic loading rate and organic carbon concentration to the saturated soil columns are also presented.

4.3.3.1 Estrogen Removal under Unsaturated Conditions

The depth of the water table in the unsaturated soil column was varied to assess the effect of the travel distance through the unsaturated zone on estrogen removal and the potential for groundwater contamination. Figures 4.25 b – d show profiles of E1, E2 and EE2 removal efficiencies as functions of column length, with variation in the length of travel of wastewater through the unsaturated zone of the soil column. At all the water table depths, wastewater was sampled from 150 mm and the column outlet (i.e. effluent). A comparison of the removals at these points with corresponding thickness of unsaturated zone has thus been made in Figures 4.25 e and 4.25 f for the column outlet and 150 mm respectively.

At WT75, the sand column showed complete removal of E1 and E2 in all samples (Figures 4.25 b and 4.25 c). EE2 removal reached about 94 % after travel through 850 mm of the soil column and was not detected in effluent samples (Figure 4.25 d). Previous studies have reported greater than 90 % removal of E1, E2 and EE2 in the upper 550 mm of soil during irrigation with sludge amended wastewater effluent (Ternes et al., 2007). A rise in water table to WT500 caused a drop in removal efficiencies of E1 and EE2. E2 removal efficiency was 100 % at the first sampling depth of 450 mm and remained so throughout the rest of the soil profile. This is consistent with results from 300 mm long aerobic biotic unsaturated soil columns packed with silica sand where about 99 % E2 removal was realised (Fox et al.,

2006). A less consistent removal of E1 with sand depth was however observed (Figure 4.25 b).

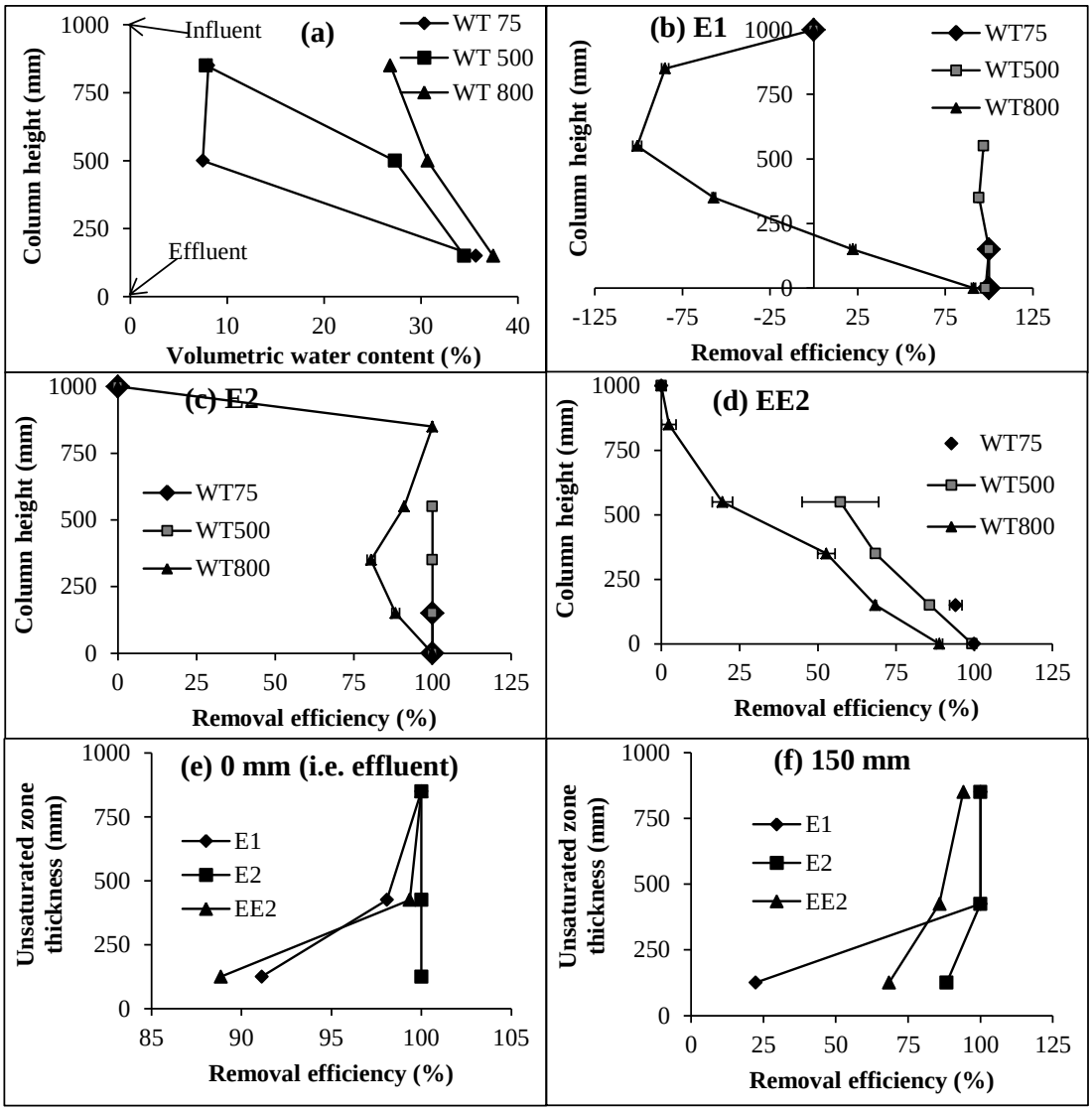

Figure 4.25 Water content and estrogen removal efficiency in unsaturated silica sand column (SC1)

(a) Water content in SC1 (b) E1 (c) E2 (d) EE2 removal efficiency at WT75, WT500 and WT800; Effect of length of travel through unsaturated zone on removal efficiency at (e) column outlet (f) 150 mm from column base (i.e. outlet). (Experimental conditions: 49 cm d^{-1} HLR, 17 mg L^{-1} DOC, 20 °C).

At 550 mm, calculated removal efficiency of E1 was 97 %. This dropped to 94 % at 350 mm and then increased to 100 % after a further 200 mm travel through the sand. E1 was once again detected in the column effluent resulting in a final removal efficiency of 98 %. As the soil column tests were repeated and similar results obtained, the transient behaviour of E1 was confirmed. In a number of studies, E2 has been observed to transform to its metabolite E1 (Colucci et al., 2001; Jürgens et al., 2002; Czajka and Londry, 2006; Stumpe and Marschner, 2009). The transformation has been attributed to abiotic oxidation processes (Colucci et al., 2001) as well as to microbial oxidation (Czajka and Londry, 2006; Stumpe and Marschner, 2009). Bacterial oxidation of EE2 to E1 has also been observed as a degradation pathway of EE2 (Haiyan et al., 2007). In this experiment, E2 was not detected in samples collected at the 550 mm point and beyond and therefore ruled out as a source of E1. The transient pattern of E1 could thus be attributed to the processes of E1 mineralisation and production from EE2 occurring simultaneously. At 150 mm, EE2 removal efficiency was found to have dropped from 94 % to 86 % at WT75 and WT500 respectively (Figure 4.25 d). At WT75, no EE2 was detected in the column effluent, hence a 100 % removal was achieved.

A further rise in water table to WT800 resulted in further decrease in removal efficiencies. There was an initial 85 % increase in the concentration of E1 at the first sampling depth (850 mm), which increased further to 100 % at 550 mm. As E2 readily biodegrades with transformation to E1 being the first step of its degradation process (Ke et al., 2007), the increase in E1 concentration within the first 450 mm of the soil column could be attributed to the transformation of E2 to its intermediate metabolite E1 by the microorganisms in the soil column. It is likely that E1

degradation occurred simultaneously, but was overshadowed by E2 and EE2 bio oxidation processes leading to their transformation to E1. Partial conversion of E1 to E2 under methanogenic conditions has also been observed by some authors, the conversion thought to have occurred as a result of the reduction of the ketone of E1 to the alcohol form of E2 (Czajka and Londry, 2006). Beyond the 550 mm column height, a reduction in E1 concentration begun, resulting in a total removal efficiency of 91 % at the outlet of the column. A removal of 2 % EE2 occurred within the first 150 mm of travel through the sand. Samples from 550 mm showed a drop in removal efficiency of EE2 from 57 % at WT500 to 19 % at WT800. Reductions in removal were also realised at 350 mm, 150 mm and in the effluent. Total removal in the column amounted to 89 %, representing an 11 % difference compared to the removal achieved at the previous water table depth (i.e. WT500).

It is clear from the results (summarised in Figures 4.25 e and 4.25 f) that the depth of the unsaturated zone increases the removal efficiency. The lower removal efficiency of the estrogens under low unsaturated zone thickness (i.e. higher water table) could be attributed to a reduction in aerobic conditions in the soil as the depth of the unsaturated zone decreased and soil water content (Figure 4.25 a) increased. The low diffusion coefficient of oxygen in water compared to that in air greatly reduces oxygen transport in the saturated zone (Blowes et al., 2005). Thus as the water table rose, redox conditions in the soil were not conducive for achieving maximum efficiency of estrogen degradation. Reduced oxygen availability could also have resulted in a reduction of nitrification zones, thus impacting negatively on degradation of EE2 in the NH_3/EE2 cometabolic process and contributing to the drop in removal efficiencies of EE2 observed. Nitrification in the unsaturated zone

followed by denitrification in the saturated zone during SAT is a crucial process for nitrogen removal, and is often optimised with appropriate lengths of the wetting and drying cycles (USEPA, 1981). The ability for the cometabolic process for the removal of EE2 to proceed without prior adaptation of nitrifying bacteria (Vader et al., 2000) is therefore advantageous in that it could provide a barrier against groundwater contamination upon the incidence of EE2 accidental or shock loading to nitrification optimised SAT infiltration basins.

At all the water table levels studied, EE2 was the least removed of the three estrogens. In previous studies, EE2 was also found to be more resistant to biodegradation or mineralisation than E1 and E2 (Colucci et al., 2001; Jürgens et al., 2002; Stumpe and Marschner, 2009). The resistance of EE2 to degradation partly stems from the presence of the ethinyl group in position 17β, which shields the compound from oxidation to E1 (Gomes and Lester, 2003).

4.3.3.2 Estrogen Removal in Saturated Silica Sand under Variable Hydraulic Loading Rates and Dissolved Organic Carbon Concentration

Figure 4.26 a – h show the removal of the estrogens under the various experimental conditions. Figure 4.26 a shows the removal efficiency of E1, E2 and EE2 through the saturated silica sand column (SC2) at a HLR of 81.5 cm d^{-1} and 17 mg L^{-1} DOC. For all three estrogens, an initial increase in concentration occurred within the first 150 mm of the sand (measured from the base of the column).

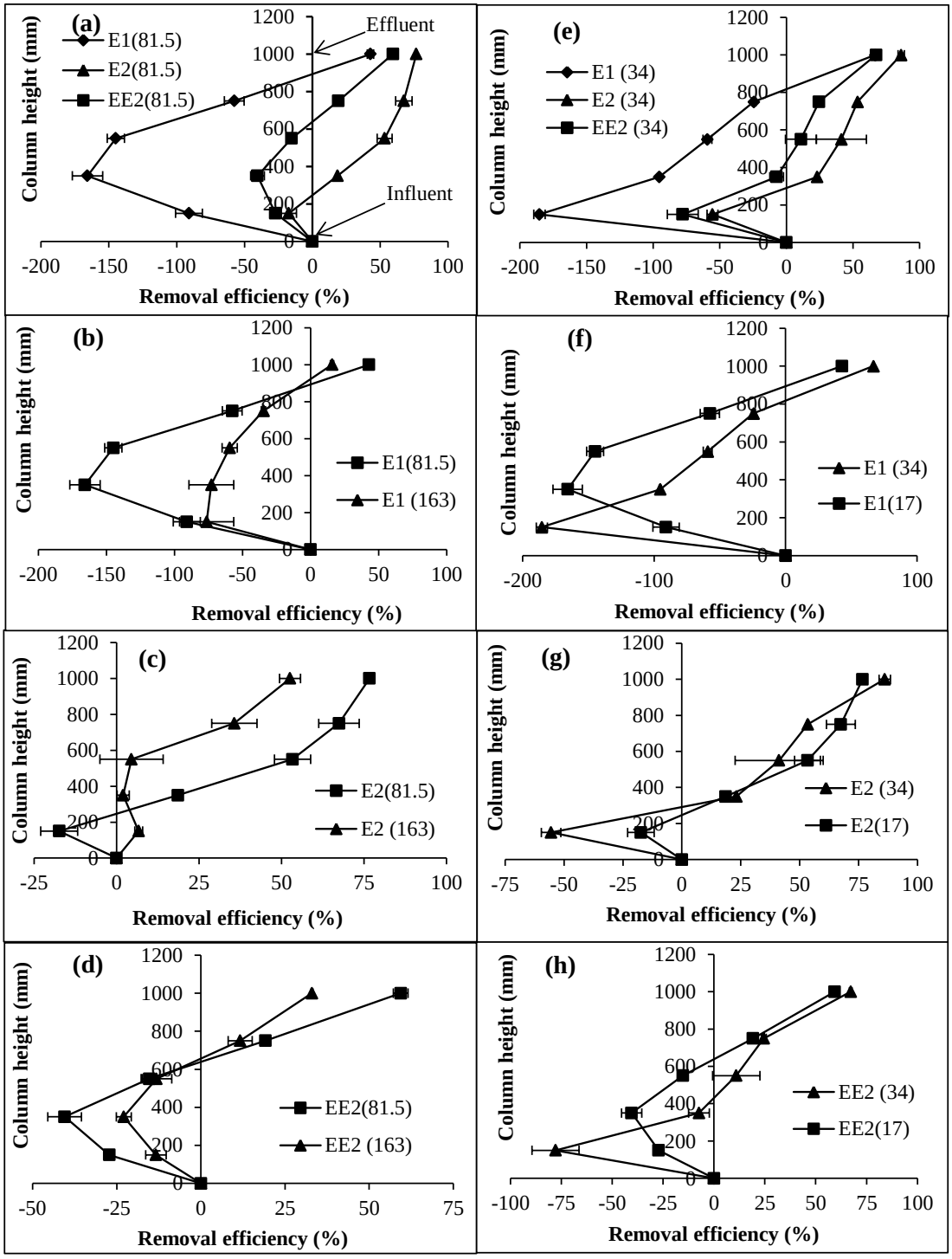

Figure 4.26 Estrogen removal efficiency in saturated silica sand column (SC2) (a) E1, E2 and EE2 removal efficiency at 17 mg L^{-1} DOC and HLR of 81.5 cm d^{-1}; Effect of HLR (17 mg L^{-1} DOC) on removal of (b) E1 (c) E2 (d) EE2; (e) Removal of E1, E2 and EE2 at 34 mg L^{-1} DOC and 81.5 cm d^{-1} HLR; Effect of DOC (81.5 cm d^{-1} HLR) on removal efficiency of (f) E1 (g) E2 (h) EE2, (T = 20 °C).

E1, E2 and EE2 concentrations increased by 90 %, 17 % and 27 % respectively. These are depicted as negative removal efficiencies in Figure 4.26. E1 and EE2 concentrations continued to increase up to 165 % and 40 % respectively within a height of 350 mm. The increase in E1 and E2 concentrations could be attributed to inter-conversion of E1 and E2 (Lai et al., 2002; Czajka and Londry, 2006; Stanford et al., 2010) and bacterial transformation of EE2 to E1 (Haiyan et al., 2007). After the 150 mm point, the concentration of E2 began to decrease reaching 77 % overall removal in the effluent. The decrease in E2 concentration suggests a marked reduction in E1 transformation to E2 and thus E2 removal became apparent.

About 99 % E2 removal in 300 mm aerobic saturated soil columns packed with silica sand and spiked with 200 ng L^{-1} of E2, estriol and testosterone and simulating 18 hours retention time in the subsurface has been previously reported (Fox et al., 2006). The lower removal efficiencies obtained in these experiments, compared to Fox et al., (2006) could be due to the shorter residence time which was of the order of 10 to 11 hours and the type of microorganisms in the soil column. It should be noted that the soil columns in the current study were fed with synthetic wastewater and bioacclimated with a synthetic seeding material as opposed to real secondary effluent in the previous studies. Therefore there are bound to be some differences in the microbial consortia in the soil columns. E1 was also not spiked into the soil column with E2 in the previous studies. Lower E2 removal efficiency observed in the current study can also therefore be attributed to the presence of E1 in the applied influent, which transformed to E2, thereby markedly increasing soil column E2 concentrations. This then had to be removed further along the soil column in addition to the concentration originally inherent in the influent.

Reduction in the concentrations of E1 and EE2 begun after 350 mm, reaching overall removals of 42 % and 59 % respectively in the column effluent. Further investigations would be required to find out the reasons for the initial increase in concentration of EE2 from the influent end. It may however be speculated that a small degree of conjugation of the estrogens with the sulphate in the wastewater may have occurred in the influent tank and that these conjugated estrogens were deconjugated into their free forms in the soil column by the microorganisms, contributing to the measurement of higher estrogen concentrations in the soil column pore water than in the influent.

Figures 4.26 b – d show the effects of increasing HLR on estrogen removal efficiency. Doubling the HLR (i.e. from 81.5 cm d^{-1} to 163 cm d^{-1}) and thus decreasing the residence time of the estrogens in the column led to a drop in overall removal efficiencies of all three estrogens. There was less production of E1 and EE2 at the higher HLR. Increase in E2 concentration also did not occur within the first 150 mm of sand at the higher HLR. These could be due to insufficient time for the microbial transformation processes occurring between the column entry point and 150 mm. At 350 mm a slight increase in E2 concentration was observed at the higher HLR. The concentration then began to decrease resulting in an overall E2 removal efficiency of about 52 % at the column outlet. On the other hand EE2 concentration increased at the higher HLR but at lower values than for low HLR. At higher HLR, the overall removal at the outlet of the column for EE2 and E1 were only 33% and 16 % respectively.

E1, E2 and EE2 removal efficiencies obtained upon doubling the DOC are shown in Figure 4.26 e. Comparison with removals of the individual estrogens is made in Figures 4.26 f – h. A similar pattern of removal of the estrogens as occurred in the previous tests at lower DOC was observed. In this case there were greater percentage increases in the concentrations of the estrogens within the first 150 mm of the soil column. The removal process after this increase was more efficient reaching 67 % for E1 and EE2 and 86 % for E2. The increased glucose concentration in the wastewater enhanced microbial respiration leading to higher estrogen removal. In previous studies on soils, this enhancement has been found to improve E2 and EE2 mineralisation in one soil type, whilst having a detrimental effect on E2 and no effect on EE2 in a different soil type (Stumpe and Marschner, 2009). Even though there was a more abundant and readily available source of carbon present by way of increase in DOC, the results show that there was no competition or preferential utilization of the wastewater DOC by the microorganisms in the soil column. This could be due to the involvement in the removal process, of certain bacterial strains capable of utilising estrogens as growth substrates (Weber et al., 2005; Yu et al., 2007).

The results suggest that increasing organic carbon concentration could be a means of improving estrogen removal, provided the organic load is not too high as to impact negatively on the redox conditions by turning them anaerobic. High biological activity occurs near the soil/water interface during SAT as this is where concentrations of biodegradable organic matter and oxygen are highest. In cases where the oxygen demand of the wastewater is very high, all the oxygen could be utilised for the oxidation of organic carbon in this zone generating anoxic conditions

at shallow soil depths (Fox et al., 2006). As oxygen diffusion in water is very slow (Blowes et al., 2005), concentrations in deeper soil layers are greatly influenced by the degree of water saturation of the soil. Microbial activity in the water-saturated soil can also quickly deplete oxygen reserves resulting in anaerobic conditions (Khanal et al., 2006) especially where there still exists an abundant supply of organic carbon and other growth substrates. An anaerobic environment would lead to very slow degradation of E2 and render EE2 recalcitrant (Czajka and Londry, 2006).

4.3.3.3 Estrogen Removal in Saturated Sand-Silt-Clay Mix under Variable Hydraulic Loading Rates and Dissolved Organic Carbon Concentration

Figure 4.27 a shows the behaviour of the estrogens in the sand-silt-clay mix soil column (SC3). No increase in E2 or EE2 concentration occurred within the first 150 mm of the sand column. Within that depth, percentage removal reached 60 % and 32 % for E2 and EE2 respectively. There was a slight reduction in the removal efficiency at the 350 mm followed by a reduction in the concentrations up to the effluent end. Overall, about 83 % E2 and 61 % EE2 removal was achieved. With regards to E1 removal, the concentration increased by about 53 % at 350 mm. Beyond this depth, removal of E1 occurred leading to an overall removal of about 34 % at the outlet of the column. Doubling the HLR (Figures 4.27 b – d) clearly resulted in lower removal efficiencies of E2 for the entire length of the column. Transformation processes leading to E1 production were reduced and E1 concentration increased by only 16 % as compared to a 53 % increase at the lower HLR. The overall removal amounted to 27 %.

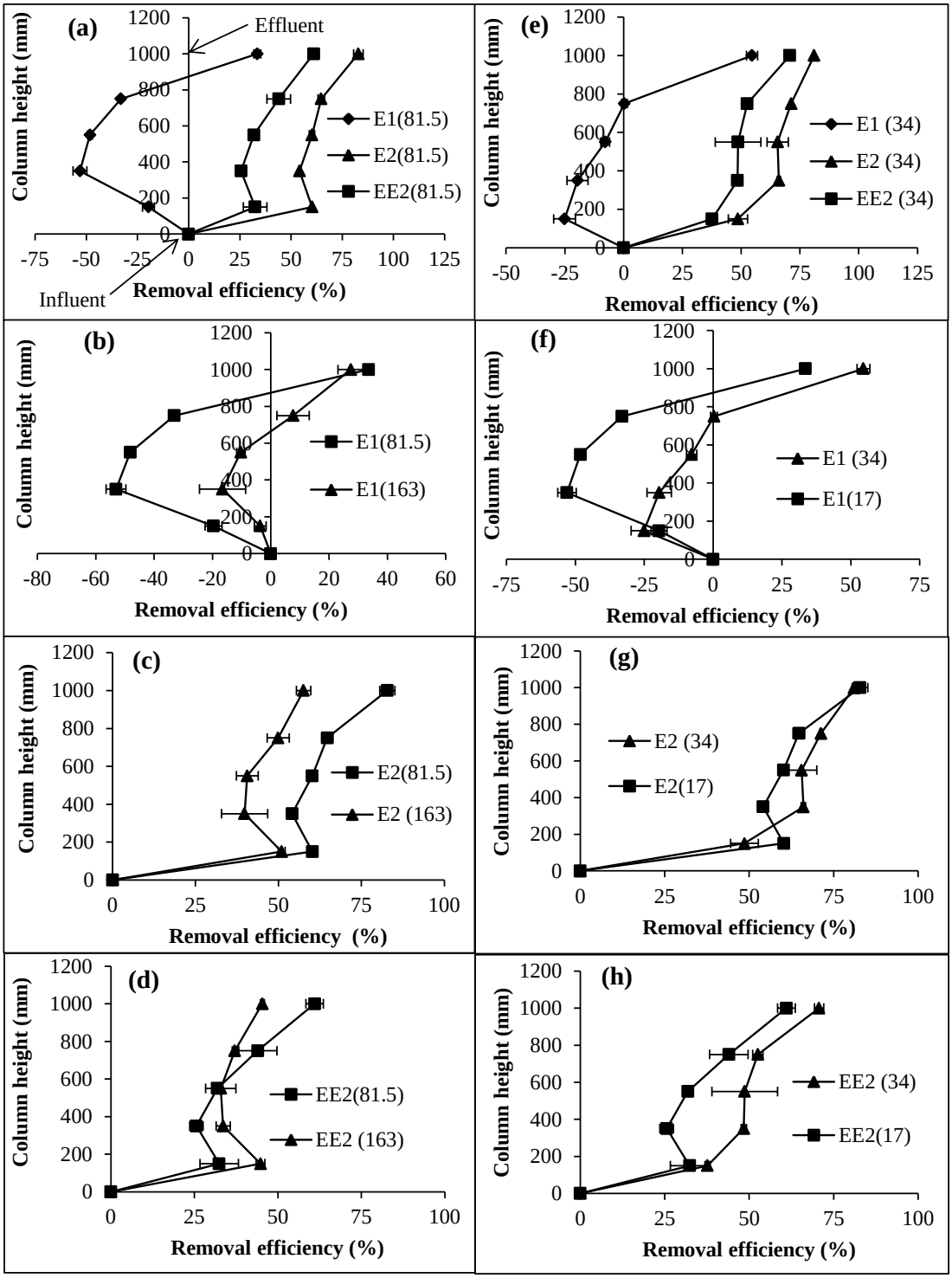

Figure 4.27 Estrogen removal efficiency in silica sand/silt/clay mix column (SC3) (a) E1, E2 and EE2 removal in SC3 at 17 mg L^{-1} DOC and 81.5 cm d^{-1} HLR; Effect of HLR on removal of (b) E1 (c) E2 (d) EE2; (e) removal of E1, E2 and EE2 at 34 mg L^{-1} DOC and 81.5 cm d^{-1} HLR; Effect of DOC on removal of (f) E1 (g) E2 (h) EE2, at T = 20 °C.

Effluent E2 and EE2 concentrations showed a drop in overall removal efficiencies from 83 % to 58 % and 61 % to 45 % respectively. The effect of increasing DOC on removal efficiencies is shown in Figure 4.27 e and is compared to that at lower DOC for each estrogen in Figures 4.27 f – h. An increase in DOC concentration resulted in improved overall removal of E1 and EE2 (Figures 4.27 f and h), while the overall removal efficiency of E2 did not change significantly (Figure 4.27 g). The figure also shows that removal efficiencies for E1 and EE2 and to some extent E2 were enhanced not only at the outlet of the column but throughout the length of the soil bed as a result of availability of more substrate for microorganisms.

Comparison of Figure 4.27 with Figure 4.26 indicates that higher removal efficiencies were obtained in SC3 (sand/silt/clay column) than SC2 (100% sand column), except for E1 in the final effluent despite having lower DOC removal efficiencies inferring lower biodegradation potential. Mechanisms for the removal and pathways for the biotransformation of estrogens during treatment are governed by their physical and chemical properties (Langford and Lester, 2003), the main mechanisms identified for their removal from the aqueous phase being volatilization, biotic and abiotic degradation and adsorption (Khanal et al., 2006). Their low Henry's law constant however limits their volatilization under normal pressure and temperature conditions. The estrogens are expected to sorb onto the solid phase due to their significant octanol-water partition coefficients (K_{ow}) which influences their partitioning and sorption. EE2 has high potential for sorption (Log K_{ow} > 4), whilst E1 and E2 would sorb moderately (2.5 < Log K_{ow} < 4) (Langford and Lester, 2003).

Although batch adsorption tests were not carried out on the soil packing materials, the relatively higher removal of estrogens in SC3 could be attributed to the presence of silt and clay. It is believed that adsorption would be higher in the presence of silt and clay due to the larger surface area provided by the small particle sizes of silt and clay and thus accounts for the higher removal efficiencies. This is supported by results of batch studies (Fox et al., 2006), where removal efficiency of E2 was better on soil having higher organic, silt and clay content than on sand. Sorption could also account for the differences in the behaviour of the estrogens observed within the earlier depths of the two columns. Sorption of estrogens onto the clay and silt in SC3 is responsible for reduced bioavailability of the estrogens, resulting in lesser transformation occurring in SC3 compared to SC2. As only small amounts of E2 and EE2 were produced, these increases in concentrations were not noticeable in SC3 due to sorption taking place in addition to degradation. The reduced permeability of the SC3 soil mix as a result of the finer clay and silt particles could also have resulted in an increase in the residence time of the estrogens in the soil leading to better removal efficiencies.

4.3.4 Conclusions

A comprehensive and systematic experimental investigation was carried out to study the effects of the length of travel through the unsaturated zone, HLR, DOC and soil type on the removal efficiency of E1, E2 and EE2. In all the experiments, E2 had the greatest removal efficiency, due to its high susceptibility to biodegradation. Increase in E1 concentrations in the columns were attributed to E2 and EE2 transformation processes. As a result of large increases in E1 concentrations from transformation processes, it had the lowest removal efficiency. A reduction in residence time due to

doubling HLR in the columns led to lower removal efficiencies. In silica sand, removal efficiencies of the estrogens improved with an increase in wastewater concentration (i.e. DOC). The presence of silt and clay also enhanced their removal efficiencies.

Deeper unsaturated zones favoured the removal of the estrogens. The efficiency of SAT for E1, E2 and EE2 removal is thus found to be dependent on the depth of the unsaturated zone with the removal process becoming less efficient as the depth of the unsaturated zone decreases.

4.4 Removal of Triclocarban during Soil Aquifer Treatment and its Effects on Chemical Oxygen Demand Removal

Triclocarban (TCC) removal during soil aquifer treatment (SAT) was simulated in a biologically active saturated laboratory soil column under aerobic conditions. This chapter presents and discusses the results obtained on the removal of TCC through the 300 mm long soil column used for the SAT simulations. The soil column was packed with silica sand with effective size (d_{10}) of 0.52 mm and average diameter (d_{50}) of 0.75 mm. Coefficients of uniformity and curvature are respectively 1.54 and 0.98. The density of the sand packing in the soil column was 1.55 g cm^{-3} and porosity 0.42. Wastewater flow direction in the soil column was downwards, from the top to the bottom of the column.

High accuracy of the TCC analysis on the high performance liquid chromatograph - mass spectrometer (LCMS) was obtained with the coefficient of correlation (R^2) for the calibration curve being 0.9633. The calibration curve is shown in Figure 3.9 of Chapter 3. Results of TCC recovery tests regarding solid phase extraction (SPE) processes carried out during the preparation of soil column samples for LC/MS analysis are also presented. In addition, the impact of TCC on chemical oxygen demand (COD) removal in the soil column is discussed.

4.4.1 TCC Solid Phase Extraction Recovery Tests

Recovery tests were carried out on the Envi-chrom P SPE cartridges in order to assess their suitability and effectiveness at retaining TCC when loaded with soil column wastewater samples. The results were important for accounting for loss of the compound during sample preparation for LC/MS analysis.

Figure 4.28 shows the measured concentrations in prepared samples that were extracted with the Envi-chrom P cartridges before LC/MS analysis against samples prepared in solvent (50:50 acetone/ methanol) and directly analysed. The recovery tests carried out using the SPE cartridges showed good recovery of the TCC applied. On the average, about 76 % recovery of TCC was obtained after the SPE process. Results obtained from LC/MS analysis were adjusted to account for the 24 % loss of the TCC analyte during the SPE phase.

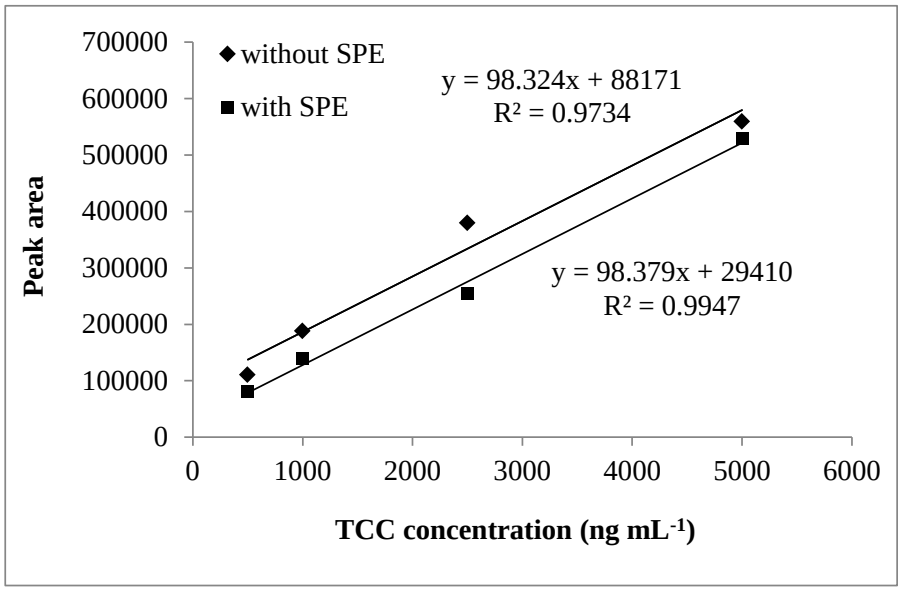

Figure 4.28 TCC solid phase extraction recovery tests

4.4.2 Soil Column Experiments

The synthetic wastewater applied to the soil column had an average COD of 67 mg L^{-1}. This was applied to the soil column at a constant hydraulic loading rate of 150 cm d^{-1}. TCC was applied to the soil column after 36 days of continuous infiltration of wastewater, during which period the COD removal in the soil column was monitored. It was confirmed from the COD removal rates in the soil column before introduction of TCC that the soil column environment was biologically active.

4.4.2.1 Influent Triclocarban Loading Rates

TCC removal in the soil column was assessed by measuring concentrations at 8 cm, 19 cm and the effluent end of the soil column over two weeks of continuous infiltration of wastewater containing TCC. Influent TCC concentrations to the column were 783 ng L^{-1}, 1112 ng L^{-1}, 2130 ng L^{-1} and 3501 ng L^{-1} on days 0, 3, 7 and 10 respectively, at a hydraulic loading rate of 150 cm d^{-1}. The applied concentration was reduced to 2372 ng L^{-1} on day 13 to observe the influence of time on removal.

4.4.2.2 Triclocarban Reduction in the Soil Column

Figure 4.29 shows the levels of TCC concentrations fed to the soil column over time and the resulting concentrations occurring at 8 cm and 19 cm depths of the column as well as in the effluent. At all TCC concentrations applied, a reduction in concentration was observed with column depth. This removal pattern is in line with studies carried out on soil amended with biosolids, where the concentration of TCC within the soil profile was found to reduce with increase in depth of soil (Xia et al.,

2010). This observation could be attributed to increased residence time and the availability of more surface area for sorption and time for biological or chemical transformation processes to occur. Effluent concentrations on the sampling days were 3.8 ng L^{-1}, 45 ng L^{-1}, 622 ng L^{-1}, 1126 ng L^{-1}, and 1607 ng L^{-1} respectively. The resulting percentage removal of TCC attained at each depth of the column is shown in Figure 4.30.

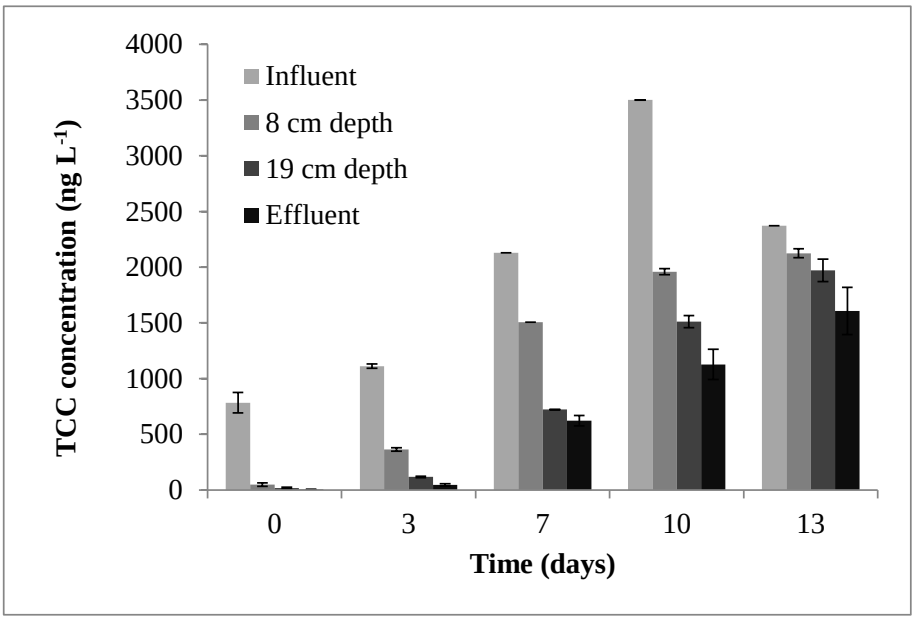

Figure 4.29 TCC concentration against time at different depths of the soil column

It can be seen from Figure 4.30 that highest TCC removals generally occurred within the first 8 cm of column depth. On the first day of infiltration of TCC at 783 ng L^{-1} concentration, about 94 % removal was attained within the first 8 cm of the soil column. The high removal efficiency within the first few centimeters of the soil column points to limited soil leaching capability of TCC (Xia et al., 2010) and also possibly high biodegradation rates, since this is the zone within which biological activity is highest in SAT systems due to copious amounts of substrate and dissolved oxygen for growth (Fox et al., 2006).

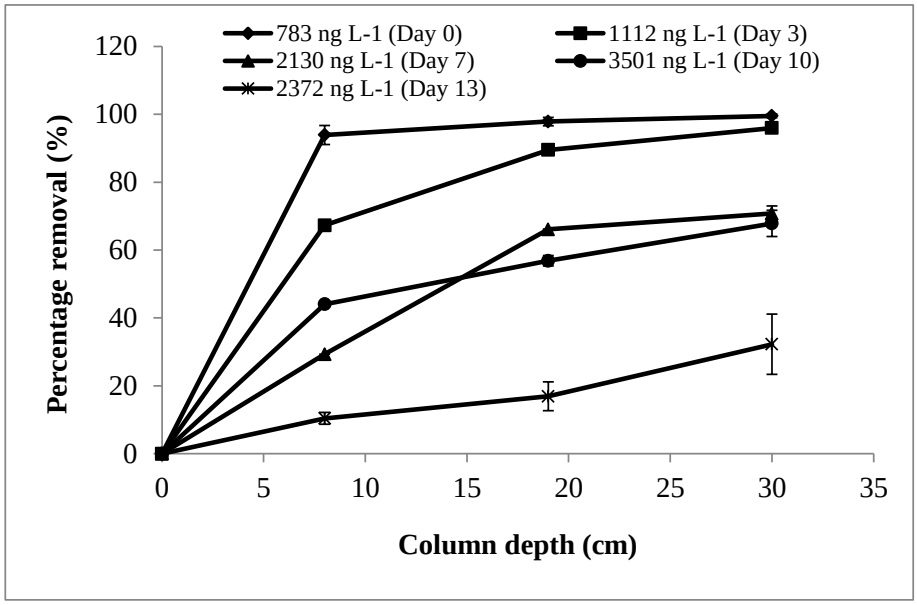

Figure 4.30 Percentage removal of TCC in the soil column

Upon an increase in influent concentration, the removal dropped to 67 % and dropped further with increase in concentration. The same pattern was observed at the 19 cm depth and at the soil column exit, where the percentage removal through the 30 cm depth of column reduced from 99.5 % observed on the first day of TCC application to 32 % at the end of two weeks. This is partly because the sorption of contaminants by soil is usually not complete, with equilibrium existing between the soil and solution, leading to the amount of TCC left in solution gradually increasing over time as the buffer capacity of the sand was approached (Yong et al., 1992).

There is limited information on the behaviour of TCC in soils that are infiltrated with municipal or industrial wastewater (Wu et al., 2009). However, triclosan (TCS), a co-contaminating (Halden and Paull, 2005) and more widely used antimicrobial agent in personal care products having similar properties as TCC (Shareef et al., 2009) has been better studied and has been found to be more persistent at higher concentrations in septic tank soil percolation systems (Svenningsen et al., 2011).

TCS has been identified as a co-contaminant with TCC in aquatic environments due to similarities in their properties, use, disposal and half-lives in the environment (Halden and Paull, 2005). Due to the similarities in antifungal and antimicrobial (Shareef et al., 2009) and other physical properties of these two compounds, it is expected that TCC would also behave in a similar fashion as TCS in soil infiltration systems, and even to a greater extent due to its higher hydrophobicity (Chu and Metcalfe, 2007) and greater environmental persistence (Higgins et al., 2011).

A decrease in influent TCC concentration on day 13 did not lead to any increase in removal efficiency implying that the removal efficiency was not only dependent on the concentration but also on the total amount of TCC fed to the column.

4.4.2.3 Evaluation of Triclocarban Removal Mechanisms in the Soil Column

It is hypothesized that both biodegradation and sorption were responsible for the removal of TCC in the soil column since these are the main removal mechanisms in SAT (Drewes, 2003). TCC sorption is an expected removal mechanism to occur in the soil column due to the properties of TCC, being high hydrophobicity, low solubility, high octanol-water partition coefficient (K_{ow}) and high soil adsorption coefficient (K_{oc}), which incline the compound to sorb onto soil and sediment particles (Heidler et al., 2006; Sapkota et al., 2007; Ying et al., 2007). Besides biodegradation (Gledhill, 1975) under aerobic conditions (Heidler et al., 2006; Ying et al., 2007; Snyder et al., 2010b), sorption onto sludge, inorganic particles and microbes (TCC-Consortium, 2002) have previously been identified as removal mechanisms for TCC in activated sludge plants (Heidler et al., 2006; Yu et al.,

2011). The contribution of sorption and biodegradation to TCC removal in the soil column were respectively assessed by measuring TCC concentrations on the sand in the soil column and evaluating coupled TCC and COD removal. A mass balance analysis was also carried out.

TCC Sorption onto Sand

TCC was extracted with acetone from sand sampled from the soil column at the 8 cm and 19 cm depths and analysed. Table 4.9 summarizes the mass of TCC sorbed on each gram of sand at 8 cm and 19 cm depths.

Table 4.9 TCC concentration in soil column sand

Time (days)	**TCC concentration (ng g^{-1} of sand)**	
	8 cm	**19 cm**
9	37.4	25.1
14	48.4	31.9
16	100.2	32.4

The results show that TCC was more concentrated in the upper layers of the sand than in the deeper layers indicating that the higher the TCC concentration in applied wastewater, the greater the sorption that would occur. This sorption behavior pertains in aquatic environments where under conditions of equilibrium, a linear relationship exists between the concentration of a contaminant in water and its concentration in soil. An increase in the contaminants concentration in the water therefore produces a corresponding constant increase in its concentration in the soil (Chiou and Kile, 2000). It is also observed from Table 4.9 that the sorbed

concentrations of TCC increased over time at all levels within the soil column, with the amount almost tripling to 100 ng g^{-1} at 8 cm in 7 days. The rate of increase was however slower in the deeper layers of the soil column. The lower amounts of TCC sorbed in the deeper layers of the soil column compared to that sorbed onto sand closer to the entrance of the soil column could be attributed to the lower concentrations available in the wastewater at that depth. The occurrence of sorption also has implications with regards to limitations on TCC bioavailability (Cha and Cupples, 2009; Wu et al., 2009). The degree of sorption to sand, besides directly reducing the TCC concentration remaining in the infiltrating wastewater, affects its movement and fate by reducing the level of concentrations in adjacent soil water thereby decreasing its exposure for biodegradation and further transport (Chiou and Kile, 2000; Snyder et al., 2010b).

The amount of sorption attainable in the soil column system would differ according to the composition of the soil (Yong et al., 1992). The transformation of TCC in the soil column is also greatly influenced by the soil properties and can vary significantly in soils with different properties (Kwon et al., 2010; Snyder et al., 2010a). It is probable therefore that enhanced TCC removal by sorption in the soil column system could be achieved if soil containing organic matter is used as the porous medium for infiltration of the wastewater (Wu et al., 2009), since contaminants, in addition to being adsorbed onto the surface of the mineral grains, partition into the matrix of the soil's organic matter (Chiou and Kile, 2000).

Effect of TCC on SAT

Before introduction of TCC into the influent wastewater, biological removal processes were efficient in the soil column. COD removal efficiency was good in the soil column reaching 70 % removal at 19 cm column depth. After the introduction of TCC into the influent wastewater, COD removal declined, rapidly falling to 19 % within 2 weeks as shown in Figure 4.31. Percentage removal at 8 cm also declined from 68.5 % to 15 % within the same number of days.

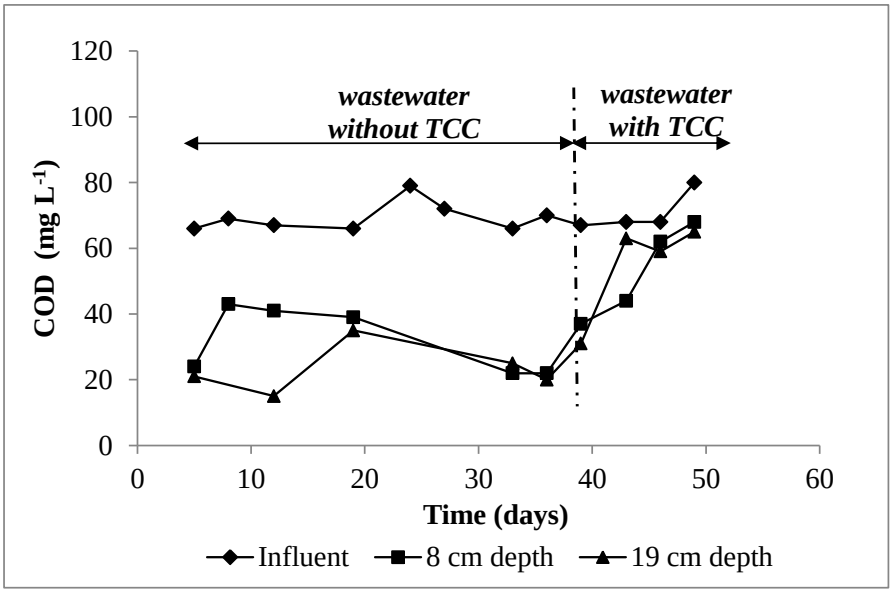

Figure 4.31 Effect of TCC addition on COD concentration in the soil column

The reduction in COD removal observed in this study upon application of TCC to the soil column suggests a negative impact on substrate utilization by the microbes in the sand, or even gradual death of some microbial populations. This is consistent with a study by Lawrence et al (2009), where TCC was found to significantly decrease the utilization of selected carbohydrates, carboxylic and amino acids by microbes. A change in the general and metabolic profile of the microbial community could also have occurred (Svenningsen et al., 2011), leading to the decreased COD

removal observed. With reference once again to TCS, environmental concentrations of triclosan (TCS) have also been found to have the potential to affect the biodegradation efficiency of wastewater percolation systems (Svenningsen et al., 2011). During Svenningsen et al's (2011) studies simulating onsite soil percolation systems for the disposal of septic tank effluents, microbial populations were found to decrease twenty two fold upon TCS exposure of 4 mg kg^{-1} of soil. The reduction in the TCC removal with a decline in COD removal confirms biodegradation as a TCC removal mechanism in the soil column. It is inferred from Snyder et al's (2010a) study that Gram negative bacteria were primarily responsible for TCC degradation in the soil column. This is because, in their study, no TCC degradation occurred upon inhibition of biodegradation with sodium azide (Snyder et al., 2010a), which is known to be acutely toxic to Gram negative bacteria whilst being less effective on Gram positive bacteria (Snyder and Lichstein, 1940; Sumbali and Mehrotra, 2009).

Given ample time however, the microbial populations in the soil column may recover from any negative impacts caused by TCC exposure through genetic mechanisms or the expansion of populations not affected by the antimicrobial (Lawrence et al., 2009). This could lead to a recovery of the soil column system with regards to TCC removal. Sustainable growth of TCC resistant Gram negative bacteria in the soil column such as the *Alcaligenaceae* family of bacteria, which are capable of utilizing TCC as their sole carbon source, is possible after persistent TCC exposure (Miller et al., 2010). Their presence in a SAT system would go a long way to promote a sustainable and long term removal of TCC from the infiltrating wastewater.

Mass Balance Analysis

In order to quantify the contribution of biodegradation to TCC removal, a TCC mass balance analysis was performed in the liquid phase of the soil column to account for all TCC losses occurring within the soil column. The amount of TCC in the aqueous phase determined from concentrations measured at the wastewater sampling points and that in the solid phase obtained from the soil column sorption soil tests were used for the analysis. The mass balance was carried out between the 8 cm and 19 cm depth. The mass balance analysis performed is illustrated in Figure 4.32 and summarized mathematically in the general form by Equation 4.13. C_8 is the TCC concentration measured at distance 8 cm from the influent end of the soil column, C_{19} is the TCC concentration measured at 19 cm and Q is the wastewater flow rate through the soil column. The total mass of TCC reaching the 19 cm depth was deducted from that leaching from the 8 cm depth. The amount of TCC that could not be accounted for after the total mass sorbed onto the sand between the depths was considered as the mass lost through biodegradation.

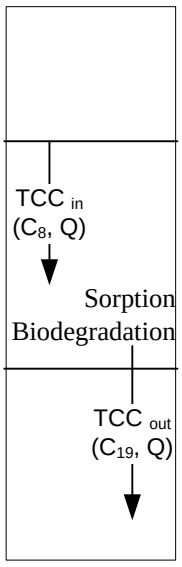

Figure 4.32 TCC mass balance in the soil column

TCC mass out

= TCC mass in - mass removed by sorption-mass biodegraded ……[4.13]

Thus the mass biodegraded is given by:

TCC mass biodegraded

= Total mass in - Total mass out-mass removed by sorption ……[4.14]

$$TCC\ total\ mass\ in = Q \times \sum_{i=1}^{i=n} (C_{8,i} \times t_i)$$

$$TCC\ total\ mass\ out = Q \times \sum_{i=1}^{i=n} (C_{19,i} \times t_i)$$

where *t* is the duration of TCC application and *i* represents the sampling number. The calculated TCC mass biodegraded was then expressed as a percentage of the mass in.

The analysis revealed that over the first 9 days, biodegradation accounted on the average for 56 % loss of the total mass of TCC applied. Removal by biodegradation dropped to about 19 % between day 10 and 14 and further down to 7 % at the end of day 16. The declining degree of biodegradation depicts unsustainable biological removal of TCC in the soil column, which coincides with a declining removal of COD. It is highly probable that the genera of microorganisms responsible for COD removal are the same as the ones responsible for TCC biodegradation. Since several steps are involved in the degradation of TCC (Miller et al., 2008) impedance of any of the steps of the degradation pathway would inadvertently result in lower biodegradation efficiency.

4.4.3 Conclusions

Results of this laboratory study confirm the ability of SAT to reduce TCC concentrations in wastewater. The removal efficiency was found to be dependent on concentration and decreased over time. Better removals are attainable with increased soil depth. Within the duration of the experimental run TCC seemed to adversely affect SAT performance indicated by reductions in COD removal efficiency.

Biodegradation and sorption were identified in these studies as mechanisms responsible for the removal of TCC from the wastewater. The amount of TCC sorbed onto the sand was found to be dependent on the TCC concentration of the wastewater applied, being larger at higher concentrations. Over time, TCC removal efficiency decreased substantially due to decreased microbial activity and sorption. Biodegradation, which has the capacity to be a sustainable treatment mechanism, was unsustainable in the soil column due to the reduced activity of the microorganisms in the column as evidenced by the continued drop in COD removal observed after application of TCC. As sorption was the predominant removal mechanism in the soil column tests following a reduction in microbial activity, the contaminant is simply immobilized and not transformed to any appreciable degree. Sorption has a finite capacity for removal of contaminants (NRC, 1994) due to a time dependent exhaustion of available sites for contaminant attachment. There is therefore the possibility in the long run for the soil in a SAT system to reach saturation with respect to TCC upon continued contaminant loading (Yong et al., 1992). The occurrence of this would result in the bulk of TCC in applied wastewater effluents being carried along with the wastewater effluent into the aquifer.

Further investigations are, however, needed to determine if the microbes in the soil column would eventually become acclimated to the presence of TCC, thereby generating better sustainability of the system with respect to removal efficiencies. Simulations would also be required under unsaturated conditions in longer soil columns or in systems employing longer hydraulic residence times to determine to what extent removal efficiencies can be improved.

CHAPTER 5

5 MODEL DEVELOPMENT

5.1 Introduction

In this chapter, the experimental data obtained for removal of chemical oxygen demand (COD) and triclocarban (TCC) under saturated conditions and estrogen removal under unsaturated soil conditions are modelled. COD removal is modelled based on its transport through the soil column by advection and dispersion. Regarding TCC and estrogen removal, the model is based on the development of empirical relations to suitably describe the treatment attained within the soil columns.

5.2 Model for Chemical Oxygen Demand Removal

The removal of COD through the 2 m long soil column was modelled by considering the soil column as a non-ideal plug flow reactor in which the fate of COD is controlled by the processes of advection, dispersion and biodegradation. The results used for the development of the model were the wastewater removal profiles obtained from the soil column when it was bioactive and after it had been sterilised. Data obtained under biotic conditions was used to determine the reaction rate and that from the abiotic experiments used to assess the sorption.

Assumptions

The assumptions made in the development of the model are:

i. Adsorption is quick and reaches equilibrium;

ii. Adsorption is linear;

iii. Flow is one dimensional;

iv. Steady state conditions are achieved.

5.2.1 Development of Fate Controlling Equations

To develop the model for the soil column, a COD mass balance was performed for a control volume V (L^3; cm^3) of cross sectional area A (L^2; cm^2) and elemental length Δl (L; cm). Let L (L; cm) be the length of the soil column, n the porosity, u (LT^{-1}; cm min^{-1}) the average linear velocity of wastewater flow in the soil column (pore water velocity) and D (L^2T^{-1}; cm^2 min^{-1}) the dispersion coefficient. The COD mass entering and leaving the control volume is depicted in Figure 5.1. The COD concentration is represented by C (ML^{-3}; mg L^{-1}).

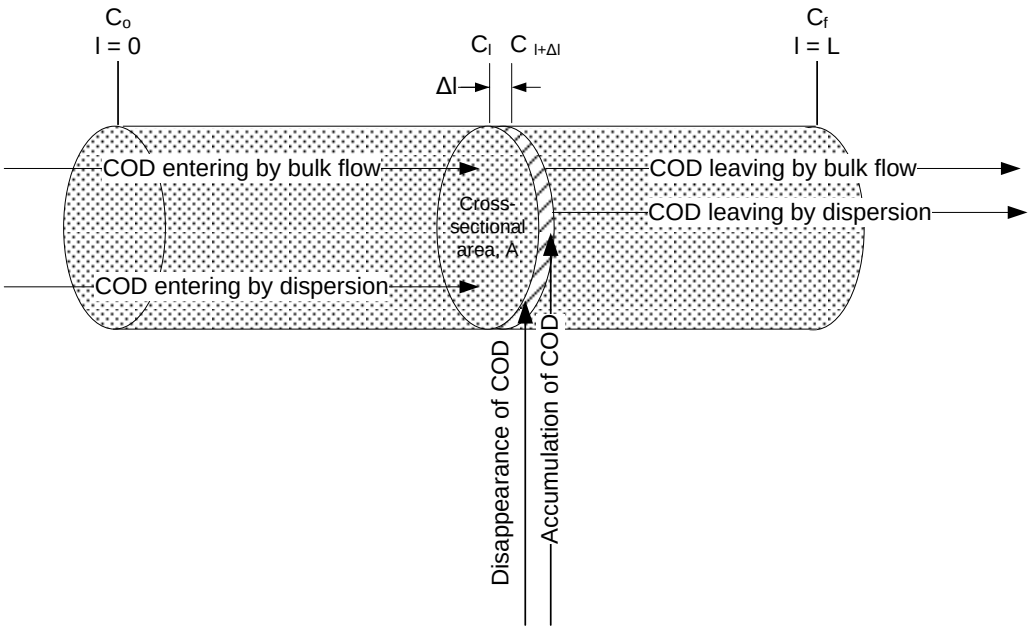

Figure 5.1 Schematic diagram of COD transport in the soil column controlled by advection, dispersion and reaction

For the control volume, a general expression for COD balance is (Levenspiel, 1999):

$$Input = Output + Disappearance + Accumulation$$

5.2.1.1 Mass Balance in the Liquid Phase

COD component entering by bulk flow

$$= n \times u \times A \times C_{l,\ t} \ldots\ldots\ldots\ldots\ldots\ldots [5.1]$$

COD component leaving by bulk flow

$$= n \times u \times A \times C_{l+\Delta l,\ t} \ldots\ldots\ldots\ldots\ldots\ldots [5.2]$$

COD component entering by axial dispersion

$$= \frac{dN}{dt} = -\left(n \times D \times A \times \frac{\partial C}{\partial l}\right)_{l,\ t} \ldots\ldots [5.3]$$

COD component leaving by axial dispersion

$$= \frac{dN}{dt} = -\left(n \times D \times A \times \frac{\partial C}{\partial l}\right)_{l+\Delta l,\ t} \ldots [5.4]$$

COD disappearance from the liquid phase would be due to reaction and also adsorption onto the soil grains. If V_l and V_s are the volumes of the liquid and solid phases respectively in the elemental slice Δl, r (T^{-1}; min^{-1}) is the rate of COD disappearance by reaction and r_s (T^{-1}; min^{-1}) is the rate of COD mass sorption per unit mass of the sand, then the:

COD component disappearing by reaction $= r \times V_l \times \Delta t$

$$= r \times n \times A \times \Delta l \times \Delta t \ldots\ldots\ldots [5.5]$$

COD component disappearing by sorption $= r_s \times \rho_s \times V_s \times \Delta t$

$$= r_s \times \rho_s \times (1 - n) \times A \times \Delta l \times \Delta t$$

where ρ_s (ML^{-3}) is the density of the sand particles.

Substituting for the bulk density, ρ_b (ML^{-3}) in the equation,

$$COD\ component\ disappearing\ by\ sorption = r_s \times \rho_b \times A \times \Delta l \times \Delta t \ldots\ldots\ldots\ldots [5.6]$$

where $\rho_b = \rho_s \times (1 - n)$.

$$COD\ Accumulation\ in\ liquid\ phase = n \times A \times \Delta l \times (C_{t+\Delta t,\, l} - C_{t,l}) \ldots\ldots\ldots\ldots\ldots [5.7]$$

The mass balance for the soil column in the liquid phase is given by (Levenspiel, 1999; Crittenden et al., 2005):

$$(In - Out)_{bulk\ flow} + (In - Out)_{axial\ dispersion} - Disappearance\ by\ reaction$$
$$- Disappearance\ by\ sorption = Accumulation \ldots\ldots\ldots\ldots [5.8]$$

Substituting Equations 5.1 to 5.7 into Equation 5.8,

$$(C_{l,t} \times u \times A \times n - C_{l+\Delta l,t} \times u \times A \times n)$$
$$+ \left(\left(-n \times D \times A \times \frac{\partial C}{\partial l}\right)_{l,t} - \left(-n \times D \times A \times \frac{\partial C}{\partial l}\right)_{l+\Delta l,\, t}\right)$$
$$- (r \times n \times A \times \Delta l \times \Delta t) - (r_s \times \rho_b \times A \times \Delta l \times \Delta t)$$
$$= n \times A \times \Delta l \times (C_{t+\Delta t,\, l} - C_{t,l})$$

Rearranging,

$$u \times A \times n\,(C_{l,\,t} - C_{l+\Delta l,\, t}) - D \times A \times n\left(\left(\frac{\partial C}{\partial l}\right)_{l,\,t} - \left(\frac{\partial C}{\partial l}\right)_{l+\Delta l,\, t}\right)$$
$$- (r \times n \times A \times \Delta l \times \Delta t) - (r_s \times \rho_b \times A \times \Delta l \times \Delta t)$$
$$= n \times A \times \Delta l \times (C_{t+\Delta t,\, l} - C_{t,l})$$

Dividing through by $n\ A\ \Delta l\ \Delta t$

$$\frac{u\,(C_{l,t} - C_{l+\Delta l,\, t})}{\Delta l\,\Delta t} - \frac{D\left(\left(\frac{\partial C}{l}\right)_{l,t} - \left(\frac{\partial C}{\partial l}\right)_{l+\Delta l,\, t}\right)}{\Delta l\,\Delta t} - r - \left(r_s \times \frac{\rho_b}{n}\right) = \frac{(C_{t+\Delta t,\, l} - C_{t,l})}{\Delta t}$$

Taking limits as $\Delta l \rightarrow 0$ and $\Delta t \rightarrow 0$ and rearranging,

$$\frac{\partial C}{\partial t} = D\frac{\partial^2 C}{\partial l^2} - u\frac{\partial C}{\partial l} - r - r_s\frac{\rho_b}{n}$$

Assuming linear equilibrium and that the adsorption follows the Freundlich isotherm,

$$r_s = \frac{\partial S}{\partial t} = K_d\frac{\partial C}{\partial t}$$

where S (MM^{-1}) is COD mass sorbed per unit mass of the sand.

Hence

$$\frac{\partial C}{\partial t} = D\frac{d^2 C}{dl^2} - u\frac{\partial C}{dl} - r - \frac{\rho_b}{n}K_d\frac{\partial C}{\partial t} \quad \text{.....[5.9]}$$

At steady state, the rate of COD accumulation in the liquid phase (Equation 5.7) will be zero. It is also recalled from the discussions in Chapter 4 Section 4.2.2.5 that COD concentration profiles obtained from the sterilised soil column indicated negligible reduction in COD and DOC. This showed that adsorption of COD was extremely minimal and therefore the COD component disappearing due to sorption can be neglected. Also, preliminary analysis of the soil column data (Section 4.2.6 of Chapter 4) to identify the reaction kinetics that pertained in the soil column for the removal of the wastewater, ignoring the effect of advection and dispersion, yielded a saturation type of reaction. Thus the rate of the reaction, *r,* is of the form:

$$r = \frac{k \times C}{K + C} \quad \text{.....[5.10]}$$

where k is the overall rate constant and K is the half saturation constant for the wastewater parameter under consideration (Tchobanoglous et al., 2003). Equation 5.10 is in the form of the Michaelis-Menten (M-M) function which defines enzyme

kinetics for a single substrate and reaction. Equations in the form of the M-M function can be used to represent kinetic reactions in wastewater treatment involving multi-substrates as well as mixed cultures (Benefield and Randall, 1980).

Equation 5.9 therefore becomes,

$$D\frac{\partial^2 C}{\partial l^2} - u\frac{\partial C}{\partial l} - \frac{k \times C}{K + C} = 0$$

Transforming the above equation into a dimensionless length scale by substituting $z = \frac{l}{L}$ and also substituting $\tau = \bar{t} = \frac{L}{u}$,

$$\frac{D}{uL}\frac{d^2C}{dz^2} - \frac{dC}{dz} - \frac{\tau k C}{K + C} = 0 \quad \text{.....[5.11]}$$

τ (T; min) is the soil column residence time.

It was evident from the experimental results carried out especially in the case of the high COD influents (HC conditions) that electron acceptor limitations were present in the soil column environment. As electron donors and electron acceptors are able to simultaneously limit the growth of microorganisms in soils and aquifers (Baveye and Valocchi, 1989) and consequently the removal efficiency of biodegradable contaminants, the modified Monod equations (Equations 5.12 a and 5.13 b) of Borden and Bedient (1986), which incorporate the influence of an electron donor during substrate utilization, were used to extend the basic biodegradation component of Equation 5.11.

$$\frac{dC}{dt} = -M_t h_u \left(\frac{C}{K_c + C}\right)\left(\frac{O}{K_o + O}\right) \quad \text{.....[5.12a]}$$

$$\frac{dO}{dt} = -M_t h_u F \left(\frac{C}{K_c + C}\right)\left(\frac{O}{K_o + O}\right) \quad \text{.....[5.12b]}$$

where:

C = concentration of organic material in pore fluid (ML^{-3})

O = concentration of oxygen in pore fluid (ML^{-3})

M_t = concentration of aerobic microorganisms (ML^{-3})

h_u = maximum rate of organic material utilization per unit mass of aerobic microorganisms (T^{-1})

K_c = half-saturation constant of the organic material (ML^{-3})

K_o = half-saturation constant of oxygen (ML^{-3})

F = ratio of oxygen to organic material consumed

In this case, the organic material is considered as the COD of the wastewater in the soil column. Equations 5.12 a and 5.12 b were further modified to suit the soil column data available by substituting $M_t h_u$ with k' (T^{-1}; min^{-1}) as an effective overall rate constant. The resulting equation for the model thus represents coupled advection-dispersion transport with biodegradation in the presence of an electron acceptor. The governing equations for the substrate and the electron acceptor are thus respectively:

$$\frac{1}{Pe}\frac{d^2C}{dz^2} - \frac{dC}{dz} - \tau k'\left(\frac{C}{K_c + C}\right)\left(\frac{O}{K_o + O}\right) = 0 \quad \text{.....[5.13a]}$$

$$\frac{1}{Pe}\frac{d^2O}{dz^2} - \frac{dO}{dz} - \tau k'F\left(\frac{C}{K_c + C}\right)\left(\frac{O}{K_o + O}\right) = 0 \quad \text{.....[5.13b]}$$

Here O represents the electron acceptors and Pe is the peclet number given by:

$$Pe = \frac{uL}{D}$$

and k' is the rate constant.

The differential equations of 5.13 were used to formulate a code in MATLAB based on the bvp4c solver function of the software (Mathworks, 2009).

5.2.1.2 Mass Balance in the Solid Phase

The mass balance in the solid phase would be ignored since COD adsorption was found to be negligible in the soil column.

5.2.2 Boundary Conditions

In order to solve the differential equations, boundary conditions were imposed at the entry and exit of the soil column. A closed-closed vessel boundary condition was assumed. Figure 5.2 shows the entry boundary at $l = 0$. To the immediate left of the entrance line, that is at $l = 0^-$, plug flow occurs and therefore there is no dispersion, likewise to the immediate right hand side of the column exit, that is at $l = L^+$. In-between these two closed points though, dispersion and reaction occur. N ($MT^{-1}L^{-2}$) is the mass flux of COD and Q (L^3T^{-1}) is the volumetric flow rate (Fogler, 1992).

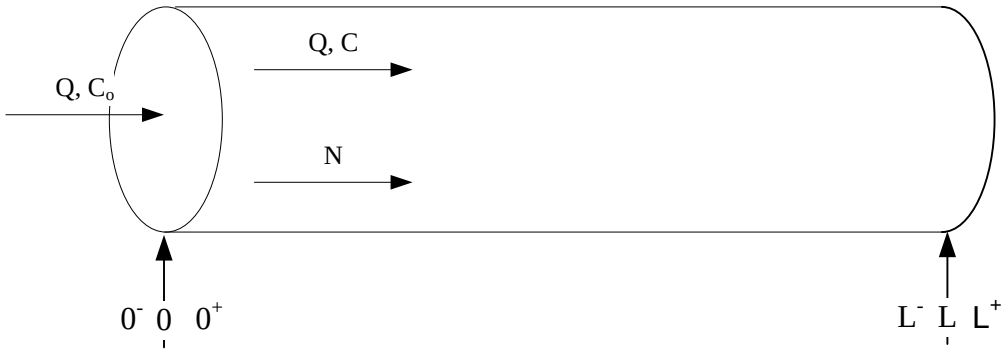

Figure 5.2 Schematic diagram of mass flow at entrance of soil column

Performing mass balance analysis at the entrance to the soil column, the boundary condition for the molar flow rate of COD, F_T is (Fogler, 1992; Said et al., 2007):

$$F_T(0^-, t) = F_T\left(0^+, t\right)$$

Thus

$$Q \times C_o = (Q \times C) + (A \times N) \quad \text{……[5.14]}$$

The axial dispersion of mass across the boundary is given by Fick's law:

$$N = -D \frac{dC}{dl} \quad \text{……..[5.15]}$$

Substituting Equation 5.15 into 5.14 and dividing through by the cross sectional area, *A*, and *Q* and rearranging,

$$C_o = C - \frac{D}{u} \frac{dC}{dl}$$

Casting the equation in dimensionless form:

$$\frac{1}{Pe} \frac{dx}{dz} = x - 1 \quad \text{……..[5.16]}$$

where

$$x = \frac{C}{C_o} \text{ and } z = \frac{l}{L}$$

At the soil column exit, the concentration gradient is zero as the concentration of substrate is continuous.

Thus at $z = 1$,

$$\frac{dx}{dz} = 0 \quad \text{……[5.17]}$$

The boundary conditions to be applied are therefore the Danckwerts boundary conditions:

$$\frac{dx}{dz} = Pe(x - 1) \qquad \textit{(entry boundary condition; z = 0)}$$

$$\frac{dx}{dz} = 0 \qquad \textit{(exit boundary condition; z =1)}$$

5.2.3 Estimation of COD Transport Parameters and Degradation Rate Constants

5.2.3.1 Hydraulic and Hydrodynamic Parameters

The values of the parameters D and τ were obtained from the soil column tracer tests, the results of which have been presented in Table 4.1 of Chapter 4.

5.2.3.2 Rate Constants

The kinetic constants, k' and K_c were obtained from the COD concentration profiles in the soil column. Since the fate of COD in the soil column is influenced by advection and dispersion in addition to biodegradation and biotransformation processes (Barry et al., 1993), the effect of two former processes could not be ignored. Due to the nonlinearity of the governing equations (Equations 5.13) k' and K_c could not be directly calculated. As a better approximation than considering the soil column system as a batch reactor, the derived equation (Equation 5.18) of Barry et al (1993) were used to obtain the values of the k' and K_c by nonlinear least squares minimization. This equation considers advection, dispersion and M-M biodegradation kinetics and is therefore suitable for use for the analysis of the soil column data. The influence of oxygen is neglected in this case.

$$0 = -l + \frac{u}{k}\left[g - C + K_c \ln\left(\frac{g}{C}\right)\right] + \frac{D}{u}\ln\left[\frac{g(K_c + C)}{C(K_c + g)}\right] \quad \text{.....[5.18]}$$

where C is the concentration of the substrate, l is the distance along the soil column and

$$g = C_o - \frac{Dk}{u^2}\,\frac{C_o - (D/u^2)\,f(C_o)}{[K_c + C_o - (D/u^2)f(C_o)][1 + Dk\,K_c/u^2(K_c + C_o)^2]}$$

where

$$f(C_o) = \frac{k \times C_o}{K_c + C_o}$$

The values of the kinetic rate constants estimated using batch analysis were used as the initial guess for the minimization. The rate constants obtained from the minimisation are summarised in Table 5.1. These values are different from others reported in literature because the characteristics of the waste undergoing treatment determines the value of the kinetic constants (Benefield and Randall, 1980).

Table 5.1 COD kinetic parameters estimated from soil column concentration profile

Parameter	***k* (min^{-1})**	***K_c* (dimensionless)**	***K_c* ($mg\ L^{-1}$)**
HC-5	0.002	0.8852	119
HC-10	0.0082	0.7876	104
HC-20	0.0221	0.7458	102

Dissolved oxygen saturation constant of 0.63 (5 mg L^{-1}) was used. This value was obtained from the analysis carried out in Section 4.2.6 to identify the kinetics of the reactions occurring in the soil column.

5.2.3.3 Ratio of Oxygen to Organic Material Consumed

In the soil column, since consumption of the three electron acceptors being dissolved oxygen, nitrate and sulphate were observed to occur simultaneously in the soil column, the ratio of oxygen to COD consumed, *F*, is redefined as the ratio of electron acceptors to COD consumed. *O* therefore represents the electron acceptors.

F was determined from the correlations made of COD mass removal rate with dissolved oxygen removal rate as the reciprocal of the slope of the curve (Figure 4.13 a of Chapter 4). To obtain a relation incorporating the role of sulphate and nitrate as electron donors during the COD biodegradation, correlations of sulphate removal rate and nitrate removal rate with dissolved oxygen were used to express these electron acceptors in terms of the dissolved oxygen. The curves have also already been presented in Chapter 4 as Figure 4.13 b. The sulphate, nitrate and dissolved oxygen correlations are:

$$Sulphate = 10.122 \times Dissolved\ oxygen$$

$$Nitrate = 0.2828 \times Dissolved\ oxygen$$

Using the half reactions for oxidation reduction processes that occur in groundwater, sulphate and nitrate were converted to the equivalent of oxygen (Freeze and Cherry, 1979). From these half reactions, the ratios of electrons that can be accepted by sulphate and nitrate to oxygen are 8/4 for $SO4^{2-}$/DO and 5/4 for NO^{3-}/DO. Summing up sulphate, nitrate and dissolved oxygen to obtain the total electron acceptor capacity in terms of dissolved oxygen therefore yields:

$$Sulphate + Nitrate + Oxygen$$

$$= \left((10.122 \times {}^{8}/_{4}) + (0.2828 \times {}^{5}/_{4}) + 1\right) \times Dissolved\ oxygen$$

Thus

$$\sum Electron\ acceptors = 21.6 \times Dissolved\ oxygen \quad \ldots\ldots\ldots\ldots [5.19]$$

A factor of 21.6 was therefore incorporated into Equation 5.13.

5.2.4 Modelling Results

Figures 5.3 to 5.5 show the fit of the model to the experimental data. The blue line indicates the modelled removal and predicts quite well the removal within the first 100 mm and the removal obtained after flow through the whole length of the soil column. At intermediate points within the soil column however, the fit was not very good. This could be due to factors such as fluctuations in the concentration of the COD and other wastewater parameters that occurred along the length of the soil column, disturbances generated in the soil column during wastewater sampling, approximations made during estimation of kinetic parameters for the model development and the conversion of sulphate and nitrate into an equivalent oxygen concentration. The code for the modelling, modified from Kierzenka (2010) is presented in Appendix D.

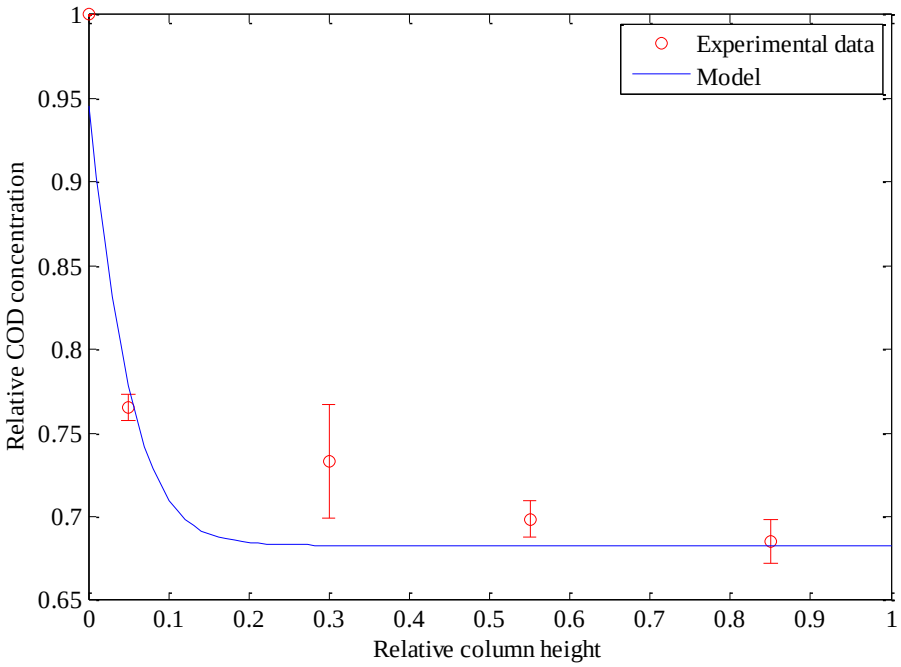

Figure 5.3 Modelled COD removal for an initial concentration of 136 mg L^{-1} applied at a HLR of 169 cm d^{-1}

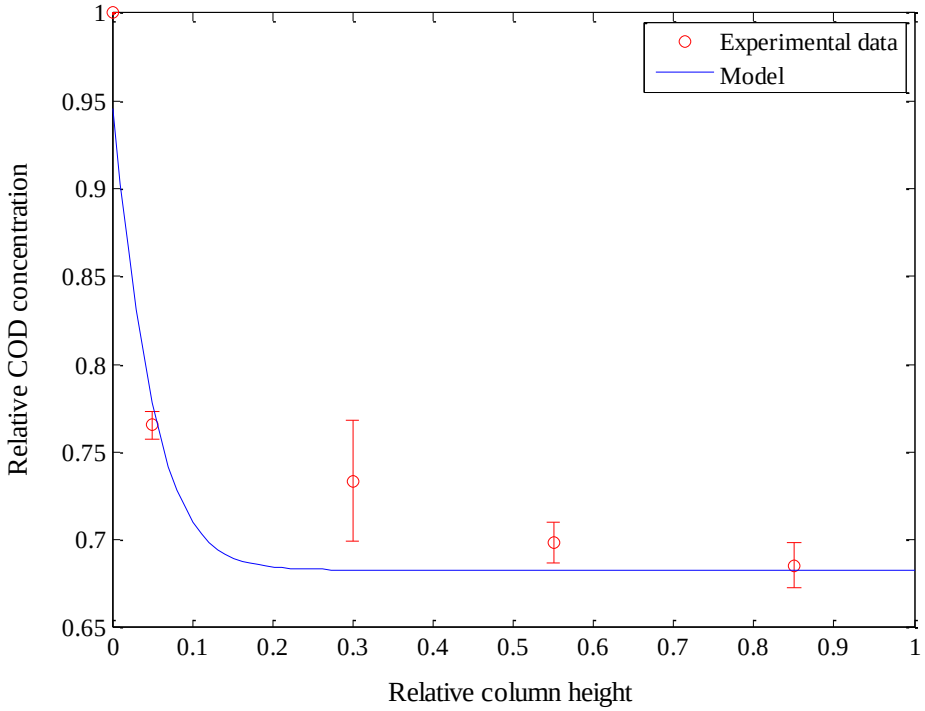

Figure 5.4 Modelled COD removal for an initial concentration of 136 mg L^{-1} applied at a HLR of 88 cm d^{-1}

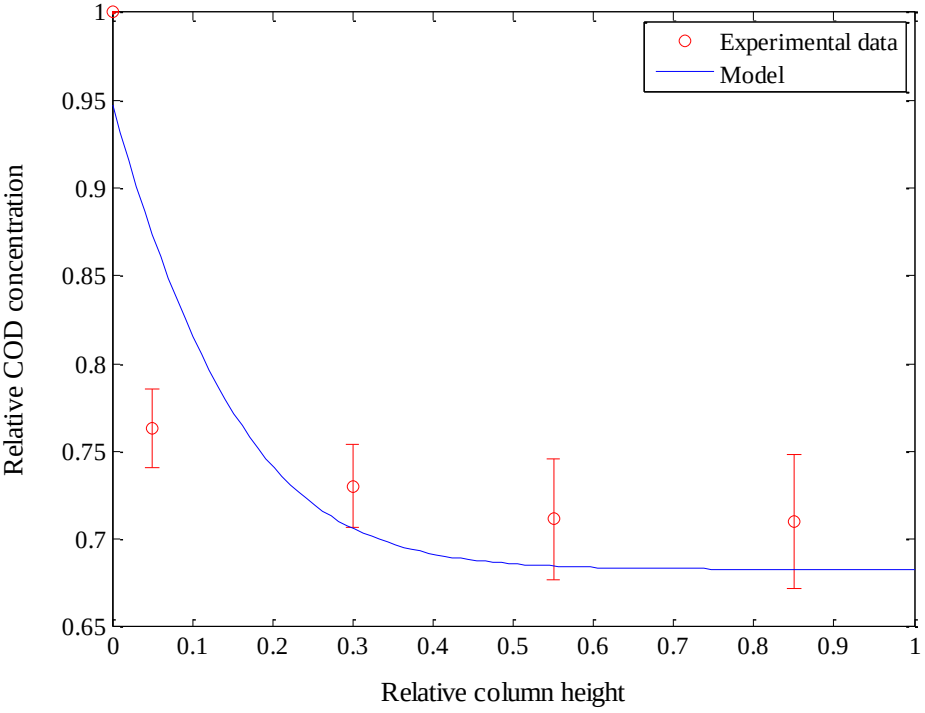

Figure 5.5 Modelled COD removal for an initial concentration of 136 mg L^{-1} applied at a HLR of 44 cm d^{-1}

5.3 Model for Triclocarban Removal

The aim of the model development was to find an expression relating the concentration of TCC in wastewater applied to the soil column and the concentration that would remain at any depth, l (L; cm), within the soil column. The model was developed using the following parameters from experiments carried out using the 300 mm soil column:

i. Influent TCC concentration, C_o (ML^{-3}; ng L^{-1});
ii. Hydraulic loading rate, q (LT^{-1}; cm d^{-1});
iii. Length of wastewater application, t (T; days);
iv. Concentration of TCC remaining at various depths within the soil column, C (ML^{-3}; ng L^{-1});
v. Soil column cross sectional area (A, cm^2).

The total cumulative mass of TCC, m_T (M; ng) applied to the soil column, since the start of application of TCC containing wastewater, on the respective sampling days (i.e. days 3, 7, 10 and 13) were calculated by multiplying the influent concentration by the hydraulic loading rate and the soil column's cross sectional area and summing up to obtain the cumulative mass for the required days. The fraction of TCC remaining in the wastewater (C/C_o) at the selected soil column depths (i.e. 8 cm, 19 cm and 30 cm) were correlated with the total TCC mass applied (see Figures 5.6 a – c). The slopes from Figures 5.6 a – c were then correlated with the sampling depths and the points fitted by regression analysis to obtain Figure 5.7. During the fitting process, trials were carried out with different functions, these being linear, logarithmic and power to obtain the best fit. The ease of manipulation of the

functions and the ability to obtain a good fit using the same function at all three depths were also taken into consideration.

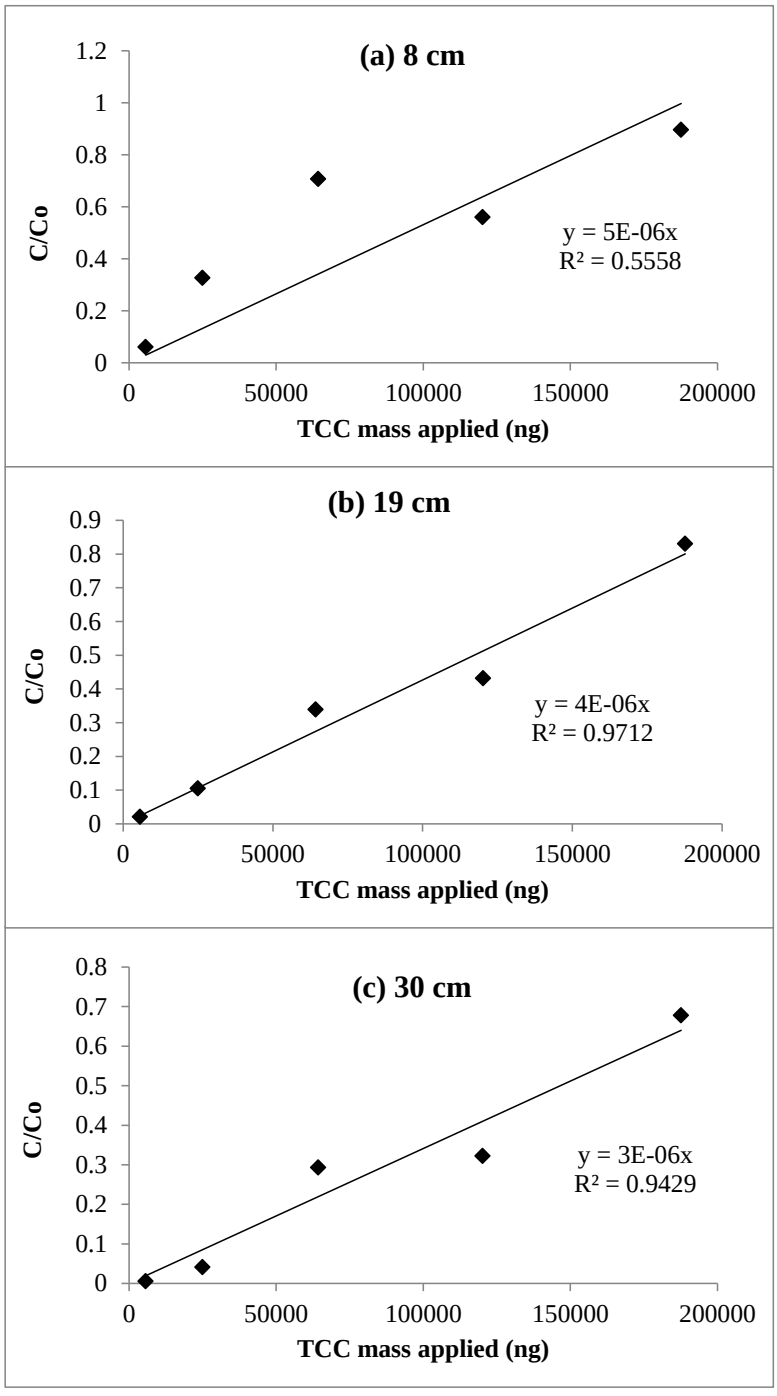

Figure 5.6 Fraction of TCC remaining against mass applied at various soil column depths

(a) 8 cm; (b) 19 cm; (c) 30 cm

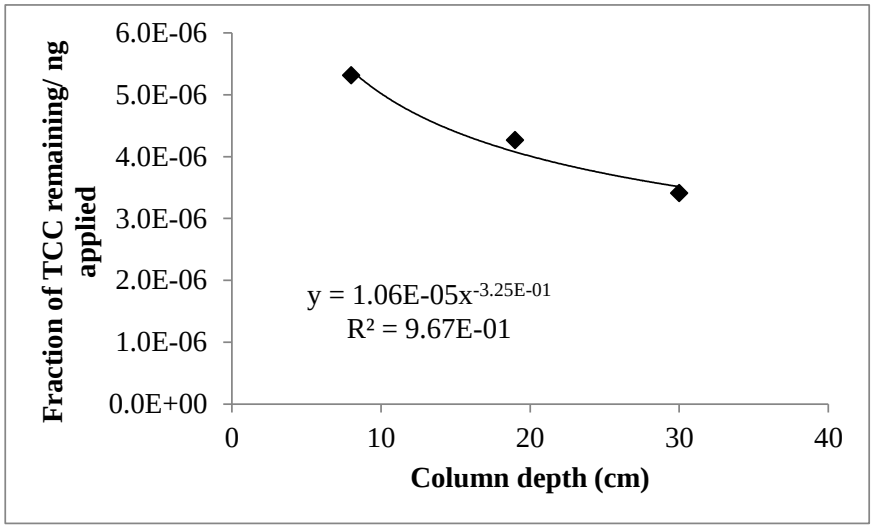

Figure 5.7 Fraction of TCC remaining per mass applied against soil column depth

From Figures 5.6 a – c the relation between the fractions of TCC remaining at any depth within the column and the cumulative mass applied can best be described in general form by Equation 5.20.

$$y = s \times m_T \quad \text{.....[5.20]}$$

where *s* is the slope of Figure 5.6 and

$$y = \frac{C_i}{C_{o_i}} \quad \text{.....[5.21]}$$

Considering that for each application cycle T_i of duration *t, where i =1,2,3,…n,* an influent TCC concentration of C_o is applied over the cross sectional area of the soil column, the total cumulative mass of TCC, m_T, applied to the soil column would be given by:

$$m_T = q \times A \left[\left(\sum_{T_1=1}^{T_1=t} C_{o_1} \times t \right) + \left(\sum_{T_2=1}^{T_2=t} C_{o_2} \times t \right) + \ldots\ldots\ldots \left(\sum_{T_n=1}^{T_n=t} C_{o_n} \times t \right) \right] \times 10^{-3} \quad \text{.....[5.22]}$$

Substituting the symbol *s* for *y* in the equation of the curve of Figure 5.7 gives the relationship as

$$s = 0.00001061 \times l^{-0.325} \quad \text{[5.23]}$$

For any application cycle, *T*, further substitution of Equations 5.21, 5.22 and 5.23 into Equation 5.20 yields:

$$\frac{C_n}{C_{o_n}} = 1.061 \times 10^{-5} \times l^{-0.325} \times q \times A \left[\left(\sum_{T_1=1}^{T_1=t} C_{o_1} \times t \right) + \left(\sum_{T_2=1}^{T_2=t} C_{o_2} \times t \right) \ldots \left(\sum_{T_n=1}^{T_n=t} C_{o_n} \times t \right) \right] \times 10^{-3}$$

……[5.24]

Rearranging the above expression, the concentration of TCC at any depth *l* within the soil column can be expressed as:

$$C_n = 1.061 \times l^{-0.325} \times q \times A \times C_{o_n} \left[\left(\sum_{T_1=1}^{T_1=t} C_{o_1} \times t \right) + \left(\sum_{T_2=1}^{T_2=t} C_{o_2} \times t \right) \ldots \left(\sum_{T_n=1}^{T_n=t} C_{o_n} \times t \right) \right] \times 10^{-8}$$

……[5.25]

Substituting for the soil column diameter in Equation 5.25 yields

$$C_n = 8.335 \times l^{-0.325} \times q \times d^2 \times C_{o_n} \left[\left(\sum_{T_1=1}^{T_1=t} C_{o_1} \times t \right) + \left(\sum_{T_2=1}^{T_2=t} C_{o_2} \times t \right) \ldots \left(\sum_{T_n=1}^{T_n=t} C_{o_n} \times t \right) \right] \times 10^{-9}$$

……[5.26]

where *d* is the internal diameter of the soil column.

Thus for the soil column,

$$C(l) = f(C_o, q, t, d, l) \quad \text{[5.27]}$$

The model was tested using TCC concentrations applied in the laboratory and the predicted concentrations compared against the measured TCC concentrations. Figure 5.8 shows the closeness of fit of the model to the measured concentrations.

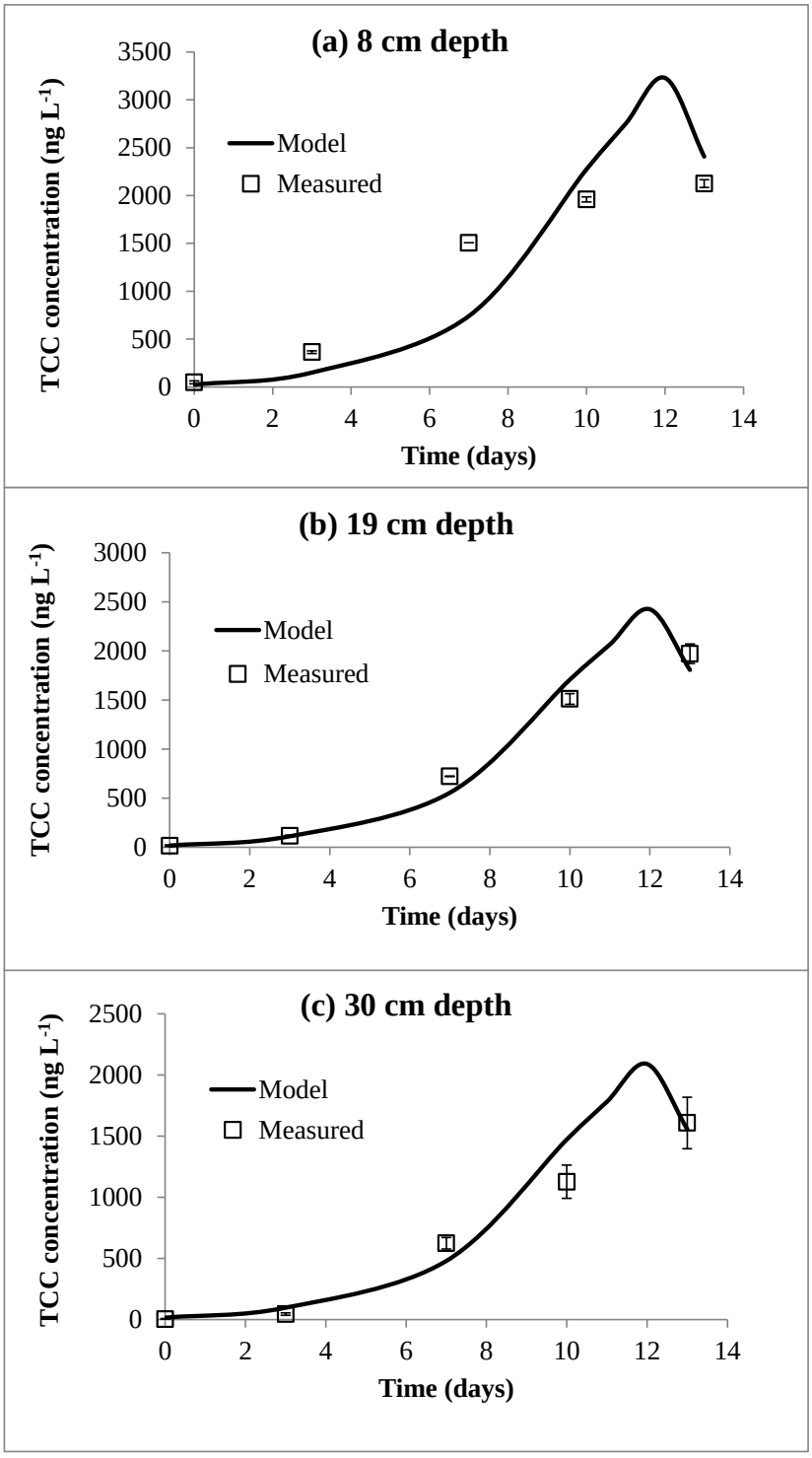

Figure 5.8 Comparison of model predicted TCC concentrations to measured concentrations at various depths

(a) 8 cm; (b) 19 cm; (c) 30 cm

Deviations are apparent between the model and the experimental data. These were smallest at the 19cm depth where the R^2 value was closest to unity. Reasons for deviations between the model predictions and the experimental data include the fitting of experimental data to linear and power functions which for the 8 cm depth did not give a very good coefficient of determination. Experimental data is also subject to errors during the sample preparation and analytical stages even though great efforts were made to minimise their occurrence. Calculated percentage errors between the predicted and the measured values are given in Table 5.2.

Table 5.2 Percentage errors between predicted and measured TCC concentrations

Sampling Depth (cm)	**Percentage error**	
	Average	**Standard deviation**
8	38	21.4
19	11	7.3
30	19	14.2

By the model predictions, it is possible to obtain higher TCC concentrations in the effluent than in the influent wastewater upon continuous infiltration over time. This is a reasonable prediction because TCC was found to have a negative impact on biodegradation in the soil column over time and as sorption alone is a not a sustainable removal mechanism, leaching of TCC from the soil over continuous TCC infiltration is a very likely occurrence.

5.4 Model for 17α-Ethinylestradiol (EE2) Removal under Unsaturated Conditions

The model development involved the determination of a relationship between the fraction of EE2 remaining at any depth in the soil column (C/C_o) and the height of water table. Variables for the development of the model are the height of water table, which dictates the depth of the unsaturated zone, and the travel distance of EE2 through the soil profile, which is controlled by the wastewater sampling depth.

For each height of water table (WT 75, WT 500 and WT 800) investigated in the laboratory, the EE2 concentrations, C (ML^{-3}; ng L^{-1}) along the soil column were expressed as a fraction of the influent concentration C_o (ML^{-3}; ng L^{-1}). The fractions obtained were plotted against the soil column depth, l (L; mm), and the points fitted by regression analysis. The resulting plots are shown in Figures 5.9 a – c. The slopes from each figure were then plotted against the corresponding thickness of unsaturated zone, h (L; mm) as shown in Figure 5.9 d.

Describing the relationship between C/C_o and soil column depth (Figure 5.9 a – c) by the general expression

$$y = (s \times l) + 1 \quad \text{……..……..[5.28]}$$

where s represents the slope of Figure 5.9, and substituting C/C_o for y yields

$$\frac{C}{C_o} = (s \times l) + 1 \quad \text{……....[5.29]}$$

An expression for the variation of s with the thickness of the unsaturated zone was obtained from the correlation curve of Figure 5.9 d, i.e.

$$s = -0.000137 \ln(h) - 0.000157 \quad \text{…….……[5.30]}$$

Substituting Equation 5.30 into 5.29 yields

$$\frac{C}{C_o} = (-0.000137\ln(h) - 0.000157) \times l + 1 \quad \text{.....[5.31]}$$

Rearranging,

$$\frac{C}{C_o} = 1 - (0.000137\ln(h) + 0.000157) \times l \quad \text{.....[5.32]}$$

The concentration at any depth can therefore be determined from Equation 5.33.

$$C = C_o \times [1 - (0.000137\ln(h) + 0.000157) \times l] \quad \text{.....[5.33]}$$

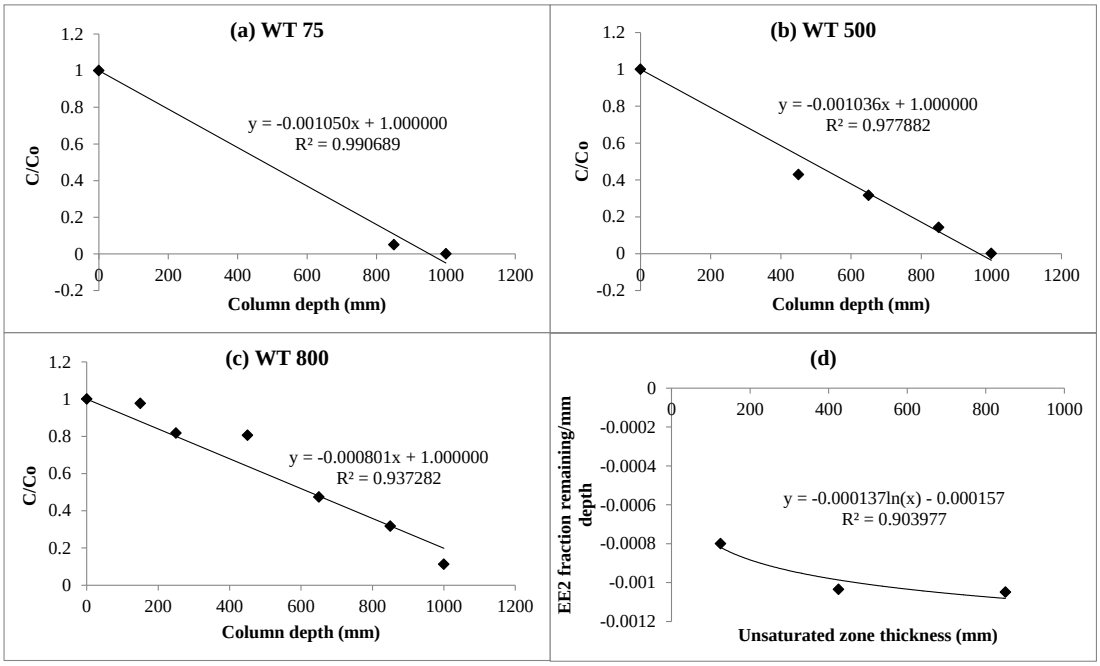

Figure 5.9 EE2 removal against soil column height in the unsaturated soil column at various water table heights

(a) WT75 (b) WT 500 (c) WT 800 (d) EE2 fraction remaining per length of wastewater travel against unsaturated zone thickness

Figure 5.10 shows the closeness of fit between the model and measured EE2 soil column concentrations. Percentage errors of the model from the experimental data are summarised in Table 5.3. Percentage errors for soil column depth of 1000 mm

for WT 75 and WT 500 were not determined (ND) because no EE2 was detected in the effluent and therefore C/C_o for the experimental data was zero.

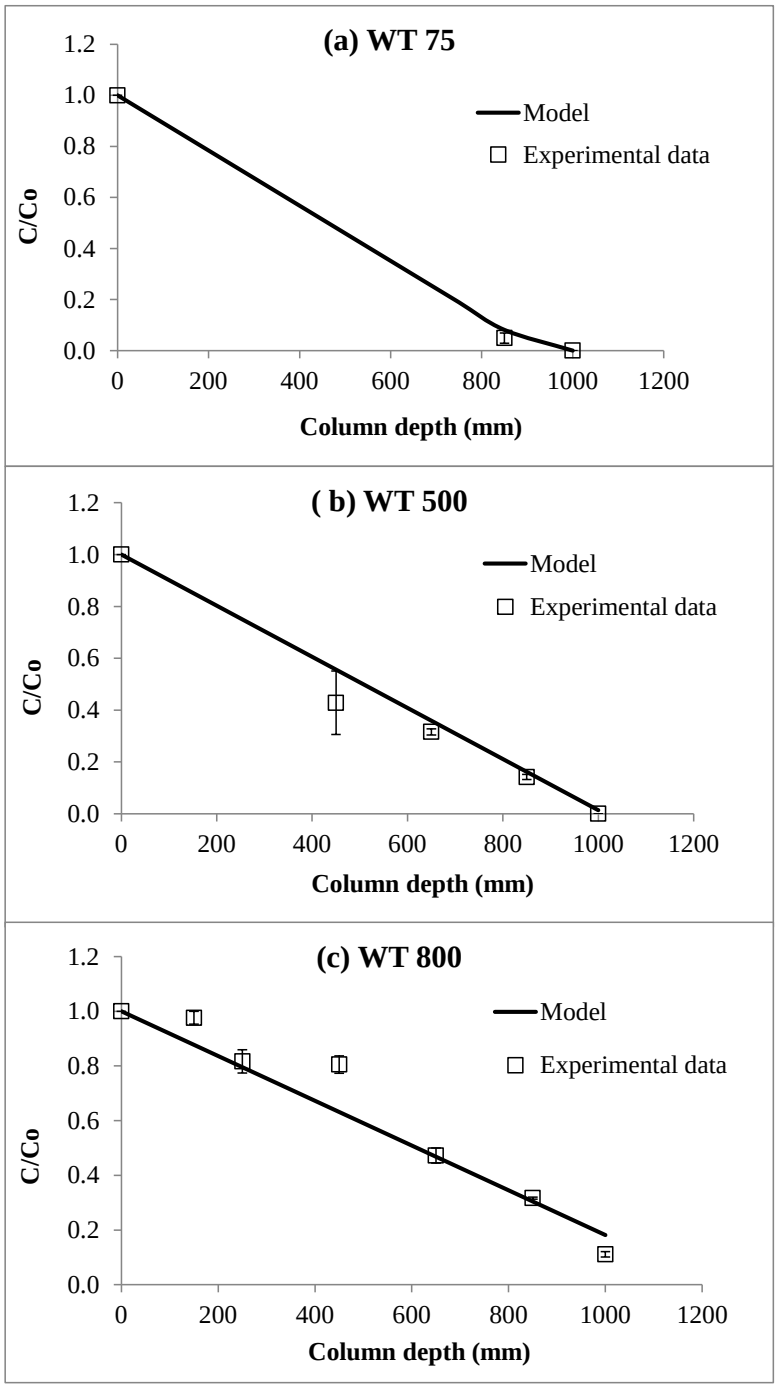

Figure 5.10 Modelled and experimental data for EE2 removal against soil column depth at various water table heights

(a) WT 75 (b) WT 500 (c) WT 800

Table 5.3 Percentage errors between predicted and measured EE2 concentrations

Soil column depth (mm)	**Percentage error**		
	WT75	**WT 500**	**WT 800**
0	0	0	0
150			-10
250			-3
450		30	-22
650		14	-1
850	65	14	-4
1000	ND	ND	63
Average % error	**33**	**14**	**3**
Standard deviation	**46**	**12**	**27**

5.5 Conclusions

Experimental data from all three soil column experiments regarding COD, TCC and EE2 removal have been modelled with satisfactory accuracy. Within the scope of the research, the models developed have not been extended to the validation stages. It is recognised that the models developed for EE2 and TCC removal need verification using external data. However the models were not validated because of the unavailability of sufficient experimental data. Field tests could not be carried out to obtain data for this purpose. Suitable data giving soil column profiles was also not obtainable from literature. It should also be noted data used to develop the models were obtained by wastewater infiltration through silica sand and not real soil. The

models in their current state are therefore not directly applicable to SAT in the field. They however successfully identify the parameters influencing the fate of EE2 and of TCC. Validation of these models could therefore constitute an item for further study.

CHAPTER 6

6 CONCLUSIONS AND RECOMMENDATIONS

6.1 Conclusions

The removal of COD, BOD, DOC, nitrogen, phosphate, the estrogens E1, E2 and EE2, and the PPCP triclocarban during simulated soil aquifer treatment were studied under different experimental conditions.

6.1.1 Removal of Chemical Oxygen Demand, Biochemical Oxygen Demand, Dissolved Organic Carbon, Nitrogen and Phosphate

The removal of COD, BOD, DOC, nitrogen and phosphate were studied under different combinations of hydraulic loading rates and organic loading rates in a saturated soil column of length 2 meters. Under all experimental conditions investigated, being different mass loadings obtained by varying the hydraulic and organic loading rates applied, a greater proportion of the removal/ transformation of COD, BOD, DOC and nitrogen occurred within the first 100 mm of the soil column. For example for the highest COD mass loading of 3 553 mg d^{-1} (experimental condition HC-20), out of the total removal efficiency of 29 %, 28 %, 53 % obtained for COD, BOD, DOC respectively, 23.5 %, 23 % and 42 % was removed within this depth. 66 % of the total organic nitrogen removal of 76 % could also be accounted for within the first 100 mm. This pattern of removal could be attributed to the microbial concentration profile within the soil column. Abiotic studies carried out in the soil column resulted in negligible removal of COD and DOC and therefore pointed to biodegradation as the main removal mechanism in the soil column.

Dissolved oxygen, nitrate and sulphate all acted as electron acceptors in the soil column. Aerobic degradation, anoxic degradation (denitrification) and anaerobic degradation (sulphate reduction) processes were therefore all found to be responsible for the biodegradation of the organic matter in the soil column, anaerobic degradation reducing with a reduction in the influent wastewater concentration. Relatively high DO to DOC, COD and BOD mass loadings were found to improve the efficiency of the removal process. The availability of dissolved oxygen as well as the rate of its replenishment to the soil column with the infiltrating wastewater therefore had a notable influence on the removal process in the soil column.

Higher mass removal rates of COD, DOC and BOD occurred at higher mass loadings rates, however at approximately the same mass loading, the removal efficiency was better when the mass applied had a lower COD concentration. On equivalent mass loading basis, a comparison of the removal efficiencies obtained for experimental condition HC-5 against condition LC-20, and HC-10 against MC-20 revealed that within the range of mass loadings investigated a strategy for improving removal efficiencies of COD, BOD and DOC in the saturated zone of SAT systems would be to lower the influent COD concentrations, not increase the contact time of the wastewater with the soil matrix. On the other hand, high concentrations and long residence times would improve nitrogen removal. Even though SAT has been previously reported as capable of performing better with primary effluents with regards to removal efficiency (Bouwer and Rice, 1984), under limiting dissolved oxygen conditions such as pertains in the saturated zone, the application of low concentration effluents through high permeability soils would achieve better removal efficiencies than infiltrating a relatively higher concentrated effluent through soils of

low permeability which allow for longer residence times. As these studies were carried out with wastewater of COD higher than that normally applied in SAT systems, this conclusion cannot be applied with certainty to very low concentrations of effluents.

With regards to phosphate, its removal was poor in the soil column and was dependent on the hydraulic loading rate, improving with a lowering of the hydraulic loading rate and therefore increased contact time with the soil matrix.

6.1.2 Removal of Estrogens

E1, E2 and EE2 removal were studied in 1 meter long soil columns under saturated and unsaturated soil conditions. The effects of the length of travel through the unsaturated zone, the hydraulic loading rate, DOC concentration and soil type on the removal efficiency of E1, E2 and EE2 were investigated. Silica sand and a soil mix constituting 65 % silica sand, 25 % silt and 10 % clay were used as packing material in the saturated soil columns.

Under all experimental conditions investigated, E2 was found to have the highest removal efficiency. This is due to its amenability to biodegradation and its ease of transformation to E1. Under saturated conditions, the concentration of E1 initially increased in the soil column before being removed. Increase in E1 concentrations in the columns were attributed to the transformation of E2 and EE2 to E1. Due to the high increases in E1 concentrations in the soil column, it had the lowest removal efficiency compared to E2 and EE2. Increases in E2 and EE2 were also apparent in the silica sand soil column, the increase in E2 being the result of transformation of

E1 to E2. It was unknown what contributed to EE2 increase in the silica sand but it may be possible that some portion of the EE2 infiltrated into the soil column was in the form of conjugates, having formed conjugates with sulphate in the wastewater influent tank. These conjugates may then have been deconjugated into the free forms leading to the observed increase in EE2 concentration. Overall removal efficiencies for E1, E2 and EE2 and a HLR of 81.5 cm d^{-1} and a DOC of 17 mg L^{-1} were 43 %, 77 % and 59 % respectively.

Increases in E2 and EE2 concentrations did not occur in the soil column containing the soil mixture and increases in E1 concentration were also smaller as a result of stronger sorption of the estrogens onto the soil due to the presence of clay. There was therefore less bioavailability of the estrogens and less transformation occurred. Less biotransformation was also due to the lower concentrations in the soil column. E1, E2 and EE2 removal efficiencies through the 1-meter length of soil column were 33 %, 83 % and 61 % respectively.

Investigations carried out into the effect of HLR on estrogen removal showed that doubling the HLR led to lower removal efficiencies of the estrogens. Increasing influent DOC concentration on the other hand had a positive effect on estrogen removal. The presence of silt and clay was also found to enhance the removal of E2 and EE2 in the soil column.

Studies carried out under unsaturated soil conditions revealed that the soil column was capable of removing all E1 and E2 and 94 % of EE2 after travel through 850 mm of unsaturated soil. Varying the length of travel through the unsaturated zone by

raising the water table showed that deeper unsaturated zones favoured the removal of the estrogens. The efficiency of SAT for E1, E2 and EE2 removal was therefore found to be dependent on the depth of the unsaturated zone with the removal process being more efficient in unsaturated soil and low soil water content.

6.1.3 Removal of Triclocarban

The removal of triclocarban was studied in a 300 mm soil column under saturated soil conditions. The removal mechanisms involved in TCC removal were biodegradation and sorption. Results from the study confirmed the ability of SAT to reduce the concentration of TCC in wastewater effluents, even though removal efficiencies decreased substantially after continuous TCC infiltration over time as a result of decreased microbial activity and sorption. The removal ranged from 99.5 % at the beginning of the experimental run to 32 % after two weeks of infiltration.

In the soil column, TCC removal increased with depth of infiltration through the soil profile and its removal efficiency was also found to be influenced by the applied concentration, decreasing with increase in influent concentration. Greater TCC sorption occurred in the shallow soil layers of the soil and at higher applied concentrations.

Within the duration of the studies, TCC had a negative impact on the efficiency of SAT, evidenced by a drop in COD removal in the soil column, which coincided with the drop in TCC removal. As indicated by the results of this study, there is a high probability of TCC affecting microbial populations and their metabolic mechanisms for the effective reduction of chemical oxygen demand in infiltrating wastewater

effluents during SAT. Unsustainable biodegradation during SAT increases the risk of TCC pollution of groundwater aquifers since sorption cannot be fully depended on as the sole removal mechanism. However as the soil column was operated for a limited period of time, further studies would be required to confirm this, since there is the possibility that given time the microorganisms could become adapted to the TCC environment and biodegradation would once again become sustainable.

6.1.4 Modelling

COD removal through the 2 meter long soil column was modelled using the advection dispersion equation and coupled Monod kinetics. Empirical models were also developed for EE2 removal as a function of the length of travel through the unsaturated zone, and for TCC removal. For TCC and EE2, the models predicted the removal profiles well. There is however the need for validation of these models.

6.2 Recommendations

The following are recommendations made for further studies.

Investigations into the increase in EE2 concentrations in saturated silica sand during infiltration are needed. This could involve soil column studies with the identification of all E1, E2 and EE2 metabolites formed during infiltration through soil. Further controlled laboratory studies are required on EE2 to determine all transformation products under different redox conditions in different soil matrices.

Further studies are also required on the transport of TCC during SAT. The identification of microorganisms indigenous to municipal wastewater and ubiquitous in SAT systems would be a step in the right direction for the development of strategies to minimise the risk of pollution of aquifers with TCC and help boost public confidence in recycled water from SAT systems. In line with the research carried out, TCC removal should be studied further over a longer duration of time in longer soil columns simulating longer residence times and also with different soils. Simulations would also be required under unsaturated conditions. These include investigating the impact of water table conditions on the transport of TCC.

The presence of several contaminants of emerging concern (CEC) in surface water and even in drinking water supplies necessitates the intensive study of their transport during SAT. With the development of new chemical products including pharmaceutical and personal care products, the routine testing of waters for only conventional wastewater parameters is no longer enough. Future research should focus more on the fate of CEC in infiltration waters. The development of more sophisticated analytical instruments and techniques that allow the identification of any CEC at any concentration in effluents without the need for rigorous sample preparation is needed. These analytical techniques should be developed in such a way as to identify all chemical and biological transformation products generated during passage of these CECs through the soil profile and also any foreign CEC that appear at the infiltration water. Transformation products should be identified and their effects and toxicity on humans assessed since the elimination of a particular CEC does not render the water devoid of it as it could have been transformed into other products that may even be more harmful than the parent CEC. These studies

are important if in the near future soil aquifer treatment is to play a major role in the recharge of aquifers for potable use.

The release and transport of arsenic during SAT could be investigated under varying water table conditions and redox potentials since factors affecting arsenic mobilisation include the redox potential of its environment (Charlet et al., 2011).

Studies are also needed on the applicability of waste stabilisation pond effluents to SAT systems. Techniques are needed to allow the infiltration of the effluents during SAT with minimal clogging by algae from maturation ponds. These studies are important for the coupling of these two low cost wastewater treatment technologies for water reuse. This would be very beneficial in developing countries where the use of low cost and low technology wastewater treatment options is prudent.

The models developed herein need to be validated and more laboratory and field tests could be carried out to obtain the required data.

REFERENCES

ADLERCREUTZ, H. & JÄRVENPÄÄ, P. (1982) Assay of estrogens in human feces. *Journal of Steroid Biochemistry,* 17**,** 639-645.

AIKEN, G. R. (2002) Organic matter in groundwater. In AIKEN, G. R. & KUNIANSKY, E. L. (Eds.) *Proceedings of the Artificial Recharge Workshop.* Sacramento, CA.

ALLINSON, M., SHIRAISHI, F., SALZMAN, S. & ALLINSON, G. (2010) In vitro and immunological assessment of the estrogenic activity and concentrations of 17β-estradiol, estrone, and ethinyl estradiol in treated effluent from 45 wastewater treatment plants in Victoria, Australia. *Archives of Environmental Contamination and Toxicology,* 58**,** 576-586.

AMIRI, F., BÖRNICK, H. & WORCH, E. (2005) Sorption of phenols onto sandy aquifer material: the effect of dissolved organic matter (DOM). *Water Research,* 39**,** 933 - 941.

AMY, G. & DREWES, J. (2007) Soil aquifer treatment (SAT) as a natural and sustainable wastewater reclamation/reuse technology: Fate of wastewater effluent organic Matter (EfoM) and trace organic compounds. *Environmental Monitoring and Assessment,* 129**,** 19-26.

AMY, G., WILSON, G. L., CONROY, A., CHAHBANDOUR, J., ZHAI, W. & SIDDIQUI, M. (1993) Fate of chlorination byproducts and nitrogen species during effluent recharge and soil aquifer treatment (SAT). *Water Environment Research,* 65**,** 726-734.

APPELO, C. A. J. & POSTMA, D. (1994) *Geochemistry, Groundwater and Pollution,* Rotterdam, A.A. Balkema.

ARCAND-HOY, L. D., NIMROD, A. C. & BENSON, W. H. (1998) Endocrine-modulating substances in the environment: estrogenic effects of pharmaceutical products. *International Journal of Toxicology,* 17**,** 139-158.

ARNON, S., DAHAN, O., ELHANANY, S., COHEN, K., PANKRATOV, I., GROSS, A., RONEN, Z., BARAM, S. & SHORE, L. S. (2008) Transport of testosterone and estrogen from dairy-farm waste lagoons to groundwater. *Environmental Science & Technology,* 42**,** 5521-5526.

ARVIN, E. & KRISTENSEN, G. H. (1983) Phosphate precipitation in biofilms and flocs. *Water Science and Technology,* 15**,** 65-85.

ARYE, G., DROR, I. & BERKOWITZ, B. (2011) Fate and transport of carbamazepine in soil aquifer treatment (SAT) infiltration basin soils. *Chemosphere,* 82**,** 244-52.

ASANO, T. (1985) *Artificial Recharge of Groundwater,* Stoneham, MA, Butterworth Publishers.

ASANO, T. & COTRUVO, J. A. (2004) Groundwater recharge with reclaimed municipal wastewater: health and regulatory considerations. *Water Research,* 38**,** 1941-1951.

AWWA (1998) Soil Treatability Pilot Studies to Design and Model Soil Aquifer Treatment Systems. AWWA Research Foundation, USA.

BALI, M., GUEDDARI, M. & BOUKCHINA, R. (2010) Treatment of secondary wastewater effluents by infiltration percolation. *Desalination,* 258**,** 1-4.

BARONTI, C., CURINI, R., D'ASCENZO, G., DI CORCIA, A., GENTILI, A. & SAMPERI, R. (2000) Monitoring natural and synthetic estrogens at activated sludge sewage treatment plants and in a receiving river water. *Environmental Science & Technology,* 34**,** 5059-5066.

BARRY, D. A., PARLANGE, J. Y. & HENSLEY, P. J. (1993) Calculation of kinetic rate constants from steady-state soil profile concentration measurements. *International Journal for Numerical and Analytical Methods in Geomechanics,* 17**,** 243-254.

BATEMAN, E. J. & BAGGS, E. M. (2005) Contributions of nitrification and denitrification to N_2O emissions from soils at different water-filled pore space. *Biology and Fertility of Soils,* 41**,** 379-388.

BAVEYE, P. & VALOCCHI, A. (1989) An evaluation of mathematical models of the transport of biologically reacting solutes in saturated soils and aquifers. *Water Resources Research,* 25**,** 1413-1421.

BDOUR, A. N., HAMDI, M. R. & TARAWNEH, Z. (2009) Perspectives on sustainable wastewater treatment technologies and reuse options in the urban areas of the Mediterranean region. *Desalination,* 237**,** 162-174.

BEAR, J. (1972) *Dynamics of Fluids in Porous Media,* New York, American Elservier Publishing Company, Inc.

BELSER, L. W. (1979) Population Ecology of Nitrifying Bacteria. *Annual Review of Microbiology,* 33**,** 309-333.

BENEFIELD, L. D. & RANDALL, C. W. (1980) *Biological Process Design for Wastewater Treatment,* Englewood Cliffs, New Jersey, Prentice-Hall Inc.

BENGTSSON, G. & ANNADOTTER, H. (1989) Nitrate reduction in a groundwater microcosm determined by N-15 gas chromatography-mass spectrometry. *Applied and Environmental Microbiology,* 55**,** 2861-2870.

BIRKETT, J. W. (2003a) Scope of the Problem. In BIRKETT, J. W. & LESTER, J. N. (Eds.) *Endocrine Disrupters in Wastewater and Sludge Treatment Processes.* London, CRC Press LLC.

BIRKETT, J. W. (2003b) Sources of Endocrine Disrupters. In BIRKETT, J. W. & LESTER, J. N. (Eds.) *Endocrine Disrupters in Wastewater and Sludge Treatment Processes.* London, CRC Press LLC.

BITTON, G. (1999) *Wastewater Microbiology,* New York, Wiley-Liss, Inc.

BITTON, G. & GERBA, C. P. (1984) *Groundwater Pollution Microbiology,* New York, John Wiley and Sons, Inc.

BLOWES, D. W., PTACEK, C. J., JAMBOR, J. L. & WEISENER, C. G. (2005) The geochemistry of acid mine drainage. In LOLLAR, B. S., HOLLAND, H. D. & TUREKIAN, K. K. (Eds.) *Environmental Geochemistry: Treatise on Geochemistry.* 2nd ed., Elservier Ltd.

BORDEN, R. C. & BEDIENT, P. B. (1986) Transport of dissolved hydrocarbons influenced by oxygen-limited biodegradation, 1. Theoretical development. *Water Resources Research,* 22**,** 1973 - 1982.

BOUWER, H. (1985) Renovation of Wastewater with Rapid-Infiltration Land Treatment Systems. In ASANO, T. (Ed.) *Artificial Recharge of Groundwater.* Boston, Butterworth Publishers.

BOUWER, H. (1991) Role of groundwater recharge in treatment and storage of wastewater for reuse. *Water Science and Technology,* 24**,** 295-302.

BOUWER, H. (2000) Integrated water management: emerging issues and challenges. *Agricultural Water Management,* 45**,** 217-228.

BOUWER, H. (2002) Artificial recharge of groundwater: hydrogeology and engineering. *Hydrogeology Journal,* 10**,** 121-142.

BOUWER, H. & RICE, R. C. (1984) Renovation of wastewater at the 23rd Avenue rapid infiltration project. *Journal Water Pollution Control Federation,* 56**,** 76-83.

BOUWER, H., RICE, R. C., LANCE, J. C. & GILBERT, R. C. (1980) Rapid-infiltration research at flushing meadows project, Arizona. *Journal Water Pollution Control Federation,* 52**,** 2457-2470.

BUNSRI, T., SIVAKUMAR, M. & HAGARE, D. (2008) Transport and biotransformation of organic carbon and nitrate compounds in unsaturated soil conditions. *Water Science and Technology,* 58**,** 2143-2153.

CANFIELD, D. & DES MARAIS, D. (1991) Aerobic sulfate reduction in microbial mats. *Science,* 251**,** 1471-1473.

CARGOUËT, M., PERDIZ, D., MOUATASSIM-SOUALI, A., TAMISIER-KAROLAK, S. & LEVI, Y. (2004) Assessment of river contamination by estrogenic compounds in Paris area (France). *Science of the Total Environment,* 324**,** 55-66.

CARLOS, K.-G. (1998) Comparative study of the electronic structure of estradiol, epiestradiol and estrone by ab initio theory. *Journal of Molecular Structure: Theochem,* 452**,** 175-183.

CARLSON, G. & SILVERSTEIN, J. (1998) Effect of molecular size and charge on biofilm sorption of organic matter. *Water Research,* 32**,** 1580-1592.

CARLSON, R. R., LINSTEDT, K. D., BENNETT, E. R. & HARTMAN, R. B. (1982) Rapid infiltration treatment of primary and secondary effluent. *Journal Water Pollution Control Federation,* 54**,** 270-280.

CARRE, J. & DUFILS, J. (1991) Wastewater treatment by infiltration basins - usefulness and limits - sewage plant in Creances (France). *Water Science and Technology,* 24**,** 287-293.

CARTER, J. P., HSIAO, Y. S., SPIRO, S. & RICHARDSON, D. J. (1995) Soil and sediment bacteria capable of aerobic nitrate respiration. *Applied and Environmental Microbiology,* 61**,** 2852-2858.

CHA, J. & CUPPLES, A. M. (2009) Detection of the antimicrobials triclocarban and triclosan in agricultural soils following land application of municipal biosolids. *Water Research,* 43**,** 2522-2530.

CHA, J. & CUPPLES, A. M. (2010) Triclocarban and triclosan biodegradation at field concentrations and the resulting leaching potentials in three agricultural soils. *Chemosphere,* 81**,** 494-499.

CHA, W., CHOI, H., KIM, J. & CHO, J. (2005) Water quality dependence on the depth of the vadose zone in SAT-simulated soil columns. *Water Science and Technology: Water Supply,* 5**,** 17-24.

CHA, W., CHOI, H., KIM, J. & KIM, I. S. (2004) Evaluation of wastewater effluents for soil aquifer treatment in South Korea. *Water Science and Technology,* 50**,** 315-322.

CHA, W., KIM, J. & CHOI, H. (2006) Evaluation of steel slag for organic and inorganic removals in soil aquifer treatment. *Water Research,* 40**,** 1034-1042.

CHALEW, T. E. A. & HALDEN, R. U. (2009) Environmental exposure of aquatic and terrestrial biota to triclosan and triclocarban. *Journal of the American Water Resources Association,* 45**,** 4-13.

CHARBENEAU, R. J. (2000) *Groundwater Hydraulics and Pollutant Transport,* Upper Saddle River, NJ, Prentice Hall Inc.

CHARLET, L., MORIN, G., ROSE, J., WANG, Y. H., AUFFAN, M., BURNOL, A. & FERNANDEZ-MARTINEZ, A. (2011) Reactivity at (nano)particle-water

interfaces, redox processes, and arsenic transport in the environment. *Comptes Rendus Geoscience,* 343**,** 123-139.

CHEN, J., AHN, K. C., GEE, N. A., AHMED, M. I., DULEBA, A. J., ZHAO, L., GEE, S. J., HAMMOCK, B. D. & LASLEY, B. L. (2008) Triclocarban enhances testosterone action: A new type of endocrine disruptor? *Endocrinology,* 149**,** 1173-1179.

CHIOU, C. T. & KILE, D. E. (2000) Contaminant Sorption by Soil and Bed Sediment. Is There a Difference? U.S. Geological Survey Fact Sheet 087-00. http://toxics.usgs.gov/pubs/FS-087-00/fs-087-00.pdf.

CHU, S. & METCALFE, C. D. (2007) Simultaneous determination of triclocarban and triclosan in municipal biosolids by liquid chromatography tandem mass spectrometry. *Journal of Chromatography A,* 1164**,** 212-218.

CHUA, L. H. C., LEONG, M. C. M., LO, E. Y. M., REINHARD, M., ROBERTSON, A. P., LIM, T. T., SHUY, E. B. & TAN, S. K. (2009) Controlled field studies on soil aquifer treatment in a constructed coastal sandfill. *Water Science and Technology,* 60**,** 1283-1293.

CHUA, L. H. C., LO, E. Y. M., SHUY, E. B., ROBERTSON, A. P., LIM, T. T. & TAN, S. K. (2010) DOC and UVA attenuation with soil aquifer treatment in the saturated zone of an artificial coastal sandfill. *Water Science and Technology,* 62**,** 491-500.

CLESCERI, L. S., GREENBERG, A. E. & EATON, A. D. (1998) *Standard Methods for the Examination of Water and Wastewater,* Washington American Public Health Association.

COLUCCI, M. S., BORK, H. & TOPP, E. (2001) Persistence of estrogenic hormones in agricultural soils: I. 17 beta-estradiol and estrone. *Journal of Environmental Quality,* 30**,** 2070-2076.

COMBALBERT, S. & HERNANDEZ-RAQUET, G. (2010) Occurrence, fate, and biodegradation of estrogens in sewage and manure. *Applied Microbiology and Biotechnology,* 86**,** 1671-1692.

CONROY, O., SAEZ, A. E., QUANRUD, D., ELA, W. & ARNOLD, R. G. (2007) Changes in estrogen/anti-estrogen activities in ponded secondary effluent. *Science of the Total Environment,* 382**,** 311-323.

COOGAN, M. A., EDZIYIE, R. E., LA POINT, T. W. & VENABLES, B. J. (2007) Algal bioaccumulation of triclocarban, triclosan, and methyl-triclosan in a North Texas wastewater treatment plant receiving stream. *Chemosphere,* 67**,** 1911-1918.

COOGAN, M. A. & LA POINT, T. W. (2008) Snail bioaccumulation of triclocarban, triclosan, and methyltriclosan in a North Texas, USA, stream affected by wastewater treatment plant runoff. *Environmental Toxicology and Chemistry,* 27**,** 1788-1793.

CORDY, G. E., DURAN, N. L., BOUWER, H., RICE, R. C., FURLONG, E. T., ZAUGG, S. D., MEYER, M. T., BARBER, L. B. & KOLPIN, D. W. (2004) Do pharmaceuticals, pathogens, and other organic waste water compounds persist when waste water is used for recharge? *Ground Water Monitoring and Remediation,* 24**,** 58-69.

CRITES, R. W., REED, S. C. & BASTIAN, R. K. (2000) *Land Treatment Systems for Municipal and Industrial Wastes,* New York, The McGraw-Hill Companies, Inc.

CRITTENDEN, J. C., TRUSSELL, R. R., HAND, D. W., HOWE, K. J. & TCHOBANOGLOUS, G. (2005) *Water Treatment - Principles and Design. 2nd Edition,* New Jersey, John Wiley & Sons, Inc.

CZAJKA, C. P. & LONDRY, K. L. (2006) Anaerobic biotransformation of estrogens. *Science of the Total Environment,* 367**,** 932-941.

D'ASCENZO, G., DI CORCIA, A., GENTILI, A., MANCINI, R., MASTROPASQUA, R., NAZZARI, M. & SAMPERI, R. (2003) Fate of natural estrogen conjugates in municipal sewage transport and treatment facilities. *The Science of the Total Environment,* 302**,** 199-209.

DAS, B. S., LEE, L. S., RAO, P. S. C. & HULTGREN, R. P. (2004) Sorption and degradation of steroid hormones in soils during transport: Column studies and model evaluation. *Environmental Science & Technology,* 38**,** 1460-1470.

DE SILVA, D. G. V. & RITTMANN, B. E. (2000) Nonsteady-State Modeling of Multispecies Activated-Sludge Processes. *Water Environment Research,* 72**,** 554-565.

DESBROW, C., ROUTLEDGE, E. J., BRIGHTY, G. C., SUMPTER, J. P. & WALDOCK, M. (1998) Identification of estrogenic chemicals in STW effluent. 1. Chemical fractionation and in vitro biological screening. *Environmental Science & Technology,* 32**,** 1549-1558.

DILLON, P., PAVELIC, P., TOZE, S., RINCK-PFEIFFER, S., MARTIN, R., KNAPTON, A. & PIDSLEY, D. (2006) Role of aquifer storage in water reuse. *Desalination,* 188**,** 123-134.

DIONEX (2001) Determination of Inorganic Anions in Wastewater by Ion Chromatography. Application Note 135. Dionex Corporation.

DOMENICO, P. A. & SCHWARTZ, F. W. (1998) *Physical and Chemical Hydrogeology,* New York, John Wiley & Sons, Inc.

DOUGHTY, M. J. (2010) pH dependent spectral properties of sodium fluorescein ophthalmic solutions revisited. *Ophthalmic and Physiological Optics,* 30**,** 167-174.

DREWES, J. E. (2003) Fate and transport of organic constituents during groundwater recharge using water of impaired quality. *IAHS-AISH Publication***,** 85-91.

DREWES, J. E. & FOX, P. (1999) Fate of natural organic matter (NOM) during groundwater recharge using reclaimed water. *Water Science and Technology,* 40**,** 241-248.

DREWES, J. E., HEMMING, J., LADENBURGER, S. J., SCHAUER, J. & SONZOGNI, W. (2005) An assessment of endocrine disrupting activity changes during wastewater treatment through the use of bioassays and chemical measurements. *Water Environment Research,* 77**,** 12-23.

DREWES, J. E. & JEKEL, M. (1996) Simulation of groundwater recharge with advanced treated wastewater. *Water Science and Technology,* 33**,** 409-418.

DROSTE, R. L. (1997) *Theory and Practice of Water and Wastewater Treatment,* New York, John Wiley & Sons Inc.

DRUGBANK (2011) Drugbank: Open Data Drug and Drug Target Database. 11th October 2011 ed., http://www.drugbank.ca/drugs/DB00286.

DYTCZAK, M. A., LONDRY, K. L. & OLESZKIEWICZ, J. A. (2008) Biotransformation of estrogens in nitrifying activated sludge under aerobic and alternating anoxic/aerobic conditions. *Water Environment Research,* 80**,** 47-52.

ESSAID, H. I., BEKINS, B. A., GODSY, E. M., WARREN, E., BAEDECKER, M. J. & COZZARELLI, I. M. (1995) Simulation of aerobic and anaerobic biodegradation processes at a crude oil spill site. *Water Resources Research,* 31**,** 3309-3327.

FENLON, K. A., JOHNSON, A. C., TYLER, C. R. & HILL, E. M. (2010) Gas-liquid chromatography-tandem mass spectrometry methodology for the quantitation of estrogenic contaminants in bile of fish exposed to wastewater treatment works effluents and from wild populations. *Journal of Chromatography A,* 1217**,** 112-118.

FETTER, C. W. (1999) *Contaminant Hydrogeology. 2nd Edition,* Upper Saddle River, New Jersey, Prentice Hall Inc.

FETTER, C. W. (2001) *Applied Hydrogeology,* New Jersey, Prentice-Hall Inc.

FILBY, A. L., SHEARS, J. A., DRAGE, B. E., CHURCHLEY, J. H. & TYLER, C. R. (2010) Effects of advanced treatments of wastewater effluents on estrogenic and reproductive health impacts in fish. *Environmental Science & Technology,* 44**,** 4348-4354.

FINDLAY, R. H. & DOBBS, F. C. (1993) Quantitative description of microbial communities using lipid analysis. In KEMP, P. F., SHERR, B. F., SHERR, E. B. & COLE, J. J. (Eds.) *Handbook of Methods in Aquatic Microbial Ecology.* Florida, CRC Press LLC.

FINDLAY, R. H., KING, G. M. & WATLING, L. (1989) Efficacy of phospholipid analysis in determining microbial biomass in sediments. *Applied and Environmental Microbiology,* 55**,** 2888-2893.

FOGLER, H. S. (1992) *Elements of Chemical Reaction Engineering,* Englewood Cliffs, New Jersey, Prentice-Hall.

FOSS (2009) The determination of nitrogen according to Kjeldahl using block digestion and steam distillation. Application Note 300. Issue No. 8.

FOX, P., ABOSHANP, W. & ALSAMADI, B. (2005) Analysis of soils to demonstrate sustained organic carbon removal during soil aquifer treatment. *Journal of Environmental Quality,* 34**,** 156-163.

FOX, P., HOUSTON, S., WESTERHOFF, P., DREWES, J. E., NELLOR, M., YANKO, W., BAIRD, R., RINCON, M., ARNOLD, R., LANSEY, K., GERBA, C., KARPISCAK, M., QUANRUD, D., AMY, G. & REINHARD, M. (2001) An Investigation of Soil Aquifer Treatment for Sustainable Water Reuse. Tempe, Arizona, National Centre for Sustainable Water Supply (NCSWS).

FOX, P., HOUSTON, S., WESTERHOFF, P., NELLOR, M., YANKO, W., BAIRD, R., RINCON, M., GULLY, J., CARR, S., ARNOLD, R., LANCEY, K., QUANRUD, D., ELA, W., AMY, G., REINHARD, M. & DREWES, J. E. (2006) *Advances in Soil Aquifer Treatment Research for Sustainable Water Reuse*, Denver, CO, AWWA Research Foundation and American Water Works Association.

FRANKENBERGER, W. T., JR., TROEH, F. & DUMENIL, L. C. (1979) Bacterial effects on hydraulic conductivity of soils. *Soil Sci. Soc. Am. J.,* 43**,** 333 - 338.

FREEZE, R. A. & CHERRY, J. A. (1979) *Groundwater*, Englewood Cliffs, New Jersey, Prentice Hall.

FROSTEGARD, A., TUNLID, A. & BAATH, E. (1993) Phospholipid fatty-acid composition, biomass, and activity of microbial communities from 2 soil types experimentally exposed to different heavy-metals. *Applied and Environmental Microbiology,* 59**,** 3605-3617.

FRYAR, A. E., MACKO, S. A., MULLICAN III, W. F., ROMANAK, K. D. & BENNETT, P. C. (2000) Nitrate reduction during ground-water recharge, Southern High Plains, Texas. *Journal of Contaminant Hydrology,* 40**,** 335-363.

GABET-GIRAUD, V., MIEGE, C., CHOUBERT, J. M., RUEL, S. M. & COQUERY, M. (2010) Occurrence and removal of estrogens and beta blockers by various processes in wastewater treatment plants. *Science of the Total Environment,* 408**,** 4257-4269.

GAO, H., SCHREIBER, F., COLLINS, G., JENSEN, M. M., KOSTKA, J. E., LAVIK, G., DE BEER, D., ZHOU, H. Y. & KUYPERS, M. M. M. (2010) Aerobic denitrification in permeable Wadden Sea sediments. *ISME Journal,* 4**,** 417-426.

GAULKE, L. S., STRAND, S. E., KALHORN, T. F. & STENSEL, H. D. (2008) 17 alpha-ethinylestradiol Transformation via Abiotic Nitration in the Presence of Ammonia Oxidizing Bacteria. *Environmental Science & Technology,* 42**,** 7622-7627.

GIBSON, R., BECERRIL-BRAVO, E., SILVA-CASTRO, V. & JIMÉNEZ, B. (2007) Determination of acidic pharmaceuticals and potential endocrine disrupting compounds in wastewaters and spring waters by selective elution and analysis by gas chromatography-mass spectrometry. *Journal of Chromatography A,* 1169**,** 31-39.

GLEDHILL, W. E. (1975) Biodegradation of 3,4,4'-trichlorocarbanilide, TCC®, in sewage and activated sludge. *Water Research,* 9**,** 649-654.

GOMES, R. & LESTER, J. N. (2003) Endocrine Disrupters in Receiving Waters. In BIRKETT, J. W. & LESTER, J. N. (Eds.) *Endocrine Disrupters in Wastewater and Sludge Treatment Processes.* London, CRC Press LLC.

GONG, R., LU, C., WU, W. M., CHENG, H., GU, B., WATSON, D., JARDINE, P. M., BROOKS, S. C., CRIDDLE, C. S., KITANIDIS, P. K. & LUO, J. (2011) Estimating reaction rate coefficients within a travel-time modeling framework. *Ground Water,* 49**,** 209-218.

GRAY, N. F. (2004) *Biology of Wastewater Treatment,* London, Imperial College Press.

GRESKOWIAK, J., PROMMER, H., MASSMANN, G., JOHNSTON, C. D., NUTZMANN, G. & PEKDEGER, A. (2005) The impact of variably saturated conditions on hydrogeochemical changes during artificial recharge of groundwater. *Applied Geochemistry,* 20**,** 1409-1426.

GRISCHEK, T., HISCOCK, K. M., METSCHIES, T., DENNIS, P. F. & NESTLER, W. (1998) Factors affecting denitrification during infiltration of river water into a sand and gravel aquifer in Saxony, Germany. *Water Research,* 32 450 - 460.

GRÜNHEID, S., AMY, G. & JEKEL, M. (2005) Removal of bulk dissolved organic carbon (DOC) and trace organic compounds by bank filtration and artificial recharge. *Water Research,* 39**,** 3219-3228.

GU, C., HORNBERGER, G. M., MILLS, A. L., HERMAN, J. S. & FLEWELLING, S. A. (2007) Nitrate reduction in streambed sediments: Effects of flow and biogeochemical kinetics. *Water Resources Research,* 43.

GUNGOR, K. & UNLU, K. (2005) Nitrite and nitrate removal efficiencies of soil aquifer treatment columns. *Turkish Journal of Engineering and Environmental Sciences,* 29**,** 159-170.

HAIYAN, R., SHULAN, J., UD DIN AHMAD, N., DAO, W. & CHENGWU, C. (2007) Degradation characteristics and metabolic pathway of 17alpha-ethynylestradiol by Sphingobacterium sp. JCR5. *Chemosphere,* 66**,** 340-6.

HALDEN, R. U. & PAULL, D. H. (2004) Analysis of triclocarban in aquatic samples by liquid chromatography electrospray ionization mass spectrometry. *Environmental Science & Technology,* 38**,** 4849-4855.

HALDEN, R. U. & PAULL, D. H. (2005) Co-occurrence of triclocarban and triclosan in U.S. water resources. *Environmental Science & Technology,* 39**,** 1420-1426.

HASHIMOTO, T., ONDA, K., NAKAMURA, Y., TADA, K., MIYA, A. & MURAKAMI, T. (2007) Comparison of natural estrogen removal efficiency in the conventional activated sludge process and the oxidation ditch process. *Water Research,* 41**,** 2117-2126.

HAYATSU, M., TAGO, K. & SAITO, M. (2008) Various players in the nitrogen cycle: Diversity and functions of the microorganisms involved in nitrification and denitrification. *Soil Science and Plant Nutrition,* 54**,** 33-45.

HEAD, K. H. (1992) *Manual of Soil Laboratory Testing Volume 1: Soil Classification and Compaction Tests,* London, Pentech Press Limited.

HEIDLER, J. & HALDEN, R. U. (2009) Fate of organohalogens in US wastewater treatment plants and estimated chemical releases to soils nationwide from biosolids recycling. *JEM Journal of Environmental Monitoring,* 11**,** 2207-2215.

HEIDLER, J., SAPKOTA, A. & HALDEN, R. U. (2006) Partitioning, persistence, and accumulation in digested sludge of the topical antiseptic triclocarban during wastewater treatment. *Environmental Science & Technology,* 40**,** 3634-3639.

HENZE, M., VAN LOOSDRECHT, M. C. M., EKAMA, G. & BRDJANOVIC, D. (Eds.) (2008) *Biological Wastewater Treatment: Principles, Modelling and Design,* London, IWA Publishing.

HIGGINS, C. P., PAESANI, Z. J., ABBOTT CHALEW, T. E., HALDEN, R. U. & HUNDAL, L. S. (2011) Persistence of triclocarban and triclosan in soils after land application of biosolids and bioaccumulation in Eisenia foetida. *Environmental Toxicology and Chemistry,* 30**,** 556-563.

HOHENBLUM, P., GANS, O., MOCHE, W., SCHARF, S. & LORBEER, G. (2004) Monitoring of selected estrogenic hormones and industrial chemicals in groundwaters and surface waters in Austria. *Science of the Total Environment,* 333**,** 185-193.

HOLZBECHER, E. O. (2007) *Environmental Modelling: Using MATLAB,* Berlin Heidelberg, Springer-Verlag

HOUSTON, S. L., DURYEA, P. D. & HONG, R. (1999) Infiltration considerations for ground-water recharge with waste effluent. *Journal of Irrigation and Drainage Engineering,* 125**,** 264-272.

HUNTER, K. S., WANG, Y. & VAN CAPPELLEN, P. (1998) Kinetic modeling of microbially-driven redox chemistry of subsurface environments: Coupling transport, microbial metabolism and geochemistry. *Journal of Hydrology,* 209**,** 53-80.

IDELOVITCH, E. & MICHAIL, M. (1984) Soil-aquifer treatment - a new approach to an old method of wastewater reuse. *Journal Water Pollution Control Federation,* 56**,** 936-943.

ISHIZAWA, S. & TOYODA, H. (1964) Microflora of Japanese soils. *Bulletin of National Institute of Agricultural Sciences Series B,* 14**,** 203 - 284.

JARUSUTTHIRAK, C. & AMY, G. (2007) Understanding soluble microbial products (SMP) as a component of effluent organic matter (EfOM). *Water Research,* 41**,** 2787-2793.

JELLALI, S., SEDIRI, T., KALLALI, H., ANANE, M. & JEDIDI, N. (2009) Analysis of hydraulic conditions and HRT on the basis of experiments and simulations on soil column. *Desalination,* 246**,** 435-443.

JOBLING, S., NOLAN, M., TYLER, C. R., BRIGHTY, G. & SUMPTER, J. P. (1998) Widespread Sexual Disruption in Wild Fish. *Environmental Science & Technology,* 32**,** 2498-2506.

JOBLING, S. & TYLER, C. R. (2003) Endocrine disruption in wild freshwater fish. *Pure and Applied Chemistry,* 75**,** 2219-2234.

JOHNSON, A. C., BELFROID, A. & DI CORCIA, A. (2000) Estimating steroid oestrogen inputs into activated sludge treatment works and observations on their removal from the effluent. *The Science of the Total Environment,* 256**,** 163-173.

JOHNSON, A. C. & SUMPTER, J. P. (2001) Removal of endocrine-disrupting chemicals in activated sludge treatment works. *Environmental Science & Technology,* 35**,** 4697-4703.

JOHNSON, A. C. & WILLIAMS, R. J. (2004) A model to estimate influent and effluent concentrations of estradiol, estrone, and ethinylestradiol at sewage treatment works. *Environmental Science & Technology,* 38**,** 3649-3658.

JOHNSON, R. R., NAVONE, R. & LARSON, E. L. (1963) An unusual epidemic of methemoglobinemia. *Pediatrics,* 31**,** 222-225.

JÜRGENS, M. D., HOLTHAUS, K. I. E., JOHNSON, A. C., SMITH, J. J. L., HETHERIDGE, M. & WILLIAMS, R. J. (2002) The potential for estradiol and ethinylestradiol degradation in english rivers. Wiley Periodicals, Inc.

KAMON, M., ZHANG, H., KATSUMI, T. & SAWA, N. (2002) Redox effect on the hydraulic conductivity of clay liner. *Soils Found.,* 42**,** 79 - 91.

KANAREK, A., AHARONI, A. & MICHAIL, M. (1993) Municipal wastewater reuse via soil aquifer treatment for non-potable purposes. *Water Science and Technology,* 27**,** 53-61.

KE, J. X., ZHUANG, W. Q., GIN, K. Y. H., REINHARD, M., HOON, L. T. & TAY, J. H. (2007) Characterization of estrogen-degrading bacteria isolated from an artificial sandy aquifer with ultrafiltered secondary effluent as the medium. *Applied Microbiology and Biotechnology,* 75**,** 1163-1171.

KHANAL, S. K., XIE, B., THOMPSON, M. L., SUNG, S., ONG, S.-K. & VAN LEEUWEN, J. (2006) Fate, transport, and biodegradation of natural estrogens in the environment and engineered systems. *Environmental Science & Technology,* 40**,** 6537-6546.

KIERZENKA, J. (2010) Solving boundary value problems with BVP4C - Tutorial + Examples. http://www.mathworks.com/bvp_tutorial. The MathWorks, Inc

KIM, J. W., KIM, J., CHOI, H. & SCHWARTZ, F. W. (2004) Modeling the fate and transport of organic and nitrogen species in soil aquifer treatment process. *Water Science and Technology,* 50**,** 255-261.

KIM, M., JEONG, S. Y., YOON, S. J., CHO, S. J., KIM, Y. H., KIM, M. J., RYU, E. Y. & LEE, S. J. (2008) Aerobic denitrification of Pseudomonas putida AD-21 at different C/N ratios. *Journal of Bioscience and Bioengineering,* 106**,** 498-502.

KLEIN, D. R., FLANNELLY, D. F. & SCHULTZ, M. M. (2010) Quantitative determination of triclocarban in wastewater effluent by stir bar sorptive extraction and liquid desorption-liquid chromatography-tandem mass spectrometry. *Journal of Chromatography A,* 1217**,** 1742-1747.

KOPCHYNSKI, T., FOX, P., ALSMADI, B. & BERNER, M. (1996) Effects of soil type and effluent pre-treatment on soil aquifer treatment. *Water Science and Technology,* 34**,** 235-242.

KWON, J.-W., ARMBRUST, K. L. & XIA, K. (2010) Transformation of triclosan and triclocarban in soils and biosolids-applied soils. *J Environ Qual,* 39**,** 1139-44.

LAGANÀ, A., BACALONI, A., DE LEVA, I., FABERI, A., FAGO, G. & MARINO, A. (2004) Analytical methodologies for determining the occurrence of endocrine disrupting chemicals in sewage treatment plants and natural waters. *Analytica Chimica Acta,* 501**,** 79-88.

LAI, K. M., SCRIMSHAW, M. D. & LESTER, J. N. (2002) Biotransformation and bioconcentration of steroid estrogens by Chlorella vulgaris. *Applied and Environmental Microbiology,* 68**,** 859-864.

LANCE, J. C., RICE, R. C. & GILBERT, R. G. (1980) Renovation of wastewater by soil columns flooded with primary effluent. *Journal Water Pollution Control Federation,* 52**,** 381-388.

LANGFORD, K. & LESTER, J. N. (2003) Fate and behavior of endocrine disrupters in wastewater treatment processes. In BIRKETT, J. W. & LESTER, J. N. (Eds.) *Endocrine Disrupters in Wastewater and Sludge Treatment Processes.* London, CRC Press LLC.

LAVAGNINI, I., MAGNO, F., SERAGLIA, R. & TRALDI, P. (2006) *Quantitative Applications of Mass Spectrometry,* Chichester, West Sussex, England, John Wiley & Sons Ltd.

LAWRENCE, A. W. & MCCARTY, P. L. (1970) Unified basis for biological treatment design and operation. *Journal of the Sanitary Engineering Division-ASCE,* 96**,** 757-778.

LAWRENCE, J. R., ZHU, B., SWERHONE, G. D. W., ROY, J., WASSENAAR, L. I., TOPP, E. & KORBER, D. R. (2009) Comparative microscale analysis of the effects of triclosan and triclocarban on the structure and function of river biofilm communities. *Science of the Total Environment,* 407**,** 3307-3316.

LECHEVALIER, M. P. (1989) Lipids in bacterial taxonomy. In O'LEARY, W. M. (Ed.) *Practical Handbook of Microbiology.* Florida, CRC Press Ltd.

LECKIE, S. E. (2005) Methods of microbial community profiling and their application to forest soils. *Forest Ecology and Management,* 220**,** 88-106.

LEE, H. B., PEART, T. E., CHAN, J. & GRIS, G. (2004) Occurrence of endocrine-disrupting chemicals in sewage and sludge samples in Toronto, Canada. *Water Quality Research Journal of Canada,* 39**,** 57-63.

LEE, M.-S., LEE, K.-K., HYUN, Y., CLEMENT, T. P. & HAMILTON, D. (2006) Nitrogen transformation and transport modeling in groundwater aquifers. *Ecological Modelling,* 192**,** 143-159.

LEE, T.-C. (1999) *Applied Mathematics in Hydrogeology,* Florida, CRC Press LLC.

LENS, P. N., DE POORTER, M. P., CRONENBERG, C. C. & VERSTRAETE, W. H. (1995) Sulfate reducing and methane producing bacteria in aerobic wastewater treatment systems. *Water Research,* 29**,** 871-880.

LEVENSPIEL, O. (1999) *Chemical Reaction Engineering,* New York, John Wiley & Sons Inc.

LIM, T. H., GIN, K. Y. H., CHOW, S. S., CHEN, Y. H., REINHARD, M. & TAY, J. H. (2007) Potential for 17 beta-estradiol and estrone degradation in a recharge aquifer system. *Journal of Environmental Engineering-Asce,* 133**,** 819-826.

LIN, C. & BANIN, A. (2006) Phosphorous retardation and breakthrough into well water in a soil-aquifer treatment (SAT) system used for large-scale wastewater reclamation. *Water Research,* 40**,** 1507-1518.

LLOYD, D., BODDY, L. & DAVIES, K. J. P. (1987) Persistence of bacterial denitrification capacity under aerobic conditions: The rule rather than the exception. *FEMS Microbiology Letters,* 45**,** 185-190.

LOGAN, B. E. (1999) *Environmental Transport Processes,* New York, Chichester, John Wiley & Sons, Inc.

MACQUARRIE, K. T. B. & SUDICKY, E. A. (2001) Multicomponent simulation of wastewater-derived nitrogen and carbon in shallow unconfined aquifers - I. Model formulation and performance. *Journal of Contaminant Hydrology,* 47**,** 53-84.

MACQUARRIE, K. T. B., SUDICKY, E. A. & ROBERTSON, W. D. (2001) Multicomponent simulation of wastewater-derived nitrogen and carbon in shallow unconfined aquifers - II. Model application to a field site. *Journal of Contaminant Hydrology,* 47**,** 85-104.

MADIGAN, M. T. & MARTINKO, J. M. (2006) *Brock Biology of Microorganisms. 11th Edition,* New Jersey, Pearson Prentice Hall. Pearson Education, Inc.

MAGDOFF, F. R., KEENEY, D. R., BOUMA, J. & ZIEBELL, W. A. (1974) Columns representing mound-type disposal systems for septic tank effluent: II. Nutrient transformations and bacterial populations. *Journal of Environmental Quality,* 3**,** 228-234.

MANSELL, J. & DREWES, J. E. (2004) Fate of steroidal hormones during soil-aquifer treatment. *Ground Water Monitoring and Remediation,* 24**,** 94-101.

MANSELL, J., DREWES, J. E. & RAUCH, T. (2004) Removal mechanisms of endocrine disrupting compounds (steroids) during soil aquifer treatment. *Water Science and Technology,* 50**,** 229-237.

MARTIN, J. P. (1945) Microorganisms and soil aggregation. I. Origin and nature of some of the aggregating substances. *Soil Sci.,* 59**,** 163 - 174.

MATHWORKS (2009) MATLAB 7.8.0 (R2009a). The MathWorks, Inc.

MATTHIESSEN, P., ARNOLD, D., JOHNSON, A. C., PEPPER, T. J., POTTINGER, T. G. & PULMAN, K. G. T. (2006) Contamination of headwater streams in the United Kingdom by oestrogenic hormones from livestock farms. *Science of the Total Environment,* 367**,** 616-630.

MICHAELIS, L. & MENTEN, M. L. (1913) Die kinetik der invertinwirkung. *Biochemische Zeitschrift,* 49**,** 333 - 369.

MILLER, C. T. & WEBER, W. J. (1984) Modeling organic contamination partitioning in groundwater systems. *Ground Water* 22**,** 584-92.

MILLER, T. R., COLQUHOUN, D. R. & HALDEN, R. U. (2010) Identification of wastewater bacteria involved in the degradation of triclocarban and its non-chlorinated congener. *Journal of Hazardous Materials,* 183**,** 766-772.

MILLER, T. R., HEIDLER, J., CHILLRUD, S. N., DELAQUIL, A., RITCHIE, J. C., MIHALIC, J. N., BOPP, R. & HALDEN, R. U. (2008) Fate of triclosan and evidence for reductive dechlorination of triclocarban in estuarine sediments. *Environmental Science and Technology,* 42**,** 4570-4576.

MIRETZKY, P., MUÑOZ, C. & CARRILLO-CHÁVEZ, A. (2006) Experimental Zn(II) retention in a sandy loam soil by very small columns. *Chemosphere,* 65**,** 2082-2089.

MIYA, A., ONDA, K., NAKAMURA, Y., TAKATOH, C., KATSU, Y. & TANAKA, T. (2007) Biological treatment of estrogenic substances. *Environmental Sciences: an international journal of environmental physiology and toxicology,* 14**,** 89-94.

MIYAZAKI, T. & SEKI, K. (2006) Effects of microbiological factors on water flow in soils. In MIYAZAKI, T. (Ed.) *Water Flow in Soils. 2nd Edition.* Boca Raton, CRC Press, Taylor & Francis Group.

MONOD, J. (1949) The growth of bacterial cultures. *Annual Review of Microbiology,* 3**,** 371 - 394.

NEMA, P., OJHA, C. S. P., KUMAR, A. & KHANNA, P. (2001) Techno-economic evaluation of soil-aquifer treatment using primary effluent at Ahmedabad, India. *Water Research,* 35**,** 2179-2190.

NOLEN, G. A. & DIERCKMAN, T. A. (1979) Reproduction and teratogenic studies of a 2:1 mixture of 3,4,4'-trichlorocarbanilide and 3-trifluoromethyl-4,4'-dichlorocarbanilide in rats and rabbits. *Toxicology and Applied Pharmacology,* 51**,** 417-425.

NRC (1994) *Ground Water Recharge Using Waters of Impaired Quality*, National Academy Press, Washington, D.C.

O'LEARY, W. M. (1962) The fatty acids of bacteria. *Bacteriological reviews,* 26**,** 421-47.

OECD (1996) Guideline for Testing of Chemicals Simulation Test-Aerobic Sewage Treatment. Technical Report. Organisation for Economic Co-operation and Development (OECD), Paris, France.

OJEDA, E., CALDENTEY, J., SAALTINK, M. W. & GARCIA, J. (2008) Evaluation of relative importance of different microbial reactions on organic matter removal in horizontal subsurface-flow constructed wetlands using a 2D simulation model. *Ecological Engineering,* 34**,** 65-75.

PARKER, J. C. & VAN GENUCHTEN, M. T. (1984) Determining transport parameters from laboratory and field tracer experiments. *Virginia Agricultural Experiment Station Bulletin***,** 1-96.

PATUREAU, D., ZUMSTEIN, E., DELGENES, J. P. & MOLETTA, R. (2000) Aerobic denitrifiers isolated from diverse natural and managed ecosystems. *Microbial Ecology,* 39**,** 145-152.

PAUWELS, B., NOPPE, H., DE BRABANDER, H. & VERSTRAETE, W. (2008) Comparison of steroid hormone concentrations in domestic and hospital wastewater treatment plants. *Journal of Environmental Engineering-ASCE,* 134**,** 933-936.

PEAVY, H. S., ROWE, D. R. & TCHOBANOGLOUS, G. (1985) *Environmental Engineering*, McGraw-Hill.

PERFECT, E., SUKOP, M. C. & HASZLER, G. R. (2002) Prediction of dispersivity for undisturbed soil columns from water retention parameters. *Soil Science Society of America Journal,* 66**,** 696-701.

PESCOD, M. B. (1992) *Wastewater Treatment and Use in Agriculture,* Rome, Food and Agriculture Organization of the United Nations.

PETERSON, E. W., DAVIS, R. K. & ORNDORFF, H. A. (2000) 17β-estradiol as an indicator of animal waste contamination in mantled karst aquifers. *Journal of Environmental Quality,* 29**,** 826-834.

POULOVASSILIS, A. (1972) The changeability of the hydraulic conductivity of saturated soil samples. *Soil Sci,* 113**,** 81 - 87.

PROCHASKA, C. A., ZOUBOULIS, A. I. & ESKRIDGE, K. M. (2007) Performance of pilot-scale vertical-flow constructed wetlands, as affected by season, substrate, hydraulic load and frequency of application of simulated urban sewage. *Ecological Engineering*, 31**,** 57-66.

PURDOM, C. E., HARDIMAN, P. A., BYE, V. V. J., ENO, N. C., TYLER, C. R. & SUMPTER, J. P. (1994) Estrogenic effects of effluents from sewage treatment works. *Chemistry and Ecology*, 8**,** 275 - 285.

QUANRUD, D. M., ARNOLD, R. G., WILSON, L. G. & CONKLIN, M. H. (1996a) Effect of soil type on water quality improvement during soil aquifer treatment. *Water Science and Technology,* 33**,** 419-431.

QUANRUD, D. M., ARNOLD, R. G., WILSON, L. G., GORDON, H. J., GRAHAM, D. W. & AMY, G. L. (1996b) Fate of organics during column

studies of soil aquifer treatment. *Journal of Environmental Engineering,* 122**,** 314-321.

QUANRUD, D. M., CARROLL, S. M., GERBA, C. P. & ARNOLD, R. G. (2003a) Virus removal during simulated soil-aquifer treatment. *Water Research,* 37**,** 753-762.

QUANRUD, D. M., HAFER, J., KARPISCAK, M. M., ZHANG, J., LANSEY, K. E. & ARNOLD, R. G. (2003b) Fate of organics during soil-aquifer treatment: Sustainability of removals in the field. *Water Research,* 37**,** 3401-3411.

RACZ, L. & GOEL, R. K. (2010) Fate and removal of estrogens in municipal wastewater. *Journal of Environmental Monitoring,* 12**,** 58-70.

RANDALL, C. W., L., B. J. & STENSEL, H. D. (Eds.) (1992) *Design and Retrofit of Wastewater Treatment Plants for Biological Nutrient Removal,* Lancaster, Pennsylvania, Technomic Publishing Company Inc.

RAO, A. M. F., MCCARTHY, M. J., GARDNER, W. S. & JAHNKE, R. A. (2007) Respiration and denitrification in permeable continental shelf deposits on the South Atlantic Bight: Rates of carbon and nitrogen cycling from sediment column experiments. *Continental Shelf Research,* 27**,** 1801-1819.

RAUCH-WILLIAMS, T. & DREWES, J. E. (2006) Using soil biomass as an indicator for the biological removal of effluent-derived organic carbon during soil infiltration. *Water Research,* 40**,** 961-968.

RAUCH-WILLIAMS, T., HOPPE-JONES, C. & DREWES, J. E. (2010) The role of organic matter in the removal of emerging trace organic chemicals during managed aquifer recharge. *Water Research,* 44**,** 449-460.

REED, S. C., MIDDLEBROOKS, E. J. & ., C. R. W. (1988) *Natural Systems for Waste Management and Treatment,,* McGraw-Hill

REEMTSMA, T., GNIRß, R. & JEKEL, M. (2000) Infiltration of combined sewer overflow and tertiary municipal wastewater: an integrated laboratory and field study on nutrients and dissolved organics. *Water Research,* 34**,** 1179-1186.

RIFAI, H. S., BEDIENT, P. B. & WILSON, J. T. (1989) BIOPLUME model for contaminant transport affected by oxygen limited biodegradation. Environmental Research Brief, EPA/600/M-89/019. Ada, United States Environmental Protection Agency.

RODGERS-GRAY, T. P., JOBLING, S., MORRIS, S., KELLY, C., KIRBY, S., JANBAKHSH, A., HARRIES, J. E., WALDOCK, M. J., SUMPTER, J. P. & TYLER, C. R. (2000) Long-term temporal changes in the estrogenic composition of treated sewage effluent and its biological effects on fish. *Environmental Science & Technology,* 34**,** 1521-1528.

ROWE, D. R. (1995) *Handbook of Wastewater Reclamation and Reuse*, CRC Press LLC.

SAID, E., FRANK, U. & CHADIA, A. (2007) Numerical Techniques for Chemical and Biological Engineers using MATLAB®. Springer Science +Business Media, LLC.

SAPKOTA, A., HEIDLER, J. & HALDEN, R. U. (2007) Detection of triclocarban and two co-contaminating chlorocarbanilides in US aquatic environments using isotope dilution liquid chromatography tandem mass spectrometry. *Environmental Research,* 103**,** 21-29.

SARFARAZ, S., THOMAS, S., TEWARI, U. K. & IYENGAR, L. (2004) Anoxic treatment of phenolic wastewater in sequencing batch reactor. *Water Research,* 38**,** 965-971.

SCHAFER, W. & THERRIEN, R. (1995) Simulating transport and removal of xylene during remediation of a sandy aquifer. *Journal of Contaminant Hydrology,* 19**,** 205-236.

SCHEURER, M., BRAUCH, H.-J. & LANGE, F. T. (2009) Analysis and occurrence of seven artificial sweeteners in German waste water and surface water and in soil aquifer treatment (SAT). *Anal Bioanal Chem,* 394**,** 1585-94.

SHACKLE, V. J., FREEMAN, C. & REYNOLDS, B. (2000) Carbon supply and the regulation of enzyme activity in constructed wetlands. *Soil Biology and Biochemistry,* 32**,** 1935-1940.

SHAREEF, A., EGERER, S. & KOOKANA, R. (2009) Effect of triclosan and triclocarban biocides on biodegradation of estrogens in soils. *Chemosphere,* 77**,** 1381-1386.

SHARMA, R. S. & MOHAMED, M. H. A. (2003) An experimental investigation of LNAPL migration in an unsaturated/saturated sand. *Engineering Geology,* 70**,** 305-313.

SHI, J., FUJISAWA, S., NAKAI, S. & HOSOMI, M. (2004) Biodegradation of natural and synthetic estrogens by nitrifying activated sludge and ammonia-oxidizing bacterium Nitrosomonas europaea. *Water Research,* 38**,** 2323-2330.

SJOBACK, R., NYGREN, J. & KUBISTA, M. (1995) Absorption and fluorescence properties of fluorescein. *Spectrochimica Acta Part a-Molecular and Biomolecular Spectroscopy,* 51**,** L7-L21.

SNYDER, E. H., O'CONNOR, G. A. & MCAVOY, D. C. (2010a) Fate of C-14-triclocarban in biosolids-amended soils. *Science of the Total Environment,* 408**,** 2726-2732.

SNYDER, E. H., O'CONNOR, G. A. & MCAVOY, D. C. (2010b) Measured physicochemical characteristics and biosolids-borne concentrations of the antimicrobial Triclocarban (TCC). *Science of the Total Environment,* 408**,** 2667-2673.

SNYDER, M. L. & LICHSTEIN, H. C. (1940) Sodium azide as an inhibiting substance for Gram-negative bacteria. *The Journal of Infectious Diseases,* 67**,** 113-115.

SNYDER, S. A., VILLENEUVE, D. L., SNYDER, E. M. & GIESY, J. P. (2001) Identification and quantification of estrogen receptor agonists in wastewater effluents. *Environmental Science & Technology,* 35**,** 3620-3625.

SOUSA, A., SCHONENBERGER, R., JONKERS, N., SUTER, M. J. F., TANABE, S. & BARROSO, C. M. (2010) Chemical and biological characterization of estrogenicity in effluents from WWTPs in Ria de Aveiro (NW Portugal). *Archives of Environmental Contamination and Toxicology,* 58**,** 1-8.

STANFORD, B. D., AMOOZEGAR, A. & WEINBERG, H. S. (2010) The impact of co-contaminants and septic system effluent quality on the transport of estrogens and nonylphenols through soil. *Water Research,* 44**,** 1598-1606.

STUMPE, B. & MARSCHNER, B. (2009) Factors controlling the biodegradation of 17[beta]-estradiol, estrone and 17[alpha]-ethinylestradiol in different natural soils. *Chemosphere,* 74**,** 556-562.

STUYFZAND, P. J. (1989) Hydrology and water quality aspects of rhine bank groundwater in The Netherlands. *Journal of Hydrology,* 106**,** 341-363.

SUAREZ, S., LEMA, J. M. & OMIL, F. (2010) Removal of Pharmaceutical and Personal Care Products (PPCPs) under nitrifying and denitrifying conditions. *Water Research,* 44**,** 3214-3224.

SUMBALI, G. & MEHROTRA, R. S. (2009) *Principles of Microbiology,* New Delhi, Tata McGraw Hill Education Private Limited.

SVENNINGSEN, H., HENRIKSEN, T., PRIEMÉ, A. & JOHNSEN, A. R. (2011) Triclosan affects the microbial community in simulated sewage-drain-field soil and slows down xenobiotic degradation. *Environmental Pollution,* 159**,** 1599-1605.

SWARTZ, C. H., REDDY, S., BENOTTI, M. J., YIN, H., BARBER, L. B., BROWNAWELL, B. J. & RUDEL, R. A. (2006) Steroid estrogens, nonylphenol ethoxylate metabolites, and other wastewater contaminants in groundwater affected by a residential septic system on Cape Cod, MA. *Environmental Science & Technology,* 40**,** 4894-4902.

TCC-CONSORTIUM (2002) High Production Volume (HPV) Chemical Challenge Program Data Availability and Screening Level Assessment for Triclocarban CAS #: 101-20-2. Report No. 201-14186A. http://www.epa.gov/HPV/pubs/summaries/tricloca/c14186.pdf.

TCHOBANOGLOUS, G., BURTON, F. L., METCALF & EDDY (1999) *Wastewater Engineering: Treatment, Disposal and Reuse. 3rd Edition,* New Delhi, Tata McGraw-Hill Publishing Company Limited.

TCHOBANOGLOUS, G., BURTON, F. L., STENSEL, H. D., METCALF & EDDY (2003) *Wastewater Engineering: Treatment and Reuse,* New York, McGraw-Hill Inc.

TERNES, T. A., BONERZ, M., HERRMANN, N., TEISER, B. & ANDERSEN, H. R. (2007) Irrigation of treated wastewater in Braunschweig, Germany: An option to remove pharmaceuticals and musk fragrances. *Chemosphere,* 66**,** 894-904.

TERNES, T. A., STUMPF, M., MUELLER, J., HABERER, K., WILKEN, R. D. & SERVOS, M. (1999) Behavior and occurrence of estrogens in municipal sewage treatment plants - I. Investigations in Germany, Canada and Brazil. *Science of the Total Environment,* 225**,** 81-90.

TOPP, E., MONTEIRO, S. C., BECK, A., COELHO, B. B., BOXALL, A. B. A., DUENK, P. W., KLEYWEGT, S., LAPEN, D. R., PAYNE, M., SABOURIN, L., LI, H. & METCALFE, C. D. (2008) Runoff of pharmaceuticals and personal care products following application of biosolids to an agricultural field. *Science of the Total Environment,* 396**,** 52-59.

TRENHOLM, R. A., VANDERFORD, B. J., DREWES, J. E. & SNYDER, S. A. (2008) Determination of household chemicals using gas chromatography and liquid chromatography with tandem mass spectrometry. *Journal of Chromatography A,* 1190**,** 253-262.

TYLER, C. R., JOBLING, S. & SUMPTER, J. P. (1998) Endocrine disruption in wildlife: A critical review of the evidence. *Critical Reviews in Toxicology,* 28**,** 319-361.

USEPA (1981) Land Treatment of Municipal Wastewater: Process Design Manual, No. EPA-625/1-81-013. Center for Environmental Research Information.

USEPA (1997) Special Report on Environmental Endocrine Disruption: An Effects Assessment and Analysis, Report No. 630/R-96/012. U.S. Environmental Protection Agency, Risk Assessment Forum, Washington, DC.

VADER, J. S., VAN GINKEL, C. G., SPERLING, F. M. G. M., DE JONG, J., DE BOER, W., DE GRAAF, J. S., VAN DER MOST, M. & STOKMAN, P. G.

W. (2000) Degradation of ethinyl estradiol by nitrifying activated sludge. *Chemosphere,* 41**,** 1239-1243.

VALENZUELA, A. & MORGADO, N. (1999) Trans fatty acid isomers in human health and in the food industry. *Biological Research,* 32**,** 273-287.

VAN CUYK, S., SIEGRIST, R., LOGAN, A., MASSON, S., FISCHER, E. & FIGUEROA, L. (2001) Hydraulic and purification behaviors and their interactions during wastewater treatment in soil infiltration systems. *Water Research,* 35**,** 953-964.

VAN GENUCHTEN, M. T. (1980) A closed form equation for predicting the hydraulic conductivity of unsaturated soils. *Soil Science Society of America Journal,* 44**,** 892-898.

VAN GENUCHTEN, M. T. & PARKER, J. C. (1984) Boundary conditions for displacement experiments through short laboratory soil columns. *Soil Science Society of America Journal,* 48**,** 703-708.

VAN HAANDEL, A. & VAN DER LUBBE, J. (2007) *Handbook Biological Waste Water Treatment - Design and Optimisation of Activated Sludge Systems,* Leidschendam, The Netherlands, Quist Publishing.

VELASCO, A., RAMÍREZ, M., VOLKE-SEPÚLVEDA, T., GONZÁLEZ-SÁNCHEZ, A. & REVAH, S. (2008) Evaluation of feed COD/sulfate ratio as a control criterion for the biological hydrogen sulfide production and lead precipitation. *Journal of Hazardous Materials,* 151**,** 407-413.

VESTAL, J. R. & WHITE, D. C. (1989) Lipid analysis in microbial ecology - Quantitative approaches to the study of microbial communities. *Bioscience,* 39**,** 535-541.

WARD, C. H., GIGER, W. & MCCARTY, P. L. (1985) *Ground Water Quality,* 605 Third. Ave., New York, John Wiley. &. Sons, Inc.

WEBER, S., LEUSCHNER, P., KÄMPFER, P., DOTT, W. & HOLLENDER, J. (2005) Degradation of estradiol and ethinyl estradiol by activated sludge and by a defined mixed culture. *Applied Microbiology and Biotechnology,* 67**,** 106-112.

WHITE, D. C., DAVIS, W. M., NICKELS, J. S., KING, J. D. & BOBBIE, R. J. (1979) Determination of the sedimentary microbial biomass by extractable lipid phosphate. *Oecologia,* 40**,** 51-62.

WIDDOWSON, M. A., MOLZ, F. J. & BENEFIELD, L. D. (1988) A numerical transport model for oxygen-based and nitrate-based respiration linked to substrate and nutrient availability in porous-media. *Water Resources Research,* 24**,** 1553-1565.

WIESSNER, A., RAHMAN, K. Z., KUSCHK, P., KÄSTNER, M. & JECHOREK, M. (2010) Dynamics of sulphur compounds in horizontal sub-surface flow laboratory-scale constructed wetlands treating artificial sewage. *Water Research,* 44**,** 6175-6185.

WILLIAMS, R. J., JOHNSON, A. C., SMITH, J. J. L. & KANDA, R. (2003) Steroid Estrogens Profiles along River Stretches Arising from Sewage Treatment Works Discharges. *Environmental Science & Technology,* 37**,** 1744-1750.

WPCF (1990) Natural Systems for Wastewater Treatment, Manual of Practice FD-16. Alexandria VA, Water Pollution Control Federation.

WU, C., SPONGBERG, A. L. & WITTER, J. D. (2009) Adsorption and degradation of triclosan and triclocarban in soils and biosolids-amended soils. *Journal of Agricultural and Food Chemistry,* 57**,** 4900-4905.

WU, C., SPONGBERG, A. L., WITTER, J. D., FANG, M. & CZAJKOWSKI, K. P. (2010) Uptake of pharmaceutical and personal care products by soybean plants from soils applied with biosolids and irrigated with contaminated water. *Environmental Science & Technology,* 44**,** 6157-6161.

WU, S. C. & LEE, C. M. (2011) Correlation between fouling propensity of soluble extracellular polymeric substances and sludge metabolic activity altered by different starvation conditions. *Bioresource Technology,* 102**,** 5375-5380.

WUTTKE, W., JARRY, H. & SEIDLOVA-WUTTKE, D. (2010) Definition, classification and mechanism of action of endocrine disrupting chemicals. *Hormones-International Journal of Endocrinology and Metabolism,* 9**,** 9-15.

XIA, K., HUNDAL, L. S., KUMAR, K., ARMBRUST, K., COX, A. E. & GRANATO, T. C. (2010) Triclocarban, triclosan, polybrominated diphenyl ethers, and 4-nonylphenol in biosolids and in soil receiving 33-year biosolids application. *Environmental Toxicology and Chemistry,* 29**,** 597-605.

XUE, S., ZHAO, Q.-L., WEI, L.-L. & REN, N.-Q. (2009) Behavior and characteristics of dissolved organic matter during column studies of soil aquifer treatment. *Water Research,* 43**,** 499-507.

YEN, S. S. C., JAFFE, R. B. & BARBIERI, R. L. (Eds.) (1999) *Reproductive Endocrinology: Physiology, Pathophysiology and Clinical Management. 4th Edition,* Pennsylvania, W.B. Saunders Company.

YI, T. & HARPER, W. F. (2007) The link between nitrification and biotransformation of 17α-ethinylestradiol. *Environmental Science & Technology,* 41**,** 4311-4316.

YING, G.-G., YU, X.-Y. & KOOKANA, R. S. (2007) Biological degradation of triclocarban and triclosan in a soil under aerobic and anaerobic conditions

and comparison with environmental fate modelling. *Environmental Pollution,* 150**,** 300-305.

YING, G. G., KOOKANA, R. S. & RU, Y. J. (2002) Occurrence and fate of hormone steroids in the environment. *Environment International,* 28**,** 545-551.

YONG, R. N., MOHAMED, A. M. O. & WARKENTIN, B. P. (1992) *Principles of Contaminant Transport in Soils,* Amsterdam, Elsevier Science Publishers B. V.

YOUNG, W. F., WHITEHOUSE, P., JOHNSON, I. & SOROKIN, N. (2004) Proposed Predicted-No-Effect-Concentrations (PNECs) for Natural and Synthetic Steroid Oestrogens in Surface Waters, R&D Technical Report P2-T04/1. Environment Agency.

YU, C.-P., ROH, H. & CHU, K.-H. (2007) 17β-estradiol-degrading bacteria isolated from activated sludge. *Environmental Science & Technology,* 41**,** 486-492.

YU, L., FINK, G., WINTGENS, T., MELINA, T. & TERNES, T. A. (2009) Sorption behavior of potential organic wastewater indicators with soils. *Water Research,* 43**,** 951-960.

YU, Y., HUANG, Q., WANG, Z., ZHANG, K., TANG, C., CUI, J., FENG, J. & PENG, X. (2011) Occurrence and behavior of pharmaceuticals, steroid hormones, and endocrine-disrupting personal care products in wastewater and the recipient river water of the Pearl River Delta, South China. *Journal of Environmental Monitoring,* 13**,** 871-878.

ZELLES, L. (1999) Fatty acid patterns of phospholipids and lipopolysaccharides in the characterisation of microbial communities in soil: a review. *Biology and Fertility of Soils,* 29**,** 111-129.

ZHANG, Z., FENG, Y., GAO, P., WANG, C. & REN, N. (2011) Occurrence and removal efficiencies of eight EDCs and estrogenicity in a STP. *Journal of Environmental Monitoring,* 13**,** 1366-1373.

ZHAO, J.-L., YING, G.-G., LIU, Y.-S., CHEN, F., YANG, J.-F. & WANG, L. (2010) Occurrence and risks of triclosan and triclocarban in the Pearl River system, South China: From source to the receiving environment. *Journal of Hazardous Materials,* 179**,** 215-222.

ZHAO, Q. L., XUE, S., YOU, S. J. & WANG, L. N. (2007) Removal and transformation of organic matter during soil-aquifer treatment. *Journal of Zhejiang University-Science A,* 8**,** 712-718.

APPENDIX A

Soil column photo gallery

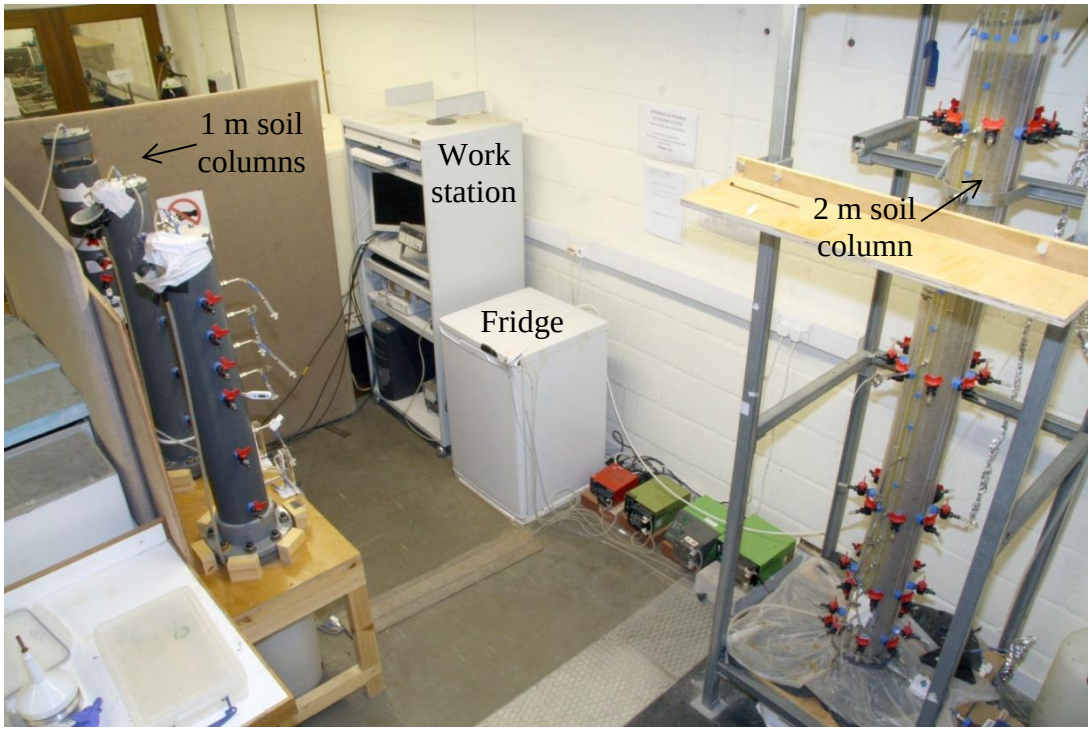

Laboratory arrangement of 1 m and 2 m soil column setup

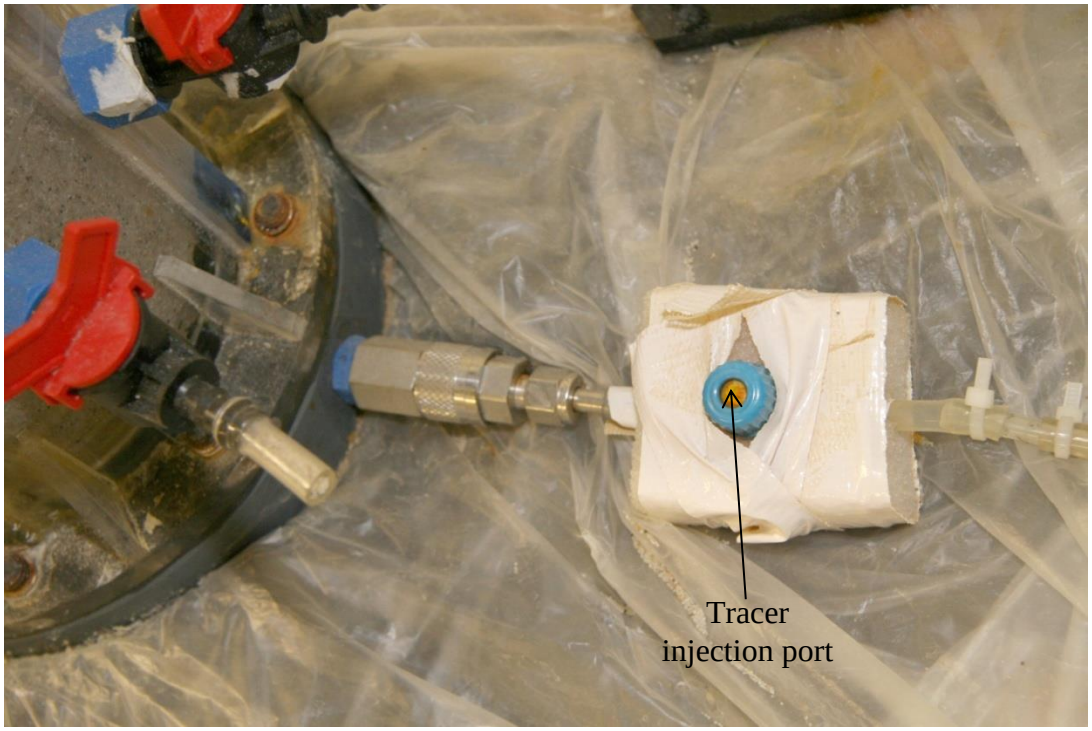

Tracer injection port to 2 m soil column

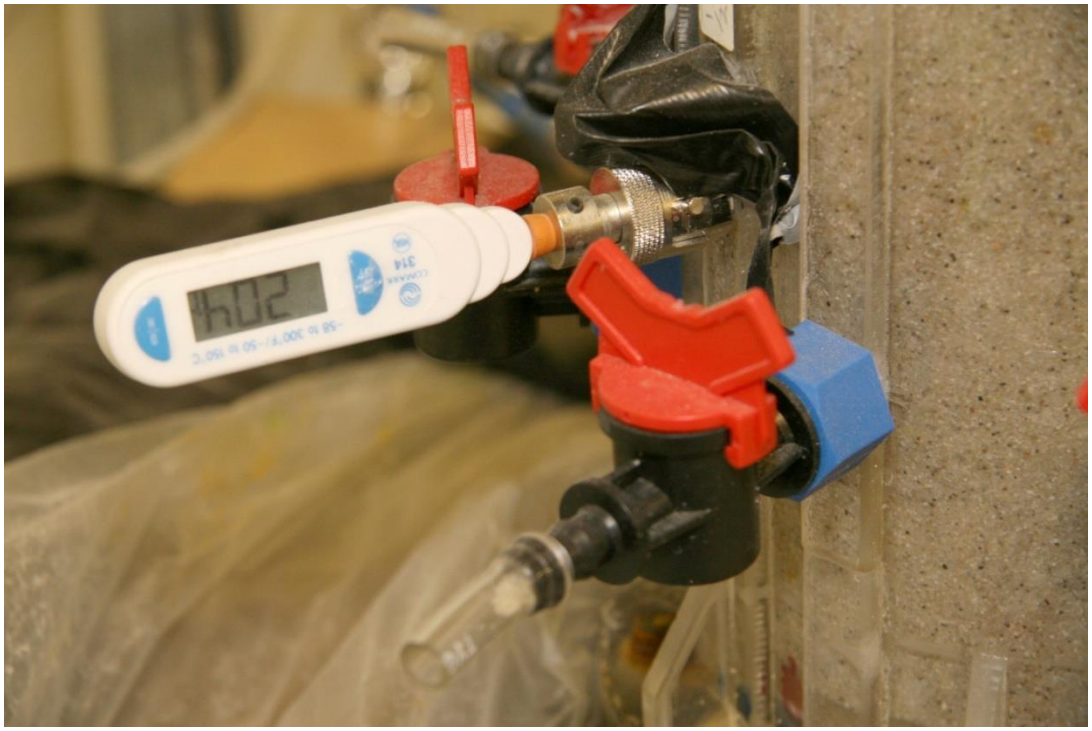

Temperature measurement

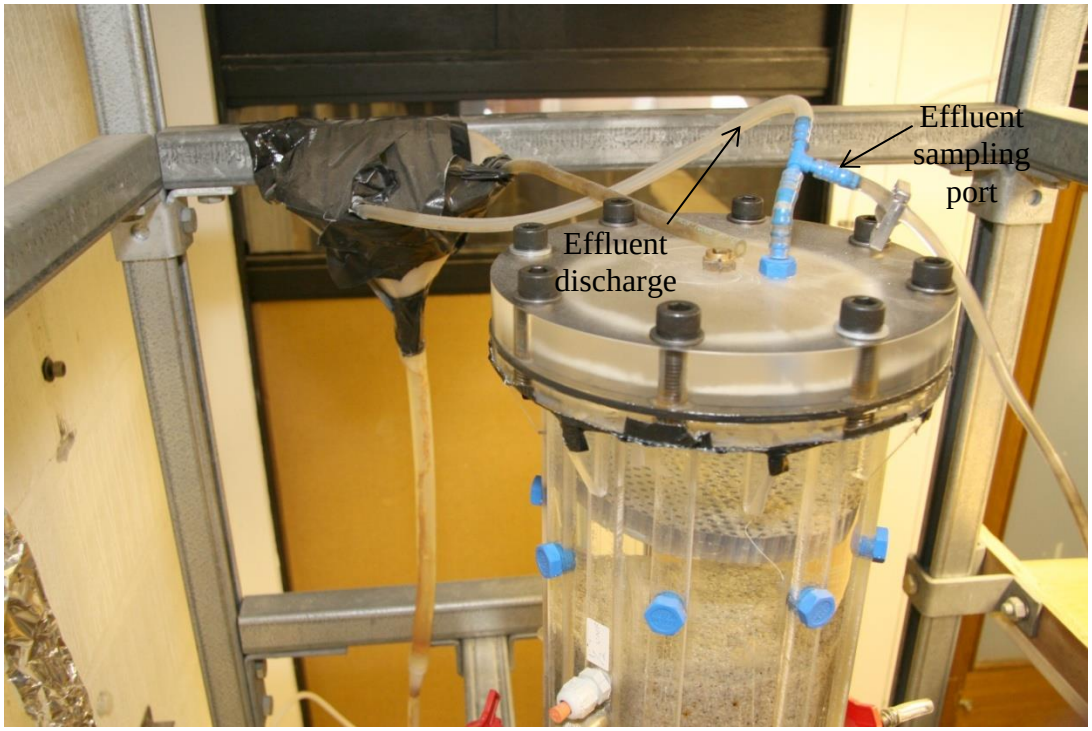

2 m soil column effluent discharge arrangement

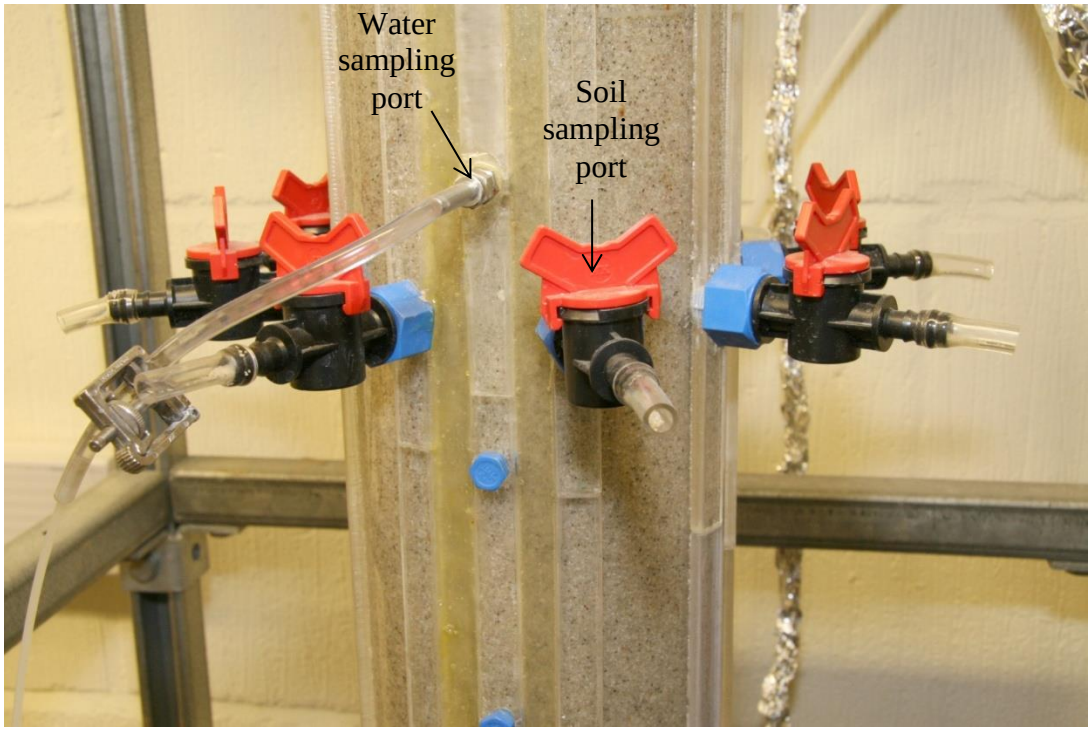

2 m soil column water and soil sampling ports

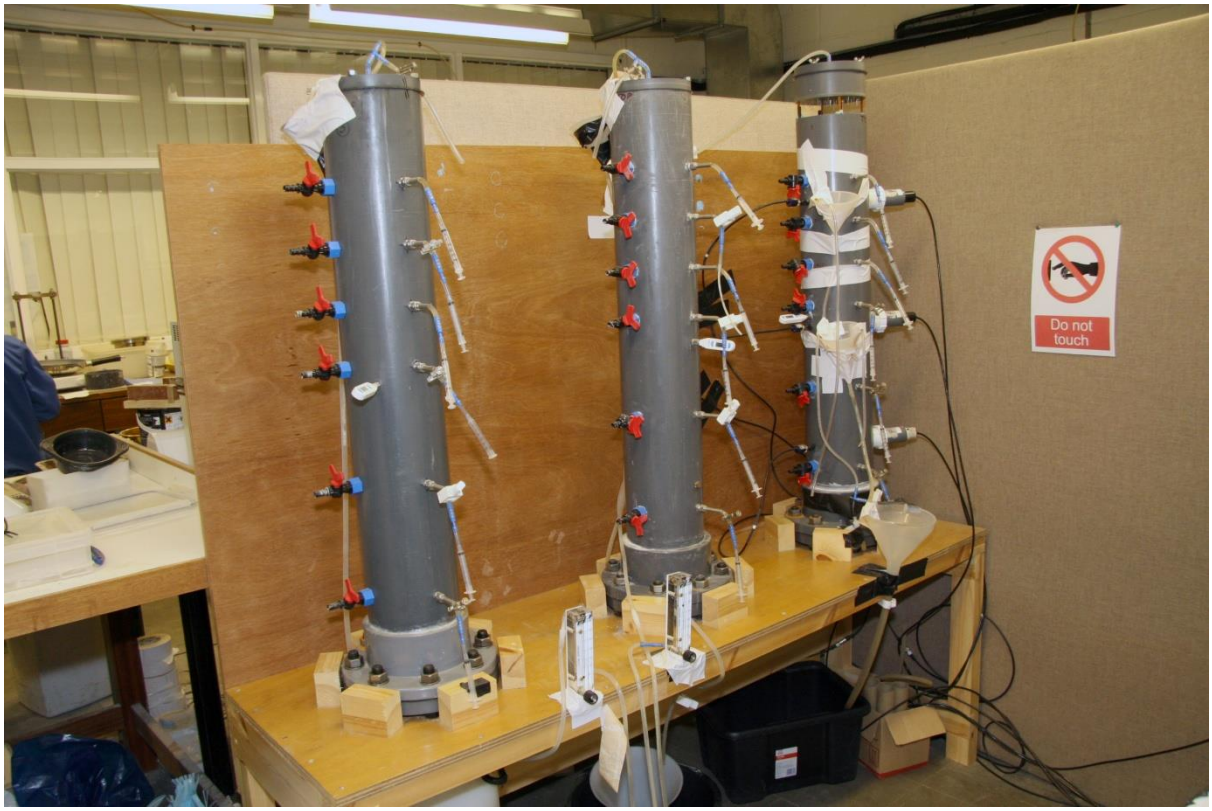

1 m soil columns setup – unsaturated soil column on extreme right

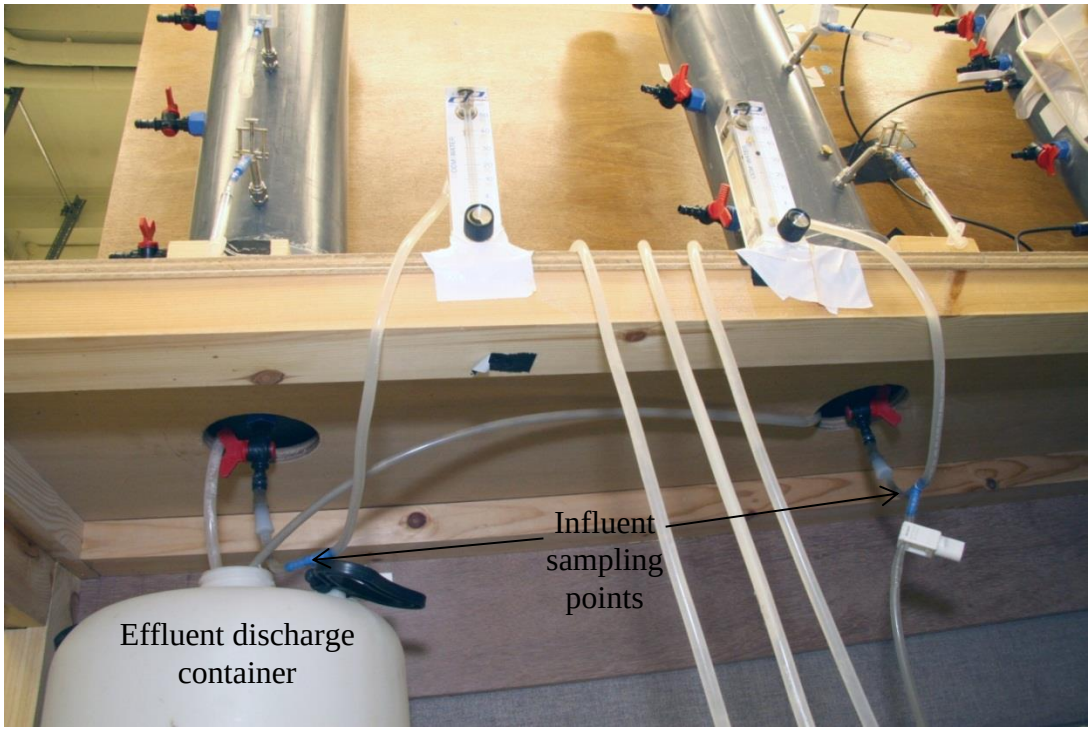

1 m saturated soil column influent sampling and effluent discharge points

1 m saturated soil column effluent sampling and discharge arrangement

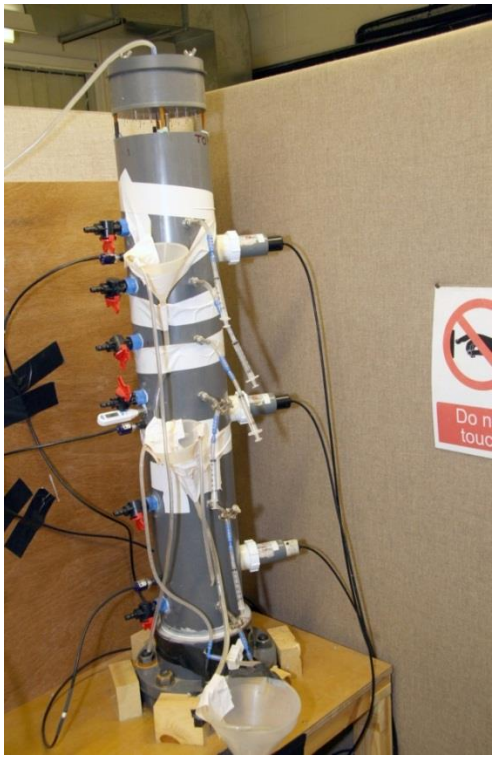

1 m unsaturated soil column

Unsaturated soil column instrumentation arrangement

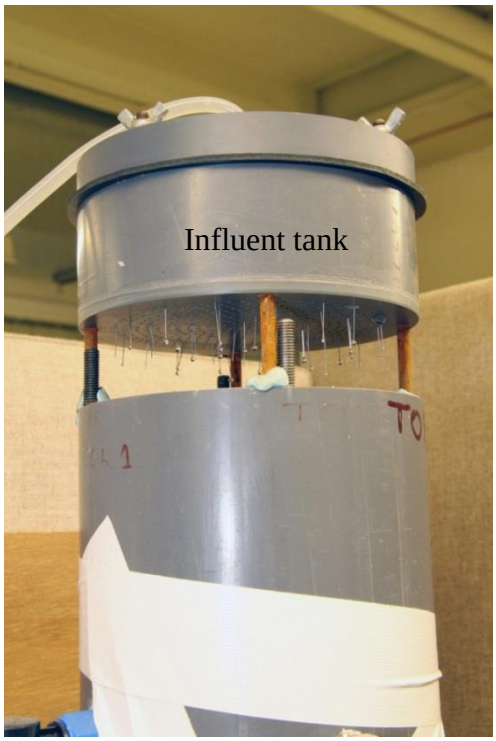

Unsaturated soil column influent application arrangement

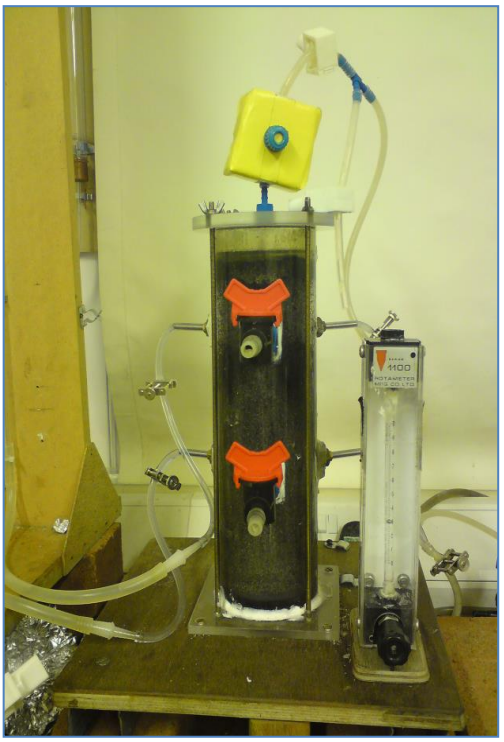

300 mm soil column

Influent and sample storage

Data acquisition system

APPENDIX B

Table B1 Mass of phosphate at various depths in 2m soil column under different experimental conditions

Depth	**Phosphate applied (mg d^{-1})**				
(mm)	**HC-5**	**HC-10**	**HC-20**	**MC-20**	**LC-20**
0	45.4	81.3	105.1	113.4	104.3
100	49.4	94.1	163.4	123.8	90.5
600	50.3	92.4	164.9	125.7	87.6
1100	49.5	93.2	165.0	126.5	92.1
1700	42.8	86.5	161.9	131.3	101.6
2000	40.3	83.8	166.1	105.7	105.2

Table B2 Removal rate of phosphate in 2m soil column under different experimental conditions

Depth	**Phosphate removed (mg d^{-1})**				
(mm)	**HC-5**	**HC-10**	**HC-20**	**MC-20**	**LC-20**
0	0.0	0.0	0.0	0.0	0.0
100	-3.9	-12.8	-58.3	-10.4	13.8
600	-4.9	-11.1	-59.9	-12.3	16.6
1100	-4.1	-11.9	-59.9	-13.1	12.2
1700	2.6	-5.2	-56.8	-17.9	2.7
2000	5.1	-2.5	-61.0	7.7	-0.9

Table B3 Mass of COD, DOC and BOD at various depths in 2m soil column under different experimental conditions

Depth (mm)	COD applied (mg d^{-1})					DOC applied (mg d^{-1})					BOD applied (mg d^{-1})				
	HC-5	HC-10	HC-20	MC-20	LC-20	HC-5	HC-10	HC-20	MC-20	LC-20	HC-5	HC-10	HC-20	MC-20	LC-20
0	910.7	1780.6	3552.5	1586.4	1083.7	340.2	661.1	1356.2	691.2	418.4	595.0	1113.1	1998.1	1124.3	680.8
100	695.3	1433.9	2719.2	1285.6	443.7	181.7	427.6	788.1	281.4	137.0	385.0	737.7	1544.1	533.6	249.7
600	665.2	1353.1	2605.5	1108.8	521.0	176.6	379.7	725.2	265.9	122.6	371.6	671.2	1288.6	483.7	118.6
1100	648.1	1251.1	2482.0	1176.5	492.3	170.7	362.1	680.6	251.1	115.7	379.3	617.5	1301.8	553.9	157.6
1700	646.9	1194.4	2434.9	1280.9	550.5	185.7	351.5	660.6	236.5	107.8	370.4	615.0	1279.3	538.3	170.1
2000	661.4	1212.7	2528.2	1376.4	501.9	168.7	339.8	639.8	241.9	109.1	348.2	637.6	1442.9	667.8	223.1

Table B4 Removal rate of COD, DOC and BOD in 2m soil column under different experimental conditions

Depth (mm)	COD removed (mg d^{-1})					DOC removed (mg d^{-1})					BOD removed (mg d^{-1})				
	HC-5	HC-10	HC-20	MC-20	LC-20	HC-5	HC-10	HC-20	MC-20	LC-20	HC-5	HC-10	HC-20	MC-20	LC-20
0	0.0	0.0	0.0	0.0	0.0	0.0	0.0	0.0	0.0	0.0	0.0	0.0	0.0	0.0	0.0
100	215.4	346.6	833.2	300.8	640.0	158.5	233.5	568.2	409.9	281.5	210.0	375.4	454.0	590.6	431.2
600	245.5	427.5	947.0	477.6	562.7	163.6	281.5	631.0	425.3	295.9	223.3	441.8	709.4	640.5	562.3
1100	262.6	529.5	1070.4	409.9	591.3	169.5	299.0	675.6	440.2	302.7	215.6	495.6	696.3	570.3	523.2
1700	263.8	586.1	1117.5	305.5	533.2	154.5	309.7	695.6	454.7	310.7	224.5	498.0	718.8	585.9	510.8
2000	249.3	567.9	1024.2	210.0	581.8	171.6	321.4	716.4	449.3	309.4	246.8	475.4	555.2	456.4	457.7

Table B5 Mass of dissolved oxygen, nitrate and sulphate at various depths in 2m soil column under different experimental conditions

Depth	**DO applied (mg d^{-1})**					**Nitrate applied (mg d^{-1})**					**Sulphate applied (mg d^{-1})**				
(mm)	**HC-5**	**HC-10**	**HC-20**	**MC-20**	**LC-20**	**HC-5**	**HC-10**	**HC-20**	**MC-20**	**LC-20**	**HC-5**	**HC-10**	**HC-20**	**MC-20**	**LC-20**
0	53.3	101.7	218.5	251.0	278.8	16.6	26.9	39.0	59.8	62.7	341.4	690.5	1654.8	1475.1	1301.6
100	23.2	33.7	67.4	77.9	82.8	1.2	4.4	5.0	4.0	6.0	7.0	77.9	249.0	712.9	990.3
600	20.7	38.5	72.6	98.9	80.7	0.8	0.0	0.0	0.0	0.0	8.2	27.2	68.2	670.9	947.6
1100	16.0	24.7	53.9	40.9	73.7	0.0	0.0	0.0	0.0	11.7	9.2	29.8	58.2	581.8	919.1
1700	18.4	43.9	94.2	43.6	94.2	0.0	0.0	0.0	0.0	11.7	10.1	30.9	49.7	510.4	836.4
2000	5.7	18.5	36.5	47.7	49.0	0.0	0.0	0.0	0.0	5.8	9.6	30.2	56.0	445.7	795.0

Table B6 Removal rate of dissolved oxygen, nitrate and sulphate in 2m soil column under different experimental conditions

Depth	**DO removed (mg d^{-1})**					**Nitrate removed (mg d^{-1})**					**Sulphate removed (mg d^{-1})**				
(mm)	**HC-5**	**HC-10**	**HC-20**	**MC-20**	**LC-20**	**HC-5**	**HC-10**	**HC-20**	**MC-20**	**LC-20**	**HC-5**	**HC-10**	**HC-20**	**MC-20**	**LC-20**
0	0.0	0.0	0.0	0.0	0.0	0.0	0.0	0.0	0.0	0.0	0.0	0.0	0.0	0.0	0.0
100	30.1	68.0	151.1	173.0	195.9	15.4	22.5	34.0	55.9	56.7	334.4	612.6	1405.8	762.2	311.3
600	32.6	63.2	145.9	152.1	198.1	15.8	26.9	39.0	59.8	62.7	333.2	663.3	1586.6	804.1	354.0
1100	37.3	77.0	164.6	210.1	205.1	16.6	26.9	39.0	59.8	51.0	332.2	660.7	1596.6	893.3	382.6
1700	34.9	57.8	124.2	207.3	184.6	16.6	26.9	39.0	59.8	50.9	331.3	659.6	1605.1	964.6	465.2
2000	47.6	83.2	182.0	203.3	229.7	16.6	26.9	39.0	59.8	56.9	331.8	660.2	1598.8	1029.3	506.6

Table B7 Mass of nitrogen species at various depths in 2m soil column under different experimental conditions

Depth	Organic-N applied (mg d^{-1})					Ammonia-N applied (mg d^{-1})					Total N applied (mg d^{-1})				
(mm)	HC-5	HC-10	HC-20	MC-20	LC-20	HC-5	HC-10	HC-20	MC-20	LC-20	HC-5	HC-10	HC-20	MC-20	LC-20
0	74.4	129.5	262.7	127.4	71.0	25.2	48.6	94.7	43.7	36.4	111.0	205.3	390.1	230.9	170.1
100	19.4	44.9	89.9	53.8	33.2	69.4	121.9	242.3	114.8	58.6	92.2	181.9	335.4	171.7	91.4
600	16.4	36.7	72.9	41.0	23.4	70.3	123.5	253.4	118.6	67.0	89.5	178.2	326.3	158.2	87.4
1100	15.1	29.2	66.6	45.4	33.0	68.3	124.2	255.0	130.1	69.6	85.8	169.0	320.4	173.5	108.2
1700	17.9	29.9	74.0	41.8	31.6	65.1	117.9	250.5	131.6	89.6	83.9	170.1	323.9	173.0	126.5
2000	21.3	33.1	63.7	39.4	30.1	64.7	115.5	251.6	137.2	79.2	82.9	164.3	316.6	174.9	111.6

Table B8 Removal rate of nitrogen species in 2m soil column under different experimental conditions

Depth	Organic-N removed (mg d^{-1})					Ammonia –N increase (mg d^{-1})					Total N removed (mg d^{-1})				
(mm)	HC-5	HC-10	HC-20	MC-20	LC-20	HC-5	HC-10	HC-20	MC-20	LC-20	HC-5	HC-10	HC-20	MC-20	LC-20
0	0.0	0.0	0.0	0.0	0.0	0.0	0.0	0.0	0.0	0.0	0.0	0.0	0.0	0.0	0.0
100	54.9	84.6	172.8	73.6	37.8	44.2	73.3	147.6	71.1	22.2	18.7	23.4	54.7	59.2	78.7
600	58.0	92.8	189.8	86.5	47.6	45.1	74.9	158.8	74.9	30.6	21.4	27.1	63.8	72.7	82.7
1100	59.3	100.3	196.1	82.0	38.0	43.1	75.6	160.4	86.4	33.2	25.1	36.3	69.7	57.4	61.9
1700	56.4	99.6	188.6	85.6	39.4	39.9	69.2	155.9	87.9	53.2	27.1	35.2	66.2	57.9	43.6
2000	53.1	96.4	199.0	88.0	40.9	39.5	66.9	156.9	93.5	42.8	28.1	41.0	73.5	56.0	58.5

Table B9 Removal efficiencies in 2 meter column under abiotic conditions

Column depth (mm)	**Removal efficiency (%)**		
	COD	**DOC**	**Ammonia-N**
0	0	0	0
100	4.2	1.1	15.4
600	6.3	2.8	23.1
1100	4.2	0.6	23.1
1700	4.2	0.6	61.5
2000	4.2	0.6	69.2

Table B10 DOC and sulphate removal efficiencies in SC1

Column height(mm)	**DOC removal efficiency (%)**			**Sulphate removal efficiency (%)**		
	WT75	**WT500**	**WT800**	**WT75**	**WT500**	**WT800**
1000	0	0	0	0	0	0
850			85			2.1
750			86			3.9
550		82	86		-9.2	4.7
350		82	85		-11.5	1.3
150	89	81	82	-0.4	-10.8	1.4
0	86	82	80	-0.7	-12.7	0.3

Table B11 Nitrogen removal efficiencies in SC1

Column height (mm)	**Nitrate increase (%)**			**Ammonia-N removal efficiency (%)**			**Organic-N removal efficiency (%)**		
	WT 75	**WT 500**	**WT 800**	**WT 75**	**WT 500**	**WT 800**	**WT75**	**WT 500**	**WT 800**
1000	0	0	0	0	0	0	0	0	0
850			190			100			88
750			194			100			88
550		73	152		90	69		55	100
350		174	270		100	69		82	94
150	371	364	51	100	90	23	100	91	100
0	590	405	67	92	100	23	85	100	71

Table B12 Estrogen percentage removal efficiencies of E1, E2 and EE2 at varying heights of water table in SC1

Column height (mm)	**Removal efficiency for WT75 (%)**			**Removal efficiency for WT500 (%)**			**Removal efficiency for WT800 (%)**		
	E1	**E2**	**EE2**	**E1**	**E2**	**EE2**	**E1**	**E2**	**EE2**
1000	0	0	0	0	0	0	0	0	0
850							-85	100	2
750							-1	85	18
650							-30	84	17
550				97	100	57	-101	91	19
350				94	100	68	-57	80	53
150	100	100	94	100	100	86	22	88	68
0	100	100	100	98	100	99	91	100	89

Table B13 DOC, dissolved oxygen, nitrate and sulphate removal efficiencies in SC2 and SC3

Column height (mm)	**DOC removal efficiency (%)**		**DO removal efficiency (%)**		**Nitrate removal efficiency (%)**		**Sulphate removal efficiency (%)**	
	SC2	**SC3**	**SC2**	**SC3**	**SC2**	**SC3**	**SC2**	**SC3**
0	0	0	0	0	0	0	0	0
150	66	65	76	81	92	100	14	12
350	73	65	77	78	100	100	8	8
550	74	65	78	71	100	100	12	11
750	75	66	55	71	92	93	13	15
1000	78	68	68	64	92	100	13	16

Table B14 Estrogen removal efficiencies of E1, E2 and EE2 at hydraulic loading rate of 81.5 cm d^{-1} and DOC of 17 mg L^{-1} for SC2 and SC3

Column height(mm)	SC3 removal efficiency (%)			SC2 removal efficiency (%)		
	E1(81.5)	E2(81.5)	EE2(81.5)	E1(81.5)	E2(81.5)	EE2(81.5)
0	0	0	0	0	0	0
150	-20	60	32	-91	-17	-27
350	-53	54	26	-166	19	-40
550	-48	60	32	-145	53	-15
750	-33	65	44	-58	67	19
1000	34	83	61	43	77	59

Table B15 Estrogen removal efficiency at hydraulic loading rate of 163 cm d^{-1} and DOC of 17 mg L^{-1} for SC2 and SC3

Column height (mm)	SC3 removal efficiency (%)			SC2 removal efficiency (%)		
	E1(163)	E2(163)	EE2(163)	E1(163)	E2(163)	EE2(163)
0	0	0	0	0	0	0
150	-4	51	45	-76	7	-13
350	-17	40	34	-73	2	-23
550	-10	41	33	-59	5	-13
750	8	50	37	-35	36	12
1000	27	58	45	16	53	33

Table B16 Estrogen percentage removal efficiency at hydraulic loading rate of 81.5 cm d^{-1} and DOC of 34 mg L^{-1} for SC2 and SC3

Column height (mm)	SC3 removal efficiency (%)			SC2 removal efficiency (%)		
	E1 (34)	E2 (34)	EE2 (34)	E1 (34)	E2 (34)	EE2 (34)
0	0	0	0	0	0	0
150	-25	49	38	-185	-55	-78
350	-20	66	48	-95	23	-7
550	-8	66	49	-59	41	11
750	0.3	71	53	-24	53	24
1000	55	81	71	67	86	67

Table B17 COD at various depths in 300 mm soil column

Day	**COD (mg L^{-1}) at**		
	0 cm	**8 cm**	**19 cm**
5	66	24	21
8	69	43	-
12	67	41	15
19	66	39	35
24	79	-	-
27	72	-	-
33	66	22	25
36	70	22	20
39	67	37	31
43	68	44	63
46	68	62	59
49	80	68	65

Table B18 TCC removal efficiency in 300 mm soil column

Column depth (cm)	**Removal efficiency (%)**				
	783 ng L^{-1} (Day 0)	**1112 ng L^{-1} (Day 3)**	**2130 ng L^{-1} (Day 7)**	**3501 ng L^{-1} (Day 10)**	**2372 ng L^{-1} (Day 13)**
0	0	0	0	0	0
8	94	67	29	44	10
19	98	89	66	57	17
30	100	96	71	68	32

Figure B1 Chloride calibration curve

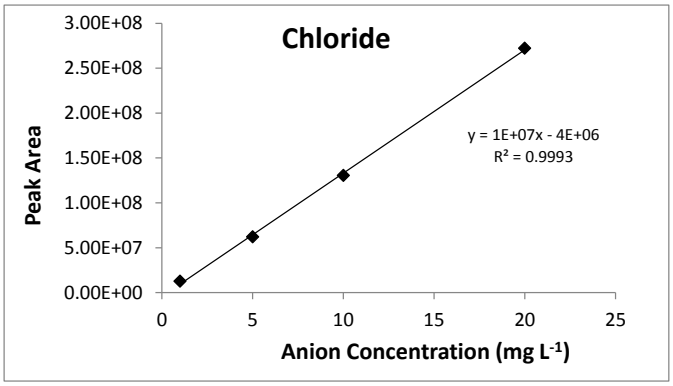

Figure B2 Bacterial Methyl Ester (BAME) calibration curves

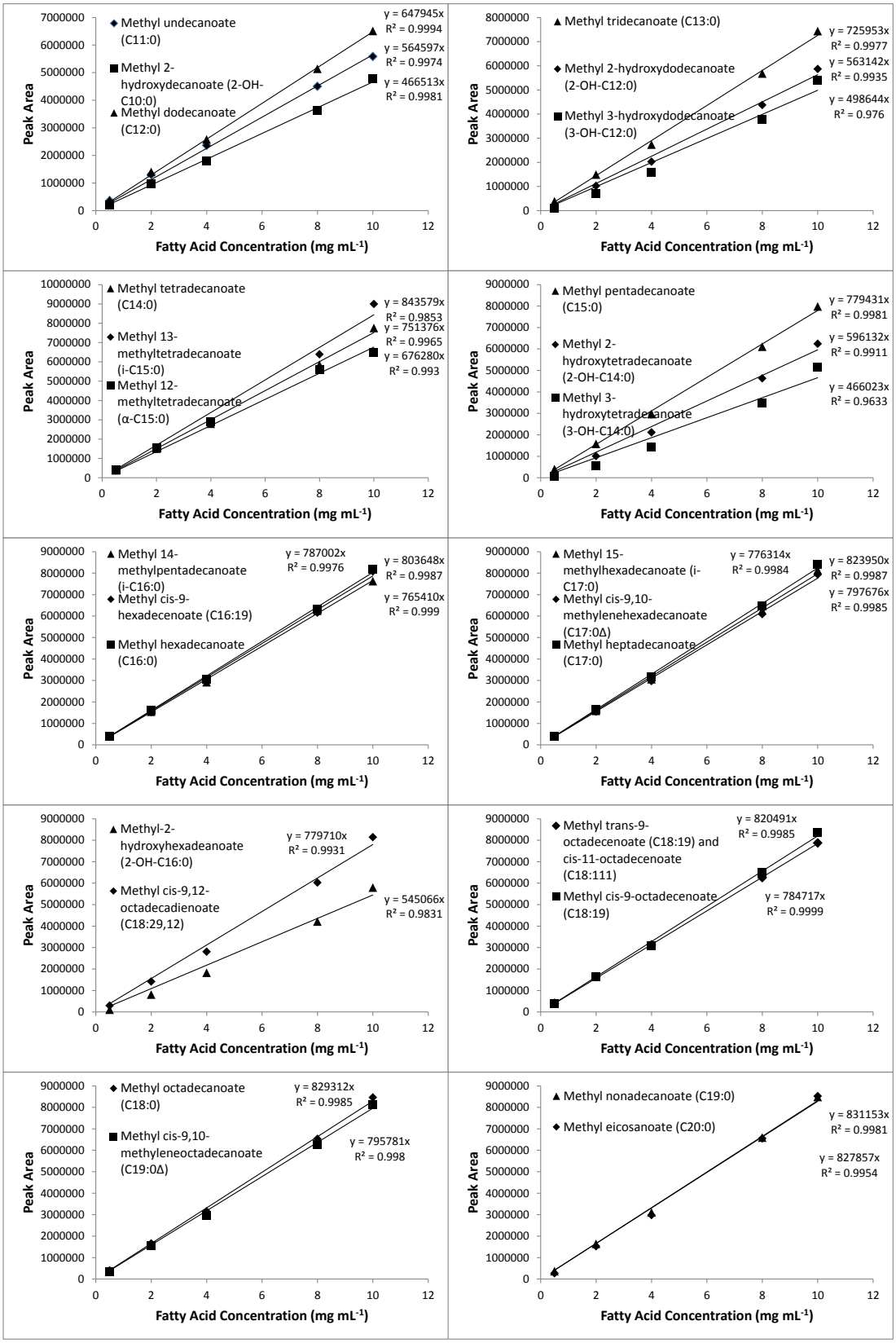

Figure B3 Sample moisture content and pressure readings in 1 meter unsaturated soil column

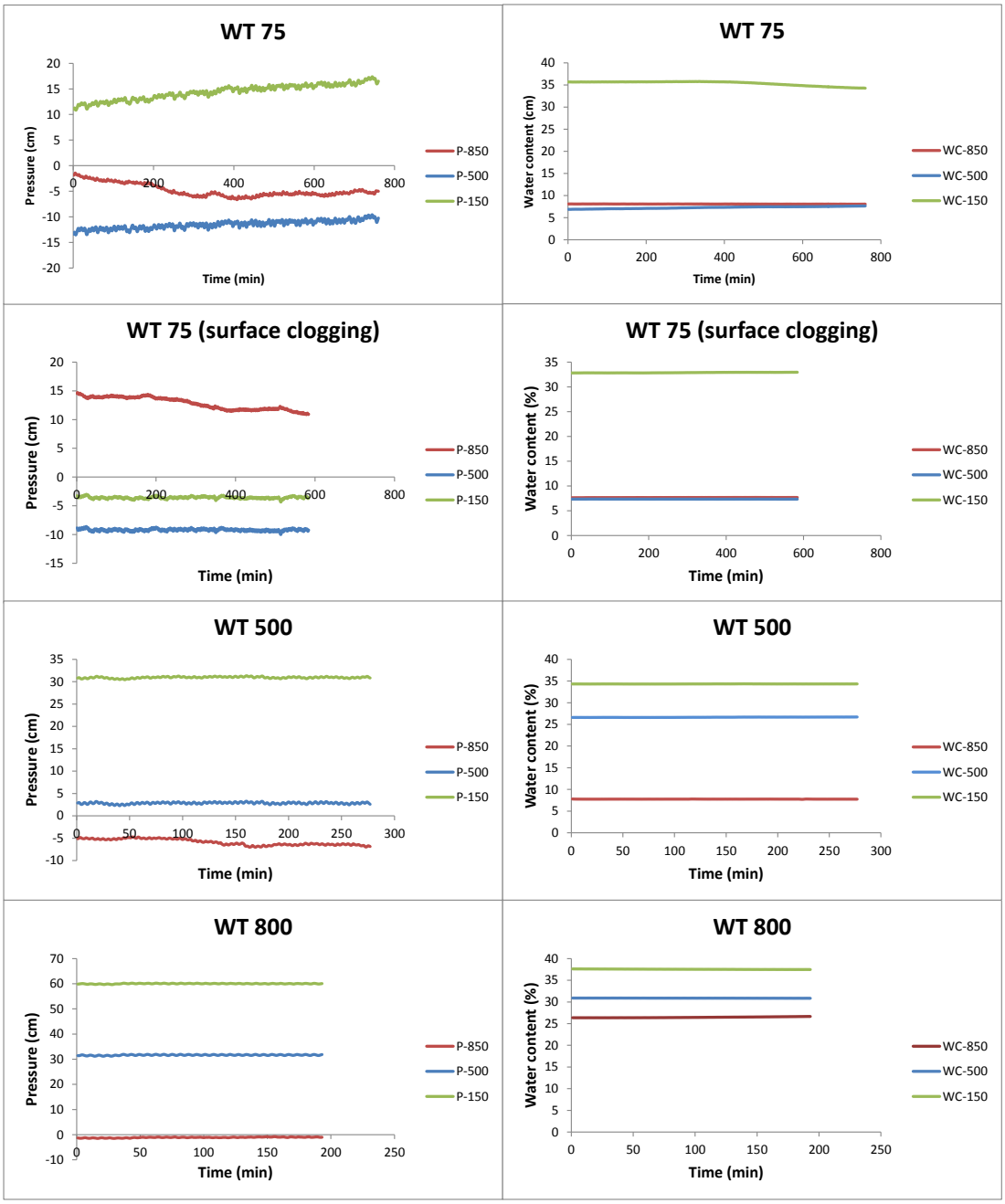

APPENDIX C

Tables C1 a – h Structures and IUPAC names of fatty acids identified in soil columns SC2 and SC3

Table C1 a

Type of Fatty Acid	**Shorthand designation**	**Quality**
Undecanoic acid, methyl ester ($C_{12}H_{24}O_2$ methyl undecanoate 	11:0	97
Dodecanoic acid, methyl ester ($C_{13}H_{26}O_2$) methyl dodecanoate 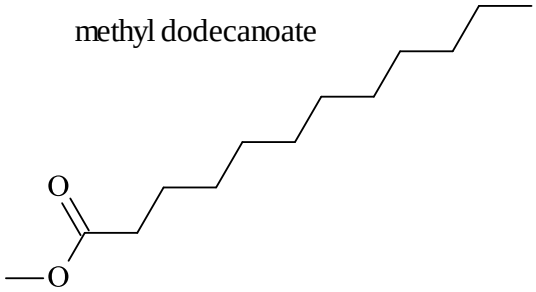	12:0	96
Tridecanoic acid, methyl ester ($C_{14}H_{28}O_2$) methyl tridecanoate 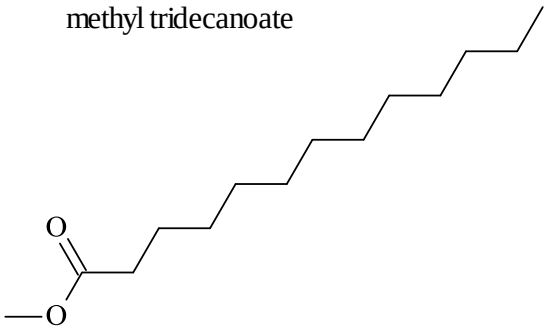	13:0	97
Tetradecanoic acid, methyl ester ($C_{15}H_{30}O_2$) methyl tetradecanoate 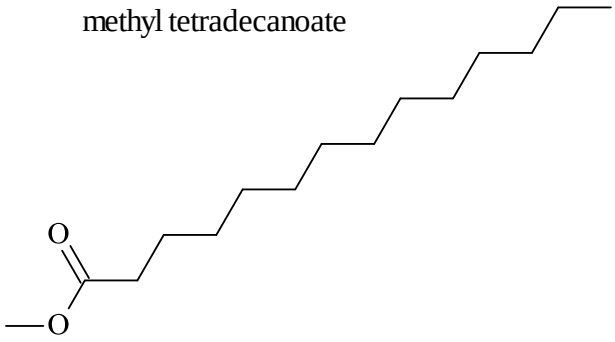	14:0	97

Table C1 b

Type of Fatty Acid	**Shorthand designation**	**Quality**
Methyl 9-methyltetradecanoate ($C_{16}H_{32}O_2$) methyl 9-methyltetradecanoate 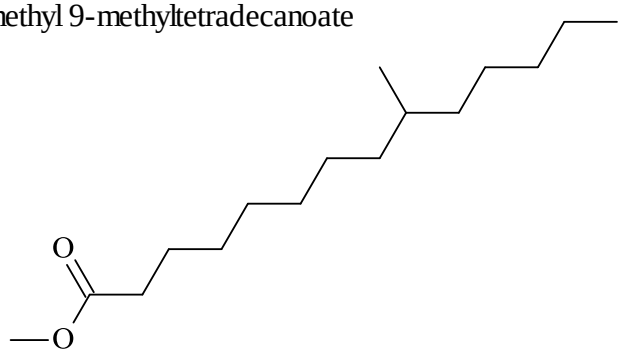	9Me15:0	95
Tetradecanoic acid, 12-methyl-, methyl ester ($C_{16}H_{32}O_2$) methyl 12-methyltetradecanoate 	a15:0	90
Pentadecanoic acid, methyl ester ($C_{16}H_{32}O_2$) methyl pentadecanoate 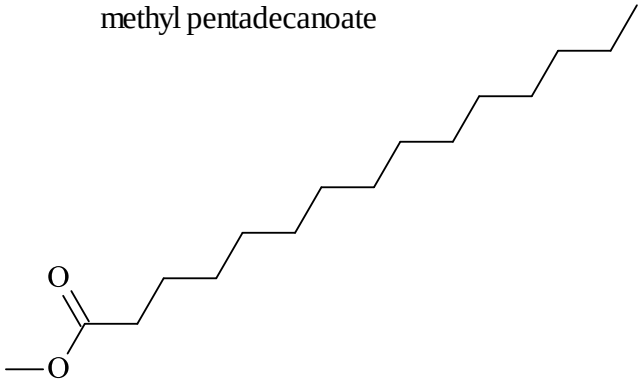	15:0	98

Table C1 c

Type of Fatty Acid	**Shorthand designation**	**Quality**
Tetradecanoic acid, 2-hydroxy-, methyl ester ($C_{15}H_{30}O_3$) methyl 2-hydroxytetradecanoate 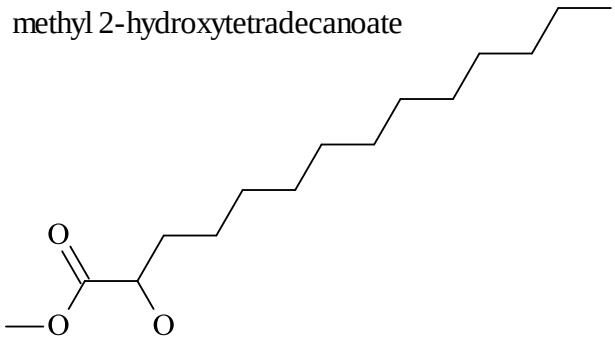	2-OH 14:0	99
Methyl 3-hydroxytetradecanoate ($C_{15}H_{30}O_3$) methyl 3-hydroxytetradecanoate 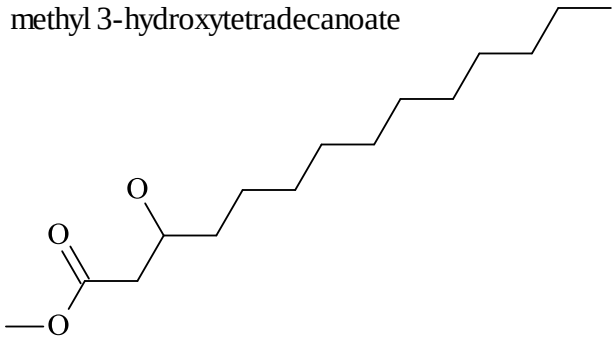	3-OH 14:0	91
Pentadecanoic acid, 14-methyl-, methyl ester ($C_{17}H_{34}O_2$) methyl 14-methylpentadecanoate 	i16:0	97

Table C1 d

Type of Fatty Acid	**Shorthand designation**	**Quality**
9-Hexadecenoic acid, methyl ester, (Z)- ($C_{17}H_{32}O_2$) methyl (Z)-hexadec-9-enoate 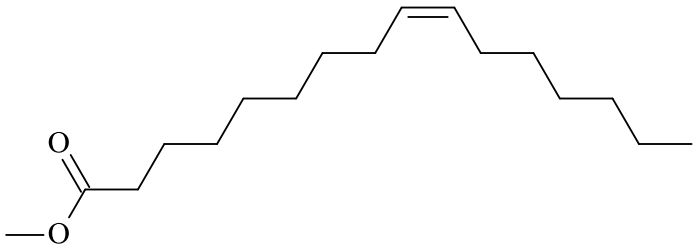	16:1ω7	99
Hexadecanoic acid, methyl ester ($C_{17}H_{34}O_2$) methyl hexadecanoate 	16:0	98
Hexadecanoic acid, 14-methyl-, methyl ester ($C_{18}H_{36}O_2$) methyl 14-methylhexadecanoate 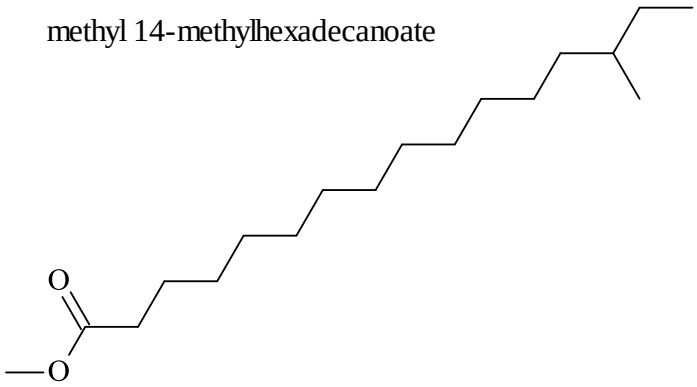	a17:0	97

Table C1 e

Type of Fatty Acid	**Shorthand designation**	**Quality**
Cyclopropaneoctanoic acid, 2-hexyl-, methyl ester ($C_{18}H_{34}O_2$) 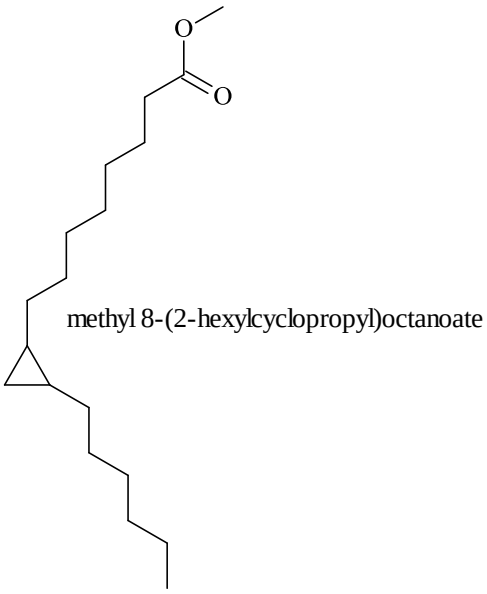	cy17:0	96
Heptadecanoic acid, methyl ester ($C_{18}H_{36}O_2$) 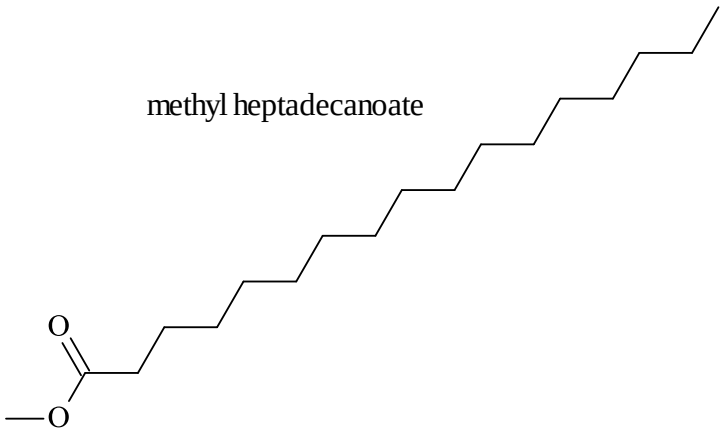	17:0	99
Hexadecanoic acid, 2-hydroxy-, methyl ester ($C_{17}H_{34}O_3$) 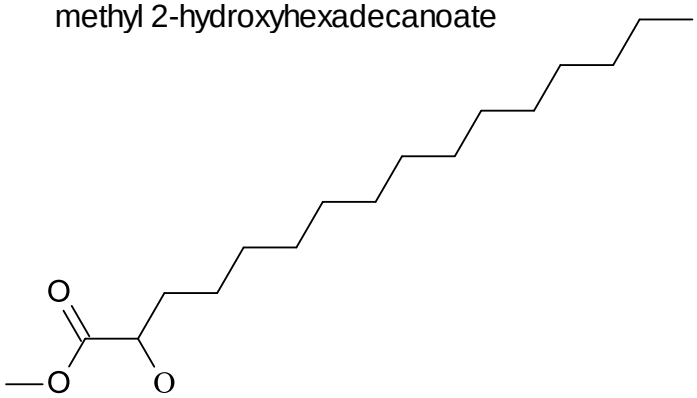	2-OH 16:0	

Table C1 f

Type of Fatty Acid	**Shorthand designation**	**Quality**
9,12-Octadecadienoic acid, methyl ester, (E,E)- ($C_{19}H_{34}O_2$) methyl (9E,12E)-octadeca-9,12-dienoate 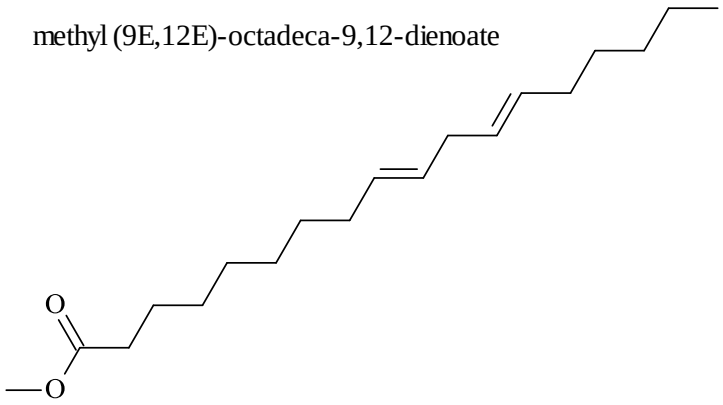	18:2ω6	99
8-Octadecenoic acid, methyl ester ($C_{19}H_{36}O_2$) methyl (E)-octadec-8-enoate 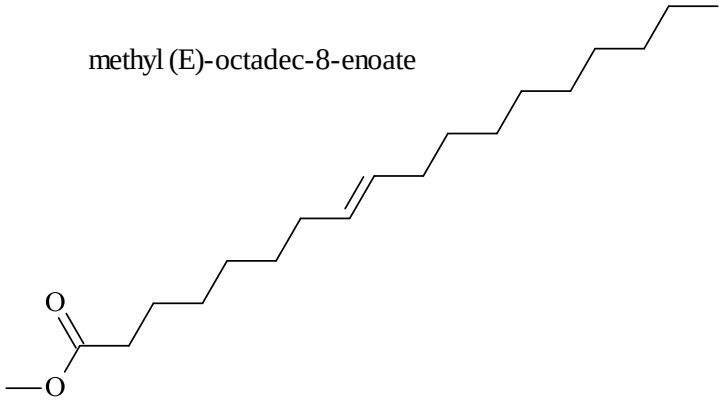	18:1ω10	99
9-Octadecenoic acid, methyl ester, (E) ($C_{19}H_{36}O_2$) methyl (E)-octadec-9-enoate 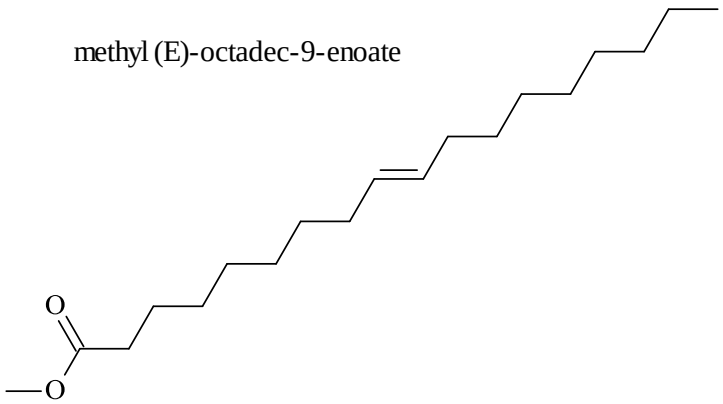	18:1ω9	99

Table C1 g

Type of Fatty Acid	**Shorthand designation**	**Quality**
Octadecanoic acid, methyl ester ($C_{19}H_{38}O_2$) methyl octadecanoate 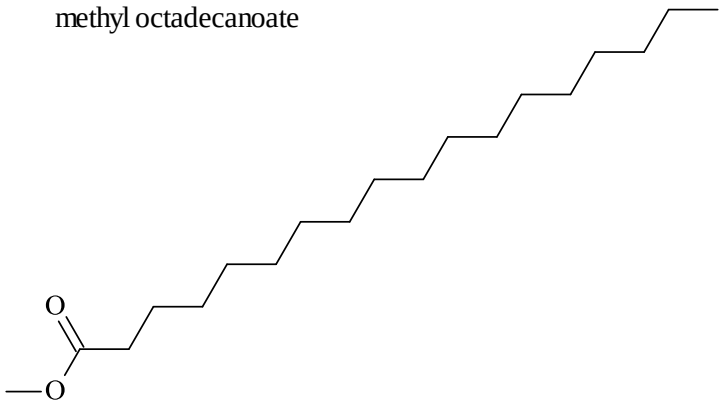	18:0	97
Cyclopropaneoctanoic acid, 2-octyl-, methyl ester ($C_{20}H_{38}O_2$) 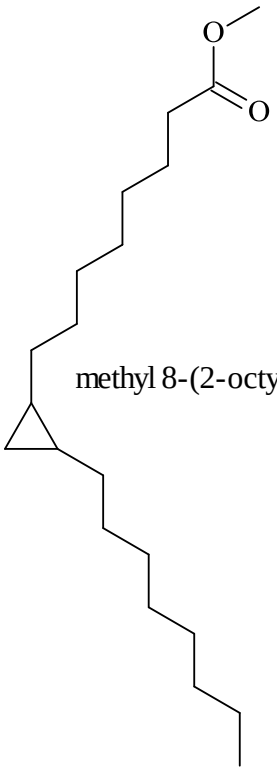 methyl 8-(2-octylcyclopropyl)octanoate	cy19:0	99

Table C1 h

Type of Fatty Acid	**Shorthand designation**	**Quality**
Nonadecanoic acid, methyl ester ($C_{20}H_{40}O_2$) 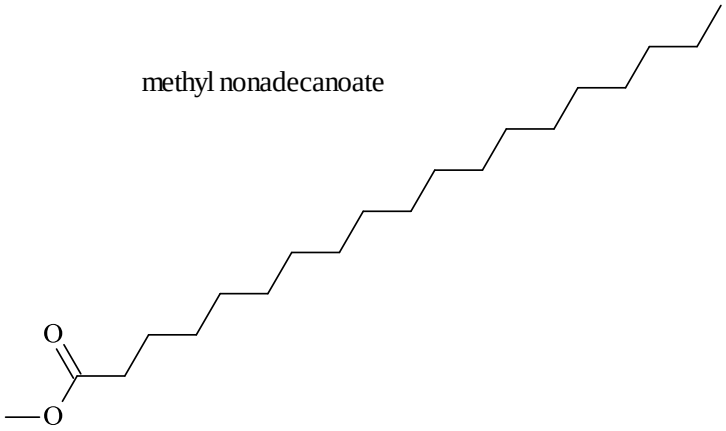	19:0	98
Eicosanoic acid, methyl ester ($C_{21}H_{42}O_2$) 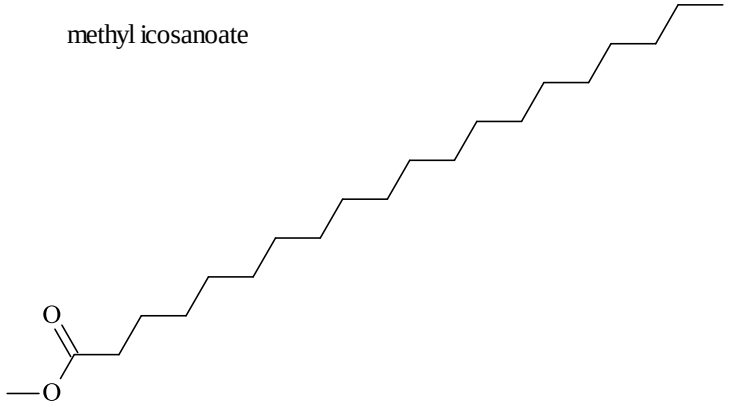	20:0	99

Figure C1 Sample chromatogram for fatty acid analysis

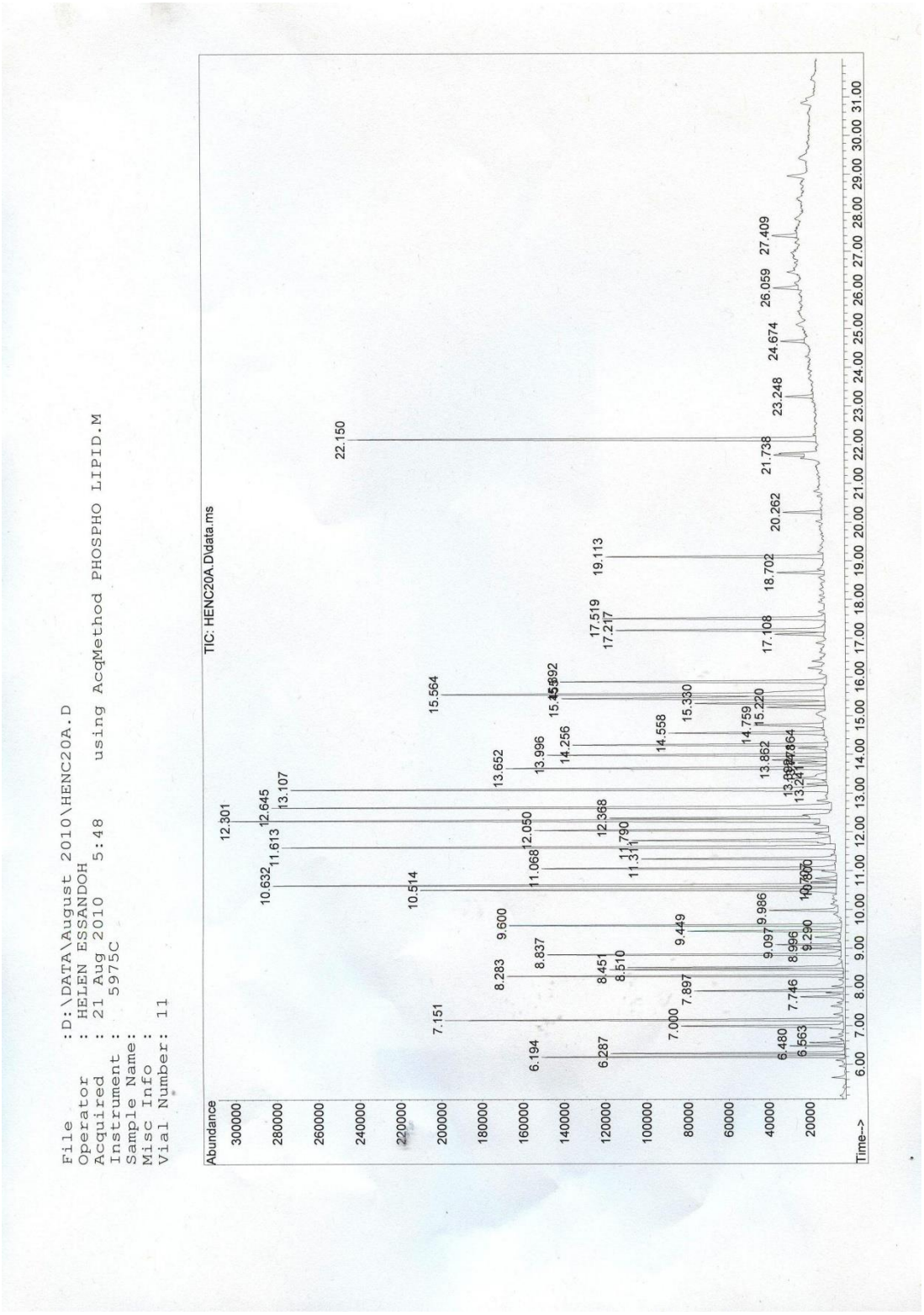

Figure C2 Sample chromatograms for 17α-ethinylestradiol (EE2), 17β-estradiol (E2) and estrone (E1) analysis

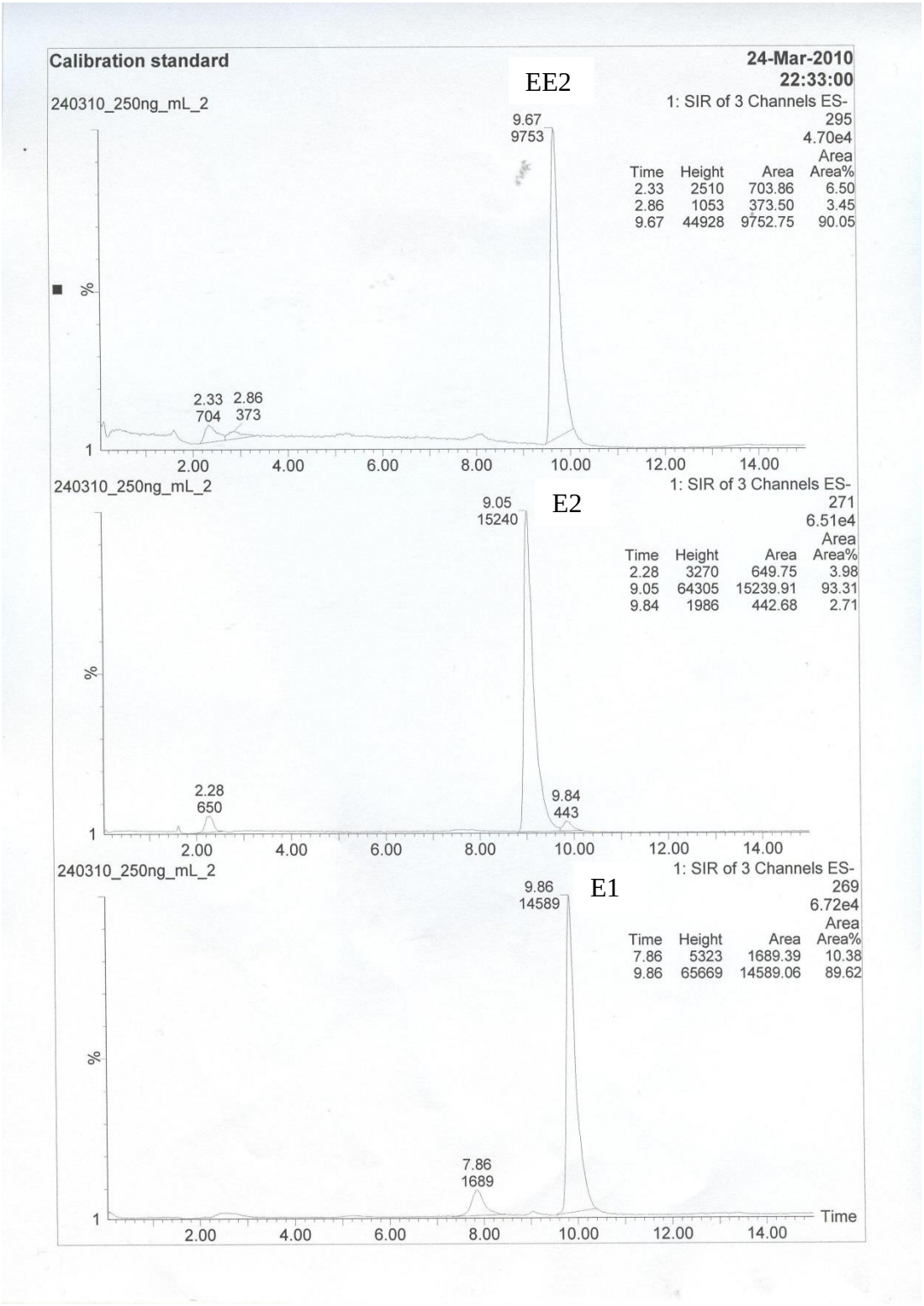

Figure C3 Sample chromatogram for TCC analysis

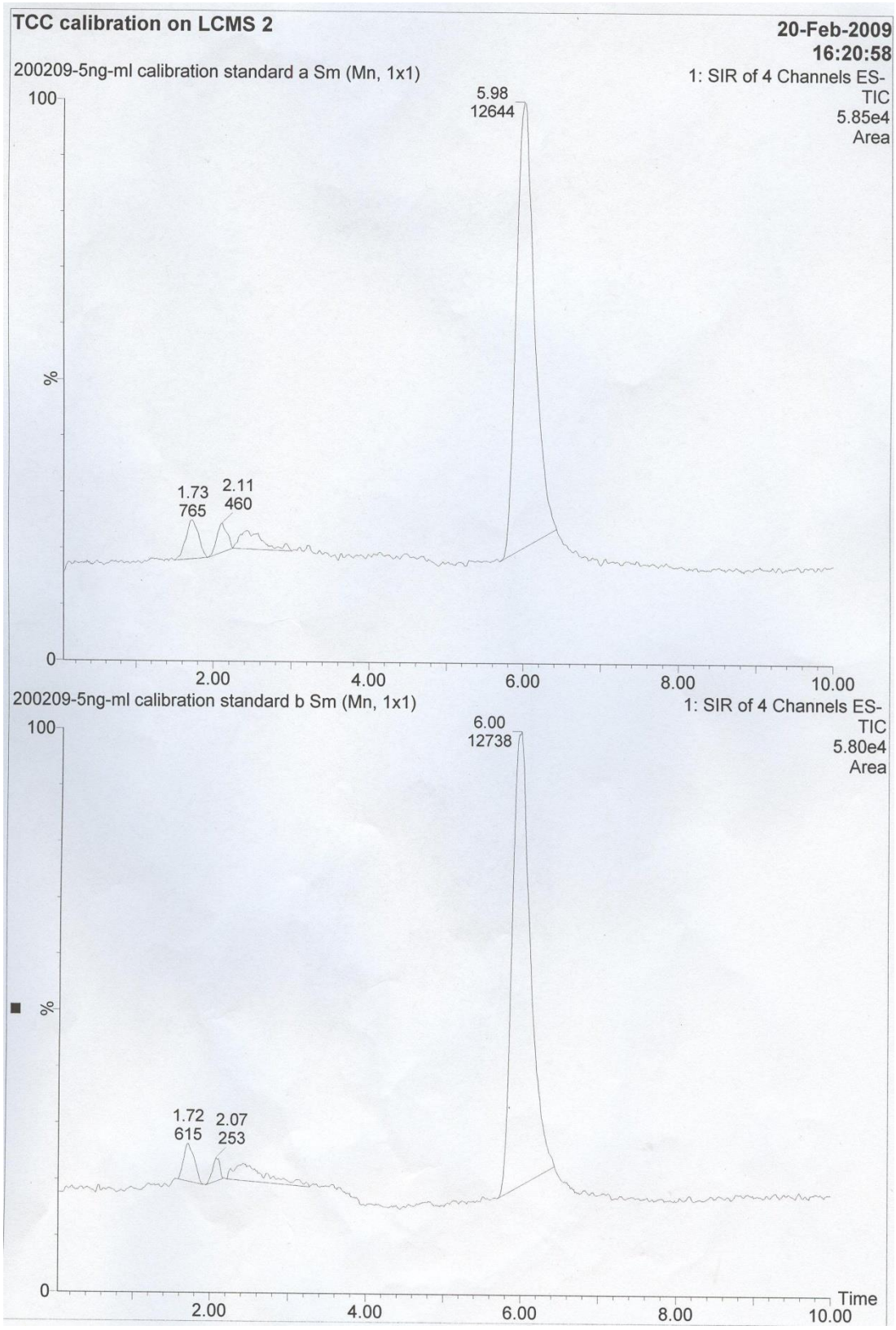

APPENDIX D

MATLAB code for estimation of COD rate constants using nonlinear squares approximation

```
function enorm = CODfitfun2(x,cdata,ydata)
%ENORM Norm of fit to function
%  g = (co - ((D * x(1)/u^2)* (co - (D/u^2)* (x(1) * co/(x(2) +
co)))/((x(2) + co - (D/u^2)*(x(1) * co/(x(2) + co)))* (1 + (D * x(1)
* x(2))/(u^2 *(x(2) + co)^2)))));
% f(c)=((u/x(1)) *(g - (c + (k(2) * log(g/c)))))+ ((D/u)* log((g
*(x(2) + c))/(c * (x(2) + g))))
%
% ENORM(X, Cdata, Ydata) returns norm(Ydata - f(Cdata))
%k = x(1), K = x(2), f(c) = l (distance along column)

% The following are known parameters for HC20.
u = 0.2861;
co = 1;
D = 0.6797;

% The following are known parameters for HC10.
%u = 0.1486;
%co = 1;
%D = 0.5833;

% The following are known parameters for HC5.
%u = 0.0743;
%co = 136.6;
%co = 1;
%D = 0.5257;


for i=1:5

f(i) = ((u/x(1)) *((co - ((D * x(1)/u^2)*(co - (D/u^2)* (x(1) *
co/(x(2) + co)))/((x(2)+ co - (D/u^2)*(x(1) * co/(x(2) + co)))* (1 +
(D * x(1) * x(2))/(u^2 *(x(2) + co)^2)))) -(cdata(i) + (x(2) *
log((co - ((D * x(1)/u^2)*(co - (D/u^2)* (x(1) * co/(x(2) +
co)))/((x(2) + co - (D/u^2)*(x(1) * co/(x(2) + co)))*(1 + (D * x(1)
* x(2))/(u^2 *(x(2) + co)^2)))))/cdata(i))))))+ ((D/u)* log(((co -
((D * x(1)/u^2)* (co - (D/u^2)* (x(1) *co/(x(2) + co)))/((x(2) + co
- (D/u^2)*(x(1) * co/(x(2) + co)))*(1 + (D * x(1) * x(2))/(u^2
*(x(2) + co)^2)))) *(x(2) + cdata(i)))/(cdata(i) * (x(2) + (co -
((D * x(1)/u^2)*(co - (D/u^2)* (x(1) * co/(x(2) + co)))/((x(2) +co -
(D/u^2)*(x(1) * co/(x(2) + co)))*(1 + (D * x(1) * x(2))/(u^2 *(x(2)
+ co)^2)))))))));
end
enorm = norm(f'-ydata);
end
```

```
clc
clear

% testCODfitfun2
% script file to test nonlinear least squares problem

% create test data for COD HC20

cdata = [1 0.765452 0.733433 0.69868 0.685423]';
ydata =[0 0.05 0.3 0.55 0.85]';

% create an initial guess
% x contains initial guess parameters[f0,K]
x0 = [0.05, 0.88]

% call fminsearch

CODfitfun = @CODfitfun2; % create handle

options = []; % take default options

% the vector parvec contains the parameters f0 and K
parvec = fminsearch(CODfitfun,x0,options,cdata,ydata);

% compute error norm at returned solution

enorm = CODfitfun2(parvec,cdata,ydata)
```

MATLAB code for modelling COD removal in the 2 meter soil column

A. Code for experimental condition HC-20

```
function codtrbvp
%BIOTRBVP  Solution for plug flow model with mixed order kinetics
%   The soil column is modelled as a non-ideal plug flow reactor %
%   with axial dispersion and biological reactions occurring.
%
%   For experimental condition HC-20
%   c'' = Pe*(c' - (k*T*c/(Kc+c))*(o/(Ko+o))) for COD and
%   o'' = Pe*(o' - (k*T*F*c/(Kc+c))*(o/(Ko+o))) for electron %
%   acceptors here represented by oxygen.
%
%
%   Here Pe is the axial Peclet number, T is the residence time, k
%   is the overall reaction rate and K is the saturation constant.
%   Let y1 = c ;  y2 = c'. Thus  y1'= c' = y2 and y2'= c''
%   Let y3 = o; y4 = o'. Thus y3'= o' = y4 and y4' = o''.
%   The resulting system of first order ODEs are therefore
%   y'(1) = y(2)
%   y'(2) = Pe*(y(2)-(k*T*y(1)/(K+y(1))*(y(3)/(Ko+y(3))))
%   y'(3) = y(4)
%   y'(4) = Pe*(y(4)-(k*T*F*y(1)/(K+y(1))*(y(3)/(Ko+y(3))))
%
%
%  DEVAL is used to get a smoother graph of y(x).

  % Known parameters, visible in the nested functions.
  Pe = 84;
  k = -0.0221;
  Kc = 0.7458;
  Ko = 0.63;
  T = 729;
  F = 0.146;

  options = bvpset('stats','on');
  solinit = bvpinit(linspace(0,1,10),[0.68 0 0.25 0]);
  sol = bvp4c(@codtrode,@codtrbc,solinit,options);

  zExpt = [0 0.05 0.3 0.55 0.85];
  cExpt = [1 0.765452 0.733433 0.69868 0.685423];
  err = [0 0.008 0.0344 0.0114 0.0130];
  errorbar(zExpt, cExpt, err,'ro');

  hold on;
  xinit = linspace(0,1);
  Sinit = deval(sol,xinit);
  plot(xinit,Sinit(1,:))
  xlabel('Relative column height')
  ylabel('Relative COD concentration')
  legend('Experimental data','Model')

  % --------------------------------------------------------------
  % Nested functions
  %
    function dydx = codtrode(x,y)
  %CODTRODE  ODE function for the soil column
```

```
    dydx = [y(2)
            Pe*(y(2)-((k*T*y(1)/(Kc+y(1)))*(y(3)/(Ko+y(3)))))
            y(4)
            Pe*(y(4)-
            ((21.6*k*T*F*y(1)/(Kc+y(1)))*(y(3)/(Ko+y(3)))))];

  end % codtrode

  % --------------------------------------------------------------------

  function res = codtrbc(ya,yb)
  %CODTRBC  Boundary conditions for the soil column
    res = [ya(2) - Pe*(ya(1) - 1)
           yb(2)
           ya(4) - Pe*(ya(3) - 1)
           yb(4)];
  end % codtrbc

  % --------------------------------------------------------------------

end  % codtrbvp
```

The solution was obtained on a mesh of 37 points.

The maximum residual is 4.031e-004.

There were 951 calls to the ODE function.

There were 68 calls to the BC function.

B. Code for experimental condition HC-10

```
function codtrbvp10
%BIOTRBVP  Solution for plug flow model with mixed order kinetics
%   The soil column is modelled as a non-ideal plug flow reactor
%   with axial dispersion and biological reactions occuring.
%
%   For experimental condition HC-10
%   c'' = Pe*(c' - (k*T*c/(Kc+c))*(o/(Ko+o))) for COD and
%   o'' = Pe*(o' - (k*T*F*c/(Kc+c))*(o/(Ko+o))) for electron
%   acceptors here represented by oxygen.
%
%   Here Pe is the axial Peclet number, T is the residence time, k
%   is the overall reaction rate and K is the saturation constant.
%   Let y1 = c ;  y2 = c'. Thus  y1'= c' = y2 and y2'= c''
%   Let y3 = o; y4 = o'. Thus y3'= o' = y4 and y4' = o''.
%   The resulting system of first order ODEs are therefore
%   y'(1) = y(2)
%   y'(2) = Pe*(y(2)-(k*T*y(1)/(K+y(1))*(y(3)/(Ko+y(3))))
%   y'(3) = y(4)
%   y'(4) = Pe*(y(4)-(k*T*F*y(1)/(K+y(1))*(y(3)/(Ko+y(3)))))
%
%
%  DEVAL is used to get a smoother graph of y(x).
```

```
  % Known parameter, visible in the nested functions.
  Pe = 51;
  k = -0.0082;
  Kc = 0.7876;
  Ko = 0.63;
  T = 1426.7;
  F = 0.146;

  options = bvpset('stats','on');
  solinit = bvpinit(linspace(0,1,10),[0.5 0 0.5 0]);
  sol = bvp4c(@codtrode,@codtrbc,solinit,options);

  zExpt = [0 0.05 0.3 0.55 0.85];
  cExpt = [1 0.805326 0.759929 0.70265 0.67082];
  err = [0 0.0185 0.0099 0.0099 0.0205];
  errorbar(zExpt, cExpt, err,'ro');

  xlabel('Relative column height')
  ylabel('Relative COD concentration')
  legend('Experimental data')

  hold on;
  xinit = linspace(0,1);
  Sinit = deval(sol,xinit);
  plot(xinit,Sinit(1,:))
  xlabel('Relative column height')
  ylabel('Relative COD concentration')
  legend('Experimental data', 'Model')

  % --------------------------------------------------------------------
  % Nested functions
  %

  function dydx = codtrode(x,y)
  %CODTRODE  ODE function for the soil column
    dydx = [y(2)
            Pe*(y(2)-((k*T*y(1)/(Kc+y(1)))*(y(3)/(Ko+y(3)))))
            y(4)
            Pe*(y(4)-
            ((21.6*k*T*F*y(1)/(Kc+y(1)))*(y(3)/(Ko+y(3)))))];

  end % codtrode

  % --------------------------------------------------------------------

  function res = codtrbc(ya,yb)
  %CODTRBC  Boundary conditions for the soil column
    res = [ya(2) - Pe*(ya(1) - 1)
           yb(2)
           ya(4) - Pe*(ya(3) - 1)
           yb(4)];
  end % codtrbc

  % --------------------------------------------------------------------

end  % codtrbvp
```

The solution was obtained on a mesh of 26 points.

The maximum residual is 9.356e-004.

There were 852 calls to the ODE function.

There were 69 calls to the BC function.

C. Code for experimental condition HC-5

```
function codtrbvp5
%BIOTRBVP  Solution for plug flow model with mixed order kinetics
%   The soil column is modelled as a non-ideal plug flow reactor
%   with axial dispersion and biological reactions occuring.
%
%   For experimental condition HC-20
%   c'' = Pe*(c' - (k*T*c/(Kc+c))*(o/(Ko+o))) for COD and
%   o'' = Pe*(o' - (k*T*F*c/(Kc+c))*(o/(Ko+o))) for electron
%   acceptors here represented by oxygen.
%
%
%   Here Pe is the axial Peclet number, T is the residence time, k
%   is the overall reaaction rate and K is the saturation constant.
%   Let y1 = c ;  y2 = c'. Thus  y1'= c' = y2 and y2'= c''
%   Let y3 = o; y4 = o'. Thus y3'= o' = y4 and y4' = o''.
%   The resulting system of first order ODEs are therefore
%   y'(1) = y(2)
%   y'(2) = Pe*(y(2)-(k*T*y(1)/(K+y(1))*(y(3)/(Ko+y(3))))
%   y'(3) = y(4)
%   y'(4) = Pe*(y(4)-(k*T*F*y(1)/(K+y(1))*(y(3)/(Ko+y(3))))
%
%
%  DEVAL is used to get a smoother graph of y(x).

  % Known parameter, visible in the nested functions.
  Pe = 31;
  k = -0.002;
  Kc = 0.8852;
  Ko = 0.63;
  T = 3106.3;
  F = 0.146;

  options = bvpset('stats','on');
  solinit = bvpinit(linspace(0,1,10),[0.68 0 0.25 0]);
  sol = bvp4c(@codtrode,@codtrbc,solinit,options);

  zExpt = [0 0.05 0.3 0.55 0.85];
  cExpt = [1 0.763518 0.730443 0.711624 0.710322];
  err = [0 0.0225 0.0239 0.0343 0.0383];
  errorbar(zExpt, cExpt, err,'ro');

  xlabel('relative column height')
  ylabel('Relative concentration')
  legend('Experimental data')
```

```
  hold on;
  xinit = linspace(0,1);
  Sinit = deval(sol,xinit);
  plot(xinit,Sinit(1,:))
  xlabel('Relative column height')
  ylabel('Relative COD concentration')
  legend('Experimental data', 'Model')

  % --------------------------------------------------------------------
  % Nested functions
  %

  function dydx = codtrode(x,y)
  %CODTRODE  ODE function for the soil column
    dydx = [y(2)
            Pe*(y(2)-((k*T*y(1)/(Kc+y(1)))*(y(3)/(Ko+y(3)))))
            y(4)
            Pe*(y(4)-
            ((21.6*k*T*F*y(1)/(Kc+y(1)))*(y(3)/(Ko+y(3)))))];

  end % codtrode

  % --------------------------------------------------------------------

  function res = codtrbc(ya,yb)
  %CODTRBC  Boundary conditions for the soil column
    res = [ya(2) - Pe*(ya(1) - 1)
           yb(2)
           ya(4) - Pe*(ya(3) - 1)
           yb(4)];
  end % codtrbc

  % --------------------------------------------------------------------

end  % codtrbvp
```

The solution was obtained on a mesh of 21 points.

The maximum residual is 5.685e-004.

There were 663 calls to the ODE function.

There were 67 calls to the BC function.

Further experimental results can be found on the accompanying CD. These include:

i. Soil column tracer tests;

ii. TCC, E1, E2 and EE2 chromatograms;

iii. PLFA chromatograms.